UNIVERSITY OF MANITOBA

"IN-SITU CHARACTERIZATION OF MATERIAL PROPERTIES FOR THE DESIGN AND EVALUATION OF FLEXIBLE PAVEMENTS"

A Thesis
Presented to the Faculty of Graduate Studies
in Partial Fulfilment of the Requirements for
The Degree of **Doctor of Philosophy**
in
the Department of Civil and Geological Engineering

by

Gani Venkataraman GANAPATHY

VOLUME 1 - Text, Figures and Tables

February, 1994

ISBN 0-315-92204-4

Canada

IN-SITU CHARACTERIZATION OF MATERIAL PROPERTIES FOR THE THE DESIGN AND EVALUATION OF FLEXIBLE PAVEMENTS

BY

GANI VENKATARAMAN GANAPATHY

A Thesis submitted to the Faculty of Graduate Studies of the University of Manitoba in partial fulfillment of the requirements for the degree of

DOCTOR OF PHILOSOPHY

DEDICATED TO

Bhagawan Sri Satya Sai Baba

without whose grace and guidance

nothing is ever possible in this Universe.

OM SRI SAI RAM

ACKNOWLEDGEMENTS

The research reported in this thesis spanned a period of over eight years between 1984 and 1992. It involved the collection of a large amount of field data from existing pavements. A work of this magnitude is never an individual effort. While the author did plan the collection of data, analyzed and interpreted the data, the work would not have been possible without the help of many individuals, agencies and organizations. It is now my privilege to acknowledge this help and thank the various individuals and organizations.

First, the author wishes to thank sincerely his advisor Dr. A.M. Lansdown of the Department of Civil Engineering of the University of Manitoba for the constant encouragement, pointed and critical advice, suggestions, and never-failing support. Above all his patience during this prolonged study period is deeply appreciated.

Secondly, the author wishes to acknowledge the valuable guidance given by the advisory committee consisting of Professors Dr. D.H. Shields and Dr. O. Hawaleshka. I shall be remiss in my duty if I forget to thank Dr. J.J. Emery who served on the advisory committee between 1984 and 1989.

Thirdly, I wish to thank the external examiner, Dr. Ralph Haas, for his comments, criticisms, and the encouraging comments on this work.

All the field data reported in this thesis, involved considerable expense to collect. The author is ever grateful to Transport Canada, Public Works Canada and the Department of Transportation and Communications of the Province of Manitoba for underwriting all the cost and expenses of collecting this data. This involved the use of the Falling Weight of Deflectometer, cores from the pavements, providing the logistics of traffic control and

providing all the construction records of the different facilities. The author also wishes to acknowledge the help provided by the three firms, Trow Ltd., John Emery Geotechnical Engineering Ltd. (JEGEL) and Dynatest Canada Ltd., which owned and operated the testing equipment. These three firms provided the equipment and the services of knowledgeable field engineers at cost to Transport Canada and to the Province of Manitoba who in turn helped the author collect the needed data. In this connection the author also wishes to acknowledge the help and encouragement provided by the following individuals in these organizations:

Mr. Glenn Argue: Chief, Professional and Technical Services Branch, Transport Canada, Ottawa.

Mr. Fred Young, Director of Materials Research, Department of Highways and Transportation of the Province of Manitoba.

Mr. Ray van Cauwenberghe, Head of Materials Research Section, Department of Highways and Transportation of the Province of Manitoba.

Dr. J.J. Emery, President, JEGL, Downsview, Ontario.

Mr. D.H. Hein, Manager, Dynatest Canada Ltd., Downsview, Ontario.

The author received considerable help from his colleagues in Transport Canada and in Public Works Canada in the testing of materials recovered from the different test sites. I wish to express my very sincere thanks to them, in particular to Messrs Rudy Labay, Ken Friesen, Roy Smith and Dan Holefeld.

While the technical part of the research was taken care of the above individuals and organizations, the author also received financial aid from many organizations. The author wishes to thank the following:

Mr. Harold Bell, Regional Director General of Aviation Group in Transport Canada (Central Region) for granting the author a leave of absence from his duties with Transport Canada so that he could devote full time in the analysis of the data and writing the thesis.

The T.J. Pounder Trust Fund and Mrs. M. Pounder for awarding the Pounder Memorial Scholarship for the year 1989-90 to the author.

Transportation Association of Canada (TAC) and Delcan Canada for the TAC scholarship for the year 1989-90.

The Department of Civil Engineering for the teaching assistantship dand sessional instructorship during the Spring of 1991.

This financial help was crucial for the author for the support of his family during his leave of absence from his regular job.

While technical and financial assistance were crucial, the author cannot thank enough the members of his family, his friends and relatives for the help and support they extended to the author throughout these years. First and foremost are my wife Sachu and my son Bharat who lived through long lonely days, months and years because of my studies and had to put up with considerable hardships during this long period. I am very grateful for their steadfast support and for their prayers for the successful completion of this project. I am very thankful to all our other relatives whose understanding, encouragement and moral support helped me go through this arduous task.

Many thanks are also due to all our friends who made sure that my family did not fade into social oblivion during these years because of my long preoccupation with my studies.

Last, but not the least, my mother whose constant prayers that this work should come to fruitful end were a source of inspiration to me all these years.

Finally, my sincere thanks to Mrs. Ingrid Trestrail who helped with the professional production of the thesis in its final form.

TABLE OF CONTENTS

LIST OF ABBREVIATIONS

AASHO	American Association of State Highway Officials (later changed to AASHTO)
AASHTO	American Association of State Highway and Transportation Officials
ASCE	American Society of Civil Engineers
ASTM	American Society for Testing Materials
CBR	California Bearing Ratio
CGRA	Canadian Good Roads Association (the forerunner of the Roads and Transportation Association of Canada - RTAC)
C-SHRP	Canadian Strategic Highway Research Program
FAA	Federal Aviation Administration (US)
FHWA	Federal Highway Administration
FWD	Falling Weight Deflectometer
HRB	Highway Research Board
HWD	Heavy Weight Deflectometer
RTAC	Roads and Transportation Association of Canada
SHRP	Strategic Highway Research Program (USA)
TAC	Transportation Association of Canada (formerly Roads and Transportation of Canada, RTAC)
TRB	Transportation Research Board (US) (Formerly HRB)
USAE	United States Army Corps of Engineers
USAF	United States Air Force
WASHO	Western Association of State Highway Officials
WES	Waterways Experiment Station (of the US Army)

LIST OF FIGURES AND TABLES

NOTE:

In general, the Figures and Tables are included at the end of each chapter. In a few cases, some smaller Tables are included in the text.

CHAPTER 3

CHAPTER 4

CHAPTER 5

CHAPTER 6

LIST OF APPENDICES

CHAPTER 1 THROUGH 3: NO APPENDICES.

CHAPTER 4.

APPENDIX 4-I: Results of pressuremeter tests at various sites (tables).

CHAPTER 5.

APPENDIX 5-I: Theory of stif 42 isoparametric solid (source: ANSYS theoretical manual).

APPENDIX 5-II: User defined codes and macros used in this thesis.

CHAPTER 6.

APPENDIX 6-I: Typical results of analyses for each site (tables).

APPENDIX 6-II: Typical results of analyses for each site (charts).

APPENDIX 6-III: Summary of moduli for each site (tables).

APPENDIX 6-IV: Summary of moduli for each site (charts).

APPENDIX 6-V: Stress distribution along the centreline of load.

CHAPTER 7.

NO APPENDIX.

NOTE: The appendices for chapter 6 contain only typical results for one station from each site. The results of complete analyses for all stations are available on 3.5-Inch or 5.25-Inch floppy disks.

ABSTRACT

In the last half a century or so, pavement engineering has evolved from an art into a science. This has been made possible by the great advancements in many related fields of such as geotechnical engineering, engineering mechanics, material science, numerical modelling, computational techniques, instrumentation and techniques of measurement of pavement response to various kinds of loading. Despite these advancements, however, there exist significant gaps in our ability to analyze, evaluate and design pavements rationally. These gaps in our knowledge pertain to two areas:

1. Measurement of the mechanical properties of the materials in the pavement structure.
2. The models used for the analysis of pavements have many restrictive assumptions that make them too simplistic .

This thesis addresses these two questions in an attempt to fill this gap. The objective of this thesis is twofold:

1. To develop a finite element model to represent the pavement as a layered elastic solid with the minimum of restrictive assumptions. In fact the only restrictive assumption is that the problem is solved as an axi-symmetrical solid, (i.e) as a plane strain problem. The model should be able to consider any number of layers. It should be able to handle material properties such as non-homogeneity, non linearity, cross anisotropy and stress-dependency.
2. To adapt in-situ testing techniques that are common in geotechnical engineering, to measure the properties of pavement materials directly as they exist in the

ground. These can then be set directly into the model and pavement responses can be predicted.

In order to achieve these objectives the following tasks were undertaken and are reported in the thesis.

1. A multi layered elastic model was developed using a commercially available general purpose finite element program, ANSYS. This program turned out to be a powerful tool for such complex analyses. One unique feature of this algorithm is the ability to run an optimization routine which would lead to a match between the observed and computed deflection basins ***consistent with the measured material properties.***
2. Five airfield pavements representing a wide range of subgrade, structural, environmental, loading and service lives were selected and tested with the Dynatest 8001 Heavy Weight Deflectometer / Falling Weight Deflectometer (HWD/FWD).
3. The pavements were cored at the test locations to ascertain the exact pavement structure and to recover materials for laboratory testing.
4. At the test location the moduli of the unbound layers were measured using the pavement pressuremeter developed by Briaud (1979).
5. The numerical model was used to backcalculate the moduli of the materials in the different layers within the bounds measured by the tests and specified in the model (see (1) above).
6. A regression analysis was carried out between the measured and the computed material properties at each site as well as by pooling all the data.

The following conclusions are drawn from this study:

1. A general-purpose finite-element method such as ANSYS presents a powerful tool to model the pavement under many different assumptions of material properties and layer geometry.
2. The most powerful method of matching the deflection basins in a backcalculation procedure appears to be when the differences between the respective "AREA" of the deflection basins (volume of the bowl in a three dimensional case) are minimized rather than a comparison to the maximum deflection only. This can be defended, philosophically, on the basis that the volume of the deflection basin represents the energy absorbed by the pavement under the applied load. Thus a match of the volume of the basin should lead to a good estimate of the true material properties.
3. Based on the above conclusion, it would be desirable to precede the ANSYS analysis with a curve fitting program such as is used by ISSEM-4. This will permit closer integration of the basin.
4. Some of the pavements tested in this investigation were aged and badly cracked. In such cases there is an abrupt deviation of the observed basin from the computed ones.
5. For cracked pavements the classical models, including the one presented herein, cannot properly analyze the pavement. The model should be capable of incorporating a "gap" element across which only partial or no load transfer will exist. The ANSYS model presented herein is capable of modelling such gap elements.

6. For the pavements tested the unbound layers exhibited cross anisotropic ratios ranging between 0.5 and 3. These are the general range reported in the literature.
7. The stress distribution appeared to be relatively insensitive to the variations in the moduli. This raises a question whether one should be overly concerned with exact values of moduli. For, in the final analysis, the stresses and strains and the climatic factors are the factors which determine the performance of the pavements.
8. Isotropic models gave better correlations between measured and computed moduli values than cross anisotropic models for both the asphalt and the unbound layers.. One should, however, remember that the asphaltic concrete layer was always considered isotropic. Taken together with the comments earlier about the insensitivity of stress distribution, it is suggested that the isotropic model for the pavement is adequate.
9. Attempts to correlate computed moduli to independently measured moduli met with limited success. It is suggested that the small data base and not considering other significant factors (see 11 and 12 below) might be the cause for the less than spectacular correlations. Yet, the modest correlations do merit further investigation.
10. In the case of asphalt moduli, three sites gave moderate correlations while the other two showed no correlation at all. When the data were pooled, there was no correlation. On further examination of the pavement history, it would appear that the younger the pave-ments are, the better is the correlation; the older the pavements are, the poorer is the correlation. This leads one back to the

conclusion regarding aged and fatigued and cracked pavements as discussed above (see # 4 above).

11. In the regression relationships presented for asphaltic concrete, no physical meaning can be attached to the intercept of the line. However, the slope may be looked upon as the ratio of dynamic to static moduli. For the material tested in this investigation this ratio is in the vicinity of two.
12. In comparing the computed moduli for the unbound materials with the pressuremeter-measured moduli, it was found that the data from individual sites showed no correlation at all. This was not surprising because in any one site, within the length of a runway, a high uniformity of material should be expected. Under such a condition the data points clustered around in a narrow region. Thus a regression analysis is not meaningful. However, when the data was pooled, a much better correlation could be seen (see # 8 above).
13. In the case of unbound materials, many other factors influence the modulus. These are gradation, moisture content and in-place density to name a few. These must be taken into account and a multivariate analysis, instead of a univariate analysis, should be done. It is expected that the correlation would be better (see # 8 above).
14. It is therefore submitted that the pressuremeter can be used to predict the moduli of unbound layers which can be directly set in a layered elastic analysis. However, additional studies are required.

15. Unlike in the case of asphaltic concrete (see # 11 above) no physical meaning can be attributed to the regression parameters for the unbound materials, neither the slope nor the intercept.

Chapter 7 of the thesis presents many suggestions for further research in the field of pavement engineering. For further discussions the reader is referred to that chapter.

CHAPTER ONE

INTRODUCTION

1.1 DESIGN AND EVALUATION OF PAVEMENTS

1.1.1 Historical Perspective

Construction of roads has been one of the major activities of mankind since the earliest periods of civilization. However, like many other activities of man, road building remained more an art than science until the dawn of the Industrial Revolution. Even then, a systematic approach to road construction was not taken until in the mid 1800's when McAdam built his first roads using broken stones. Later, in this century, came new surfacing materials such as portland cement concrete and asphalt. With rapid industrialization and growth of motorized traffic the need for stronger, longer lasting and all-weather pavements became a priority. Thus much attention was paid to portland cement concrete and asphalt both from the point of view of materials technology and construction techniques. Much less attention was paid to the properties and behaviour of granular materials or of subgrade. The "design" of a pavement was still a matter of experience passed from one generation of engineers to the next. Such experience was necessarily confined to a local area and was not readily transferable to another region. Pavement engineers from different regions could not compare notes on a quantifiable basis.

Then in the early 1930's soil mechanics evolved as a new discipline within the field of civil engineering. Its impact on pavement engineering was almost instantaneous. Terzaghi evolved the concept of subgrade modulus and suggested a method to measure it in the field

(the plate load test). This concept was later used in the theoretical works of Biot (1937), Westergaard (1939) and Burmister (1943). The ASTM staged a symposium (1949) on plate load tests where many papers were presented dealing with the application of this test to pavement engineering.

With the ability to apply loads approximately at the same magnitude and contact pressure as the actual truck or aircraft wheel and measure the deflections under the loads, the carrying capacity of a pavement could be determined for any ***pre-determined deflection level.*** The test could be carried out at different levels of the pavement (such as subgrade, base or surface) so that the required thickness of structure could be determined. Hence the problem was one of arriving at a suitable ***"tolerable"*** deflection based on experience and performance of the pavements. Thus the design of pavements was still left to be based on an empirical basis. Not much attention was paid to the theoretical developments mentioned earlier. It is suspected that this was primarily due to the complexity of the mathematics and the extremely onerous computational effort involved. Even today (1993) the plate load test forms the basis of pavement design and evaluation for many agencies who are responsible for airfields.

However, the evolution of soil mechanics did provide a means of quantifying the characteristics of pavement materials such as subgrade and granular layers. Thus the concept of Group Index was born. The Group Index is a number based on the clay fraction and plasticity characteristics of the soil (Yoder and Witczak, 1974). Later it was shown by many researchers that these factors could be indirectly linked to the shear strength and compressibility characteristics of the soils (for example Skempton, 1964). These latter factors are the ones that govern the deformation and rutting of pavements. Thus, for the first time, pavement engineers from different regions of the country could compare their exp-

eriences based on a numerical, albeit empirical, index. Until recently, the Group Index formed the basis of design for many agencies including the Federal Aviation Administration (FAA) and United States Air Force (USAF).

While pavement design has been making the transition from experience based on empirical evaluation to some elementary form of soil testing, great strides were being made in the field of geotechnical laboratory testing. Tests such as unconfined compression test, Proctor and California Bearing Ratio (CBR) tests and triaxial tests were being developed and perfected. Along with the development of laboratory techniques, geotechnical engineers were also introducing analytical methods using these laboratory parameters for solving foundation engineering problems. This had its impact on pavement engineering. Many highway agencies attempted to use triaxial test results for the design pavements. This did not lead to any great success because pavements differed from foundations in certain basic ways. Some of these are:

	FOUNDATIONS	**PAVEMENT**
1.	Continuous static loading	Repetitive dynamic loading
2.	Half Space	Layered System
3.	Reasonably homogeneous	Heterogeneous
4.	Moderate strains	Very low strains
5.	Minor environmental effect	Environment major factor
6.	Localized problem	Wide area affected

The response of the pavement materials on a stretch of highway varied so much that laboratory testing provided little help during design or subsequent evaluation. Thus the hope

for a rational and fundamental design procedure faded till early to mid 1960's.

At this time two developments, one on either side of the Atlantic, provided great impetus for theoretical development in pavement engineering. In Europe a group of researchers at the Shell Research Centre in Amsterdam, Holland, were pursuing Burmister's theoretical work and were developing techniques to model and to analyze the pavement as a layered elastic system. In the U.S.A. the Americans launched the most ambitious and comprehensive full-scale road test to that date using different types of construction and materials and subjecting them to actual vehicle loads until the sections failed. These tests came to be known as the AASHO (American Association of State Highway Officials) Road Tests. Many valuable research papers were published, based on these efforts in two international conferences on pavement design (the Ann Arbor conferences of 1962 and 1967). The data from the road tests are still being analyzed and re-analysed based on more recent concepts and theories. From these developments evolved two fundamentally different philosophies of pavement design and evaluation.

The Europeans continued the development of a mechanistic design procedure where the material properties would be measured either in the laboratory or in-situ. Based on these measured properties a theoretical analysis would be carried out to calculate the stresses and strains at critical locations in the pavement. These calculated stresses or strains would be compared to the tolerable strain or stress for the required number of repetitions of the design load using some type of a fatigue law (eg. Miner's Hypothesis). Design charts were prepared on these concepts to aid the practising engineer (Shell Design Manual 10, 1961, Dorman and Metcalf, 1965). This came to be known as the Shell Design Procedure (Claessen et al., 1977).

In North America the results of the AASHO Road Tests were synthesised in the form of an "Interim Guide to the Design of Flexible Pavements" in 1972. In contrast to the stress and strain concept in the Shell method, the underlying philosophy in the AASHO procedure was the serviceability of the pavement. The serviceability depends on a host of factors such as the rideability, cracking, deformations, other distresses, maintenance needed etc. and is expressed in terms of a Present Serviceability Index (PSI). Using statistical methods to analyze the large amount of data collected from the Road Test, empirical equations were derived to compute the PSI. Nomographs were prepared to design the structural section of a pavement for a given traffic mix. Input to these nomographs were the traffic, material properties, and climatic factors. The AASHO method was still essentially empirical in its approach. Individual States modified some of the factors suggested by AASHO to suit their local and regional conditions. Despite these minor modifications, the method remained intact and is still being used by many North American highway departments as well as by many countries around the world. The data collected from the Road Test still forms a valuable data-base for research in pavement engineering. During the last decade deficiencies in the empirical approach are becoming more apparent and there is a move towards a mechanistic approach in North America as well. To reflect this trend AASHO revised the Interim Guide in 1986 and again in 1993 which leans definitely towards a mechanistic approach to the design and evaluation of pavements.

1.1.2 Current Trend in Pavement Engineering

Both the mechanistic and the empirical methods have not been without their problems. The availability of high-speed computers, the capacity to store very large amount of data

relatively inexpensively and the development of powerful and sophisticated analytical techniques (such as the finite-element method) have overcome the difficulties of mathematical computations faced by engineers some twenty years ago. However, the determination of the material parameters that are needed for these analyses has remained a thorny problem. Thanks to the advanced technology of microprocessors, the laboratory and measuring techniques have improved immensely. However, the relevance of those parameters measured in the laboratory to real-life pavement materials has not been demonstrated. On the other hand the extrapolation of empirical test results, such as the AASHO Road Tests, to other parts of the world has not been entirely satisfactory.

To fill this gap AASHTO and the FHWA (US Federal Highway Administration) launched in 1987 another ambitious research program known as the Strategic Highway Research Program (SHRP). In Canada there is a corresponding program called C-SHRP. Many other countries around the world are also participating in this venture. Therefore, it would not be amiss here to say that the state-of-the-art process in pavement design at this time (1993), is to use a mechanistic approach. The material parameters for the analysis would be determined at conditions as close as possible to those existing in the road structure. In fact, the trend is to evaluate these properties by nondestructive testing of the actual facilities, using such techniques as deflection testing, in-situ geotechnical tests and geophysical methods such as wave propagation. Laboratory testing is still useful in isolating and studying the effect of individual factors on the overall response of the material in a controlled environment. Thus one should not lose the advantage of the modern laboratory facilities and techniques.

In what follows a brief discussion of the concepts underlying the mechanistic design and the material characterization is presented leading up to the objectives and the scope of

the research developed in this thesis.

1.1.2.1 Layered Elastic Systems

Layered elastic systems will be discussed in a little more detail in Chapter 2. The discussion at this point is simply to suggest that there is a need to model the pavement more adequately and realistically.

It is now generally accepted that pavements are best modelled as a layered system consisting of layers of various materials (concrete, asphalt, granular base, subbase etc.) resting on a natural soil deposit or the subgrade. The behaviour of such a system can be analyzed using the classical theory of elasticity as demonstrated by Burmister (1943, 1945). Classical theory of elasticity was developed strictly for continuous media as approximated closely by metals, some natural products such as wood and to a lesser extent by some man-made products such as concrete. It is well recognized by pavement engineers that the materials used in the construction of pavements do not form a continuum but rather are particulate materials (Josselin de Jong, 1963; Sokolowski, 1967; and Hardin et al. 1989). Moreover, soils are not elastic even at moderate strains. For these reasons, geotechnical engineers nowadays attempt to use the theories of plasticity and flow for foundation problems in preference to elastic theory. However, as mentioned earlier, pavements differ from foundations in some aspects. One of these is the strain levels which can be tolerated for satisfactory performance.

Fig. 1.1[1] shows the typical stress-strain response of a soil in the laboratory. The

---

[1] Figures and tables are included at the end of each chapter.

circled area which is shown enlarged would probably be appropriate for pavements. For such small strains and for the transient loads that the pavements will be subjected to, the assumption of elastic behaviour is defensible. Further, as can be seen, under repetitive loading the materials generally tend to show elastic behaviour with the area of the hysteresis loop being relatively small even under moderate strains.

In modelling the pavement as a layered system, the following assumptions are made:

1. Each layer is linearly elastic, isotropic and homogeneous.
2. Each layer (except the subgrade) is finite in thickness and infinite in the horizontal plane.
3. The subgrade is a semi-infinite half space.
4. The loads are applied vertically on top of the uppermost layer.
5. There are no shear forces acting on the loaded surface.
6. There is perfect contact between the layers at their interfaces.

Because of assumption 1, the constitutive relationship for such materials would involve only two elastic constants; the modulus of elasticity (E) and the Poisson's ratio (μ) or the bulk modulus (K) and the shear modulus (G). While some authors (eg. Domaschuk and Wade, 1969; Naylor, 1978; Pappin and Brown, 1980; Bowles, 1988) feel that K and G are preferable to E and μ to characterize earth materials, it is customary to use E and μ in all geotechnical and pavement engineering computations. Because of the transient or repetitive nature of the loading in pavement engineering, the elasticity modulus E is replaced by M_R, the resilient modulus. The resilient modulus is defined as the recoverable strain divided by the stress.

While it has been traditional, both in geotechnical and in pavement engineering, to treat soils and pavement layers as isotropic and homogeneous, the last fifteen years have seen

number of models assuming soils to be cross-anisotropic. A cross-anisotropic material is one where there is one axis of symmetry with respect to the elastic properties[2]. By nature of their deposition and subsequent stress history soils are anisotropic. There is more and more evidence that many soil deposits can be better modelled by assuming them to be cross-anisotropic (Barden, 1963; Lo et al., 1977; Wroth and Houlsby, 1985; Graham and Houlsby, 1983; Lee and Rowe, 1989; Graham et al., 1989).

Some investigators have shown that compacted soils in a pavement can exhibit cross anisotropy (Gerrard, 1968; Stock and Brown, 1980; Uzan, 1985; Stewart et al., 1985). Thus an argument can be made that pavement layers are probably better modelled by treating the materials as cross-anisotropic. With cross-anisotropic material one needs to define five elastic constants instead of just two for the isotropic material. This poses a problem in testing. Some of these will be discussed in the next section.

1.1.2.2 Laboratory Characterization of Materials

As can be seen from the foregoing discussions, in order to analyze the pavement as a layered elastic system, one has to determine two or five elastic constants depending upon whether one treats the structure as isotropic or cross-anisotropic. It was shown that the traditional plate load tests could not be used to determine any of these parameters unless one assumes the pavement to be a halfspace. The plate load test yields one composite stiffness value for the entire pavement. Breaking down a composite modulus into the moduli of

---

[2] Some authors (e.g. Wroth and Houlsby, 1985) call this an orthotropic medium. In the literature on continuum mechanics, the term orthotropy usually refers to symmetry in three planes whereas cross-anisotropy refers to symmetry in six or more planes. The former requires nine elastic constants while the latter requires only five.

component layers can be done only in an arbitrary fashion. The traditional method in geotechnical engineering for the determination of the moduli is to use the triaxial apparatus. For pavement design, where one is seeking the resilient modulus, the traditional setup will not be adequate. The apparatus had to be modified for repeated loading and should be instrumented to read very small strains; therefore the need exists for increased sophistication in the instrumentation (see for example, Seed et al., 1967; Nair and Chang, 1973; Boyce and Brown, 1976; Lam, 1982; Emery, 1983). If anisotropy is to be considered, the testing becomes even more complicated. The usual method of determining the anisotropic parameters is to measure the sample in three different orientations, vertical, horizontal and at some inclination, generally at 45° (Gibson, 1967, 1974; Chowdhury, 1972; Atkinson, 1975). Some researchers feel that a truly anisotropic test can be done only if all the three principal stresses can be independently varied, a three-axial test as against the traditional triaxial test (Yuen, 1976; Lo et al., 1977). One of the independent parameters for a cross-anisotropic soil is the vertical shear modulus G_{vh}. Some authors have suggested that this can be obtained only with torsional testing and have developed a torsional triaxial apparatus (Sada and Ou, 1973). It is not difficult to see that the laboratory testing for the parameters required in pavement engineering can become quite complicated, time-consuming and expensive. Moreover, as has been said before, only a few samples can be tested to represent a large volume of materials. Finally, there is always the perennial criticism that the laboratory sample might not represent the field conditions faithfully. Marcuson and Townsend (1976) have shown that reconstituting the sample for cyclic triaxial tests can affect the test results substantially. They found that the sampling procedures, the manner of remolding the sample, cementation, stratigraphy and the grain size distribution all affected the results in the case of

the shell and foundation material used for the Fort Peck dam in Montana. Details of some of the laboratory tests referred to here will be discussed in a subsequent section. It is the intention here to demonstrate that there is a gap in our ability to characterize pavement materials adequately.

1.1.2.3 *In-Situ* Testing

Because of the difficulties in adequately characterizing earth materials by laboratory testing, particularly for pavement engineering purposes, attention was directed to *in-situ* testing. The plate load test, which was discussed earlier, is one type of *in-situ* test. As mentioned earlier, however, it is inadequate in characterizing the material properties of individual layers. Other types of tests in this group are deflection testing, *in-situ* geotechnical tests and geophysical tests.

Surface deflection is one of the best determinants of pavement response. Deflection testing was first introduced by Benkelman during the WASHO (Western Association of State Highway Officials) tests. It was used in the AASHO Road Tests. However, the Benkelman beam test suffers from the same shortcoming as the plate load test in that the response is measured at only one point. Individual layer properties cannot be assessed. Also, like the plate load tests, the rate of loading is different from that imposed by the traffic loads. To overcome this criticism researchers in Europe developed equipment which would measure the pavement deflections under dynamic loading conditions at several points in addition to directly under the load. The first of these dynamic deflection measuring equipment was developed by the Shell group (Heukelom and Foster, 1960; Heukelom, 1961; Heukelom and Klomp, 1964). Thus a ***deflection basin*** would be defined. Then using the inverse process

of analysis, the modulus value for each layer would be calculated that would yield a deflection basin matching the measured deflections. This process is known as the backcalculation procedure.

Considerable improvements have been made to these machines since the days of Heukelom. The modern deflection testing machines are very sophisticated, totally automated and have a very high degree of repeatability and precision in their measurements. Some of the more commonly used equipment currently employed to measure pavement deflections are Dynaflect, Road Rater, FHWA Thumper, California Travelling Deflectometer, LaCroix Deflectographe, the Falling Weight Deflectometer (FWD) and the Heavy Vehicle Simulator. Of these only the Dynaflect, Road Rater, the LaCroix Deflectographe and the FWD are commercially available. The rest are one of a kind developed by different agencies for research purposes and are also being used for routine evaluation in their jurisdictions. Excellent reviews of these machines can be seen in reports by Clayton Sparks and Associates (1980), Hoffman and Thompson (1982), Kennedy (1982), Bush et al. (1985), and several papers in the two international symposia on Non-Destructive Testing (NDT) in Baltimore under the auspices of ASTM (1988) and the second under the auspices of TRB (1991) and the two international conferences sponsored by the US Army Corps of Engineers (1989, 1991). The three international symposia on the bearing capacity of roads and airfields (Trontheim 1986, Nottingham 1989 and Trontheim 1991) also contain very good papers on this subject. Of the different deflection testing machines discussed in these forums, the FWD appears to be the most used by many agencies. It has been also chosen as the standard test equipment for the SHRP and the CSHRP programs curently running in the USA and in Canada. This was also the machine used in the field testing phase of the research reported

in this thesis. Deflection testing and back-calculation procedures are discussed in some more detail in Chapter 2.

Several in-situ geotechnical tests have been developed in the past 15 years. The more common of these are the cone penetration tests, the pressuremeter and the flat plate dilatometer. In reality these test procedures have been around for longer than 15 years, particularly in Europe. However, interest in them grew vastly in the past 15 years due to some of the concerns about the relevance of laboratory testing. Of these only the pressuremeter and the dilatometer measure a modulus value directly. Because of the geometry of the equipment, a rigorous mathematical treatment is possible only for the pressuremeter test. It was for this reason a special pressuremeter for testing pavement layers was developed (Briaud, 1979; Briaud and Shields, 1979). Further demonstration of the potential of this equipment has been reported by Cosentino (1987), Briaud and Cosentino (1987) and Briaud et al. (1989). In this thesis data from additional pressuremeter tests at some Canadian airfields will be presented.

Geophysical test methods such as seismic refraction, reflection, down-hole and cross-hole seismic tests have long been used by geotechnical engineers to identify soil stratification, depth to rock and permafrost. Recently they have been used to measure more specific properties such as the elasticity and shear moduli and Poisson's ratios. One such method, the Surface Wave method, is drawing increasing attention from pavement engineers (Nazarian, 1989). It would be later suggested in this thesis that the surface wave method together with the pressuremeter holds the greatest potential in perfecting a pavement model as a layered elastic medium having non-homogeneous, non-linear and cross-anisotropic properties.

1.1.2.4 Problems and Shortcomings

Based on the above discussions, the problems facing pavement engineers can be summarised as below:

1. Characterization of materials in the pavement layers is a major problem facing pavement engineers. Sophisticated laboratory testing techniques are available to test the pavement materials in the laboratory. However, these are very time consuming and expensive. Moreover, laboratory tests do not represent the actual material properties adequately; in particular, it is impossible to perform enough number of tests to adequately cover the variations that can occur in a stretch of highway.
2. Pavement engineers have not taken advantage of in-situ tests to characterize the materials of construction.
3. While a high level of confidence can be placed in deflection measurements by some of the modern equipment, the analyses of the data have not been satisfactory. The lack of match between backcalculated properties of material and measured ones points to the need for more work.
4. In particular, existing analysis methods are too restrictive in their assumptions. They cannot consider visco-elastic properties of the asphalt surface; they cannot consider anisotropy in the layers; they cannot consider yield criteria of the material; they cannot solve the problem when one imposes limits for the material properties for the various layers whether such properties are obtained from laboratory tests, in-situ tests or known from one's experience or previous research. In other words, they cannot optimize the solution to fit the given

pavement structure.

5. With the improved ability to measure properties and the ability to compute complicated models better, more realistic models of pavement should be built and analyzed.

It is in this context this thesis is presented. It is an attempt to suggest a more realistic model of the pavement structure and a method to determine the necessary parameters.

It may be appropriate here to state that the pavement engineer faces other problems which make the analysis of pavements difficult. While these are not directly relevant to this thesis, they are related to pavement evaluation and pavement management. They are simply enumerated below for the sake of completeness:

1. A high degree of error is associated with the estimates of traffic loads;
2. Another problem is the adequate modelling of the pavement performance
3. Currently considerable difficulty is encountered in modelling the effects of climate on the materials and on their performance;
4. The interaction of loads and climatic effects are not clearly understood.
5. A high variance is associated with the construction not only with respect to pavement structure but also with the materials and construction quality.
6. The effect of maintenance and local repairs cannot be adequately considered at present.

1.2 SCOPE OF THE THESIS

1.2.1 Objectives of the Study

The primary objective of this study is to characterize the materials in the pavement structure. This is a twofold assignment relating to:

a) The development of a model which can be used to analyze a layered elastic system with both isotropic and anisotropic properties as well as stress dependent variation of layer moduli. It is believed that such a model will be more general, more realistic and more useful than the current models.

b) Field measurements to validate the model and to demonstrate how the required elastic parameters can be measured.

It is recognized that there is no single equipment existing at present which can be used to measure all the five parameters required for the characterization of an anisotropic medium. At present these parameters can be measured only in the laboratory. In this thesis, reliance is placed on published results from laboratory tests by other investigators on anisotropic behaviour of soils at the test sites. However, suggestions are made for the development of an instrument to measure the five parameters.

1.2.2 Methodology of the Study

1.2.2.1 An Analytical Model for Pavements

The theoretical model to be studied in this thesis is still the layered elastic system. However an attempt is made to consider cross anisotropy of the layers. The existence of such cross anisotropy in all the layers has been suggested in the literature. Considerable work has been done by geotechnical engineers on cross-anisotropic half space. A cross-anisotropic

layered system has been studied by Gerrard (1967; 1968), Bhattacharya (1968) and by Gerrard and Harrison (1971). The earlier work by Gerrard and his associates considered a two-layer system for two specific ratios of anisotropy (i.e. ratio of vertical to horizontal elastic moduli). The latter work by these authors considered a multi-layer system with no numerical evaluation. The work by Bhattacharya dealt with a homogeneous cross-anisotropic medium subjected to a point load. No further work seems to have been done in the intervening period (1970-1993) and no computational algorithms appear to exist to analyze pavements as cross-anisotropic layered systems. The method of solution in these earlier works involved the use of finite differences. It is submitted that these earlier works are too limited in scope to be of much practical use. This thesis will, therefore, attempt to extend these previous works by:

1. Formulating a finite element model to analyze the pavements as an elastic, cross-anisotropic layered system (Chapter 3).
2. Suggesting a method for the *in-situ* measurement of the elastic parameters needed in the analysis (Chapters 3 and 4).
3. Verifying the model by comparing the analytical solutions to actually measured pavement responses as well as to published results in the literature (Chapters 4 and 5).

Non-homogeneity and stress-dependency of the material will be considered in an indirect way by dividing any layer into sub layers in the finite element model. However, it will be emphasized that the model that is suggested in this thesis is a general purpose finite element program that can solve the layered elastic structure under the most generalised assumptions. Details of the model, of the finite element setup and the stress dependency of the moduli in

different layers are discussed in Chapter 3.

1.2.2.2 Field Testing

In order to verify the model, deflection tests were conducted at five airport sites in the Prairie provinces in Canada. The sites selected were Thunder Bay in NW Ontario, Brandon and St. Andrews in Manitoba and Regina and Saskatoon in Saskatchewan. It is submitted that these sites represent a wide spectrum of pavements with respect to geotechnical, environmental, load and traffic conditions, and age of the pavements. More particulars of the test sites are given in Chapter 4.

1.2.2.3 Material Characterization

All the pavements tested had an asphaltic concrete (AC) surface, though some were of composite construction (AC overlay on Portland cement concrete pavements). The pavement construction was determined by actually coring through the pavements. This helped establish the pavement structure as well as recover materials from each layer for subsequent laboratory testing to determine their properties.

For the bituminous materials the mix characteristics (density, composition, percent binder etc.), gradation of aggregates, consistency of the binder (both viscosity and penetration measurements) were determined.

For the unbound materials laboratory investigation consisted of basic classification and consistency tests. The elastic properties of the materials that are required in the model are to be determined using the pavement pressuremeter. Since there are five parameters to be evaluated and the pressuremeter can at the most yield only two of these, different numerical

expediencies are necessary to infer the other three. One such expediency would be to use the device suggested by Graham and Houlsby (1983). Alternatively, the bounds suggested by Pickering (1970), Uriel and Canizo (1971) and Nayak (1973) could be used to infer the missing parameters with sufficient accuracy. The former approach relies on the regression analysis of a large number of high quality triaxial tests. This was not feasible in this study because, such tests were not carried out. This study is primarily aimed at measuring these parameters *in-situ*. The cross-anisotropy of the soils at the test sites in this study have been studied by others (Yuen, 1976; Lo et al., 1977; Graham and Houlsby, 1983). Thus it is possible to draw from their studies and infer the missing parameters using the bound values suggested by these authors.

1.2.2.4 Pavement Response

In addition to the pressuremeter tests, the response of the pavements to three different levels (low, medium and high) of loading at the five test sites was measured with the Falling Weight Deflectometer (FWD). The pavement structures at these sites were analyzed using a commercially available general purpose finite element program for both the isotropic and cross-anisotropic cases. The results of the finite element analyses are then compared to the measured FWD deflection basins to evaluate whether:

1. The model can predict the deflection basins within specified tolerances and whether such a match would be compatible with the measured material properties.
2. The isotropic or cross-anisotropic model better matches the actual pavement response. The details of these analyses are discussed in more detail in

Chapter 3 and Chapter 5.

3. The techniques of determining the in-situ material properties, as described in this thesis, are adequate or at least hold some promise.

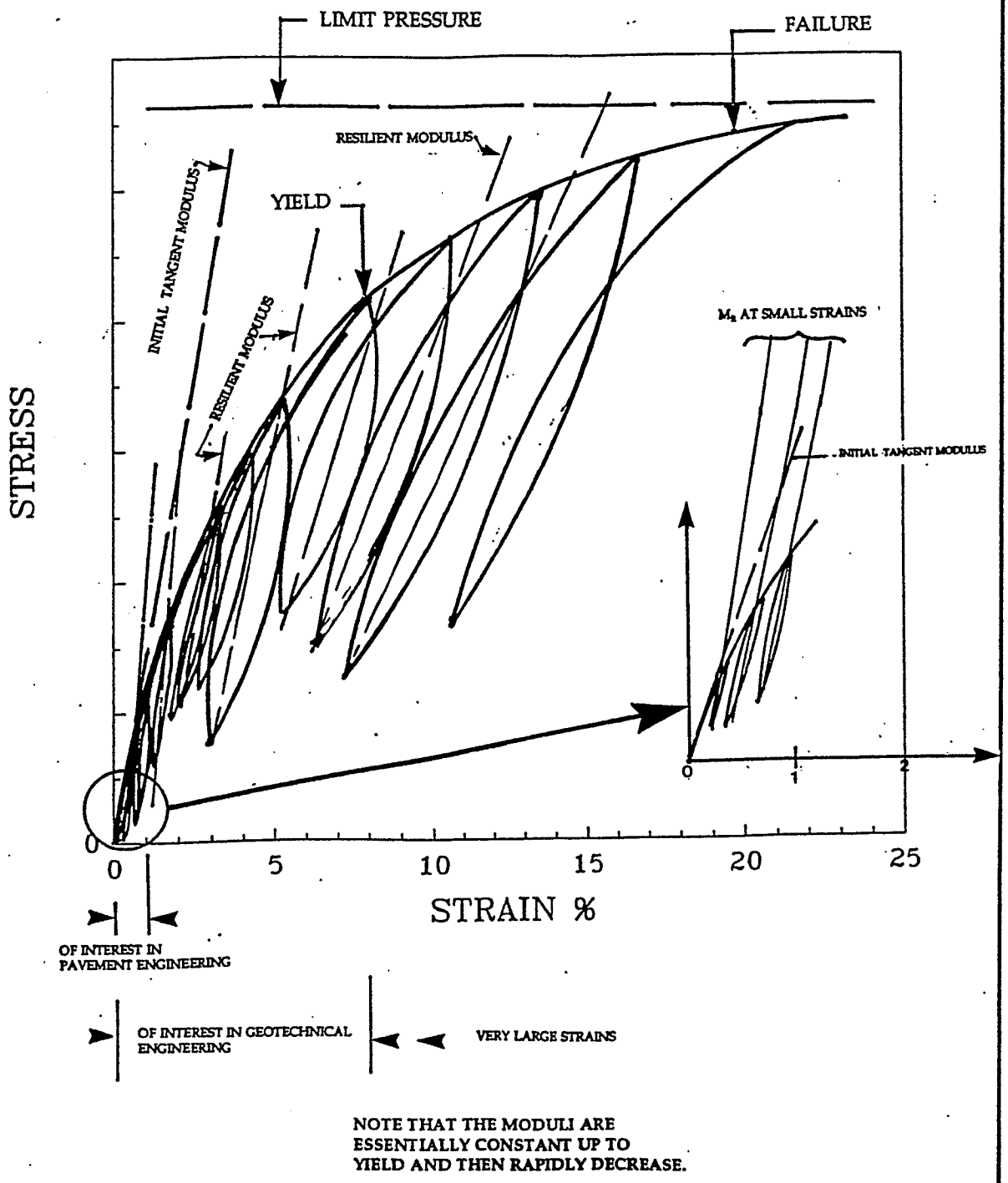

FIG.1.1. TYPICAL STRESS-STRAIN CURVE FOR PAVEMENT MATERIALS AND THE RANGE OF INTEREST IN PAVEMENT ENGINEERING.

CHAPTER TWO

REVIEW OF LITERATURE

2.1 ANALYSIS: LAYERED ELASTIC SYSTEMS

Pavements are generally analyzed by modelling them as layered elastic systems. The assumptions involved in this theoretical model were given in Chapter 1. Because of the geometry of the problem one can analyze the system as an axisymmetrical case. The equation of equilibrium for an axisymmetrical problem in polar coordinates, can then be written as:

$$\frac{\partial \sigma_r}{\partial r} + \frac{\partial \tau_{zy}}{\partial z} + \frac{\sigma_r - \sigma_\theta}{n} = 0 \qquad (1)$$

$$\frac{\partial \tau_{zv}}{\partial r} + \frac{\partial \sigma_z}{\partial z} + \frac{\tau_{zv}}{r} = 0 \qquad (2)$$

where σ_r, σ_θ are the normal components of stresses, τ_{zr} is the shear stress and r, θ and z are the coordinate directions. The z-axis is assumed to be vertical. The loads are generally assumed in the form of Fourier series or Fourier integrals or Hankel Transforms (Gerrard, 1967). The series approach will apply to periodic loading at regular intervals (e.g. railway loads). The integral formulation will apply to finite loading such as highway loads. The Hankel transform is more suitable for axi-symmetrical problems form the computational point of view. One of the assumptions made (see Section 1.1.2.1) is that the surface of the system is loaded only by vertical forces and there are no shear forces acting on the surface. The loading is usually taken as sine (odd) and cosine (even) functions. For an axi-symmetrical

case the odd function will result in zero loading (no shear loads) and the even functions will result in a net force (vertical stresses).

The solution to the set of Eqns. (1) and (2) are generally given by a stress function Φ in the form of a Bessel series as below (Burmister, 1943; Gerrard, 1967):

$$\phi = J_0(mr)\ [Ae^{mz} - Be^{-mz} + CZe^{mz} + DZe^{-mz}] \qquad (3)$$

where

Φ = the stress function to satisfy $\nabla^4 \Phi = 0$

∇ = the LaPlace operator

J_o = Besel function of order 0

r = radial distance from the load and

m, A, B, C and D are constants of integration to be determined from the boundary conditions.

Since there are four constants for each of the layers, for an *n-layer* system one has to evaluate 4n constants. The 4n simultaneous equations required to determine the 4n constants are supplied by the following boundary conditions:

1. Two equations relating to the loads at the surface (i.e. the vertical stress is equal to applied stress and shear stress is equal to zero).
2. Two equations at the lower boundary at infinity (stresses and deformations must be equal to zero).
3. 4(n-1) equations at each of the n-1 boundaries.

Solutions for such a system with isotropic materials for a two-layer system were given by Burmister (1943, 1945). His work was extended by many. Table 2.1 summarizes some of the known results.

Limited solutions for a system with cross-anisotropic properties were given by Gerrard (1967) and Gerrard and Harrison (1971) (see also Poulos and Davis 1974, pp. 187 and Appendix B). The differential equations and the solution methodology still remain the same as for the isotropic case except that some of the parameters would now include the five elastic constants needed to characterize a cross-anisotropic medium. It can be shown that the isotropic layer is a special case of the cross-anisotropic problem (Gerrard 1967). The solutions, given by Eq. (3), for stresses are functions of the elastic properties of the materials, the elasticity and shear moduli and the Poisson's ratios. From the stresses, the strains are calculated using the constitutive equations for the materials. These are obtained from the general theory of elasticity. In what follows these constitutive equations are simply stated first for the most general Hookean material (linear elastic material) and how it will simplify in the case of cross-anisotropic and isotropic materials. For more detailed discussions the reader is referred to the extensive literature on continuum mechanics and theory of elasticity (eg. Timoshenko and Goodier, 1949; Lekhnitskii, 1963; Jaeger, 1969; Melvern, 1974). This will be followed by a review of literature on the application of elasticity theory for soils and pavements for both isotropic and anisotropic cases. Finally in this section some of the existing theoretical and computer models for pavement analysis are discussed.

2.1.1 General Theory of Elasticity

Fig. 2.1[1] shows an infinitesimal parallelepiped with sides of dimensions dx, dy and dz in equilibrium in an elastic continuum. Fig. 2.2 shows the coordinate system and a soil element in polar coordinates for an axi-symmetrical case. In order to completely define the state of stress, in the most general case, one has to define the nine stress components shown in Fig. 2.1.

These are the normal stresses and the six shear stress components: σ_x; σ_y; σ_z; (τ_{xy}, τ_{yx}); (τ_{yz}, τ_{zy}); (τ_{zx}, τ_{xz}). Of these the pairs of shear stress components shown can be shown to be equal from consideration of the moment equilibrium of the element. Thus one is left with six components of stresses to define the stress state of the parallelepiped. These six stress components are linearly related to the corresponding normal strains and shear strains by Hooke's law. These relationships can be written in tensor notation as below:

$$\begin{Bmatrix} \epsilon_x \\ \epsilon_y \\ \epsilon_z \\ \gamma_{xy} \\ \gamma_{yz} \\ \gamma_{zx} \end{Bmatrix} = \begin{bmatrix} C_{11} & C_{12} & C_{13} & C_{14} & C_{15} & C_{16} \\ C_{21} & C_{22} & C_{23} & C_{24} & C_{25} & C_{26} \\ C_{31} & C_{32} & C_{33} & C_{34} & C_{35} & C_{36} \\ C_{41} & C_{42} & C_{43} & C_{44} & C_{45} & C_{46} \\ C_{51} & C_{52} & C_{53} & C_{54} & C_{55} & C_{56} \\ C_{61} & C_{62} & C_{62} & C_{64} & C_{65} & C_{66} \end{bmatrix} \begin{Bmatrix} \sigma_x \\ \sigma_y \\ \sigma_z \\ \tau_{xy} \\ \tau_{yz} \\ \tau_{zx} \end{Bmatrix} \qquad (4)$$

Because of the requirement of positive strain energy (i.e. work cannot be extracted from a body when it is being strained), the coefficient matrix [C] must be symmetrical (e.g. Jaeger, 1969, pp. 62). Thus the number of independent constants for a general linear elastic body can

---

[1] Figures and Tables are appended at the end of each chapter.

be obtained by considering only the top half of the diagonal (in Eqn. 4) as shown below leaving only 21 independent constants[2].

$$\begin{Bmatrix} \epsilon_x \\ \epsilon_y \\ \epsilon_z \\ \gamma_{xy} \\ \gamma_{yz} \\ \gamma_{zx} \end{Bmatrix} = \begin{bmatrix} C_{11} & C_{12} & C_{13} & C_{14} & C_{15} & C_{16} \\ & C_{22} & C_{23} & C_{24} & C_{25} & C_{26} \\ & & C_{33} & C_{34} & C_{35} & C_{36} \\ & & & C_{44} & C_{45} & C_{46} \\ & & & & C_{55} & C_{56} \\ & & & & & C_{66} \end{bmatrix} \begin{Bmatrix} \sigma_x \\ \sigma_y \\ \sigma_z \\ \tau_{xy} \\ \tau_{yz} \\ \tau_{zx} \end{Bmatrix} \tag{5}$$

If the material possesses planes of elastic symmetry (i.e. planes in which the elastic properties are equal) then by successive rotation of the axes it can be shown that some of the constants will become zero leaving fewer and fewer constants. As mentioned in Chapter 1 a cross-anisotropic material is one which has six planes of symmetry.

Curiously, a material which possesses more than six planes of symmetry also behaves like the one having the hexagonal symmetry. For such a case it can be demonstrated that the stress strain relationship shown above will degenerate as shown in Eq. (6) below (Lekhnitskii, 1963, pp. 24; Jaeger, 1969, pp. 63-65).

$$\begin{Bmatrix} \epsilon_x \\ \epsilon_y \\ \epsilon_z \\ \gamma_{xy} \\ \gamma_{yz} \\ \gamma_{zx} \end{Bmatrix} = \begin{bmatrix} C_{11} & C_{12} & C_{13} & 0 & 0 & 0 \\ & C_{11} & C_{12} & 0 & 0 & 0 \\ & & C_{33} & 0 & 0 & 0 \\ & & & C_{44} & 0 & 0 \\ & & & & C_{44} & 0 \\ & & & & & 2(C_{11}-C_{12}) \end{bmatrix} \begin{Bmatrix} \sigma_x \\ \sigma_y \\ \sigma_z \\ \tau_{xy} \\ \tau_{yz} \\ \tau_{zx} \end{Bmatrix} \tag{6}$$

---

[2] In Eq. (5) and in many subsequent matrix formulations only the coefficients in the top half are shown for the sake of clarity. The coefficients are symmetrical with respect to the primary diagonal.

Thus five elastic constants are needed to define the stresses in the cross-anisotropic material.

An isotropic material has complete symmetry about all axes. For such a case:

$$C_{11} = C_{33} \; ; \quad C_{12} = C_{13} \; ; \quad C_{44} = 2(C_{11} - C_{12}) \tag{7}$$

Thus the stress strain relationship will be as follows, leaving only two elastic constants:

$$\begin{Bmatrix} \epsilon_x \\ \epsilon_y \\ \epsilon_z \\ \gamma_{xy} \\ \gamma_{yz} \\ \gamma_{zx} \end{Bmatrix} = \begin{bmatrix} C_{11} & C_{12} & C_{13} & 0 & 0 & 0 \\ & C_{11} & C_{12} & 0 & 0 & 0 \\ & & C_{11} & 0 & 0 & 0 \\ & & & 2(C_{11}-C_{12}) & 0 & 0 \\ & & & & 2(C_{11}-C_{12}) & 0 \\ & & & & & 2(C_{11}-C_{12}) \end{bmatrix} \begin{Bmatrix} \sigma_x \\ \sigma_y \\ \sigma_z \\ \tau_{xy} \\ \tau_{yz} \\ \tau_{zx} \end{Bmatrix} \tag{8}$$

In terms of engineering parameters these coefficients can be written as below (Lekhnitskii, 1963).

For an isotropic material:

$$C_{11} = 1/E \; ; \quad C_{12} = -\mu/E \; ; \quad 2(C_{11} - C_{12}) = \frac{2(1-\mu)}{E} = 1/G \tag{9}$$

where

E = modulus of elasticity

G = shear modulus

and μ = Poisson's ratio.

Then Eqn. (8) can be written in the familiar form:

$$\begin{Bmatrix} \epsilon_x \\ \epsilon_y \\ \epsilon_z \\ \gamma_{xy} \\ \gamma_{yz} \\ \gamma_{zx} \end{Bmatrix} = \frac{1}{E} \begin{bmatrix} 1 & -\mu & -\mu & 0 & 0 & 0 \\ -\mu & 1 & -\mu & 0 & 0 & 0 \\ -\mu & -\mu & 1 & 0 & 0 & 0 \\ 0 & 0 & 0 & 2(1-\mu) & 0 & 0 \\ 0 & 0 & 0 & 0 & 2(1-\mu) & 0 \\ 0 & 0 & 0 & 0 & 0 & 2(1-\mu) \end{bmatrix} \begin{Bmatrix} \sigma_x \\ \sigma_y \\ \sigma_z \\ \tau_{xy} \\ \tau_{yz} \\ \tau_{xz} \end{Bmatrix} \qquad (10)$$

For a cross-anisotropic material the constants in Eqn. (9) can be written as below using the engineering parameters (Gerrard, 1967; Pickering, 1970).

$$\begin{aligned} &C_{11} = 1/E_{11} \; ; \; C_{12} = -\mu_1/E_{11} \; ; \; C_{13} = -\mu_z/E_{11}; \\ &C_{33} = 1/E_3 \; ; \; C_{44} = G_{13} = G_{31} \\ &2(C_{11} - C_{12}) = G_{12} = G_{21} \end{aligned} \qquad (11)$$

Thus Eqn. (9) can be written with the familiar engineering units as below (Eqns. 11 and 12). Since most of us are more at ease with cartesian or polar coordinates, the axes are changed to the familiar x,y,z and r,Θ,z. The coordinate axes are shown in Fig. 2.2.

Cartesian Coordinates

For the sake of clarity the zeroes are not shown.

$$\begin{Bmatrix} \epsilon_x \\ \epsilon_y \\ \epsilon_z \\ \gamma_{xy} \\ \gamma_{yz} \\ \gamma_{zx} \end{Bmatrix} = \begin{bmatrix} 1/E_x & -\mu_x/E_x & -\mu_z/E_x & 0 & 0 & 0 \\ -\mu_z/E_x & 1/E_x & -\mu_x/E_x & 0 & 0 & 0 \\ -\mu_x/E_x & -\mu_x/E_x & 1/E_z & 0 & 0 & 0 \\ & & & & 2(1+\mu_x)/E_x & 0 \\ & & & & 1/G_{xz} & 0 \\ & & & & & 1/G_{xz} \end{bmatrix} \begin{Bmatrix} \sigma_x \\ \sigma_y \\ \sigma_z \\ \tau_{xy} \\ \tau_{yz} \\ \tau_{xz} \end{Bmatrix} \qquad (12)$$

Polar Coordinates

$$\begin{Bmatrix} \epsilon_r \\ \epsilon_\theta \\ \epsilon_z \\ \epsilon_{r\theta} \\ \epsilon_{\theta z} \\ \epsilon_{rz} \end{Bmatrix} = \begin{bmatrix} 1/E_r & (-\mu_r/E_r) & (-\mu_z/E_r) & 0 & 0 & 0 \\ (-\mu_z/E_r) & 1/E_r & (-\mu_r/E_r) & 0 & 0 & 0 \\ (-\mu_r/E_r) & (-\mu_r/E_r) & 1/E_z & 0 & 0 & 0 \\ & & & 2(1+\mu)/E_r & 0 & 0 \\ & & & & 1/G_{rz} & 0 \\ & & & & & 1/G_{rz} \end{bmatrix} \begin{Bmatrix} \sigma_r \\ \sigma_\theta \\ \sigma_z \\ \tau_{r\theta} \\ \tau_{\theta z} \\ \tau_{rz} \end{Bmatrix} \quad (13)$$

2.1.2 Application of Elastic Theory to Analysis of Pavements

As can be seen from Table 2.1 application of the theory of elasticity to the design of pavements had undergone three different phases of evolution over the past one hundred years. These three phases can be identified with the following three analytical models.

1. The Boussinesq model. (Halfspace model.).
2. The Burmister model. (Layered elastic systems.)
3. Computer based models, particularly based on the finite-element approach.

In this section the application of these models to the analysis of pavements will be discussed.

2.1.2.1 Boussinesq Model

The first practical and usable solution for a homogeneous, isotropic linear elastic halfspace loaded on its upper boundary either by a single load P or by a uniform load over a finite area is generally credited to Boussinesq. While Boussinesq gave the equations for complete state of stresses, only those for the vertical stress and vertical deformation at any depth z are given here since these are of most interest.

$$\sigma_z = \frac{3}{2\pi\left[1 + \left(\frac{r}{z}\right)^2\right]^{5/2}} \cdot \frac{P}{Z_2} \qquad (14)$$

$$\Delta_z = \frac{P\,(+\,\mu)\,a}{E}\left[\frac{z}{a} \cdot A + (1 - \mu)\,H\right] \qquad (15)$$

Here P is the load intensity, r the radial distance from load, z the depth, E the Young's modulus, μ the Poisson's ratio, A and H are influence factors. Ahlvin and Ulery (1962) have published extensive tabular values for this case.

As pointed out in Chapter 1, Boussinesq's model has wide application in foundation engineering provided one is not concerned with anisotropy or non-homogeneity. However, in the absence of a method to calculate stresses and displacements in a layered system, Boussinesq's method was employed for analyzing pavement systems.

The theory was applied in two ways. Some engineers ignored the contribution of the upper layers and treated the roadbed and the subgrade as an elastic halfspace. Thus in the ASTM symposium on plate load tests (STP 79, 1949) the papers which attempted to analyze the plate load test results did so on the basis of the classical theory of halfspace (Palmer, McLeod, and Osterberg discussing Mcleod's paper). Between 1945 and 1960 the US ARMY Corps of Engineers tested full-scale test pavements with instruments and found that the classical theory of halfspace predicted the stresses reasonably closely to the measured values (Foster and Fergus, 1949; Turnbull et al., 1961). Vesic and his colleagues came to the same conclusions between 1960 and 1965 (Sowers and Vesic, 1961; Vesic, 1962, Vesic and Domaschuk, 1964).

Another school of thought is to consider the upper layers but to incorporate it in the computations as an equivalent layer having the same modulus as the supporting foundation subgrade. Thus the pavement would be converted into a homogeneous halfspace satisfying Boussinesq's assumption (Steinbrenner, 1947; Palmer and Barber, 1940; Odemark, 1949; Vesic, 1962; Thenn de Barros, 1966; Ueshita and Meyerhof, 1967; Briaud, 1979; Ullidtz and Peattie, 1980). The various methods of finding equivalent single loads (eg. see Yoder and Witczack, 1974) are also based on this concept. Once the equivalent halfspace is found the stresses and displacements can be calculated at any depth. At least one backcalculation method for FWD deflections (the ELMOD method) uses this concept (Ullidtz and Stubstad, 1985).

Poulos and Davis (1974) have reviewed some of these methods by comparing them with the exact solutions proposed by Burmister. Steinbrenner's method works well for layered systems in which the modulus increases with depth. However, there are significant discrepancies in computed radial and vertical displacements in some cases. Odemark's solutions suffer from the same criticisms. The ELMOD program often gives results which are at variance with other accepted algorithms such as ELSYM 5 or ILLIPAVE. Some of the expressions for finding the equivalent modulus are fairly complicated (Odemark, 1949; Ueshita and Meyerhof, 1967). In general the equivalent modulus is given by:

$$E_{eq} = \sum \frac{(h_i \cdot E_i)^n}{h_i} \qquad (16)$$

where,

E_{eq} = Equivalent modulus

h_i = thickness of the ith layer

E_i = modulus of the ith layer

n = an exponent (generally around 3)

The variation between Boussinesq's distribution and the one predicted by layered theory by Burmister would depend on the relative stiffness of the layers. This may be part of the reason why experimental sections such as used by Sowers and Vesic (1961) or the US Army Corps of Engineers (Foster and Fergus, 1949; Turnbull et al., 1961) did not show much differences between the two theories. It is suggested that the compaction and construction techniques in a test pit would not produce the same stiffnesses as in an actual construction. This was explicitly recognized by Foster and Fergus (1949). Instrumented sections of actual airfield pavement sections show significant differences between Boussinesq's and observed stress distribution showing the effect of the stiff upper layer. Thus, Boussinesq's model cannot be accepted as valid for most primary and heavy duty pavements.

2.1.2.2 Burmister's Model

Burmister was the first to develop solutions for layered systems and in particular application to airfield pavements. He still kept the assumptions regarding homogeneity, isotropy and linear elasticity in his theoretical developments. Other assumptions involved in the analysis of layered systems were given in Chapter 1. His original work (1943, 1945) was for a two-layer system which he later extended to three-layer systems (1958). He also published a set of curves giving influence factors which could be used to compute surface deflections under the imposed load. At first he considered Poisson's ratio of 0.5. In a further paper (1962) he published curves with different Poisson's ratios. In general, the theoretical

expressions for layered systems are very involved and cumbersome to handle. Hence multi-layered systems could not be analyzed without recourse to tabulated values, graphs and charts. When the number of layers exceeeded three, the evaluation of the factors became unwieldy and a high speed computer would be needed.

Burmister's work was extended by many (see Table 2.1). The extensions consisted mainly in considering a third layer, working with many more ratios of thicknesses and modulus values (and combination of these) so that these theoretical solutions can be approximated as closely as possible to the practical field problems.

2.1.2.3 Extensions to Burmister's Model

The most notable and probably most used of these additional works were due to Acum and Fox (1951), Jones (1962), Peattie (1962) and Ueshita and Meyerhof (1967, 1968). By this time the Shell Design method (see Chapter 1) was already in place and many computer programs had been developed based on finite-element methods. The finite-element method also took the layered elastic system one step further in that stress-dependent moduli as well as non-homogeneous material could be considered in the computations. Also the number of layers was theoretically unlimited.

Acum and Fox (1951) extended Burmister's method to a three-layer system. The loading was a uniform load on a circular area. The numerical computations were based on four parameters which were functions of the radius of the loaded area (a), the thicknesses of the two finite layers (h_1 and h_2) and the modular ratios (E_1/E_2 and E_2/E_3). The results were somewhat limited because only factors for stresses were given. No factors for strains or displacements were given. Only one Poisson's ratio (0.5) was considered. Also relatively few

cases were considered. The results were presented in the form of tabulated values rather than charts or graphs so that interpolation would be necessary. Since the solutions were very complicated and non-linear such interpolations could introduce significant errors. However, this work should be considered a big contribution because it evaluated a three-layer system which was more practical and commonplace than a two-layer system. Also the results were in a form more readily usable by the practising engineer than mathematical formulae.

The next major breakthrough came with the publication of more extensive charts and tables by Jones (1962) and by Peattie (1962). Jones extended the earlier work by Acum and Fox (1951) to include a much wider range of the same parameters considered by the earlier workers. However, the Poisson's ratio was still kept at 0.5. Again Jones chose to publish his results in the form of tables though, because of the wider range of parameters, interpolation was not necessarily as risky as in the earlier work. Peattie used the same parameters as the other investigators and computed a few more values to "tighten up" the interpolation range. More interestingly, though, he presented these results in an ingeneous graphical way consisting of curvilinear grids. Fig. 2.4 shows an example of Peattie's curves. The works by both Jones and by Peattie were still concerned only with stresses in the layers. No factors were derived for deformations or strains.

Ueshita and Meyerhof (1967, 1968) attempted to fill this gap by deriving deflection factors for a three-layer system and presenting them in the form graphs and charts. The Poisson's ratio in these investigations were assumed to be 0.5. They also compared their results with approximate methods suggested by Odemark (1942) previous workers and found good agreement for specific conditions (i.e. progressively decreasing layer moduli). Ueshita and Meyerhof also verified their results by model tests in the laboratory and concluded that

the theory of a layered elastic system is valid for the type of pavements they tested. Finally, as mentioned in an earlier section, they also derived equivalent moduli for multi layer systems.

No further attempt at numerical evaluation or further extension to Burmister's model has been reported in the literature. By this time the Shell Design Method had been in place for some years and many computer based algorithms were being developed. With these programs one can theoretically analyze an n-layer system though the computational effort becomes too large if the number of layers exceeds five. Also the accuracy obtainable with increased effort does not seem to warrant such effort. In the next section a few of these computer-based techniques, their advantages and capabilities and deficiencies are discussed.

2.1.2.4 Currently Used Computer Models

This section describes some of the better known computer programs for the design and evaluation of flexible pavements. All models assume isotropic, homogeneous and linear elastic layer properties. Some can consider non-linearity because they are based on finite-element techniques. Thus different constitutive equations can be written for different elements and the non-linearity can be considered. There are basically two types of models:

1. Analysis models
2. Distress models

The oldest known computer based analysis model is probably BISTRO which formed the basis of the Shell design procedure. This was later improved and issued as BISAR (Claessen et al., 1977). The improvements considered were horizontal loads, variable interface friction and revised stress-strain relationships of asphalt based on further laboratory data. The capability of considering visco-elastic behaviour of asphalt was included in the

program. Also the fatigue criteria for subgrade and asphalt material were modified to take into account field and laboratory test data. BISAR can also consider any number of layers. Thus by dividing the layers into a number of sub-layers the program can be made to consider non-linearity of the materials. The program can also consider multiple wheel loads. The drawback of the program is the long computational time required.

Other analysis models that are often referred to in the literature are CHEVRON and CHEVRON-N programs. The CHEVRON is the older version which could consider only three layers. CHEVRON-N is the modified version to handle any number of layers much the same way BISAR considered multi-layer pavements.

ELSYM 5 is a multi-layer analysis program developed at the University of California, Berkeley and forms the basis of design management systems of many agencies. This is a finite-element-based program using layered elastic theory. The original development of ELSYM 5 followed the CHEVRON-5 program. However, there have been numerous improvements and modifications so that this has evolved to be an independent algorithm by itself. The program can accept a multiple-wheel configuration defined by coordinates with reference to a set of axes. The output, then, would give stresses and strains at any point with reference to this coordinate system. As a default, the program assumes rigid bottom at infinite depth, but depth to rigid bottom can be specified. Though the program is based on finite-element analysis, only linear elastic material characteristics can be input. Modifications have been made to the source code so that non-linearity can be considered. For this purpose the program was modified to consider up to 50 layers. Details of the working of the program can be seen in the FHWA report FHWA-TS-87-206 (1987).

ILLI-PAVE is an analysis tool developed at the University of Illinois (Gomez-Gomez-Achecar and Thompson, 1984, 1986). This is a complex finite-element-based program. The pavement is considered to be an axi-symmetrical solid of revolution. Non-linear material properties are incorporated in the program. In addition, the Mohr-Coulomb failure criterion is also included in the model. As input, the program requires pavement geometry (layer thicknesses), material constants to define the stress dependent material response and seed moduli for each layer. The computations are done iteratively to match the computed deflection basin with the observed deflection basin measured with the FWD. Thereby at each point the material response model and the Mohr-Coulomb failure criteria must be obeyed.

The program is specifically oriented towards highway pavement design. The program validation was done on a large number of highway sections in Illinois where deflection measurements were taken with the FWD. Thus the analyses are all done for a circular load of 40 kN and 600 kPa tire pressure (9,000 lb, 80 psi) corresponding to single wheel of the single-axle highway truck. The program is being continuously upgraded to consider more and more pertinent design factors. Thus, recently the effect of climatic factors on material and pavement response was included (Dempsey et al., 1985). ILLI-SLAB is the sister program to ILLI-PAVE written to analyse rigid pavements.

ELMOD is an analysis program developed by Dynatest Inc. who manufacture the FWD. This is strictly not a layered elastic algorithm. The pavement is first converted to an equivalent halfspace using Odemark's theory (Ullidtz and Peattie, 1980). Then using the Boussinesq model the stresses, strains and moduli are calculated. Finally, the moduli are broken into individual layer moduli. The program takes the deflection values directly from

FWD test files. At this point the operator has the option of indicating the surface condition of the pavement. Later in the analysis part the user has the option of modifying the computed moduli based on the state of distress of the pavement. The program evaluates up to four layers. It can consider non-linear and seasonal variation of the modulus as well as viscoelastic behaviour of asphalt. It can also consider stabilized bases. Different loads and load configuration can be considered by the program. There is a rehabilitation option to the program which would compute the remaining life of the pavement and the required overlay thickness. ELCON is a companion program to ELMOD, but specifically for concrete pavements.

ISSEM-4 is another numerical evaluation program marketed by Dynatest to specifically evaluate FWD data. The source code is in FORTRAN. Unlike ELMOD this program does not read the field FWD files directly. The data has to be re-worked in a specific format dictated by the FORTRAN language. The pavement is reduced to an axi-symmetrical plane-strain problem. The authors call the model generated "a finite cylinder". The program has two parts:

1. A curve-fitting program.
2. Back analysis.

The curve-fitting part uses the data generated by the FWD and interpolates the intermediate points to fit into a smooth asymptotic curve. Deflections are generated in this way at every 20 cm from the centre of the load to the outer boundary of the model. Once a satisfactory curve has been generated, the data is fed in to the analysis part. It could happen sometimes that if the asymptote cannot be properly defined, then the program cannot generate

a satisfactorily fitting curve and will abort. Physically this means that the seven sensors in the FWD do not define the deflection bowl adequately.

ISSEM-4 uses ELSYM as the subroutine for the analysis part. Based on the load and deflection data ELSYM attempts to arrive at possible values for the different layers. The program can abort even at this stage if a satisfactory match between the calculated and measured deflections cannot be found. The program can vary the modulus of either the top layer (AC) or the base layer but not both. The program can consider a maximum of four layers. For pavements having more layers equivalent moduli can be computed and given as input for the program. After the calculations, one has to derive the individual moduli of this composite layer.

Distress models are those which attempt to predict the distresses likely to occur in the pavement based on the computed stresses and strains. These are basically analysis programs as discussed above but also incorporate additional response models for predicting fatigue cracking, rutting, thermal cracking etc. The best known in this category is VESYS developed by the FHWA (Kenis, 1982). At the time of this writing (1993) it is undergoing trial as VESYS IV. There are other computer programs developed by many consulting engineers and State Highway Departments. They are used for analysis as well as for selecting rehabilitation options (e.g. Rauhut et al., 1979; Finn and Monismith, 1984; Smith et al., 1986; Ali and Khosla, 1987).

2.1.2.5 Finite-element Techniques

Over the past twenty years analysis of stresses, strains and displacements in soil and rock masses as well as beneath the pavements has been frequently carried out by the finite-

element method. The first application of the finite-element method to pavement analysis was illustrated by Duncan et al. (1968) and Barker (1972). Subsequently, the application of the method in general geotechnical engineering was shown by Girijavallabhan and Reese (1968), Radhakrishna and Reese (1970), and Desai (1979). As was described in the previous section most modern multi-layer algorithms are based on finite-element techniques. The greatest advantage of this technique lies in its ability to consider such complex behaviour as non-linearity, non-homogeneity, and anisotropy. However, the technique is a numerical one and care should be taken that the successive iterations will converge rapidly and not oscillate about a value. Certain values of the material parameters can lead to such a situation. Thus, for instance, in the ELSYM 5 program Poisson's ratio can never take a value between 0.748 and 0.752 nor can it be equal to unity. In some formulation of constitutive equations for cross-anisotropic soils by the classical theory of elasticity Poisson's ratio of 0.5 would lead to results which would exceed the definition of infinity by the computer. In such cases expediencies such as setting $\mu = 0.49$ should be adopted (Raymond, 1972; Uriel, 1973). In all cases a rigid boundary below the bottom layer must be specified or provisions must be made for a default value. Similarly the lateral extent of the load distribution which is an unknown to start with should be specified . The choice of the mesh itself affects the convergence rate. Some modern finite-element software can automatically choose a mesh configuration depending on the problem. Finally, regardless of how sophisticated the program is, the results are only as good as the model or the material parameters that go in as input values.

There appear to be some divergent opinions about the utility and reliability of the various programs. Rauhut et al. (1979) quote from an unpublished report from the University

of Texas and state that all the programs yield essentially same results within about 1 percent, the maximum difference being 3 percent. In contrast, Ali and Khosla (1987) presented results which compared four different algorithms. The ratio of predicted resilient modulus to laboratory measured modulus varied form a low of 0.18 to a high of 18.3. The same program when analyzing different sections of pavements showed wide variations. With some the variations of the maximum and minimum ratios of computed and laboratory measured moduli were within a factor of two while with others the factor was as high as 30. Hoffman and Thompson (1982) show that the ILLI-PAVE and BISAR algorithms can yield quite different results. Bush et al. (1985) analyzed deflection basins produced by different equipment and analyzed by a layered elastic program developed by Waterways Experiment Station (WES) and showed that they all yielded totally different results. Brown et al. (1986) compare the results obtained from analyses run with the BISTRO and CHEVRON programs and show that these could yield seriously divergent results. In their discussion of the paper by Bush et al., Uddin et al. (1985) suggest that the deflection results of each equipment should be analyzed by the special algorithm developed for that equipment. Since linear elastic systems should be strictly independent of the method of testing, load level (as long as it is well within the elastic range), sequence and time of testing, the argument by Uddin et al. cannot be accepted. However, it does point out that there is a need to re-examine the layered elastic model. The computer programs should be able to consider stress dependency of the moduli, non-homogeneity and probably even anisotropy. In many recent international forums (Purdue 1985, Ann Arbor 1987, Baltimore 1988 and West Lebanon 1989, Nottingham 1991, Nashville 1991) significant discrepancy between measured and computed moduli was reported by

numerous authors. Therefore there is a need to reexamine the theoretical model in the analysis of pavements.

In comparing these different algorithms and the reviews about these it appears that the models are sensitive to:

1. the pavement geometry, i.e. thicknesses of the layers; and
2. the material characteristics i.e. the modulus, the type of stress-strain relationships they are assumed to have, and the state of stress during testing.

There is not much one can do about wrong inputs regarding the layer thicknesses. Even when the thicknesses are taken from actual cores obtained from the pavement some of the programs show some variations. Therefore the major weakness in the programs lies in the inadequate characterization of the materials. The following section discusses the characterization of pavement materials based on a review of existing literature.

2.2 MEASUREMENT OF MATERIAL PARAMETERS

The properties of the pavement materials can be determined in two ways. The first is laboratory determination and the second is *in-situ*. Laboratory investigations are useful in that the influence of the many variables governing the response of the materials can be studied in isolation and under controlled conditions. This aspect is very important to understand the fundamental behaviour of the material. On the other hand it is very nearly impossible to reproduce the field conditions faithfully in a laboratory. In pavement engineering this is quite important because the response of the structure is affected by relatively short-term changes in the field conditions. Therefore, *in-situ* tests are very useful. This section attempts to review the research reported in the literature, on both these evaluation methods.

2.2.1 Laboratory Investigations

Since the materials used in the construction of pavements are essentially earth materials, the method of testing reported in the literature is primarily the triaxial test method used extensively in geotechnical engineering. In contrast to geotechnical engineering, the objective here is not so much to determine the strength parameters or the elasticity modulus at a particular stress or strain level as it is to measure the resilient modulus. The resilient modulus is defined as the ratio of the recoverable strain after a loading and unloading cycle at the associated stress level (Fig. 2.5). Thus the resilient modulus can be expressed as:

$$M_R = \sigma_d / \epsilon_r \qquad (17)$$

where,

M_R = resilient modulus

ϵ_r = recoverable strain (ϵ_{rr} → radial; ϵ_{vr} → vertical)

q_r = deviator stress level

Many factors affect the value of the resilient modulus. Some of these are:

1. Type of material;
2. Moisture content;
3. Confining pressure;
4. Stress history of the material;
5. Stress level of loading and unloading;
6. Number of cycles of loading and unloading; and
7. Type of loading.

The following review is divided into two parts, one dealing with the fine-grained materials (subgrade: generally silts and clays) and the other with granular materials (bases and subbases: generally crushed rock, gravels and sand).

2.2.1.1 Resilient Modulus of Fine Grained Materials

Some of the earliest investigations on the resilient modulus of fine-grained soils were due to Seed and his associates at the University of California at Berkeley (1955, 1956, 1958, 1960, 1962, 1967). In these tests a silty clay was compacted at low and high degree of saturation and subjected to different levels of deviator stress, different ratios of principal stresses and different stress histories. It was found that clayey soils tend to soften during the initial cycles of repetitive loading. However, at large number of cycles of loading they could show a stiffening effect. Based on the series of tests between 1955 and 1962 Seed and his associates formulated a model for the resilient modulus for fine- grained soils which is shown in Fig. 2.6. The equations to the two parts of the curve shown in Fig. 2.6 are usually given as follows (Yoder and Witczak, 1974):

$$M_R = K_2 + K_3 [K_1 - (\sigma_1 - \sigma_3)] \qquad 0 < (\sigma_1 - \sigma_3) < K_1 \qquad (18)$$

$$M_R = K_2 + K_4 [(\sigma_1 - \sigma_3) - K_1] \qquad K_1 < (\sigma_1 - \sigma_3) \qquad (19)$$

Stress history and frequency of loading had significant influence on the failure strain of the clays. Thixotropic soils, at high degree of saturation, can recover strength and show considerably increased stiffness under repeated loading (Fig. 2.7).

Dehlen (1969) summarized the results of various previous researchers, including Seed and his associates, up to 1969. All the investigators found that the resilient modulus of

the fine grained soils decreased rapidly by as much as four hundred percent up to a deviator stress between 100 and 150 kPa (14 psi. to 21 psi.). Beyond this stress level there is a slight stiffening effect (see Fig. 2.6). The initial decrease in the resilient modulus is attributed to the shear strain (strain-softening effects) and the breakdown of structure. The stiffening part is attributed to:

1. The overriding effect of the mean normal stress over the shear stress effects;
2. Structural changes in the clay particle arrangements;
3. Densification of clay and consequent increase in strength and stiffness (Seed and Chan, 1958).

However, Dehlen suggested that the strains at which the stiffening effect was usually observed would be far in excess of the rut criteria suggested by Dorman and Metcalf (1964). Thus he would seem to suggest that this part of the curve would be of little practical importance in pavement analysis. However, it may be argued that at any stress level the resilient modulus increases after about 1000 repetitions as shown in Fig. 2.8 (Seed, Chan and Lee, 1962). This is a relatively low number of repetitions in the life of a pavement and hence is likely to be reached at an early age. Seed et al. (1967) had summarised the Berkeley series of tests on the resilient modulus of fine grained soils:

1. Resilient deformations decrease as the number of load applications increases. Conversely M_R increases.
2. Resilient modulus increases as the intensity of stress decreases.
3. Methods of compaction which result in a dispersed structure in the clay (wet of optimum) produce lower resilient modulus.

4. As the compaction curve shifts towards the saturation line, the resilient modulus decreases.
5. As a corollary to (3) and (4) above, increase in water content after placement decreases the resilient modulus. On the other hand increase in dry density increases the modulus.
6. Thixotropic materials show an increase in modulus after a small number of load repetitions and long rest periods. However, at large number of load repetitions, thixotropy does not seem to have any effect on the resilient modulus. Also the effect of thixotropy can be seen only at high degree of saturation.

Seed et al. recognized that the resilient modulus depended on a number of factors which could not be always controlled. One such factor is the effect of time. The laboratory results are based on accelerated test procedures. However, the authors felt that this would give conservative values for the design. Another factor is that the induced stresses in the field would vary both in the vertical and horizontal directions i.e. the effects of non-linearity and non-homogeneity could not be considered in the tests. Further the validity of the laboratory-determined modulus was accepted based on the good agreement between these results and the plate load tests. However, the plate load tests could yield only one deflection. Matching the maximum deflection does not necessarily mean that the behaviour of the pavement has been properly characterized by the measured modulus. Further, Seed et al. (1967) report that the laboratory specimens were recovered at the end of plate load tests in test pits. In view of their findings that the resilient modulus is significantly influenced by the stress history, it should be questioned whether the sample after a repeated plate load test would be the same as before that test. Thus the significance of their result that the laboratory results agree

closely with the prototype plate load tests is not clear. It is suggested that they are not comparing the same two specimens of the soil. Similar objections can be found in Argue (1970). Based on the series of tests Seed et al. recommended using an equivalent modulus which would give the same deformation as the actual layered structure (cf. Section 2.1.2.1). They justify their recommendation based on tests on prototype pavements by McMohan and Yoder (1960), Sowers and Vesic (1961) who concluded that the halfspace model represents the pavements quite adequately. The objection to such prototype pavement tests (e.g. Turnbull et al., 1961) has been already mentioned (see Section 2.1.2.1).

Marcuson and Townsend (1976) and Townsend (1977) report on the effect of reconstituting samples for cyclic triaxial testing. Their report was specifically directed to the shell and foundation materials for the Fort Peck Dam in Montana. In the 1977 report Townsend quotes a number of other workers from different parts of the world who had obtained similiar results. From these works it would appear that reconstituted materials show 15% to 100% lower strength and modulus than in-situ materials. Further, it was suggested in their report that most natural soils are anisotropic and that reconstitution would destroy the fabric and the anisotropic character. Thus it is suggested that neither cyclic tests on remolded samples nor small-scale tests in the laboartory are likely to be representative of the actual conditions in the field. The question of anisotropy will be discussed in a subsequent section.

At the time of the Berkeley tests in the sixties and seventies (e.g. Seed and Chan 1958; Dehlen, 1969; Hicks and Monismith, 1971; Deacon, 1970;) techniques determining anisotropic parameters had not been developed. The Berkeley tests have shown that the resilient modulus of fine-grained subgrade materials is influenced by the stress history of the

soils. Due to the manner of their deposition, subsequent consolidation and probable load-relief these soils do possess inherent anisotropy (e.g. Graham et al., 1989). Very often the construction techniques such as compaction in thin lifts induce anisotropy (e.g. Ingold, 1980; Harris, 1984b). The implication of considering anisotropy in the analysis of pavements is discussed in a subsequent section. In the remainder of this section a few other models for fine-grained soils are reviewed.

Kondner (1963) suggested a hyperbolic model for the stress strain relationship for clays.

$$(\sigma / \epsilon) = E = 1 / (a + b\epsilon) \qquad (20)$$

One can rewrite this to yield the modulus:

$$(\frac{1}{E}) = a + b \cdot \epsilon \qquad (21)$$

Therefore, a plot of 1/E and ϵ will be a straight line the slope of which will give inverse of the secant modulus at any strain level and the intercept of the line will be the inverse of the initial tangent modulus. This model has been accepted by many (Duncan and Chang, 1970; Briaud et al., 1983, 1986). However, there are a few objections to this model when applied to pavement engineering. Kondner's paper aimed primarily at the prediction of the ultimate strength of the clay. He recognized that except for small strains (less than 4%) the model predicted the triaxial test results from many other investigators fairly well. However, in all cases the experimental data differed significantly from the prediction of the model in the range of small strains. Pavement engineers are mainly concerned with strains in this small range. For example Dorman and Metcalf (1964) suggest tolerable subgrade strains between 600 and

1500 microinches per inch (or between 0.006 and 0.015 percent) depending on the number of repetitions. Thus it is clear that the model is a poor one for small strains that are of concern to the pavement engineer. In discussing Kondner's paper, Brinch Hansen (1963) suggested a modified parabolic relationship as given below:

$$\sigma = \sqrt{\frac{\epsilon}{(a - b\epsilon)}} \tag{22}$$

This, however does not lend itself to calculation of the moduli as easily as does the hyperbolic model. Furthermore, Kondner's work does not deal with repetitive loading or resilient modulus. Thus it is suggested that the model is not suitable for pavement analysis.

Brown et al. (1975), and Brown (1982) suggested a relationship as below:

$$M_R = \frac{K}{(q_r / \sigma_3')^n} \tag{23}$$

where,

M_R = resilient modulus

q_r = cyclic deviator stress

σ_3' = confining pressure

and K and n are constants.

This model will be referred to as the Nottingham model in this thesis. This relationship was shown to fit data on laboratory samples of Keuper marl prepared from slurry and consolidated to varying degrees of consolidation. The over-consolidation ratio (OCR) ranged between 1 and 20. The results are shown in Fig. 2.9.

It would be interesting to compare the Berkeley and the Nottingham models. The Berkeley model does not recognize the effect of the confining pressures explicitly. Thus, for a given pavement structure as the load increases the modulus will decrease and the deflections will increase. However, if the subgrade would be restrained against deformation the apparent or the effective modulus will increase with a consequent reduction in the deflection. Such restraints can be due to inherent anisotropy, reinforcement by a geogrid, by stabilization or in partially saturated soils due to soil suction. Richards (1966), Dehlen (1969), and Monismith (1992) showed that soil suction had significant effect on the resilient modulus (Figs. 2.10 and 2.11). Fredlund (1989) presented similar results. Brown et al. call this the effect of the initial confining pressure and consider this in their model by a power of (σ_3'). Fig. 2.12 shows the relationship between the resilient modulus and the ratio of deviatoric stress to this effective confining pressure as suggested by Brown et al.

Both the Nottingham and Berkeley models require extensive and elaborate laboratory setup to arrive at the suitable material constants in Eqns. (17) to (19) (e.g. Boyce and Brown, (1976); Finn and Monismith, (1984)). Therefore attempts have been made to relate the resilient modulus to simple soil index properties. Thus Kirwan and Snaith (1976) and Jones and Witczak (1977) have tried to relate water content, plasticity index, degree of compaction etc. While these are useful, there is an amount of empiricism involved which make these unsuitable as predictive models. These relationships have to be established for local conditions with a large data base. Therefore these are not further discussed here.

Moosazadeh and Witczak (1985) suggest a model as shown below:

$$M_r = K_1 (\sigma_d)^{K_2} \quad (24)$$

where,

M_r = resilient modulus

σ_d = deviator stress

K_1 and K_2 are material constants.

By analyzing nearly 3,900 pavement test data from different parts of U.S.A. and using regression techniques, they could suggest range of values for the constants K_1 and K_2. K_1 varies between 1 and 200 while K_2 varies between 0 and 1. They also attempted to correlate the values K_1 and K_2 to other physical parameters such as dry density, moisture content, liquid limit, PI etc.

K_1 increases as dry density increases, is directly proportional to liquid limit and PI but is inversely proportional to plastic limit. K_2 decreases as the dry density increases and is insensitive to the limits. K_1 and K_2 are relatively independent of each other. This model is similar to the Berkeley model. The resilient modulus is explicitly related to the deviatoric stress but only implicitly to the confining pressure, through the constants K_1 and K_2. As one can see, the factors which affect these constants are in turn affect the effective confining stress. However, it is suggested that a model, such as the Nottingham model, which would explicitly relate the modulus to both the deviatoric stress and the confining stress is preferable to others.

2.2.1.2 Resilient Modulus of Granular Materials

As in the case of fine-grained soils, the earliest investigations on granular materials were carried out by Seed and his associates at Berkeley (see previous section for the relevant references). Their primary conclusions based on those tests were:

1. The resilient modulus of granular materials depends on the confining pressure. The resilient modulus can be expressed as:

$$M_R = K_1 \cdot \sigma_3^{k_2} \tag{25}$$

Alternately it can be also expressed as:

$$M_R = K_1' \cdot \theta^{K_2'} \tag{26}$$

where,

M_R = resilient modulus

σ_3 = lateral confining stress

θ = first stress invariant

and K_1, K_2 ,K_1' and K_2' are material constants.

The constants can be determined easily by plotting the results of the repeated load triaxial tests on a log-log scale (Fig. 2.13). This model is generally referred to as the K-θ model in the literature.

2. The modulus increases as the density increases.

3. The modulus increases with increasing angularity of the aggregates.

4. The modulus decreases with increasing moisture content or degree of saturation.

5. The number of stress repetitions has no effect on the modulus.

6. The sequence of loading has no effect on the modulus.

7. Load duration and frequency have no effect on the modulus.

Following the pioneering work by Seed and his associates, there have been a number of investigations into the resilient modulus of granular materials. Some of these investigations continued the laboratory tests while others determined the modulus by back calculation from the measured deflection bowls. A review of the data shows that practically everybody, who determined the modulus in the laboratory, came to the conclusion that the K-θ model would be satisfactory. However, those investigators who attempted to evaluate the modulus from *in-situ* tests or by backcalculating from deflection tests found poor correlation with the K-θ model. At the present time there is an increasing consensus that laboratory measurements of the modulus of granular material is not satisfactory (eg. D'Amato and Witczack (1980); Brown and Pappin (1981, 1985); May (1981); Kehdr, (1985)).

D'Amato and Witczak (1980) conducted a series of deflection tests using the FHWA road rater equipment. Their conclusion was that the theoretically-predicted deflections based on laboratory-measured moduli are two to four times greater than the actual measured deflections. By inference, the laboratory-determined modulus values are one-half to one-quarter of the actual *in-situ* moduli. Thus the laboratory tests consistently underestimated the moduli. The authors suggested an "adjustment factor" to the K-θ model as follows:

$$M_R = K_1 \cdot k_1 \cdot \theta^{k_2} \qquad (27)$$

Here the symbols have the same significance as before except k_1 which is the "adjustment factor". Before defining the adjustment factor, one other concept has to be explained. This is the factor called "deflection ratio", R_d. R_d is the ratio of predicted to measured deflections.

For any given pavement section a unique k_1 can be determined in such a way that the predicted and measured deflections are equal (i.e. $R_d = 1.0$). This value of k_1 is called k_1 ($R_d = 1.0$). By repeating the theoretical iterative layer-elastic program D'Amato and Witczak arrived at unique k_1 values for different pavement sections but only for the centre deflections. Their attempt to find such unique k_1 values for deflections at other points measured by the road rater was unsuccessful. They justified this approach because they were essentially extending a previous study by Jones and Witczak (1977) who used the Benkelman Beam to measure the actual deflection. The Benkelman Beam as well as the plate load test measure only the maximum centreline deflections. Hence the "adjustment factor" suggested by D'Amato and Witczak is valid for only one point under the load. Thus one may conclude that the K-θ model is a poor one to represent the true response of the pavement. A valid model should be able to match not only the maximum deflections but also the deflection basin as suggested by Hoffman and Thompson (1982).

The value of the adjustment factor k_1 ($R_d = 1.0$) decreases with weaker pavements, higher loads, and increasing deflections. That indicates the stress dependency of the modulus. D'Amato and Witczak explained this as being due to increasing shear strains in thinner pavements, higher loads or increasing deflections. Thus they suggest that these bases show a strain-softening effect. These conclusions were later supported by May (1981) and May and Witczak (1981) who continued the studies by D'Amato and Witczak.

Pappin and Brown (1980), Brown and Pappin (1981, 1985) also noted that the K-θ model was inadequate for granular materials and have proposed what is known as the Contour Model. They note that when using the K-θ model in a finite-element back-calculation program the peak stresses calculated in each step of the iteration might exceed the shear

strength of the material; or the material might experience tension. In either case the computer algorithm would arbitrarily reduce the stresses and recalculate the modulus. Brown and Pappin argue that such manipulations do not consider the yield criteria for soils nor do they recognize that the soil might arrive at a stress state by any number of stress paths. For example, the stress path in the conventional repeated load tests would be as shown in Fig. 2.14. Here the soil is stressed from point A to point B. Because of the constant confining pressure the slope of this path would be 3 to 1. However, in a pavement the stress path can have any slope as shown in Fig. 2.15 depending on the loading sequence, the mean normal stresses and the initial stress condition. The figure shows the initial stress condition, the path taken as well as the mean normal stress and the resilient deviatoric stress. In an actual pavement, where a large number of repetitions of loading can occur, there could be any number of stress paths likely as shown in Fig. 2.16. If any of these stress paths crosses the yield line then local yielding would occur. If a number of neighbouring points experience such stress state then that area of the pavement can show excessive deformation. Now, the strains in the soil are complex and can be resolved into two components, the volumetric and the shear strains. Pappin and Brown (1981) demonstrate that the volumetric strain is essentially path independent while the shear strain is path dependent. Thus the path along which the material is stressed becomes important.

By conducting a large number of triaxial tests one can develop a set of strain contours for both volumetric and shear strains for different materials (hence the name contour method) in the p'-q space (Fig. 2.17). Thus for any given stress path the shear and volumetric strains can be determined. It should be noted that the two elastic parameters used by these authors are the bulk modulus and the shear modulus (see Section 1.1.2.1). Since the resilient

volumetric and shear strains are computed as outlined above and the bulk stress and the deviatoric stress are known these two parameters can be computed and set in the elastic layer model. They come to the conclusion that the elastic layer model is a reasonable approximation to the pavement system.

The contour model was originally developed for dry materials so that the effective stresses can be measured directly. Subsequent work in Nottingham showed that the model can be applied to partially saturated soils if effective stresses are used (Brown and Pappin, 1985).

Finally, they stipulate the Mohr-Coulomb yield criterion for the material to ensure that failure does not take place. In their model and the finite-element program, called SENOL, they try to incorporate these fundamental geotechnical concepts. It might be recalled that for fine-grained soils similar model was suggested by Gomez-Achecar and Thompson (1986).

The contour model is probably the first attempt to consider fundamental geotechnical aspect of materials. However, it relies heavily on laboratory testing of prepared samples. It would be recalled that the strain contours for each type of material should be established first. This requires a large number of tests on each type of material to be performed in the laboratory. The equipment needed for these tests are much more sophisticated than the conventional triaxial equipment (Brown and Snaith, 1974; Boyce and Brown, 1976). The inability to reproduce field conditions in the laboratory, particularly with respect to stress history and lateral stresses has been already discussed. Yet, the concept behind the contour model is probably the most promising to date in assessing the modulus on a sound physical basis. It would be more advantageous to determine these quantities *in-situ*. Uzan (1985)

reviewed the existing hypotheses to characterize the granular layers in the pavement structure. The models examined were:

1. the K-θ model → $M_R = K_1 . \theta^{K2}$

2. the hyperbolic model → $1/E = (a + b\epsilon)$

3. the contour model due to Brown and Pappin.

Uzan produces the results of tests conducted on a dense graded aggregate and shows that the K-θ model fits the test results quite well if the first stress invariant is plotted against the resilient modulus (Fig. 2.17(a)). However, if the same results are plotted as resilient modulus vs. resilient vertical strains the theoretical predictions and actual test results differ markedly (Fig. 2.17(b)), showing that the K-θ model is a poor representation of the material response, particularly in the lower strain ranges. Fig. 2.18(a) shows the comparison between the K-θ model and the model suggested by Brown and Pappin. These results were for crushed limestone, different from those represented in Fig. 2.17(a) and Fig. 2.17(b). However, the trends of the K-θ model and the contour model are still valid. Fig. 2.18(b) shows that the contour model appears to predict the test behaviour better than the theoretical predictions by the K-θ model (Fig. 2.18(a)). The decrease in the resilient modulus for lower strains may be explained by the tendency of dense packed granular materials to dilate at low shear strains. Therefore it would appear that the K-θ model fails to recognize the effect of shear strain on the modulus. Uzan suggests a modification to the K-θmodel to include the strain effect on the modulus. His equations are as below:

$$M_r = K_1 \cdot \theta^{k_2} \cdot \epsilon_a^{k_3} \qquad (28)$$

or

$$M_R = K_1 \cdot \theta^{k_2} \cdot \sigma_d^{k_4} \qquad (29)$$

where, ϵ_a and σ_d are the resilient axial strain and the deviatoric stress respectively, and K_1, K_2, K_3 and K_4 are material constants. These constants are to be evaluated by regression analyses of a large number of test results. Uzan compared these equations with the contour model as well as some other test results (Fig. 2.18a and Fig. 2.18b). From these evaluations it would appear that the equations agree well with the contour model but the agreement is not satisfactory with the test results except in a very small range and relatively low confining pressures. At high confining pressures the model is entirely unsatisfactory. Uzan suggests that the discrepancies arise because of the residual stresses in the compacted granular base which would imply that the response of the granular base depends on the initial effective stresses or the stress history just as in the case of fine-grained soils.

The existence of locked-in stresses (or residual stresses) in both compacted fine-grained and granular fills has been documented (Sowers et al., 1957; Broms, 1971, Carder et al., 1977, 1980; Ingold, 1979, 1980; Stock and Brown, 1980; Ofer, 1982; Harris, 1984b). These investigations are concerned primarily with stresses in backfill behind retaining walls. They included field measurements, experimental retaining walls, as well as laboratory experiments with small scale cylindrical containers. They all refer to a much earlier work by Whiffin, in 1954, who measured the stresses under actual rollers, both static and vibratory.

The mechanism of residual stresses in compacted fills has been explained as follows. Consider a point in a loosely placed fill. This point will be subjected to an effective vertical

stress σ_v' and an effective horizontal stress σ_h' (Fig. 2.19). The ratio of the effective vertical and horizontal stresses is the coefficient of earth pressure at rest K_o.

$$K_o = \sigma_h' / \sigma_v' \qquad (30)$$

Now, due to the operation of the roller the fill is subjected to an additional vertical and a corresponding horizontal load. The initial and the final state of stress due to the operation of the roller are represented by points a and b on the stress path shown in Fig. 2.19. It has been assumed that the increase in stress will follow the K_a line. This could be true for most of the roller operation when the soil would yield a little laterally under the roller. Once the roller leaves the effective vertical stress will revert back close to the level at A (note that compaction would increase the effective unit weight). However, the unloading path will be b-c-d. The point C will lie on the K_p line (the passive pressure line). Since the lateral pressure cannot exceed the passive pressure this will be the upper limit. When the unloading curve reaches the K_p line the soil yields and there is a reduction in the lateral stresses. The depth at which this yielding occurs is called the critical depth. Below the critical depth there is no reduction in the horizontal stresses. Therefore, from Fig. 2.19 it is clear that after the compaction is completed the horizontal stresses in the fill are higher than in the original condition giving rise to residual stresses or higher initial effective stresses. Since the resilient modulus depends on the initial effective stresses these have to be considered in analysing pavements. From the above discussions it is clear that the magnitude of the residual lateral stresses will depend on the location of the point b (Fig. 2.19) on the stress path, which is dictated by the compactive effort and the thickness of the layer. If the fill is placed in one thick lift then the pressure is likely to be as shown in Fig. 2.20(a). However, fills are

compacted in thin lifts of 150 to 200 mm so that the pressure distribution is more likely to be as in Fig. 2.20(b).

The tests and results reported by these authors can be summarized as below:

1. Compaction of fills produces lateral stresses that are considerably in excess of what would be predicted by classical theories.
2. Compaction, essentially, produces overconsolidation in the fill. Overconsolidation, in turn gives rise to high K_o value increasing the value of lateral stresses Fig. 2.21 (Brooker and Ireland, 1965; Mayne and Kulhaway, 1982).
3. In a deep fill the maximum lateral stress occurs at some depth Z_c below the top surface (Fig. 2.20). This depth is called the critical depth by these investigators. In a pavement because of the compaction of the hot asphalt on top of the granular layers one can expect that the critical depth would move close to the interface between the asphalt and granular layers. Thus one can expect high lateral stresses in the granular layer of the pavement.
4. The magnitude of the lateral stresses depended on the type of compacting equipment. From Whiffin's study quoted by the other authors it would appear that vibratory rollers produced more than twice the stresses measured under static loads. It depended upon the intensity of stresses under the roller and the amplitude of vibrations. Since modern rollers are much heavier than those in Whiffin's days and can exert much higher vibratory loads it could be assumed that high locked-in stresses would be measured in the granular base layers of today's pavements. This writer is not aware of any recent work similar to Whiffin's.

5. The lateral stresses in clays increase with increasing compactive effort and decrease with increasing moisture content. While no such definitive relationships were reported for granular soils, high lateral stresses were measured in these. K_o values much greater than 1.0 have been reported (Ingold, 1979, 1980; Brown and Pappin, 1985).
6. The lateral stresses tend to drop slightly with time in the case of clays while no such reduction was observed with sands (Broms, 1971; Carder et al., 1977).

Residual transverse stresses have been measured even in such coarse material as railway ballast by Stewart et al., (1985). In their view the current procedures of computing resilient modulus of granular materials fall into two categories:

1. Ones that do not recognize the development of tensile stresses at the bottom of the granular layers.
2. Ones that do but artificially assign low M_R values near failure stresses and eliminate the tensile stresses, (compare with the discussions on the contour model).

Stewart et al. argue that both these approaches cannot be accepted because, in case of (1) the Mohr-Coulomb failure criterion will be violated and in case of (2) large permanent deformations would develop. These are in contradiction to observed performance both in field and in the laboratory. They describe laboratory tests in a large box where railway ballast was subjected repeated loads. Large horizontal stresses on the sides of the box are reported giving rise to K_o values as high as 12 at about the mid point of the box. Considering that they were testing high quality, angular and free draining ballast, such K_o values are possible. The important point, though, is the existence of high residual lateral stresses. Stewart et al. conclude that the existence of such high residual stresses is responsible for eliminating tensile stresses or permanent deformations. Brown and Pappin (1985) demonstrate that even at

K_o = 1.0 the necessary horizontal compressive stresses would be developed to eliminate tensile stresses in a typical pavement structure.

Kehdr (1985) reviewed the permanent and resilient deformation behaviour for a range of crushed limestone generally used for road construction in Ohio state. While the principal objective of his study was to propose a predictive equation for permanent deformation of granular base course, he did review many of the previous research efforts in characterizing granular materials. He noted that most researchers used a static or constant confining pressure. He adopted a dynamic confining pressure approach whereby the axial and lateral stresses were varied simultaneously. A few other investigators have used this technique before (e.g. Allen, 1973; Pappin and Brown, 1980; Lam, 1982). Using this approach and a series of linear stepwise regression Khedr concluded that the K-θ model holds reasonably for bulk stress levels greater than 70 kPa. He noticed that below this stress level some of the samples showed a decrease in M_R with increasing θ. It is suggested that this might be the range where the stress path might cross the failure line. (Compare discussion of Uzan's paper above.) Unfortunately, unlike Uzan, Kehdr does not go into a discussion of the observed results.

The existence of high lateral stresses would suggest that granular pavement layers should, perhaps, be modelled as elastic cross-anisotropic layers. That the stress induced anisotropy can exist even in pluvially deposited granular materials has been suggested by Sada et al. (1976), Belloti et al. (1989). It will be recalled here that in reviewing the literature on the resilient modulus of fine-grained soils, in the previous section, it was noted that there was an increasing consensus that anisotropy should be considered in problems involving earth masses. Cross-anisotropy will be discussed in a subsequent section.

In using the hyperbolic model, it should be noted that the modulus decreases as the strain increases. While this could be true for small strains, both the K-θ model and the contour model suggest otherwise. Therefore, the hyperbolic model is even a less appropriate model for granular bases.

Boyce (1980) suggests a non-linear, elastic model characterized by the secant bulk modulus, K, and the secant shear modulus G. He calls this the G-K model. The basic assumptions behind this model are:

1. The material is elastic and isotropic.
2. The modulus is stress dependent and non-linear.
3. The moduli apply to any stress path; the state of stress is a unique function of the state of strain.
4. Though granular materials are particulate materials, and would be subjected to crushing and slippage at the contact points, hysteresis and plastic yielding do not play a role at the small strain levels being considered (cf., for example, Hardin and Banford, 1989).

Boyce starts from a constitutive relationship in terms of G and K as follows:

$$\epsilon_{ij} = \frac{1}{3K}\,\delta_{ij}\,p + \frac{1}{2G}\,S_{ij} \qquad (31)$$

where, ϵ_{ij} = a component of strain tensor

p = the mean normal stress

S_{ij} = component of the deviatoric stress tensor

and δ_{ij} = the Kroenecker delta

He then shows that the moduli are functions of the first and second stress invariants. Using these concepts, he derives expressions for the increments of volumetric and shear strains as below:[3]

$$\dot{\epsilon}_v = \left[\frac{1}{k} - \frac{p}{k^2}\frac{\partial k}{\partial p}\right]\dot{p} - \frac{p}{k^2}\cdot\frac{\partial k}{\partial q}\cdot\dot{q} \qquad (32)$$

$$\dot{\epsilon}_s = \left[\frac{1}{3G} - \frac{q}{3G^2}\cdot\frac{\partial G}{\partial q}\right]\dot{q} - \frac{q}{3G^2}\cdot\frac{\partial G}{\partial p}\cdot\dot{p} \qquad (33)$$

It will be noted that both the strains are functions of mean normal as well as deviatoric stresses in contrast to the K-θ model. Noticing that all the previous research (e.g. Hicks and Monismith, 1971; Allen and Thompson, 1974) indicated that the stiffness of the granular material is related to the mean normal stress by a power law Boyce proposes the following formulation for K and G:

$$K = K_1\, p^{(1-n)} \qquad (34)$$

$$G = G_1\, p^{(1-n)} \qquad (35)$$

In his paper he then demonstrates that the model explains the results of the previous workers, in particular the dilatancy that was noted by others as given by high values of resilient Poisson's ratio. However, he also states that the effect of cross-anisotropy cannot be ruled out as the cause for the high Poisson's ratio.

The G-K model is somewhat cumbersome to use in numerical technique. Yet, this forms the basis of the SENOL software program developed by the Nottingham University.

---

[3] Note that the dot notation here refers to the increment in the strain and not the strain rate as commonly understood.

To summarize the laboratory characterization of material properties one can state:

1. Most of the earlier work (till mid seventies) were done using repeated load triaxial tests where the confining pressure was kept constant and the deviator stress was pulsated to simulate traffic loads.
2. Such tests showed that the resilient modulus of fine-grained soils depended mainly on the deviatoric stress while that of the granular material was a function of the mean normal stress.
3. These models proved to be unsatisfactory because they could not predict the measured deformations of a pavement structure with acceptable accuracy. The discrepencies are particularly noticeable with dense dilatant granular materials.
4. Improved models considered the dependency of the modulus on the stress path. They also stipulated a failure criterion commonly acceptable in geotechnical engineering. Usually this is the Mohr-Coulomb criterion.
5. Of all the models proposed to-date the Nottingham model appears to be most promising.
6. It has been suggested that a model based on bulk and shear moduli would better represent granular layer response than a resilient modulus based on resilient axial strain and Poisson's ratio.
7. Many researchers presented results that could not be explained by linear elastic and isotropic materials. It would appear that cross-anisotropy could explain some of these results.
8. There is evidence in the literature that the construction activities, such as compaction, can introduce significant anisotropy both in granular and in the subgrade layers.

9. There is also evidence in the literature that reconstituted laboratory samples underestimate the moduli, because they destroy the fabric and with it the cross-anisotropic characteristics of the *in-situ* materials. Similar objections have been levelled against small scale sand box tests.

10. In view of these uncertainties with laboratory results and because laboratory testing cannot adequately represent the materials under a long stretch of road or runway, it is suggested that *in-situ* charaterization of the graunular and subgrade materials is a viable alternative to characterize pavement materials.

11. Finite-element techniques are best suited to model the pavement structure given the complex nature of the materials making up the structure.

2.2.2 Field Measurements of Resilient Moduli

In the previous section it was noted that material parameters have been, traditionally, determined using the repeated load triaxial tests. Such tests have given much insight to the fundamental nature of the material response to repeated or transient loading; however, on a quantitative basis the parameters determined from these tests could not predict the response of actual pavements in a satisfactory manner. This is primarily due to the fact that the laboratory test results cannot represent the materials in the pavement structure at each test point at the time of testing. Hence much attention has been devoted to determine these material parameters by *in-situ* tests. The *in-situ* tests fall into three categories:

1. Deflection Testing.
2. Geophysical methods.
3. *In-situ* geotechnical methods.

This section reviews and discusses the literature on these three methods of investigations.

2.2.2.1 Deflection Testing

Deflection of the pavement under an applied load is the best indicator of the stiffness and load carrying ability of the structure. This was recognized by pavement engineers as early as the 1940's when Terzaghi proposed a method to conduct plate load tests. At the present time deflection testing for pavement evaluation is done by one of three means listed below:

1. The plate load test.
2. The Benkelman Beam test.
3. Modern deflection testing machines.

In what follows these methods will be reviewed and discussed briefly. These discussions are done from the perspective of test methods, interpretation of the results and from the operational point of view. The last mentioned aspect is important because, it provided the strongest motivation in the development of the modern deflection testing machines.

1. Plate Load Test

Fig. 2.22(a) shows the schematic of the test. Fig. 2.22(b) shows the setup of the test. The test consists of loading a rigid steel plate either 300 mm or 760 mm in diameter and loaded vertically against a heavy enough reaction. The settlement of the plate under a given load is observed by a set of dial gages or transducers mounted on the ends of a diameter of the plate. The deflection at the centre of the plate is taken to be the average of the dial gage or the transducer readings. The test is usually performed as a cyclic test i.e. at each load level the pavement will be loaded and reloaded a few times and the settlements noted. After these

cycles the load will be increased to the next higher level and the process repeated. Generally, the load levels would cover a range of loading from below the design wheel load to one and one half to twice the design load. Fig. 2.23 shows the typical results that would be obtained from the plate load tests.

The evaluation of the results of a plate load test varies from agency to agency. Thus in the ASTM symposium (1949) Palmer (U.S. Navy) suggested a deflection of 0.2 inch (5 mm) as a limit to determine the carrying capacity. On the other hand many authors at the ASTM symposium have suggested anything between 0.1 and 0.5 inch (2.5 to 12.5 mm) as the limiting deflection. McLeod suggested that the limiting criterion for the deflection should be 12.5 mm after 10 load repetitions on a 760 mm diameter plate.

Generally, all agencies conducted plate load tests at different levels of the pavement structure, i.e. subgrade, base and on the surface. However, the limiting deflection criterion was always the same, at a specified value. As has been pointed out by Nevitt, in discussing Palmer's paper the strains in the subgrade would be totally different in both the cases. Thus any attempt to correlate the bearing capacity of the entire pavement structure to the subgrade support value would lead to unsatisfactory results as seen from the results presented by Palmer (Fig. 2.24). McLeod attempted to circumvent this problem by deriving a series of conversion factors (Table 2.3) which would convert the surface load to load at any level of the pavement. This was based on extensive tests at Canadian airports. However, it should be recognized that these are essentially empirical factors applicable only to circumstances at which these tests were conducted. Looking at Table 2.3 one recognizes that a unique conversion factor as suggested by Mcleod would be an oversimplification of the problem when so many variables were involved. What the does not show are the many other factors,

such as the perimeter to area ratio of the plate, the type of base and subgrade, the influence of plate size on the deflection etc. on these factors. McLeod, of course, considered these in arriving at the factors shown in Table 2.3. McLeod's recommendation still forms the basis of design for the Canadian Ministry of Transport. Similarly, Palmer's criteria were the basis of design till recently for the US Navy and the US Air Force.

Apart from the difficulty of setting a reliable criterion for the limiting deflection, there are other problems with the plate load tests. The capacity of the lower layers is generally determined in test pits after removing the upper layers. The size of these pits in relation to the size of the plate is significant because of the influence of the surcharge provided by the pavement structure above the level of testing. In addition, if the tests are done in the same test pit for all the layers, the loading on the upper layers would have pre-loaded the lower layers. Thus the base and subgrade are subjected to a different load history in the test pit from that at any other typical location in the pavement. As was mentioned in the previous section, many investigators have shown that the stress history has a significant influence on the resilient modulus of the material, at least for the fine-grained materials. If one carries out these tests in different pits for different layers then one is actually testing different spots on the pavement. Thus the properties determined for any one layer need not necessarily be consistent with the others. Moreover such a test setup would require a number of test pits which should be spaced sufficiently far apart to avoid mutual influence. This is operationally a nuisance as well as excessively destructive to the pavement. These and other difficulties have been more fully discussed by Argue (1970).

The plate load test is a static test whereas the loading on a pavement is dynamic. Thus the plate load deflection has a larger irrecoverable creep component than would be observed

under the wheel load. Thus except for facilities such as loading docks, aircraft parking aprons etc., the plate load test is not a representative test. Though many agencies adopt the repetitive plate load tests the test is essentially, a static test.

The plate load test yields only limited information if only the maximum deflection is measured, as is usually the case. Two pavements can yield the same centreline deflection and still have very different load spreading capabilities. Thus the shape of the deflection bowl is a significant factor in judging the stiffness of the pavement. With one deflection value the layer moduli of a multi-layer system cannot be evaluated. In order to define the deflection and the curvature of the deflected shape one has to measure multiple deflection values under a given load.

The theory of elasticity can be applied to the results of plate load tests to obtain the modulus of the materials. Since there is only one measured result (the maximum deflection under the load) the analysis can be done strictly for the Boussinesq model only. The Boussinesq solution for the maximum deflection under a uniformly loaded rigid circular plate is:

$$\Delta = \frac{\pi}{2} \frac{(1 - \mu^2)}{E} \cdot p \cdot h \qquad (36)$$

where,

Δ = the measured deflection

p = the contact pressure

r = the radius of the plate

and μ = Poisson's ratio

For a flexible plate (simulating a tire load) this expression is modified as below (Burmister, 1949; Osterberg, 1949):

Burmister:

$$\Delta = \frac{2(1 - \mu^2)}{E} p \cdot r \qquad (37)$$

Osterberg:

$$\Delta = C_s \cdot \frac{p \cdot b}{AE} (1 - \mu^2) \qquad (38)$$

In these expressions:

p	=	the contact pressure
r	=	radius of the plate
s	=	settlement under the plate
b	=	width of footing
μ	=	Poisson's ratio
C_s	=	a constant to account for the size, shape and rigidity of the plate.

For a two-layer system Burmister modified this expression as below:

$$\Delta = \frac{2(1 - \mu^2)}{E} \cdot p \cdot r \cdot F \qquad (39)$$

Here the symbols have the same significance as before and F is an influence factor that is a function of the ratio of the moduli of the two layers. As discussed in Section 2.1.2.3, Jones (1962) and Peattie (1962) extended these solutions for a three-layer system. The solutions for more than three layers become very complex and are not possible without computer

modelling. Burmister (1949) also gives the following expression for an elastic halfspace where the modulus varies linearly with the depth.

$$\Delta = \frac{\pi}{2} \frac{(1 - \mu^2)}{(E_0 + C_r)} \cdot p \cdot r \qquad (40)$$

where, E_0 is the modulus at the surface and C_r is the increment in the modulus for unit depth. Finally, Skempton (1952) and Burmister (1949) suggest a method to determine the stresses and the modulus from laboratory compression tests using the expression below:

$$\epsilon_L = \frac{\Delta_L}{4r_L} \cdot \frac{\sigma_L}{E} \qquad (41)$$

where,

ϵ_L = strain in the laboratory sample

σ_L = stress in the laboratory sample

r = radius of the laboratory specimen

E = modulus of elasticity

This is based on the premise that most of the observed settlement in field is caused by the soil contained within the ($0.1\ \sigma_L$) isobar (Fig. 2.25). Burmister postulated that the field test can be approximated as a cylindrical compression test of a cylinder of diameter 2R and height 4R. In the laboratory the dimensions will be 2r and 4r (Fig. 2.25). For any deflection in the field the strain can be calculated. For an equal strain in the laboratory sample the axial compression can be determined, and using the expression above the modulus can be calculated. Both Burmister and Skempton used this approach more to compute the stresses in the soil under the plate load than to arrive at the modulus value. Equating the expression for axial strain in

the field and laboratory cylindrical specimens (see Fig. 2.25) and assuming $\mu = 0.5$, σ which is the stress in the soil under the plate can be seen to be:

$$\sigma_F = 3.4\ \sigma_L \tag{42}$$

or

$$\sigma_L = 0.29\ \sigma_F \tag{43}$$

Here the subscripts F and L refer to field and laboratory samples respectively. No such simple expressions are possible for multi-layered systems.

In summary:

1. Plate load tests do not represent the conditions imposed by the traffic except for stationary loads.
2. The bearing capacity or the support value obtained from the plate load tests is not an inherent material property but represents a stiffness of a particular structure for the specified deflection.
3. Application of the elastic theory to the test can be valid only for the Boussinesq medium. For the multi-layer system no unique solution is possible because, only one value of deflection is measured.
4. Layer moduli cannot be obtained from the plate load tests. Pavements showing similar deflections under similar loads are not necessarily equivalent because, their load spreadability can be quite different from one another.
5. Operationally the test is disruptive and if done at different layers it is also destructive.

6. The test is too time-consuming and expensive so that not enough locations can be tested to be representative of a stretch of highway or runway.

2. Benkelman Beam Test

The Benkelman Beam test is another deflection test conducted at creep speeds of an actual vehicle. The test is shown schematically in Fig. 2.26a. Fig. 2.26b shows the actual set-up of the test. The test equipment consists of two arms pivoted at a point such that the ratio of the lengths of the two arms is 2:1. The probe is at the end of the longer arm while a deflection gage is attached at the end of the shorter arm. The probe is first positioned between the duals of a standard truck axle which carries precisely 80 kN (18 kips) (Fig. 2.26a). The tires are standard ply and are inflated to 600 kPa (80 psi). This was, generally, the legally permitted tire pressure and axle load in most jurisdictions when the test was originally developed. The truck is driven away at creep speed and the rebound of the pavement is measured. Further details of the test and some theoretical background can be found in the CGRA Manual 11 (1959) and in a paper by CGRA in the 1962 Ann Arbor conference. If the tire pressure and the resilient deflection are known, a resilient stiffness can be computed. However, the Benkelman Beam test results have not been used in this way. Many agencies have correlated the Benkelman Beam deflection to the bearing capacity obtained from the plate load test (e.g. see Sebastyan, 1962; Fig. 2.27). By comparing the deflections on the pavements that are performing satisfactorily, a measure of allowable Benkelman Beam deflection has been established. Thus when the rebound values from the Benkelman Beam tests exceed the allowable limits the pavement would need rehabilitation.

Performing Benkelman Beam tests is more economical and much faster than doing plate load tests.

The Benkelman Beam test suffers from many of the same criticisms levelled at the plate load tests. The test is not representative of the actual traffic but measures only the response under creep load. The deflections are measured at only one location so that the test gives no indication of the load spreadability of the structure. Layer moduli cannot be calculated using the Benkelman beam results. The test vehicle is a normal highway truck so that the heavier pavement structures or pavements on strong subgrades are insensitive to the test procedures. Also, if Bousinesq's theory or the elastic layer theory is to be applied to the Benkelman Beam tests, one has to find an equivalent load for the test load. The movement of the probe is sensitive to exposure to direct sunlight, asphalt temperature and moderate winds. In fact, the effects of temperature of such pavements will be more critical than the loads themselves. In the original WASHO procedure where the deflections rather than the rebound values were observed, there could be negative residuals (i.e. an apparent heave after removal of the load) depending on the structure and the geometry of the apparatus. In such cases the pivot as well as the probe would find themselves within the deflection bowl so that on rebound the probe may end up higher than the reference level giving an apparent heave or negative residuals. This was the reason for the revision by the CGRA of the Beam design. Further details of these and other problems are discussed in the 1962 CGRA paper. While the tests are much faster than the plate load tests they are still operationally disruptive.

3. Deflection Testing Machines

Under this category are included the modern machines which apply a pulsating or impulse load, can collect deflection data at many points outside the loaded area and are fully automated. These machines are very sophisticated, and can measure the applied load and the resulting deflections with a high degree of accuracy, precision and reproducibility. Since these are almost completely computer-driven it is possible to feed into the machine further information regarding the condition of the structure which can then be considered in some fashion during the analysis of the data. The data collected are invariably analysed by layered elastic theory. Some recent reviews of these machines can be found in papers by Kennedy (1982), Hoffman and Thompson (1982), and Elkins et al. (1988).

Basically there are two types of deflection measuring devices: (1) the moving type and (2) the stationary type. The LaCroix Deflectometer and the Califorina profilometer are examples of the moving type. They actually travel with the traffic stream and collect data. They are relatively simple to operate and are fast. However, it is difficult to establish an unmovable reference point during a measuring cycle. By far the most common type of machines are the stationary type. Examples of this type are the FHWA Thumper, the Road Rater, the Dynaflect and the Falling Weight Deflectometer (FWD). These machines are positioned over the test point and either a steady state sinusoidal vibration or an impulse force is applied to the pavement through a rigid steel plate. The resulting vibrations are sensed by a set of sensitive accelerometers positioned at different distances from the load point. The accelerations are integrated by the computer and stored as deflections for later analysis. The stationary type of machines can, in themselves, be classified in three different categories as shown below:

	Type	Commercial Version
a)	Stationary, Dynamic, sinusoidal loading at a fixed frequency of 8 Hz. peak-to- peak	Dynaflect
b)	Stationary, dynamic impact type of loading at fixed frequency of 35 Hz. Impact load variable.	Falling Weight Deflectometer of different designs (e.g. Dynatest, Kuab and Phoenix)
c)	Stationary, dynamic impact type of load with variable frequency and loads.	Road Rater, The Thumper and the Heavy Vehicle Simulator (South Africa, Australia and FHWA)

The Dynaflect Fig. 2.28a and 2.28b is one of the earliest commercially available and automated deflection measuring equipment. A static weight of approximately 9.5 kN is applied through a pair of two rigid steel wheels. The dynamic load is generated by a set of eccentrically loaded flywheels operating at 8 Hz. This applies a sinusoidal force of 4.5 kN peak-to-peak which superimpose on the static load. The resulting deflections are sensed by a set of five accelerometers and recorded by an on-board computer. When the deflections are recorded the equipment is moved to the next test location.

The Road Rater (Fig. 2.29) carries a vibrator which applies a vibration to a steel mass which is the source for its dynamic loading. Loads can be varied between 2.0 and 42 kN at variable frequencies between 5 and 70 Hz., depending on the model used. The load, frequencies, and the deflections are measured by transducers and recorded automatically. The deflections are measured at four locations, including under the load. Like the Dynaflect the Road Rater applies a static load, due to the weight of the equipment, through two square steel pads. In the analysis these are replaced by equivalent circular loads (Fig. 2.29). The dynamic load is superposed on the static loads.

The Thumper and the Heavy Vehicle Simulators are essentially research-type equipment used by the agencies which developed them.

The Falling Weight Deflectometer (FWD) (Fig. 2.30) is of the impact type which drops a weight on to a rigid steel plate dampened by rubber buffers (Fig. 2.31). The lighter version of the model Dynatest 8000 (Fig. 2.32a) can apply loads up to 107 kN while the heavier version the Heavy Weight Deflectometer (Fig. 2.32b) can apply loads up to 240 kN. The frequency of the load is approximately 35 Hz. The deflections are measured directly under the load and at six other locations, thus defining a deflection basin.

It is not proposed here to give any comparative evaluation of specific equipment. The author does not have personal experience with all of them and hence is not competent to undertake such an evaluation. This has been done by others based on personal research and the reader is referred to these papers in the literature (Clayton Sparks and Associates, 1980; Bush, 1980; Hoffman and Thompson, 1982; Kennedy, 1982; Bush et al., 1985; Smith and Lytton, 1985; Tholen et al., 1985; Elkins et al., 1988). However, some general comments are in order here.

1. Moving vs. stationary test devices: The moving devices travel with the traffic and collect deflection data at very close spacing so that one obtains practically a continuous strength profile of the road. However, as mentioned earlier, it is difficult to have a fixed reference point with this type of testing. On the other hand, the stationary equipment cannot reproduce the actual stress-strain conditions generated by the moving vehicle. In the case of the moving vehicle the principal stresses rotate (see Fig. 2.33) as the vehicle approaches and passes over the point. Since the response of pavement materials are stress and frequency dependent the response

measured under a stationary loads may not be representative of a moving load. None of the loading modes of the stationary equipment, the sinusoidal loading of the Dynaflect, the vibratory loading of the Road Rater or the single impact load of the FWD, matches the actual loading by a moving vehicle, although there is general consensus that the FWD simulates the traffic load the closest (Hoffman and Thompson, 1982; Kennedy, 1982; Bush et al., 1985; Smith and Lytton, 1985; Elkins et al., 1988). The difficulty is attributed to the inertial effects attendant to the vibratory- or impact-type stationary loads. With moving vehicles the inertial effect is not present or at least not to the same extent as the stationary loads.

2. Sinusoidal, vibratory vs. impact loads: As mentioned above none of these modes really matches the actual frequency vs. time signals from a moving truck. However, the FWD signals are as close as one can get with current technology (Hoffman and Thompson, 1982).

3. Variable vs. fixed frequency: Pavement materials response depend on the load level as well as the frequency of loading. Since different wheel configurations or combinations will generate different load- and frequency-patterns, equipment with a single frequency (Dynaflect, FWD) cannot truly represent the traffic loading. Equipment capable of applying loads at variable frequencies is clearly preferable to that with fixed frequency.

4. Load levels: The significance of this is fairly obvious. Except for the WES (Waterways Experiment Station) Thumper and the heavy-vehicle simulators, all of the equipment uses light loads. However, the heavier version of the FWD can impart energy at levels comparable to some of the modern heavier aircraft. In this respect

the Dynaflect and the Road Rater are said to have serious deficiencies. On the other hand carrying heavy loads will seriously hamper the portability of these equipment. It may be recalled that portability was the primary motivation in the design of these equipment.

5. Number of sensors and locations: Depending on the structure and the materials the shape and size of the deflection basins will be different. Hence the deflection measuring sensors should cover a wide enough area to define satisfactorily the deflection basin. In this respect the Dynatest FWD is better than the other machines including the KUAB or the Phoenix FWD's because the Dynatest machines have seven sensors and can be positioned at variable distances. It is the author's understanding that the equipment used for research by the USAF has eleven sensors instead of the usual seven. It might be added that the boundary of the loaded area is a special point of load discontinuity in the analysis. Hence one sensor must be placed here to actually measure the deflection rather than interpolate between others.

6. Loaded area: All devices load the pavement with a circular rigid steel plate. The pressure distribution under a rigid plate is not uniform but has the shape of an inverse saddle (see for example Timoshenko and Goodier, 1949; Terzaghi, 1942). However, in all the analyses the pressure is taken to be uniform. Observations with instrumented pavements show that, depending on the ratio of the thickness of the surface layer to plate diameter the pavement response could be different from that theoretically predicted. Some equipment manufacturers have attempted to overcome this difficulty by an alternative design of the loading plate (Tholen et al., 1985). There is also evidence that a single plate does not correctly represent the loading imparted by

closely spaced tandem wheels, such as found under a Hercules C-130 aircraft. Recently Roque et al (1992) have published a theoretical evaluation of a dual plate loading system for the FWD.

7. Temperature effects: It is well known that the ambient and pavement temperatures affect the magnitude of the measured deflections. These are material characteristics and in analyzing deflection data one should correct these to a standard or design temperature (e.g. Lytton and Smith, 1985). There is also quite a different equipment-related temperature problem. Foxworthy and Darter (1986) observed that the deflections measured under the FWD could vary during different times of the day due to the effect of temperature on the rubber pad under the rigid steel plate of the FWD that is used to dampen and distribute the impact load. They also suggests some corrections for these albeit only for concrete pavements.

2.2.2.1 Analysis of the Deflection Data

Though the deflections are measured under vibratory or impulse loads, the analysis is generally carried out as if it were a static problem. The technique, which is known as a "back-calculation", is an iterative procedure. The pavement is modelled as a homogeneous, isotropic, linear and elastic layered system. To start the procedure most algorithms require the user to input a seed modulus value for each of the layers as well as the thickness of each layer except the subgrade layer, which is assumed to be infinitely thick. If there are reasons to believe that there would be a rigid bottom (e.g. bedrock) at shallow depths, then this information would be needed. From this point on, the computations are automatic whereby the computer software attempts to compute the stresses and strains at each point in the

pavement structure in accordance with the specified material model. The material model is, generally, one of the models discussed in the previous section. Finally, the surface displacements are calculated and compared with the measured deflections. The computations are terminated when the calculated deflections match the observed deflections within the specified tolerance limits which can be chosen by the user. In general a variation of five percent or less is deemed to be satisfactory. The final set of moduli, stresses and strains are then assumed to be the actual conditions in the pavement. From the design point of view, the calculated stresses and strains are compared with the allowable stresses and strains.

The back-calculation procedures that are available currently have been, at best, unsatisfactory. There are a few reasons for this:

1. The models or the constitutive equations used in most of the computer algorithms to describe the stress-strain behaviour are not realistic. Most of these relationships have been obtained from laboratory tests described in the previous section. The merits and drawbacks of this method were discussed at length in that section.
2. The multi-layer problem is essentially indeterminate. Thus a number of different combinations of the layer moduli can produce an acceptable match between observed and computed conditions. In other words, the uniqueness of the solution is not certain.
3. When a pavement is tested at any particular point in time its response has been modified by the stress history prior to the test. Many of the current algorithms do not, or cannot, consider this factor. As far as the author is aware of, ELMOD is the only program which allows for a consideration of stress history. On the other hand,

the equivalent-layer concept which is the basis of the ELMOD program has its drawbacks.

4. Linear elastic theory permits tension in the pavement layers. However, pavement materials, particularly the unbound layers, are incapable of sustaining any tension. Hence arbitrary adjustments are made to the stress and strain conditions to avoid these theoretical paradoxes. Therefore the derived moduli and, more importantly, the computed stresses and strains, need not necessarily be the true material values. In this respect the Nottingham model and ILLIPAVE are superior because of the incorporation of acceptable failure models based on geotechnical principles.

5. Residual stresses and cross-anisotropy cannot be considered by any of the current models. Since there is mounting evidence that these factors play an important role in the response of materials, the models should be capable of considering these.

6. While many algorithms have considered matching the maximum deflections and the deflection basin, their algorithms do not properly consider the contribution of the individual layers to the total deflection at each point during the iterative calculations. Instead arbitrary adjustments are made so that in each iterative cycle the match will be better than the previous trial. This sometimes leads to untenable layer moduli. This is explained in subsequent paragraphs in discussing the characteristics of the deflection basin.

Characterization of the Deflection Basin

It has been recognized for some time that it is not sufficient to match the maximum deflection alone, in arriving at the layer moduli (Vaswani, 1971; Majidzadeh, 1982; Hoffman

and Thompson, 1982). These authors have quantified the shape of the deflection basin with various parameters.

Vaswani introduced the concept of spreadability based on his work with the Dynaflect. The spreadability is defined as below:

$$S\% = \frac{D_0 + D_1 + D_2 + D_3 + D_4}{5D_0} \times 100 \qquad (44)$$

where D_0, D_1, D_2, D_3, D_4 are the deflections at the centre and at the four other sensors with the Dynaflect. He then developed an empirical method relating the spreadability and the maximum deflection for Virginia subgrades. This approach is somewhat limited for the following reasons:

1) The spreadability was based on the calculation of the area of the basin based on a Boussinesq medium. Thus he arrives at a unique value for the minimum spreadability. The rationale for this is not quite obvious. Instead it should be calculated as the area of the basin normalised to the maximum deflection (see for example Hoffman and Thompson, 1982).

2) In further developing his nomographic charts, he suggests an expression for the averege modulus for the pavement structure as below:

$$E_{av} = \frac{h_1 E_1 + h_2 E_2 + \ldots}{h_1 + h_2 + \ldots} \qquad (45)$$

This expression does not agree with the ones suggested by others (e.g. Ueshita and Meyerhof (1967, 1968), Briaud et al. (1983)). These authors suggest some form of a power functions (see Eqn. 16) to arrive at the equivalent modulus. It is suggested that a simple weighted average as proposed by Vaswani is not realistic.

3) In some of the examples he has shown pavements with lower spreadability deflect far less than those with higher spreadability. One of his examples is reproduced as Fig. 2.34. Thus the pavement (a) in this figure acts as a rigid pavement because the thin sandwich layer is completely confined and acts as part of the much more rigid confining layers. Similarly the pavement (d) with its thick sandwich layer acts essentially as a two-layer system. The third layer acts as a rigid bottom. The majority of the deflection in this structure takes place in the sandwich layer. The point here is that it is not enough to consider the area alone or some measure of spreadability or rigidity of the pavement. Instead the curvature of the basin as well as the contribution of the individual layers should be accounted for.

Huang (1971) introduced the concept of using the curvature of the structure to the evaluation of pavements. He carried out theoretical studies relating deflection, curvature of the surface, the tensile strain at the bottom of asphalt layer and the compressive strain at the top of the subgrade. He derived dimensionless parameters with these quantities and expressed them as functions of vertical and radial stresses and the modular ratios. These functions could be evaluated with published data by Jones (1962) or Peattie (1962). Huang published tabulated values relating deflections, surface curvature, asphalt tensile strain, and subgrade compressive strains to the ratios of layer thicknesses and the modular ratio. While his results are useful for parametric studies they are of much less use in direct application in the evaluation of deflection basins obtained from the modern deflection testing machines.

Majidzadeh (1982) related the concepts of curvature directly to the deflection basins obtained by Dynaflect. He introduced the various curvature indices such as the Surface

Curvature Index (SCI), the Base Curvature Index (BCI) as well as the Spreadability. He also pointed out the significance of the deflection recorded by the fifth sensor under the Dynaflect.

The various indices are given by:

$SCI = W_1 - W_2 =$ Deflection differential between the first and second sensors.

$BCI = W_4 - W_5 =$ Deflection differential between the fourth and the fifth sensors.

Spreadability is still defined according to Vaswani, Eqn. (44). Based on studies on pavements in Ohio State, Mazidzadeh makes the following observations:

1. The SCI is a strong indicator of fatigue cracking in the asphalt layer. SCI is dependent on the thickness of the surface layer as well as the ratio E_1/E_2. For thick pavements, SCI decreases with an increasing E_1/E_2. For thin pavements the variation of SCI with E_1/E_2 depends on the thickness of the surface layer. This is not quite in accordance with Huang's theoretical results (see Fig. 2.35). According to Huang, for thick pavements ($h_1/a > 1.0$ in Fig. 2.35 the modular ratio E_1/E_2 has very little influence. For thinner pavements the thickness will have a strong influence because of excessive radial strains; however the modular ratio has little influence.
2. SCI is also a strong indicator of vertical strains in the subgrade.
3. BCI is a good indicator of stresses and strains in the base course. Some states specify tolerance limits to BCI to ensure adequate performance of the pavements.
4. The fifth sensor reading W_5 is a unique parameter which depends on the subgrade modulus and is practically independent of the stiffness of the pavement structure.
5. Spreadability, by itself, is not a very useful concept in determining the adequacy of the pavement structure (compare the discussion of Vaswani's results above).

Hoffman and Thompson (1982) forwarded the idea of the "AREA" of the deflection basin. The "AREA" is literally the area of the deflection basin computed by the trapezoidal rule as shown in Fig. 2.36. For a curvilinear profile, such as the deflection basin, Simpson's rule would be better suited. The difference between the two methods of computation would amount between 5% and 12%. The area has the units of length and for the Boussinesq case will be 11 [in or cm or m] and for a perfectly rigid body will be 72 [in or cm or m] when using the FWD with seven sensors. In the case of Road Rater where there are four sensors, the "AREA" works out to be 11 and 36 for the two cases mentioned above. Hoffman and Thompson tested a number of road sections in Illinois using the ILLI-PAVE algorithm. Their principal conclusion was that, while there could be a number of combinations of surface and subgrade moduli which would yield satisfactory match of the maximum deflection or the "AREA" individually, the unique solution is the one which matches both simultaneously.

Anani (1979) and Wang and Anani (1981) report a method of analyzing deflection basins obtained from Road Rater tests in Pennsylvania. Starting from the stress function solution (Eqn. 3) for the differential equations for the stresses in a layer (Eqns. 1 and 2) they find an expression for the surface deflection at any radial distance, r, from the load point as:

$$\delta(r) = \left(-1.5\ \frac{q \cdot a}{E_1}\right) \int_0^{\infty} J_0(mr)\ (A_1 m^2\ e^{-m} - B_1 m e^{m} - C_1 e^{-m} + D_1 e^{m}) \qquad (46)$$

where,

q = the load per unit area

a = radius of the loaded area

r = radial distance of the point from load point

E_1 = modulus of elasticity (= resilient modulus)

J_o = Bessel function of 0- order

m = a dummy variable

A, B, C and D are constants of integration to be determined from boundary conditions.

Then they compute the change in surface deflections for a change in the layer moduli E_i for the ith layer. Thus they could determine which layer contributes to deflections at a certain distance from the load point. They have analyzed specific structures and specific deflection points which are the sensor locations of the Road Rater. Based on their analyses for a four layer system they conclude that:

$$\delta_4 = f_4 (E_4) \tag{47a}$$

$$\delta_3 = f_3 (E_3, E_4) \tag{47b}$$

$$\delta_2 = f_2 (E_1, E_2, E_3, E_4) \tag{47c}$$

$$\delta_1 = f_1 (E_1, E_2, E_3, E_4) \tag{47d}$$

It is seen that from Eqns. (47a) and (47b) δ_4 and δ_3 can be determined uniquely. owever, E_1 and E_2 cannot be determined as uniquely since both deflections will be affected by change in either of them. Therefore, one has to resort to some type of parametric analysis. For the Pennsylvania conditions, Wang and Anani fixed the ratio E_1/E2 at 0.7 and proceeded with the analysis. The ratio 0.7 was obtained from laboratory investigations on the materials in the pavements analyzed.

All the works cited so far have dealt with deflection basins generated by Dynaflect or Road Rater. The number of sensors is four for the Road Rater and five for the Dynaflect. Thus, it is relatively easy to identify the contributing layer to the deflections sensed by a particular sensor (see for example Wang and Anani cited above). Such discussions are not found in the literature for the FWD deflections though the analysis programs such as ISSEM-4 (which uses the ELSYM-5 as an analysis subroutine) can indicate the radial influence of the layers (Fig. 2.37). In general, based on the study reported in this thesis, it is found that the sensors 5 to 7 will be influenced primarily by the subgrade, sensors 3 and 4 are influenced by all layers below the surface while all the layers influence deflections 1 and 2. Brown et al. (1986) have published somewhat similar results (Fig. 2.38). In these figures Δ_{ij} is the difference in deflections between the i-th and j-th sensors. Thus from Fig. 2.38 one concludes that the deflections 1 and 2 are most sensitive to the stiffness of surface (there is some contribution from the other layers too) while deflections 2 to 4 are governed by base layers and the rest primarily by subgrade. It is suggested that a detailed study of the FWD deflection bowls will be useful to establish criteria similiar to those found for the Dynaflect or the Road Rater.

The above discussions were meant to focus the attention on the difficulty one encounters in interpreting the deflection basin obtained from any of the deflection- measuring devices. In order to get an acceptable solution it is necessary to know the contribution of individual layers to the overall deflection at each sensor point. Then one can isolate the contribution of each layer to the entire deflection basin. The area of the deflection basin for which any layer is responsible would be inversely proportional to the stiffness of that layer. Thus, in the numerical analysis of the basin, for each iteration the modulus value for each

layer should be adjusted in accordance with its contribution to the overall deflection basin or in inverse proportion to the area of the deflection basin calculated in that iteration. This is the conceptual framework that will be employed in the numerical evaluation proposed in this thesis (Chapter 3).

2.2.2.3 Geophysical Methods

During the past five to ten years geotechnical and pavement engineers are finding geophysical test methods increasingly useful to characterize material properties (Nazarian et al., 1987; Sanchez-Salinero et al., 1987; Nazarian, 1989). Of these the Spectral Analysis of Surface Wave (SASW) method and the down-hole or cross-hole seismography are probably most relevant to pavement engineering.

1. Fundamentals of Geophysical Testing

This method of testing involves imparting energy to the pavement or soil by means of a hammer-blow, dropping weights or a small explosive charge. Such an energy source generates three basic types of waves:

1) the compression or P-waves,
2) the shear or S-waves, and
3) the Rayleigh or R-waves (surface waves).

The velocity of propagation of these waves in any medium (such as concrete, asphalt, or earth materials) is a measure of the material properties such as density, rigidity, or stiffness modulus. Each type of wave travels at its own characteristic wave form and velocity and decays at different rates. Therefore, by suitably positioning the receivers the different waves

can be captured at different physical and time intervals and their velocities of propagation calculated which, in turn, are related to the material properties.

It is said (Nazarian, 1989) that in an isotropic homogeneous elastic medium approximately two-thirds of the energy is carried by the Rayleigh waves while the remainder is carried by the P- and S-waves. The P-waves attenuate at a rate inversely proportional to the square of the distance while the S-waves do so at a rate inversely proportional to the square root of the distance. Thus receivers stationed close to the source will receive primarily P-waves while those farther away will collect primarily S-waves. Also the P-waves travel faster than the S-waves. The ratio of the velocities of the P- and S- waves is a measure of the Poisson's ratio. The shear modulus of a material can be obtained from the relationship:

$$G = \rho \cdot V_s^2 \qquad (48)$$

where G = shear modulus

ρ = mass density

and V_s = velocity of the shear wave

Knowing G and μ, the modulus of elasticity E can be calculated using the relationship $E = 2G/(1+\mu)$. Thus in any geophysical testing the objective is to generate and capture the different waves using a source of impulse energy and a receiver (geophone).

2. Spectral Analysis of Surface Wave (SASW) Method

Fig. 2.39 shows the test setup for the SASW method. This method is based on the generation and detection of Rayleigh waves. Since Rayleigh waves travel close to the velocity of shear waves, the elastic parameter that will be measured (or interpreted) will be the shear

modulus G. In a homogeneous medium Rayleigh waves are not frequency-dependent. However, in a layered medium, such as a pavement structure, the velocity of the R-waves is frequency- dependent. Thus the wave spectrum will be dispersed. Details of obtaining the dispersion curve, the assumptions behind the theory of the SASW method and the factors affecting the test can be seen in papers by Douglas and Eller (1986) and Nazarian (1989).

It might be recalled that while discussing the anisotropy of the soil medium, it was mentioned that the independent shear modulus, G_{vh}, is difficult to measure. The laboratory setup requires testing the sample at three different orientations calling for three triaxial samples. It is suggested that the SASW method will yield more information with much less effort and resources. Together with the FWD test and some of the *in-situ* geotechnical tests which will be described in the next section, the SASW method offers the best hope for complete *in-situ* determination of material properties for pavement design.

Another method to determine the shear modulus with depth is the down- hole or cross-hole seismic method. The cross-hole method would be of little practical interest in pavement investigations because it requires at least pairs of holes for each test location and the test setup is more elaborate than the down- hole method. The technology of down-hole seismic tests exists to a sufficient degree of sophistication for use in pavement investigation at present (Campanella et al., 1986). The research by Campanella et al., was aimed at logging very deep holes for long piles and off shore structures. Hence the instrumentation in the associated equipment is fairly sophisticated and expensive. However, for pavement investigations, because of the shallow depths involved, the instrumentation can be adapted in an inexpensive way. A schematic view of the down-hole seismic test is shown in Fig. 2.40. Again an energy source at the surface generates all types of waves of which the shear wave

alone is captured by a horizontal geophone in the borehole. The time of arrival can be captured by an oscilloscope or by a spectral analyzer for later analysis (Campanella and Robertson, 1986; Campanella et al., 1986). It is suggested that the development of a simple *in-situ* apparatus combining the features of a pavement pressuremeter (Briaud, 1979) but operated by gas, and the features of down-hole seismography would be a worthwhile research effort for the future. Such an instrument could measure the necessary five parameters for treating the pavement as a layered, cross-anisotropic elastic medium. For example, Fig. 2.41 shows a cone pressuremeter developed by Campanella et al., (1986) and a seismic cone suggested by Robertson et al., (1985). Some of the sophisticated electronics and piezometer parts in these can be dispensed with and the two pieces of equipment can be combined into one for pavement investigation purposes.

The application of geophysical methods to pavement engineering is still relatively new. Hence, extensive data is not available to review this method more thoroughly. However, its use in geotechnical engineering is well accepted. The few reported correlations in pavement engineering offer much encouragement and promise (Fig. 2.42). It is seen in Fig. 2.42 that the maximum discrepancies occur in the upper layers, particularly in the unbound granular layers. However, it is in this layer where most of the discrepancies between different computer based algorithms also occur. Further, lack of agreement with the backcalculauted moduli should not necessarily distract one from the merits of this method. As discussed in the previous sections, considerable improvements are still needed in the backcalculation procedures.

2.2.2.4 *IN-SITU* Geotechnical Methods

In response to the increasing consensus that it is often impossible to reproduce the field conditions in the laboratory, geotechnical engineers have developed a number of *in-situ* tests in the past fifteen years (Bauer et al., 1973; Bauer and McRostie, 1986; Bauer and Tanaka, 1988; Mitchell, 1988). Furthermore high-quality samples are very expensive, particularly in deep holes. In pavement engineering the variations in any given stretch of a highway can be so great that *in-situ* tests are of more relevance than laboratory tests.

There is a variety of *in-situ* tests available currently as listed below:

1. Cone penetrometer (mechanical or electrical);
2. Pressuremeter;
3. Flat blade dilatometer;
4. Vane shear equipment;
5. Bore hole shear;
6. Screw plate.

It is not the intention to go into the details of all the tests here. Nor are all of them relevant or applicable to pavement investigations. Of these equipments only the flat plate dilatometer, the screw plate and the pressuremeter can measure modulus directly. Because of the geometry, only the pressuremeter is amenable to rigorous mathematical treatment. Therefore, in this section, only the use of the pressuremeter for pavement investigations will be discussed.

1. The Pressuremeter

The development of the first practical pressuremeter is generally credited to Menard. Fig. 2.43 shows schematically the Menard pressuremeter. As seen in the figure, the instrument is a tri-cell apparatus with a measuring cell in the middle and two guard cells, one above and the other below the measuring cell. The purpose of the guard cells is threefold:

1. to eliminate the end effects of restraint when the measuring cell is inflated.
2. The middle cell would thus exert a uniform pressure on the cavity wall.
3. The guard cells also ensure that the middle cell expands only radially.

This is shown schematically in Fig. 2.44. Therefore, the expansion of the pressuremeter can be modelled as the expansion of a long cylindrical cavity. Rigorous mathematical solutions are available for this problem (see for example Baguelin et al., 1978, Ch. 4). The Menard pressuremeter, useful as it is in foundation engineering, is a large apparatus, quite cumbersome and complicated in its operation and maintenance. Field and laboratory tests have shown that if the length-to-diameter ratio is kept at seven or more, the end restraints have no influence on the stress field at the centre of the probe (Briaud et al., 1985; Hughes et al., 1986). Thus the cavity expansion theory would still be valid. Therefore, if one can build a pressuremeter with a long probe to satisfy the length-to-diameter ratio then the guard cells can be eliminated. This would result in an equipment which is far less complicated or cumbersome to operate and maintain than the Menard pressuremeter. Many modern pressuremeters such as the OYO, Cambridge, Texam and the PENCEL are of the mono-cellular design. Except PENCEL, most modern pressuremeters are also gas operated instead of fluid operated. The use of gas as an inflating medium ensures instant response so that transient or dynamic loading conditions (such as under traffic loads) can be more realistically

simulated. Of all these instruments, the PENCEL pressuremeter is of particular interest because it was specifically developed for pavement investigations (Briaud, 1979; see also Sanders and Horak, 1992).

2. The PENCEL[4] Pressuremeter

The PENCEL pressuremeter was first developed by Briaud (1979) for use in pavement investigations. The forerunner of the PENCEL was developed by Menard and was known as the "mini-pressuremeter". It was a tri-cell instrument like the standard Menard pressuremeter. Briaud modified it as a nono-cell apparatus for use in pavement investigations. The original Briaud version was a laboratory prototype with triaxial-test-type volumeter etc. It was later redesigned in a more compact format and marketed as the PENCEL pressuremeter. Fig. 2.45 shows the version used in this investigation.

The requirement of a pavement pressuremeter is somewhat different from that used for foundation investigations. The overall depth to be investigated for pavements is shallow, seldom greater than 5 m; however, there will be many tests at one location and many more locations for any given pavement project than for a geotechnical foundation project. Therefore, the instrument has to be simple, robust but able to be dismantled, moved around and reassembled easily and quickly. Also because the pavement layers are rather thin, the entire probe should be short enough to be able to be buried completely in the layer for the test to be meaningful. Keeping in mind the restriction about the length-to-diameter ratio, the instrument will, therefore, have to be of small diameter, slender and long. The PENCEL is

---

[4] PENCEL is the registered trade mark of ROCTEST Inc. of Montreal, Quebec, Canada.

38 mm in diameter and 600 mm long, the inflatable part being 230 mm long. The operation of the PENCEL pressuremeter has been described elsewhere (RocTest Manual (1981); Briaud and Cosentino, (1989)).

Fig. 2.46-A shows, schematically the pressuremeter test in a pavement and typical *in-situ* results. It also shows the raw curve that would be obtained from a field test. Fig. 2.46-B shows this curve on an enlarged scale and explains the different stages of the test. The part A of the curve is usually the phase when the probe expands in the bore hole before making any contact with the surrounding soil. At point **A** the probe is in firm contact with the cavity wall and it is generally accepted that at this point during the test the original stress condition in the ground has been reestablished. The part **AB** is a psuedo elastic range where the stress-strain relation is practically linear. The point **B**, where the curve starts to deviate from the straight line, denotes the approximate start of yielding of the soil. The part **BD** denotes the yielding phase of the soil. In some cases a shear failure may be achieved. Fig. 2.46 shows an unload-reload cycle, the unloading starting at some point in the range **AB**. The secant of the hysteresis loop of the unload-reload cycle is a measure of the horizontal shear modulus of the soil from which the resilient modulus can be calculated if Poisson's ratio can be assumed. Poisson's ratio may also be inferred from the test results as follows. Since the point **A** represents the re-establishment of the existing geostatic conditions, the pressure at point **A** is approximately the lateral stress in the ground. From the lateral stresses K_o, and hence Poisson's ratio, can be calculated using the following relationship: (Feda, 1978, pp. 21).

$$K_0 = \frac{\mu}{1 - \mu} \tag{49}$$

Feda (pp. 27-28) has also suggested other relationships between K_o and anisotropic parameters which are discussed later. Lamb and Whitman (1969, pp. 159) suggest an expression for the young's modulus, E_v, which relate the modulus to the initial vertical principal stress, σ_v, and K_o:

$$E_v = \sqrt{\sigma_v \frac{(1 + 2\,K_0)}{3}} \tag{50}$$

Referring to Fig. 2.47 and using the notations shown there the resilient modulus is given by Eq. 51 below (Briaud and Cosentino, 1989):

$$E = (1 + \mu_r)\,(\sigma_{m2} - \sigma_{m1})\,\frac{\left[\left(1 + \frac{\Delta R_1}{R_0}\right)^2 + \left(1 + \frac{\Delta R_2}{R_0}\right)^2\right]}{\left[\left(1 + \frac{\Delta R_1}{R_0}\right)^2 - \left(1 + \frac{\Delta R_2}{R_0}\right)^2\right]} \tag{51}$$

Briaud suggests that the modulus is influenced by many factors, in particular, by the stress level, the strain level, the rate of loading and the number of cycles of loading. He proposed to consider these influences by incorporating different models suggested by many previous workers. Thus for the influence of the stress level he takes Janbu's model as modified by Duncan and Chang (1970):

$$E_o = K \left(\frac{\theta}{p_a}\right)^{n_1} \tag{52}$$

For the influence of strain level he uses Kondner's hyperbolic model:

$1 / E = a + b\,\epsilon$ (See Eqn. (20), Section 2.2.2.1).

For the rate of loading he uses a model proposed by Riggins (1981):

$$\frac{E_{t_1}}{E_{t_0}} = \left(\frac{t_1}{t_0}\right)^{n_2} \tag{53}$$

Finally for the cyclic effect of loading he uses the model proposed by Idriss et al.(1978):

$$\frac{E_n}{E_1} = N^{-n_3} \tag{54}$$

Briaud combines these individual models to obtain the following expression for the resilient modulus:

$$E = \frac{1}{K\left(\frac{\theta}{p_a}\right)^{n_1} + b_c} \cdot \left(\frac{t_1}{t_0}\right)^{-n_2} \cdot N^{-n_3} \tag{55}$$

With the use of these models one is left with the task of measuring five material constants: n_1, n_2, n_3, K and b.

Briaud and Cosentino (1989) suggest a field procedure to conduct cyclic pressuremeter tests whereby all the five parameters can be evaluated from a single test. According to Briaud the test could be completed in 45 to 60 minutes. He also presented field results to verify the model (Fig. 2.48 to Fig. 2.50). In presenting their results Briaud et al. (1987) attempted a three way correlation between pressuremeter based results, cyclic triaxial tests in accordance with the U.S. Army WES procedure and the observed deflections using the Dynatest FWD. ILLI-PAVE was used to compute the deflections from the pressuremeter or the cyclic triaxial test results. The following comments can be made on these results:

1. Neither the pressuremeter nor the cyclic triaxial test yields an exact match with the observed deflections.

2. The deviation from the observed values is about the same in both cases though the pressuremeter results appear to be marginally better, if one would choose the appropriate model. It should be quickly added that there are too few results and further research and more extensive correlation are needed before definitive statements can be made.

3. The results appear to be dependent on the site. This should be more appropriately interpreted as a dependence on the type of subgrade and materials used in the construction of the three pavements.

4. The need to know beforehand the appropriate model (stress or strain level model) in the case of pressuremeter tests is a disadvantage when one is using the tests for design. However, it is suggested that with further research and more extensive correlations criteria can be established to select the appropriate model for design.

5. The comparison of moduli value (Figs. 2.48 to 2.50) between the three procedures appears to lead to nowhere. The two geotechnical procedures (the cyclic triaxial and the pressuremeter) which measure the moduli directly appear to correlate better between themselves than either of them with the backcalculated moduli. Therefore, the backcalculation procedure should be more suspect than the two geotechnical test methods.

6. There is a need to continue the research on the application of pressuremeter testing to pavement design and evaluation.

In the following paragraphs a brief review of the theory of pressuremeter is given. This is followed by a discussion on the relevance of the parameters measured during a pressuremeter test to pavement engineering.

3. Theory of Pressuremeter

The theory of pressuremeter is based on the theory of expansion of long cylindrical cavity. Consider an infinitely long cylinder subjected to an internal pressure p_o which would be gradually increased to p (Fig. 2.51 B and C). Under the increasing pressure, the walls of the cavity strains the surrounding medium. Fig. 2.51 shows the strains that will be caused by such an expansion of the cavity. Since this is a long cavity the problem can be treated as a plane strain problem and one need to consider only the diametrical plane. Therefore, the radial and the circumferential strains become the principal strains. These directions remain the principal directions throughout the test. Referring to the notations in Fig. 2.51 one can then write: (see Baguelin et al., pp. 336-341).

Radial strain:

$$\epsilon_r = \frac{\mu}{r} \tag{56}$$

Circumferential strain:

$$\epsilon_\theta = \frac{du}{dr} \tag{57}$$

Using the geometry given in Fig. 2.51 one can arrive at the following expressions for the volumetric strains:

$$\varepsilon_0 = \frac{\Delta V}{V_0} \tag{58}$$

$$\varepsilon_0 = \frac{\Delta_V}{V} \tag{59}$$

Here, V_0 refers to the original volume and V refers to the deformed volume. Eqn. (58) holds for small strains and Eqn. (59) for large strains. The essential difference in these two cases is that with Eqn. (58) the strain is with respect to the original volume V_o while in Eqn. (59) the strain is with reference to the deformed volume V. Since the strains during pavement investigations are small and in the pressuremeter test it is rather difficult to know the exact volume in the deformed state, it is suggested that the use of Eqn. (58) is justified.

The stresses in the soil mass during a pressuremeter test can be calculated using the equations of equilibrium given at the beginning of the chapter (Eqns. 1 and 2). For an axisymmetrical plane strain case, in the plane of symmetry and considering small strains these two equations will reduce to one equation as given below (because there are no shear stresses on this plane and there is no variation in the stresses in the z-direction):

$$\frac{\partial \sigma_v}{\partial r} + \frac{\sigma_r - \sigma_\theta}{r} = 0 \tag{60}$$

The constitutive relations for an elastic, homogeneous and isotropic medium was given by Eqn. (10). Noting that the terms containing shear stresses and shear strains will vanish Eqn. (10) can be rewritten, for incremental stresses and strains, as:

$$\epsilon_\theta = \frac{1}{E} \left[\Delta\sigma_\theta - \mu\,(\Delta\sigma_z + \Delta\sigma_r)\right] \tag{61}$$

$$\epsilon_r = \frac{1}{E} \left[\Delta\sigma_r - \mu\,(\Delta\sigma_\theta + \Delta\sigma_z)\right] \tag{62}$$

$$\epsilon_z = \frac{1}{E} \left[\Delta\sigma_z - \mu\,(\Delta\sigma_r + \Delta\sigma_\theta)\right] \tag{63}$$

Noting again that the strain in the vertical direction, ϵ_z, should vanish one can express the incremental stresses in the z-direction, $\Delta\sigma_z$, in terms of the incremental stresses in the other two directions, Eqn. (64).

$$\Delta\sigma_z = \mu\,(\Delta\sigma_r + \Delta\sigma_\theta) \tag{64}$$

Substituting these in Eqns. (61) and (62) and after some arithmetic manipulations (see Baguelin et al., 1978, pp. 347) and substituting the result in Eqn. (60) one can, finally, write the differential equation for the radial displacement as below:

$$r^2 \frac{d^2u}{dr^2} + r \frac{du}{dr} - u = 0 \tag{65}$$

For a cross-anisotropic medium with the plane of isotropy perpendicular to the axis of symmetry the differential equation will still be Eqn. (65). The general solution to Eqn. (65) is given by:

$$u = r^n \tag{66}$$

By substituting this in Eqn. (64) it can be shown that the exponent n will have roots ± 1. Thus the solution for u is written as a combination of all roots of n as below:

$$u = Ar + \frac{B}{r} \tag{67}$$

The constants A and B should be determined from the boundary conditions. These are:

1. At large distances from the probe the displacement u = 0. Therefore A = 0.
2. At the cavity wall ($r = r_o$) the displacement is $\epsilon_o r_o$. Therefore $B = \epsilon_0 r_0^2$.

Thus the displacement u can be finally written as:

$$u = \frac{\epsilon_0 r_0^2}{r} \tag{68}$$

Noting that the circumferential and radial strains are given by u/r and du/dr respectively, one can write:

$$\epsilon_\theta = \frac{\epsilon_0 r_0^2}{r^2} \tag{69}$$

and

$$\epsilon_r = -\frac{\epsilon_0 r_0^2}{r^2} \tag{70}$$

From these the stresses can be computed as (see Baguelin et al., 1978, pp. 347-348):

$$\sigma_\theta = p_0 + \Delta\sigma_\theta = p_0 - 2G\frac{\epsilon_0 r_0^2}{r^2} \tag{71}$$

$$\sigma_r = p_0 + \Delta\sigma_r = p_0 + 2G\,\frac{\epsilon_0\, r_0^2}{r^2} \qquad (72)$$

At the cavity wall the stress is equal to the inflation pressure inside the probe, so that the pressure at the wall is given by:

$$p = p_0 + 2G\epsilon_\theta = p_0 + 2G\,\frac{u_0}{r_0} \qquad (73)$$

Eqns. (71) and (72) can be plotted in the σ-r space and Eqn. (73) as a stress-strain diagram as shown in Figs. 2.52 and 2.53. It will be noted that σ_r and σ_θ are symmetrical about p_o. They are equal in magnitude and opposite in signs. Thus the inflation of the probe does not produce any rotation of principal axes nor does it produce any distortions. The stress-strain diagram given by Eqn. (73) plots as a straight line the slope of which is the shear modulus and the intercept the *in-situ* lateral stress. For an isotropic and elastic medium the Young's modulus or the modulus of deformation can be obtained from the shear modulus G using the relationship $E = 2G(1+\mu)$ if the Poisson's ratio is known. Poisson's ratio can be also obtained from p_o in Fig. 2.53 using Eqn. (49).

For an anisotropic soil the pressuremeter yields the horizontal shear modulus, G_{hh}, and the Poisson's ratio in the horizontal plane, μ_{hh}. From G_{hh}, E_{hh} can be calculated as mentioned above (μ_{hh} is known). The other three parameters should be determined by some other means. This will be discussed in a subsequent section.

4. Relevance of Pressuremeter Moduli for Pavement Design and Evaluation

There have been many concerns or objections regarding the relevance of the pressuremeter tests to determine the resilient modulus of the pavement layers. These are:

1. The validity of using the theory of expansion of the long cylindrical cavity when evaluating properties of materials at shallow depths (eg. base material under the surface layer);
2. Probe geometry to satisfy the assumptions in the theory of expansion of a long cylindrical cavity;
3. The effect of stress level, strain level, creep, and number of cycles to truly measure the resilient modulus;
4. The fact that the pressuremeter measures a horizontal modulus. In pavement the deformations are vertical and hence the relevance of the measured modulus to pavement calculations is questionable.

These concerns are discussed in the following sections.

One of the concerns in using a pressuremeter for pavement purposes is the shallow depths at which the tests would be done, particularly when base layers are being tested. When the free surface of the soil is very near the centre of the probe it is conceivable that the inflation pressures might push the soil upward around the probe. In such cases the assumption of a plane-strain condition (the strain in the vertical direction is zero) is not valid anymore. Nor can these movements be predicted. Thus the results discussed in the previous section would not be valid.

This question was investigated by Briaud and Shields (1981). They argued that if the proximity of a free surface should have an influence then there should be a critical depth

(similar to the critical depth concept in other geotechnical problems) below which the plane strain theory would hold, while above this depth the influence of vertical strains would have to be considered. They tested their hypothesis by laboratory triaxial, and sand box tests on clean sand, and by field tests in a silty clay under a grain silo. The laboratory tests were done with both the Menard and the PENCEL (actually the prototype of the PENCEL) pressuremeters. Their essential results are reproduced in Figs. 2.54 to 2.56. As can be seen, the larger diameter Menard equipment showed a clear break in the modulus profile. It would appear that for this pressuremeter the critical depth appears to be around 1.20 m, confirming some earlier conclusions by Baguelin and Jezequel. However, for the PENCEL pressuremeter no such influence is seen. The results from all the tests (triaxial, sandbox and field tests) showed similar profiles indicating only the influence of increasing overburden but not of a critical depth. It is, therefore, suggested that the moduli measured with the PENCEL equipment are valid results and that the plane strain theory is applicable to tests in the base layer.

Another concern, which was mentioned briefly at the beginning of this section, is the validity of the theory of expansion of a long cylindrical cavity to simulate the pressuremeter test. This is essentially a problem of the geometry of the probe, specifically the length to diameter ratio (L/D Ratio) of the probe. Briaud et al. (1985) addressed this problem in connection with the standardisation of the pressuremeter tests. They quote many previous works and recommend that in order to apply the long cylindrical expansion theory the length to diameter ratio should be 6.5 or more. The PENCEL probe has an L/D ratio of over sixteen. The alternate theory would be to use the expansion of a spherical cavity in an elastic medium. In the same paper these authors show that even in the extreme case of L/D = 1

(expansion of a sphere) the error introduced by assuming long cylindrical cavity expansion is only in the order of 35 percent. However, spherical expansion theories are also available to obtain exact solutions. Houlsby and Withers (1988) show an ingenious method whereby the same form of the differential equation (Eqn. 65) can be used with a slight modification as shown below:

$$r^2 \frac{d^2u}{dr^2} + m \frac{du}{dr} - m \frac{u}{r} = 0 \qquad (74)$$

In this equation setting m = 1 will apply to the cylindrical case and m = 2 to the spherical case. The solution (Eqn. 66) can be rewritten as:

$$u = Ar + \frac{B}{r^m} \qquad (75)$$

The stresses and strains are then written as:

$$\epsilon_\theta = - \frac{B}{\gamma^{m+1}} \qquad (77)$$

$$\epsilon_r = - m\epsilon_\theta = + \frac{mB}{\gamma^{m+1}} \qquad (78)$$

$$\sigma_\theta = 2G\ \epsilon_\theta \qquad (78)$$

$$\sigma_r = - 2mG\ \epsilon_\theta \qquad (79)$$

Other factors which could influence the pressuremeter modulus are the effect of stress level, strain level, creep, number of cycles and the method of insertion. These factors were

investigated by Briaud et al. (1986). Based on this investigation they recommended using the models mentioned before. These were:

1. Kondner's hyperbolic model for strain level;
2. The K-Θ model for stress level;
3. Riggin's model for creep; and
4. The effect of loading cycles model by Idriss.

Finally, they recommend pre-boring the hole for the least disturbance. As can be seen from Figs. 2.48 to 2.50, comparison of FWD deflections and deflections using these above models has not proven conclusively the advantage of the models. Moreover, some of the objections to the hyperbolic model and the K-Θ model were discussed earlier. While pre-boring the hole may be the best method of installation, full displacement pressuremeters give reasonably close results (Houlsby and Withers, 1988). Therefore for pavement investigations full displacement pressuremeter or the cone pressuremeter (Briaud et al., 1986) should give sufficiently accurate results. The rate of loading might be a drawback in the case of pressuremeters using a fluid for determining transient loads such as the traffic loads. This could be overcome by using a gas operated equipment similar to the OYO pressuremeter but keeping the size of the PENCEL. It is suggested that the PENCEL could be modified to suit this need though in this investigation only the water inflated probe was used.

Another criticism of the pressuremeter modulus is that the pressuremeter measures a horizontal modulus rather than a vertical modulus while the loading is vertical. It is submitted that this is not a valid criticism if one is to analyze the pavement layers as elastic, isotropic and homogeneous medium. For such a medium, by definition, the moduli in all directions must be equal. The criticism is quite legitimate, however, if one recognizes that

pavement layers are indeed anisotropic. In such a case one has to, of course, determine the five elastic constants which can be done, at present, only in the laboratory. *In-situ* procedures for the determination of anisotropic parameters have not been reported in the literature. As has been mentioned previously, the current backcalculation algorithms cannot consider anisotropic layers. In addressing this question Briaud (1979), and Briaud and Cosentino (1989) maintain that the error involved is no more than 15 percent in the calculation of the deflections. It is suggested that the pressuremeter test combined with down-hole shear wave propagation methods would be useful in this respect. For example seismic cone and cone pressuremeters have been developed and are in use (Campanella and Robertson, 1986; Campanella et al., 1986; Mitchell, 1988).

2.3 CONSIDERATION OF ANISOTROPY OF PAVEMENT LAYERS

2.3.1 Elastic Halfspace

Table 2.4 shows the research or publications on linear elastic cross-anisotropic halfspace or layered systems. The earliest attempt to consider anisotropy of soil masses is attributed to Michell in 1900. Subsequently in 1935 Wolf published some results assuming equal Poisson's ratio in all directions. Thus Wolf's solutions were restricted in applications (Barden, 1963; Feda, 1978, pp. 66). Following Wolf, the first attempt to analyze cross-anisotropic halfspace seems to be by Koning (1957). He gave a general analysis and limited numerical evaluation for the stresses and displacements in a cross-anisotropic halfspace . His results are summarised in Fig. 2.57 (b). Barden (1963) used Michell's solutions and published results for stresses and displacements in an anisotropic medium. However, Barden made an untenable assumption regarding the shear modulus G_{vh} (Dooley, 1964). He assumed that the

shear modulus is the same in the plane of anisotropy and in a plane at 45° to this plane i.e. the shear modulus is independent of the rotation of the coordinate axes. The result of this assumption was that Barden could characterize the anisotropic medium with only four instead of five constants. The two essential results from Barden's work are shown in Figs. 2.57 (a) and 2.58. It is easy to see from Fig. 2.57 that the general shape and form of the curves due to Koning and due to Barden are very similar. In reviewing these works Feda (1978) comments that despite Barden's unacceptable assumptions, his analysis leads to acceptable solutions in some cases (Feda, 1978, pp. 68). One can observe a few interesting characteristics in Figs. 2.57. As the anisotropy factor (i.e. the ratio of the horizotal to vertical moduli) increases the maximum deflection decreases and there is a tendency for the stress bowl to spread out to a greater distance from the load point. Since we are assuming a linear elastic layer, the displacements will have the same shape as the stress distribution. Thus Fig. 2.58 can be looked upon as deflection basins (with a scale factor of 1/E) for the halfspace. It is clear then that anisotropy has a tendency to flatten the deflection bowl. In terms of the spreadability concept (Vaswani, 1971), anisotropy leads to greater spreadability. Looking from the point of view of curvatures (Majidzadeh, 1982) anisotropy would result in smaller curvature indices. Therefore, one could use Fig. 2.57 (Barden's or Koning's results) as a template and compare the observed deflection basin with these to gain an idea of the anisotropy of the medium. Fig. 2.58 from Barden suggests a simple means to compute the deflection in a cross-anisotropic medium if deflections can be computed for an isotropic medium. According to Gibson (1974) and Feda (1978) these results appear to work fairly well in some cases.

Subsequently, Pickering (1970) published a rigorous treatment of elastic cross-anisotropic soils. Since then until the early 1980's, there have been many other publications dealing with this problem. This section reviews these works and discusses how these can be applied to the layered medium.

At the beginning of this chapter constitutive equations for an elastic cross-anisotropic medium were given (Eqns. 12 and 13). It was noted that a cross-anisotropic medium is characterized by five elastic constants. These are usually taken as E_v, E_h, μ_{vh}, μ_{hh}, and the independent shear modulus G_{vh}. While these are independent constants, they cannot take any arbitrary values. They have to satisfy the following conditions and inter-relationships (Pickering, 1970):

1. E_v, E_h and G_{vh} must be all positive;
2. $-1<\mu_{hh}<1$;
3. $2\mu_{vh}^2 < n(1-\mu_{hh})$.

where n is the anisotropy factor equal to E_h/E_v. Noting that in condition (3) above, n is always positive it follows that $(1-\mu_{hh})-2\mu_{vh}^2$ must be positive. Setting these terms to zero, Pickering arrives at the bounding surface for elastic constants in an n,μ_{hh},μ_{vh} space (Fig. 2.59). As is seen in Fig. 2.59 the bounding surface is a paraboloid. Any section parallel to the (μ_{vh} - n) plane and any section parallel to the (μ_{hh} - μ_{vh}) plane is a parabola. The paraboloid is bounded on the open side by a plane having limiting values $\mu_{hh} = 1$ (see condition (2) above). Thus in this diagram, looking down the n-axis one obtains a set of parabolas (Fig. 2.60) relating n, μ_{hh}, and μ_{vh} (Nayak, 1973). It is therefore possible that if some of the parameters can be measured in the field others can be determined because of the above conditions. Of course, it would be ideal if these parameters could be all measured independently in the field.

This would require certain modifications to the current equipment, testing procedures or both. The question of field measurement will be discussed in a later chapter. It should be noted that the n-(μ_{hh}-μ_{vh}) space does not contain the independent shear parameter G_{vh}. This will have to be measured independently. One method is the down-hole seismic test as suggested in the previous section. Some of the developments in the analytical treatment of cross-anisotropic soils were directed toward approximating the problem in such a way so that only three instead of five parameters need to be measured or determined. Gibson (1974) showed that for an incompressible soil ($\mu_{hh} = \mu_{hv} = \mu_{vh} = 0.5$) only three elastic parameters (E_{hh}, E_{vh} and G_{vh}) need to be known. For this case he also showed that the anisotropic factor, n, should satisfy the limiting condition $0 < n < 4$. Further he showed that the deflection of a cross-anisotropic incompressible medium could never exceed 2.7 times the isotropic case. For $E_h/E_v = 4$ the medium is rigid and no settlement will occur.

Van Cauwelaert (1977), who specifically deals with pavement structures, proposes that under certain conditions only three constants need to be determined to characterize the pavement materials. These would be E_v, n and μ_{vh}. His definition of the parameters is shown in Fig. 2.61. He then proceeds to rotate the axes by an angle and transforms the elastic constants to the rotated coordinate axes. The transformation constants are essentially as given by Lekhnitskii (1963). Using Lekhnitskii's transformation constants for $\theta = \pi/4$, G_{vh} can be shown to be:

$$G_{vh} = \frac{E}{1 + n + 2\mu} \qquad (80)$$

Here he assumes the invariance of the shear modulus G_{vh}, i.e it is independent of the rotation of axes (cf. discussion of Barden's work above). Therefore G_{vh} is given by Eqn. (80). By

using a similar argument for the Poisson's effect along the Y-axis due to a tangential stress in the plane XZ, he arrives at the following relationship:

$$\mu_{vh} = \frac{\mu_{hh}}{n} \tag{81}$$

Thus, having managed to express two of the five constants in terms of the others, one is left with only three constants to determine. In a subsequent discussion of his paper he concedes that his analysis is not rigorous; however, he justifies his assumptions as follows:

1. The independence of the shear modulus to the rotation of axes is just another way of saying that the average modulus in the anisotropic planes are considered.
2. The correlation of computed values of the elastic constants of pavement materials with laboratory measured values appear to be within tolerable limits in engineering practice.

His distractors, however, point out that when his method is applied to crystals and plastics the correlations are poor. There is little doubt that van Cauwelaert's method is theoretically and conceptually unsound. However, from the results he has presented, and from the independent comments of Gibson and Feda regarding Barden's approach, it would appear that soils do not behave as regular crystals or plastics. Perhaps such approximations may be acceptable at least until methods are developed for the determination of all the five constants in-situ. Further research into this aspect will be useful.

Graham and Houlsby (1983) and Graham et al. (1989) suggest a method whereby the anisotropic parameters can be determined from triaxial tests. Since only three parameters can be measured in a triaxial test they devise a matrix formulation relating the mean normal stresses and the deviator stress to the volumetric and axial strains as shown below:

$$\begin{bmatrix} \delta p' \\ \delta q' \end{bmatrix} = \begin{bmatrix} K & J \\ J & 3G \end{bmatrix} \begin{bmatrix} \delta_v \\ \delta_\varepsilon \end{bmatrix} \tag{82}$$

Here K and G are the bulk and shear moduli respectively while, J is a coupling parameter linking mean normal stresses, $\delta p'$, to the shear strain, δ_ϵ, and the deviator stress, $\delta q'$, to the volumetric strain, δ_v. They show how these three can be in turn related to the five anisotropic parameters through four other constants. These four constants are evaluated by multiple regression analysis of a large number of triaxial tests. The model is validated using the data collected for the Winnipeg clay over the years. This is a novel approach. Its application to routine pavement engineering is, however, limited. Their methodology is also not directly applicable to *in-situ* tests such as pressuremeter tests because not enough parameters can be measured in such a test. However, their results are used later in the anslysis of the data collected during the field tests for this thesis.

Gazetas (1981, 1982) analyzed the problem of stresses and deformations in a cross-anisotropic soil. In the first paper he analyzed the problem of strip footings on a cross-anisotropic medium. Treating this as a plane-strain problem, he formulates the stress-strain relations as below:

$$\begin{aligned} \sigma_x &= C_{11}\ \epsilon_x + C_{13}\ \epsilon_z \\ \sigma_y &= C_{12}\ \epsilon_x + C_{13}\ \epsilon_z \\ \sigma_z &= C_{13}\ \epsilon_x + C_{33}\ \epsilon_z \\ \tau_{xz} &= G_{V_H}\ \gamma_{xz} \end{aligned} \tag{83}$$

He, then uses a constraint proposed by Carrier in 1946 to express the shear modulus in terms of the four constants C_{ij} above,

$$G_{v_H} = \frac{C_{11} \cdot C_{33} - C_{13}^2}{C_{11} + 2C_{13} + C_{33}} \qquad (84)$$

He demonstrates that Carrier's constraints are realistic by comparing computed and measured values of the shear modulus published in literature (Table 2.5). Thus the number of constants are reduced to four, E_h, E_v, μ_{hh}, and μ_{vh}. In the second paper he carries out a series of parametric analyses to show that the influence of μ_{hh} is insignificant compared to that of μ_{vh} (Fig. 2.62). Also, since μ_{hh} varies within a narrow range (0 to 0.5) an error in its value might not result in any error of practical significance (see Fig. 2.63, for instance). Thus in extreme cases one could even arbitrarily assume μ_{hh} without any serious error. These results are, to a certain extent, similiar to van Cauwelaert's intuitive reasoning (see above). However, the correlation for the independent shear modulus is much better according to Gazetas than according to van Cauwelaert. The difficulty still remains that in the pressuremeter test only two parameters can be measured. This will be discussed in Chapter 4 when field tests are described.

From the above discussions it would appear that solutions for the analysis of cross-anisotropic halfspace exist. While five parameters are needed, there could be ways to reduce these to three, which can be measured in a triaxial test.

2.3.2 Cross-anisotropic Elastic Layered Systems

In contrast to foundation engineering, concepts of anisotropy have not found application in pavement engineering. It is suspected that most analytical procedures are based on the theory of Burmister (1943). This analysis was mathematically overwhelming by itself without the added complication introduced by considering anisotropy. Secondly, until deflection basins could be measured accurately and back-analysed, the shortcomings in the analysis procedures treating the pavement as isotropic system could not be ascertained. Deflection testing is of recent origin. Finally, that anisotropy could be a factor in the analysis of pavements was not realised until recently when Stewart et al. (1985), Kehdr (1985) and Brown and Pappin (1985) published results concerning residual stresses.

Curiously though, analytical solutions for layered elastic, cross-anisotropic media were published in the late 1960's and early 1970's mainly by Gerrard and his associates in Australia (Gerrard and Mulholland, 1966; Gerrard, 1967, 1968; Gerrard and Harrison, 1971) and by Bhattacharya (1968). In the first of these Gerrard and Mulholland suggest a finite-difference technique to arrive at numerical solutions to the complex analytical expressions involved. They also suggest a Bessel series solution but did not go into great details. In the 1967 and 1968 papers Gerrard continued the development of the Bessel series method and based on a suggestion by Taylor on the discussion of the 1966 paper used integral transforms (Fourier or Hankel transforms) to evaluate the Bessel integration. In these papers Gerrard deals with 10 cases with one or two layers, in plane-strain or axi-symmetrical loading and for uniform circular loads or linear shear loads (Table 2.6). As can be seen these cover a very limited range. The 1971 publication by Gerrard and Harrison gives analytical solutions with no numerical evaluation. Therefore it is suggested that these solutions have to be extended

to other cases. With powerful finite-element methods now available this should be now feasible. In addition, the numerical solutions have to be validated by field observations.

Bhattacharya (1968) also used finite difference methods to compute the stresses and deformations. He restricted himself to the Boussinesq model of a homogeneous anisotropic half-space with a point load at the surface. He worked out elaborate mathematical solutions and tabulated influence coefficients for stresses, strains and deformations at various points in the half-space and at the surface. He demonstrated the validity of his solutions for the extreme cases of Boussinesq (homogeneous, isotropic solid) and of Westergaard (homogeneous solid reinforced with strips of stiff horizontal layers). However, there was no validation by field observations.

Thus the work, found in the literature to date, on anisotropic half-space or layered systems is of limited value. With more powerful numerical techniques (eg. finite-element method) available at present, pavements should be modelled more realistically as layered elastic systems and analyzed. Also, with the deflection-measuring equipment available currently, the results from the analytical models can be verified.

The remaining chapters of this thesis will attempt to address these concerns. A numerical model will be presented in Chapter 3. Field work, involving deflection measurements, will be described in Chapter 4. Chapter 5 presents the analysis and results while Chapter 6 presents a discussion of the results.

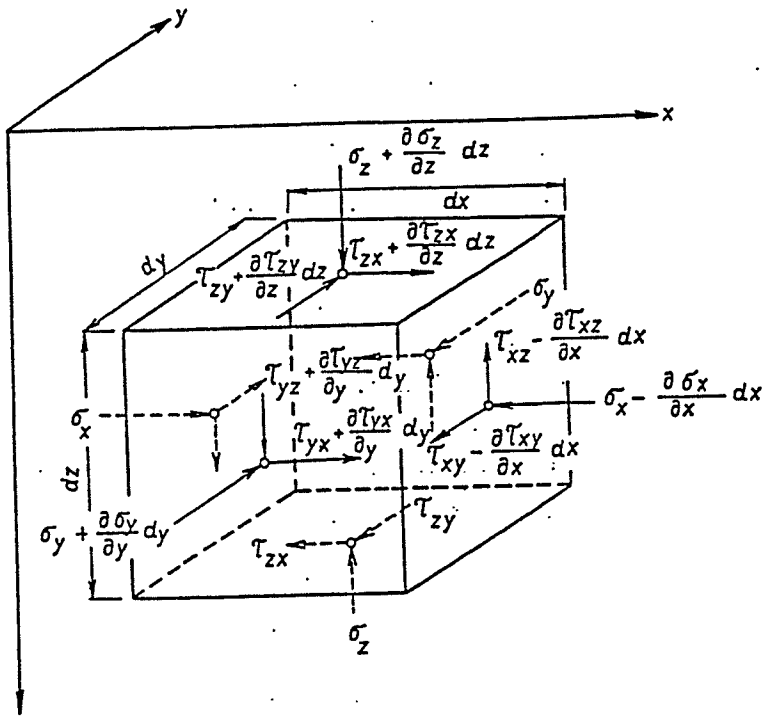

Fig. 2.1. STRESS COMPONENTS IN CARTESIAN COORDINATES.

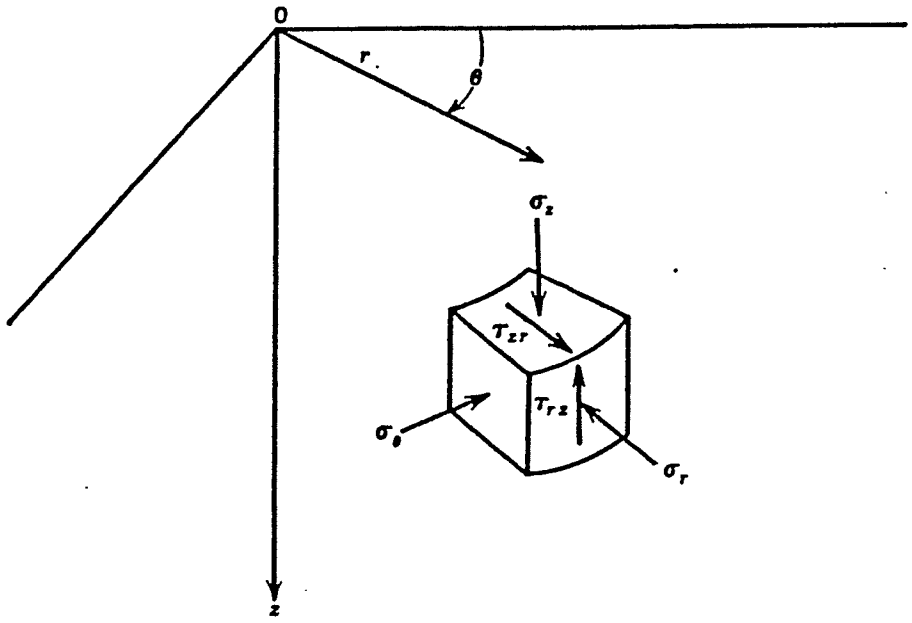

FIG. 2.2. STRESS COMPONENTS IN CYLINDRICAL COORDINATES.

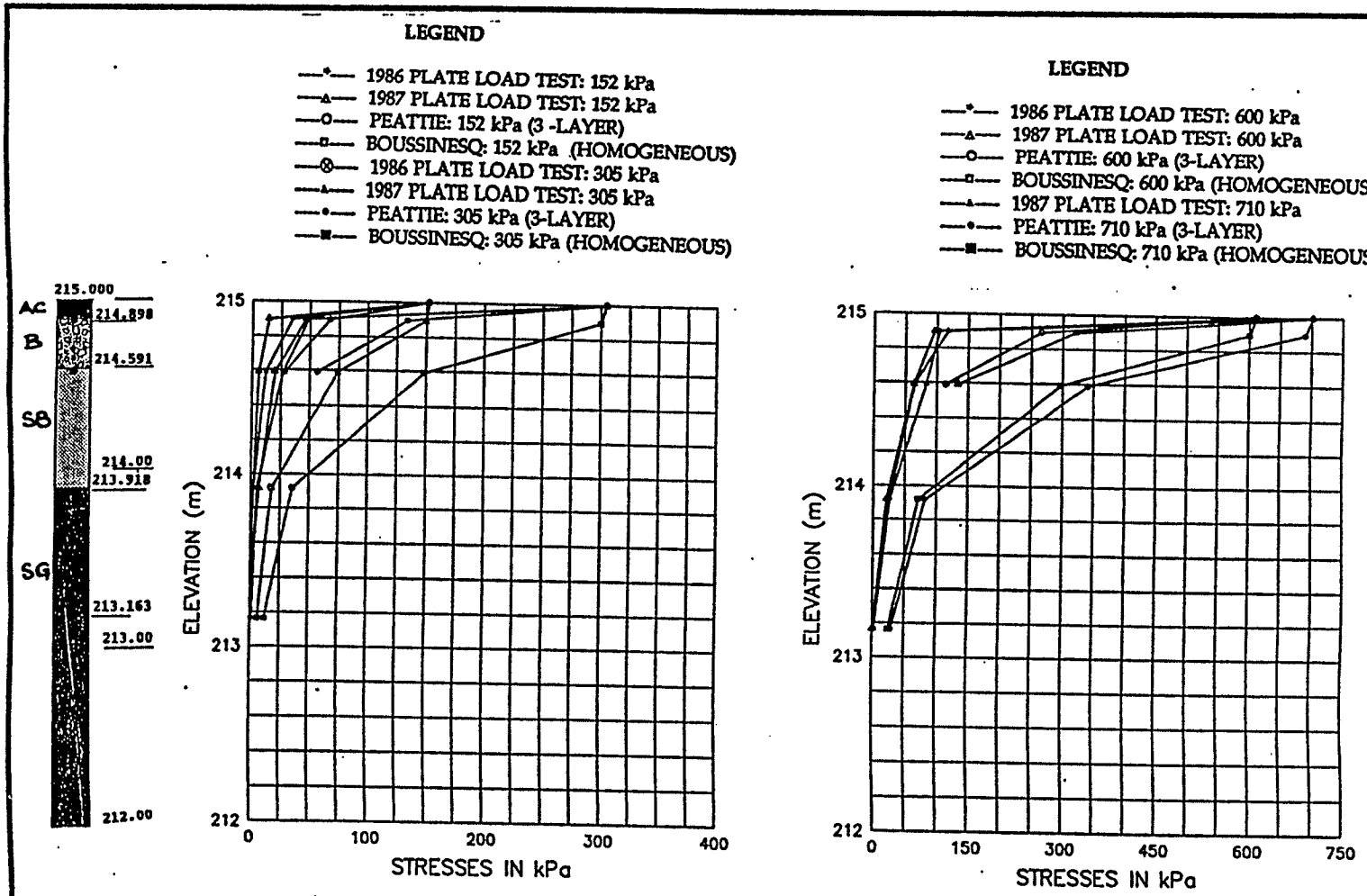

FIG. 2.3: EXAMPLE OF STRESS DISTRIBUTION IN AN INSTRUMENTED PAVEMENT.

(COMPARISON WITH CLASSICAL THEORIES)

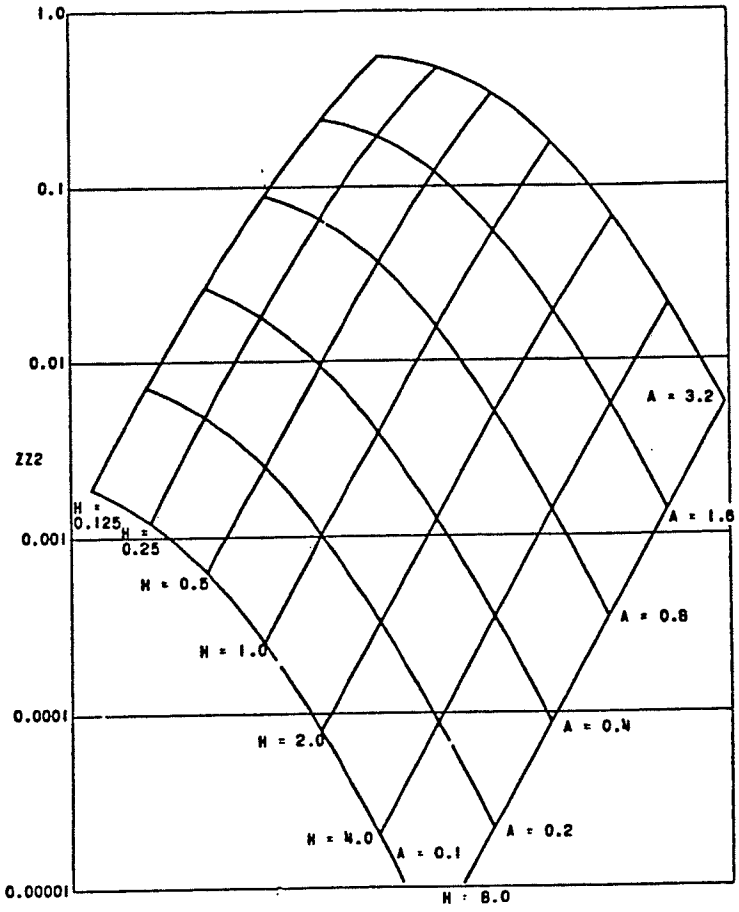

Vertical stress factor ZZ2 for $K_1 = K_2 = 20.$

FIG. 2.4. EXAMPLE OF THE CURVILINEAR GRID BY PEATTIE (AFTER PEATTIE, 1962)

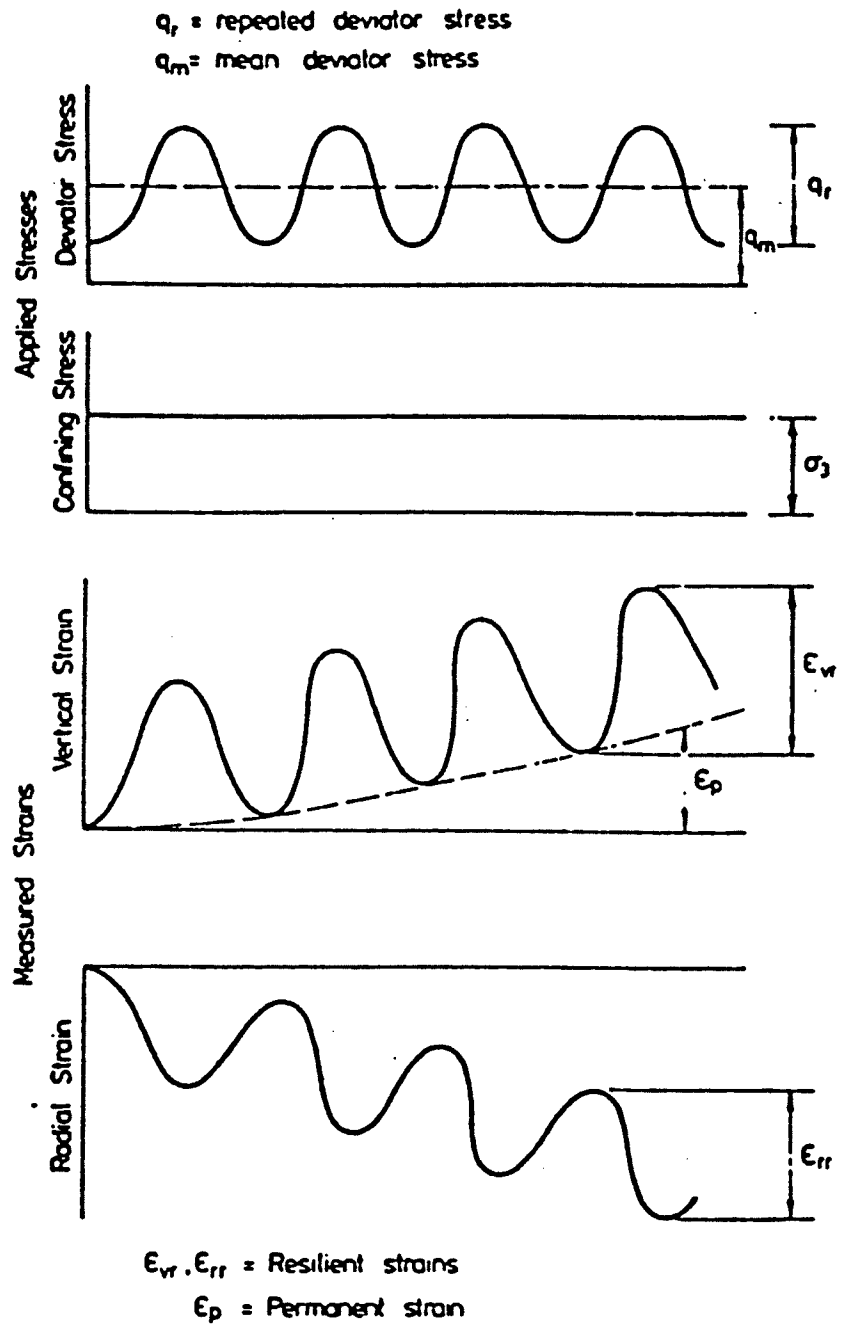

FIG. 2.5. DEFINITION OF RESILIENT MODULUS (AFTER BROWN, 1982)

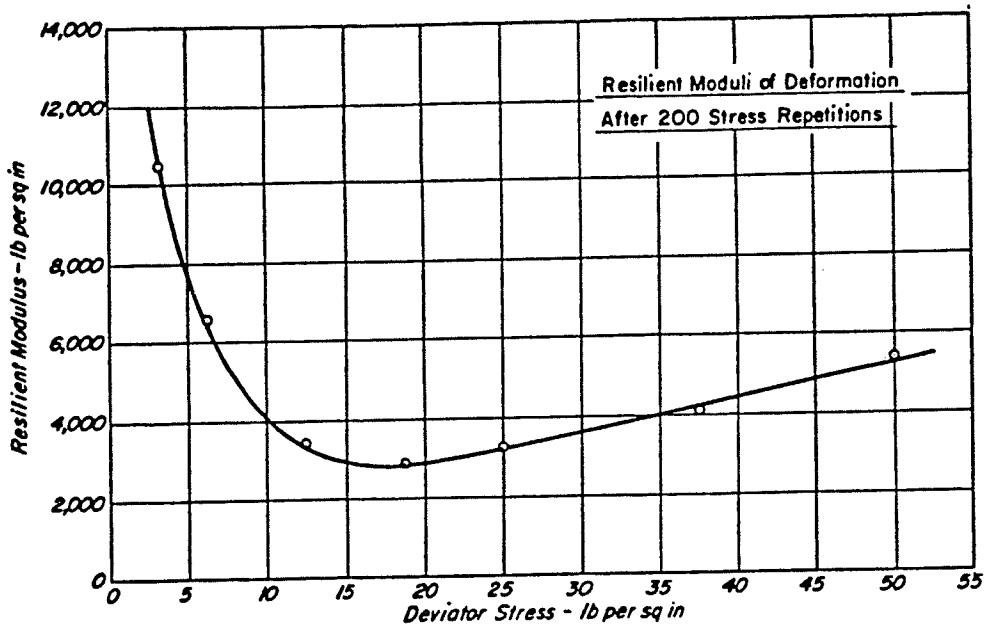

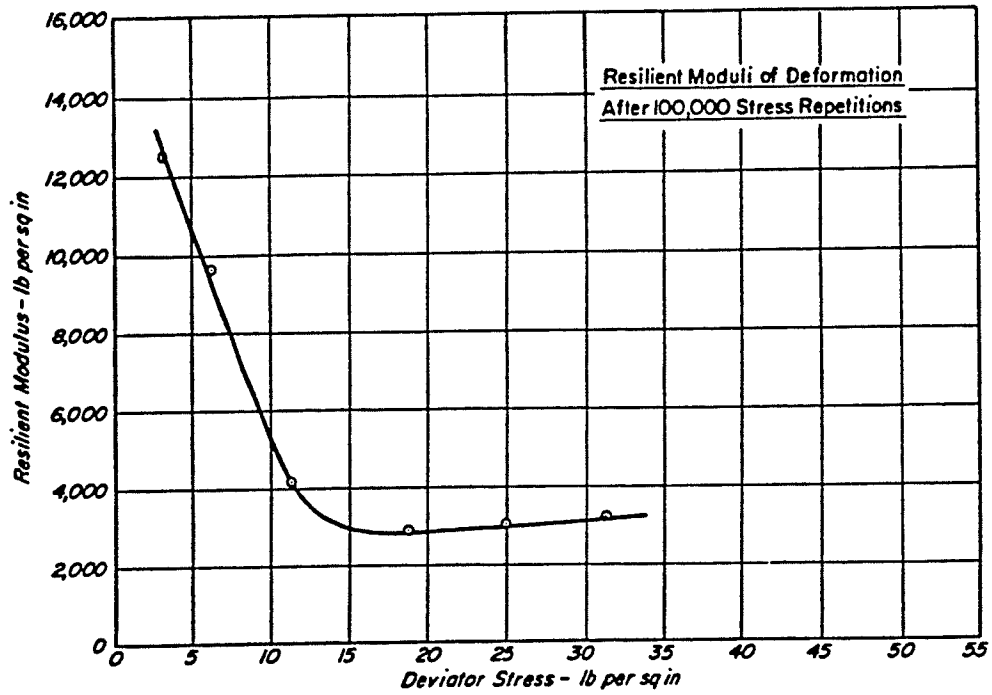

FIG. 2.6. VARIATION OF RESILIENT MODULUS WITH DEVIATOR STRESS (AFTER SEED ET AL, 1967)

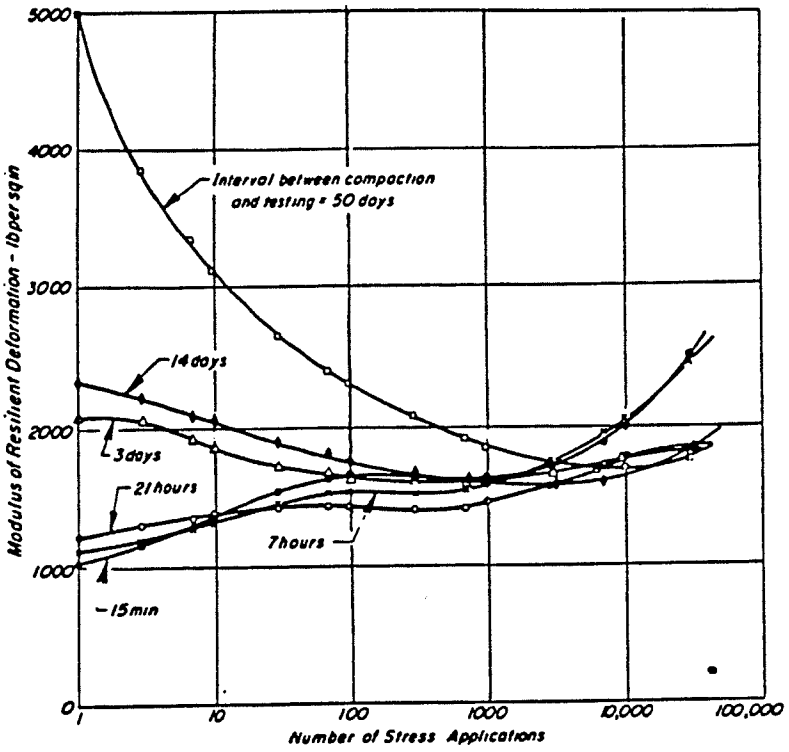

FIG. 2.7. EFFECT OF THIXOTROPY ON THE RESILIENT MODULUS OF A CLAY (AFTER SEED ET AL, 1967)

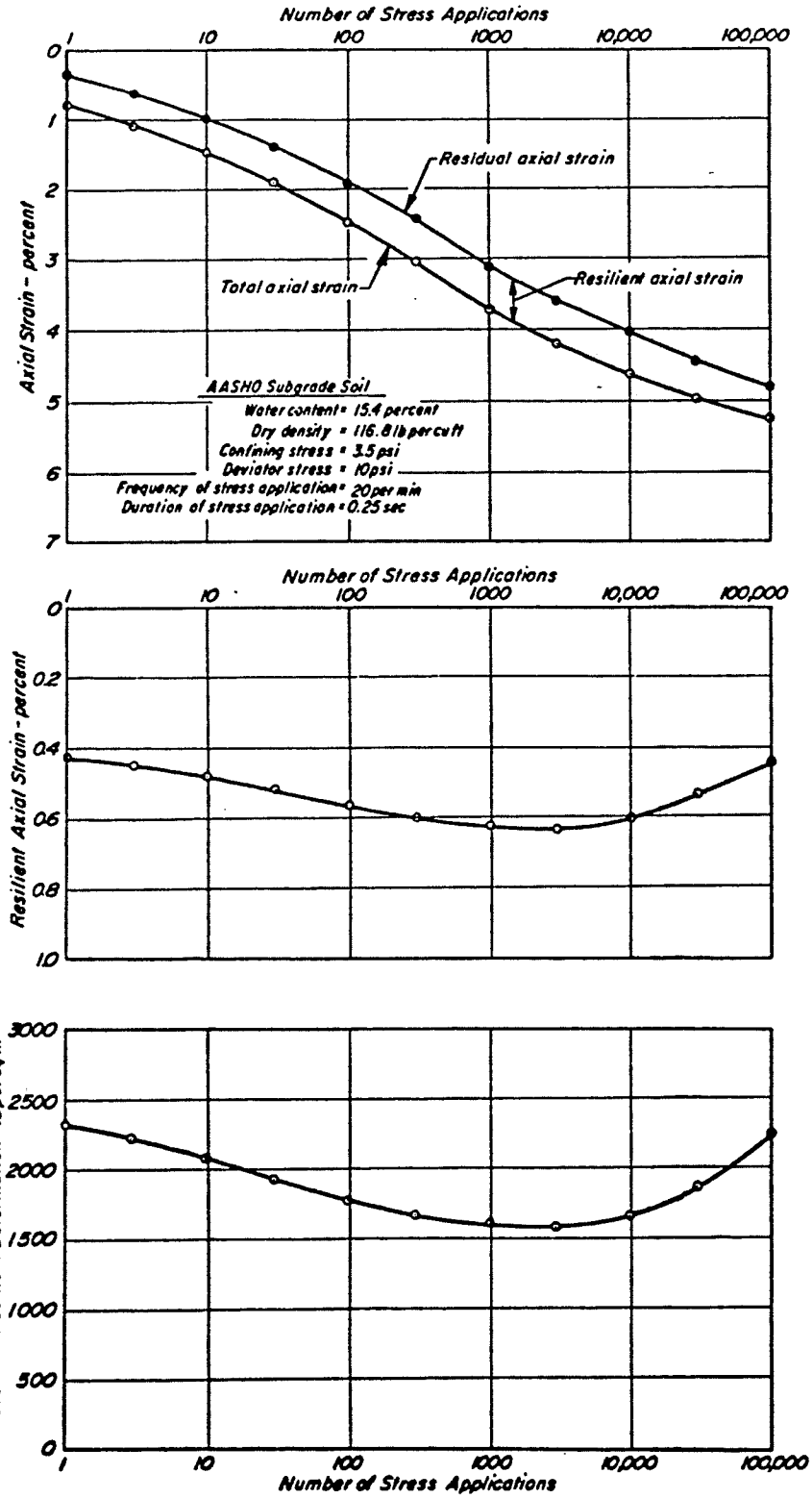

FIG. 2.8. EFFECT OF NUMBER OF CYCLES OF LOADING ON THE RESILIENT MODULUS OF SUBGRADE (AFTER SEED

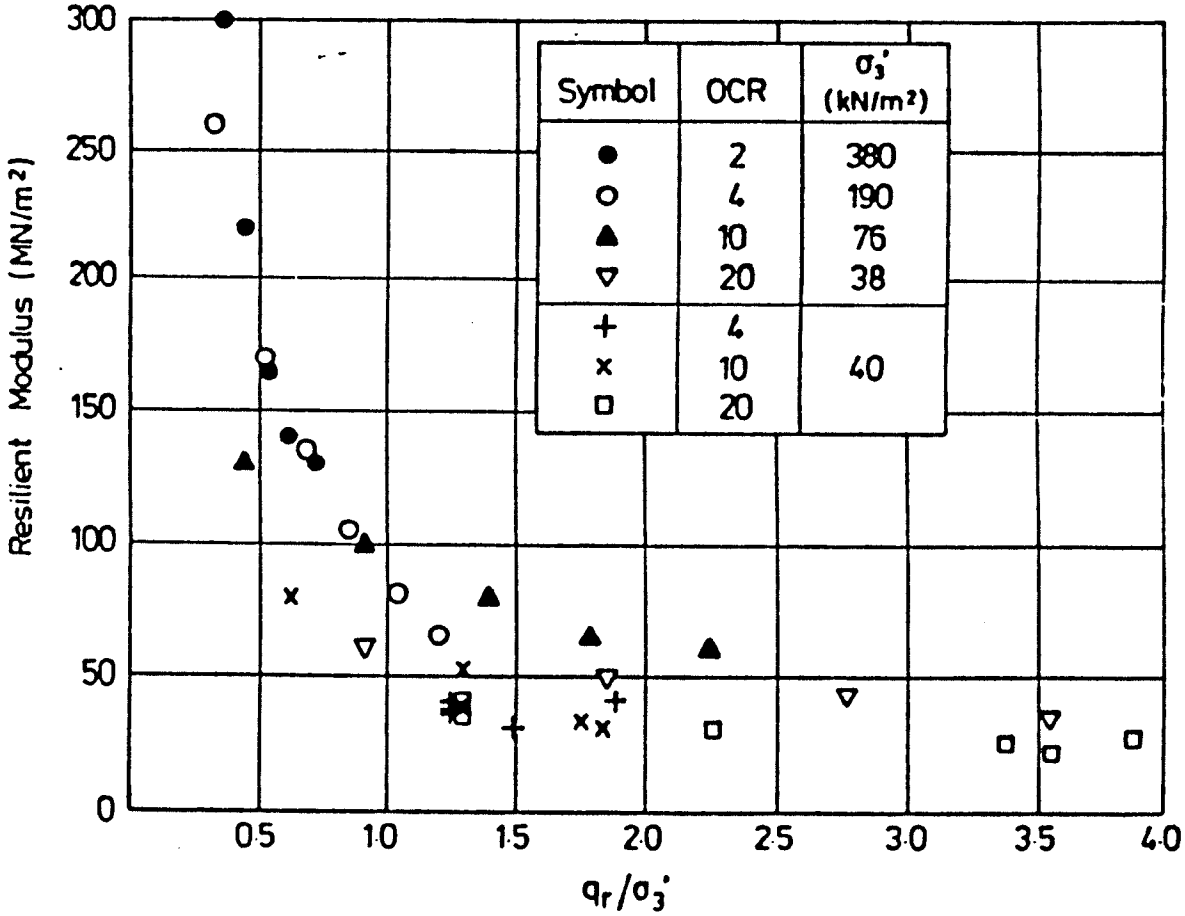

FIG. 2.9. RESILIENT MODULUS OF A SILTY CLAY AS A FUNCTION OF DEVIATOR STRESS AND CONFINEMENT (AFTER BROWN, 1982)

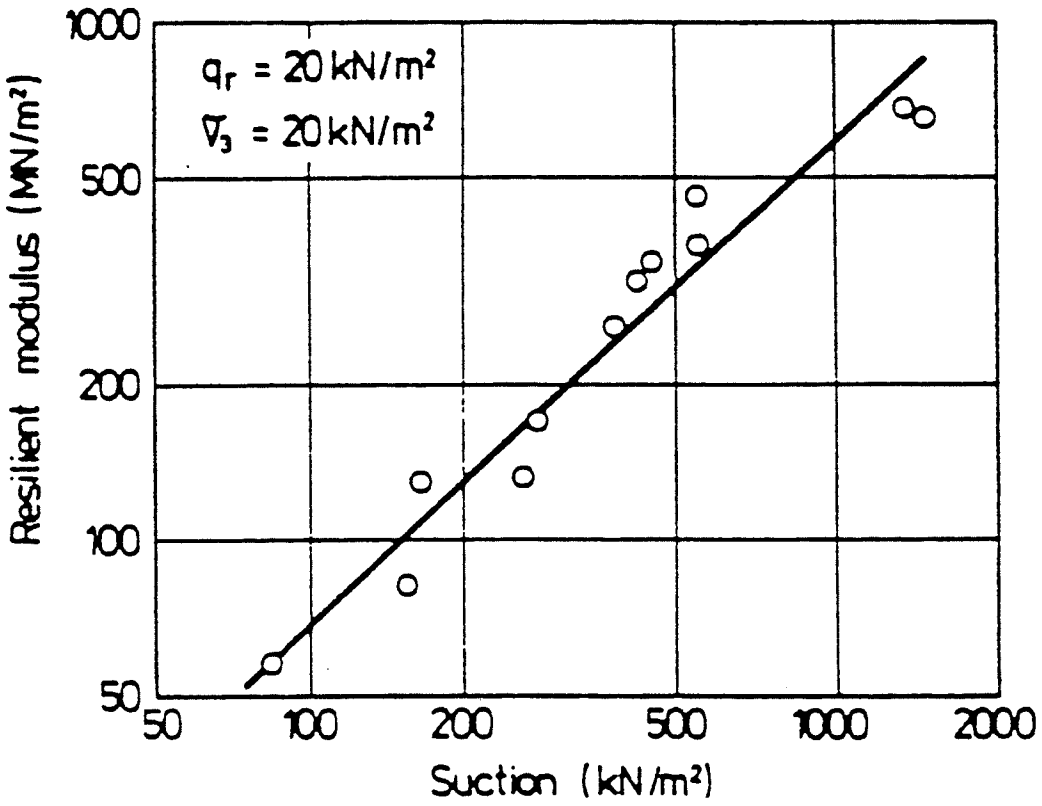

FIG. 2.10. EFFECT OF SOIL SUCTION ON THE RESILIENT MODULUS (AFTER DEHLEN, 1969)

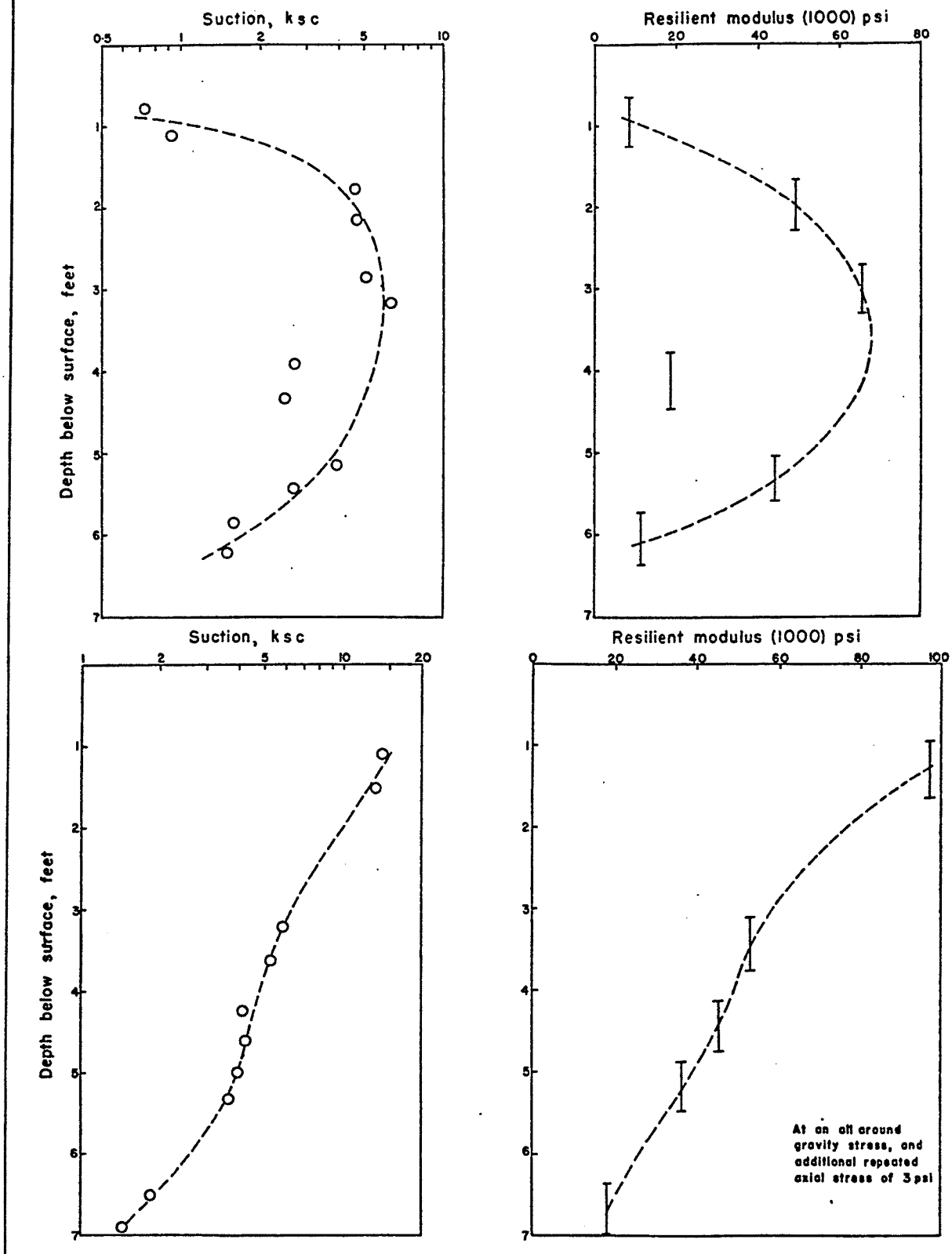

FIG. 2.11: VARIATION OF SUCTION WITH DEPTH AND RELATIONSHIP BETWEEN SUCTION AND RESILIENT MODULUS (MONISMITH, 1992)

$$\textit{Resilient Modulus}\quad M_r = \left[\frac{q_r}{\sigma_3'}\right]^n$$

q_r = deviatoric stress

σ_3' = effective confining pressure

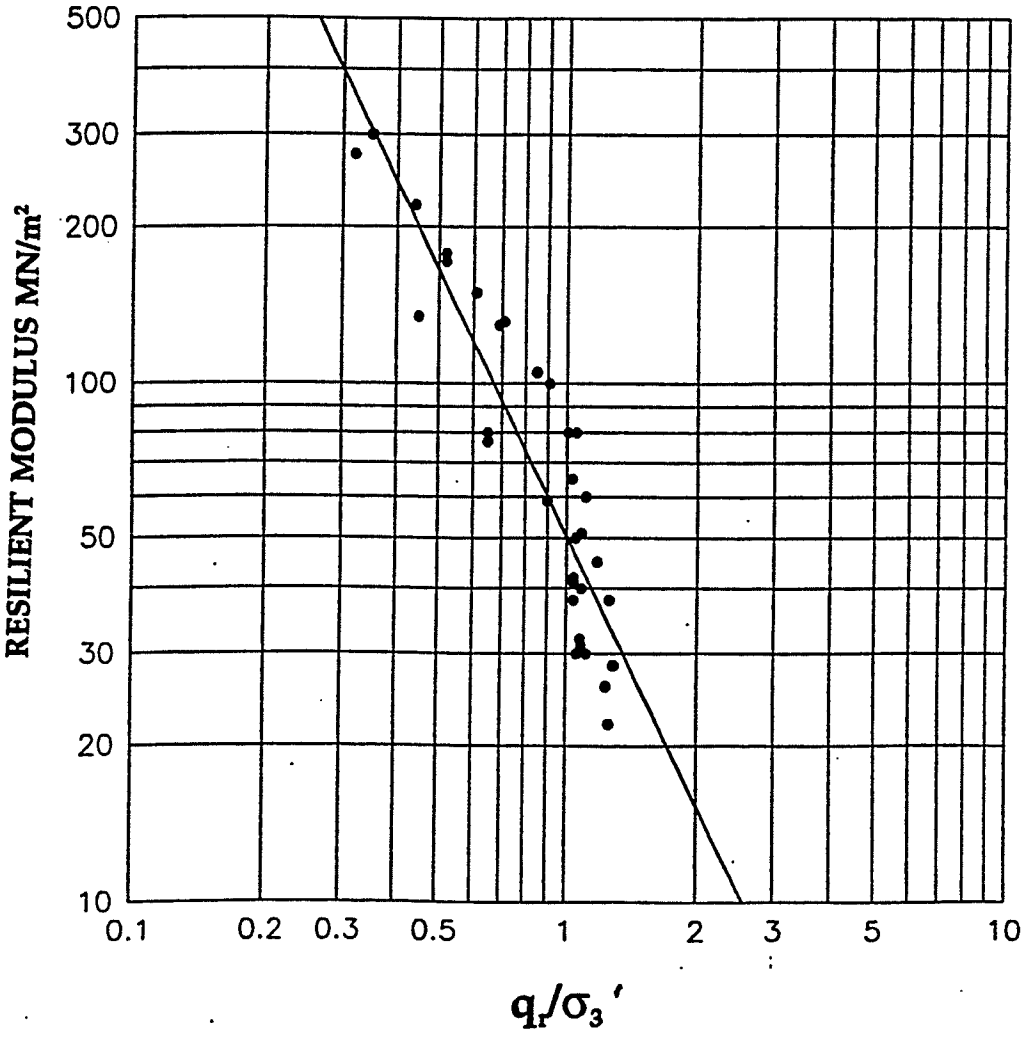

FIG. 2.12. THE NOTTINGHAM MODEL FOR THE RESILIENT MODULUS OF GRANULAR MATERIALS (AFTER BROWN ET AL 1975, BROWN 1982)

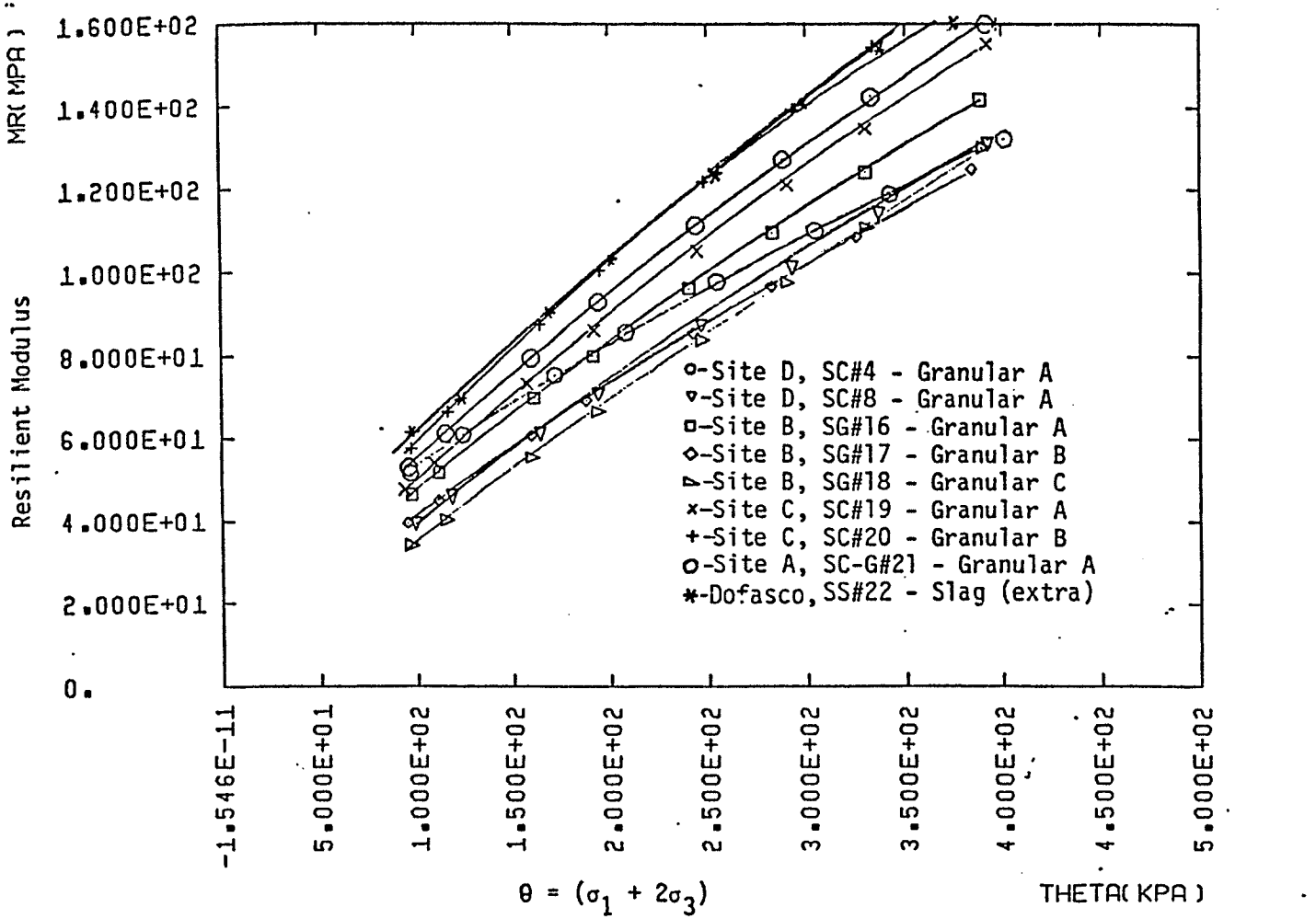

FIG. 2.13. VERIFICATION OF THE K-θ MODEL FOR VARIOUS ONTARIO GRANULAR MATERIALS (AFTER LAM, 1982)

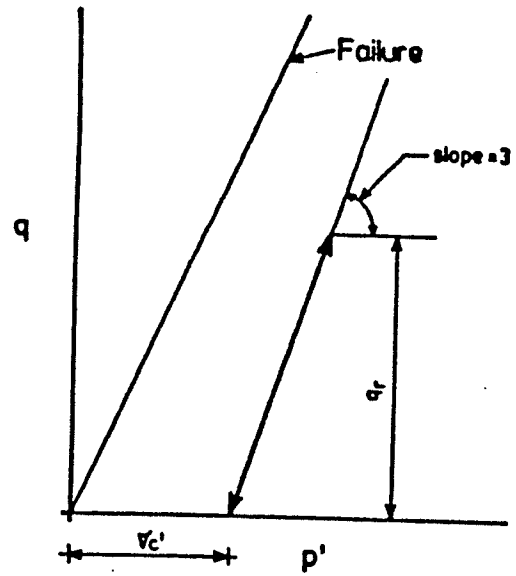

A. CONSTANT CONFINING STRESS

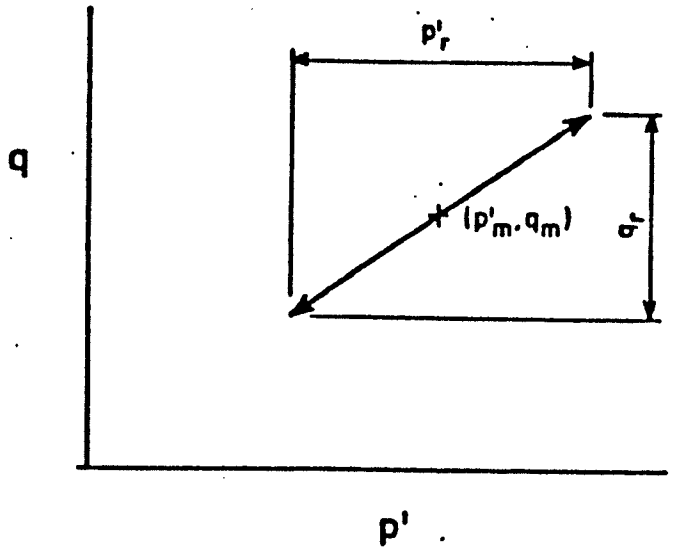

B. GENERALISED STRESS PATH IN A PAVEMENT.

FIG. 2.14. STRESS PATHS AND FAILURE ENVELOPES FOR UNBOUND MATERIALS IN A PAVEMENT. (AFTER BROWN AND PAPIN, 1985)

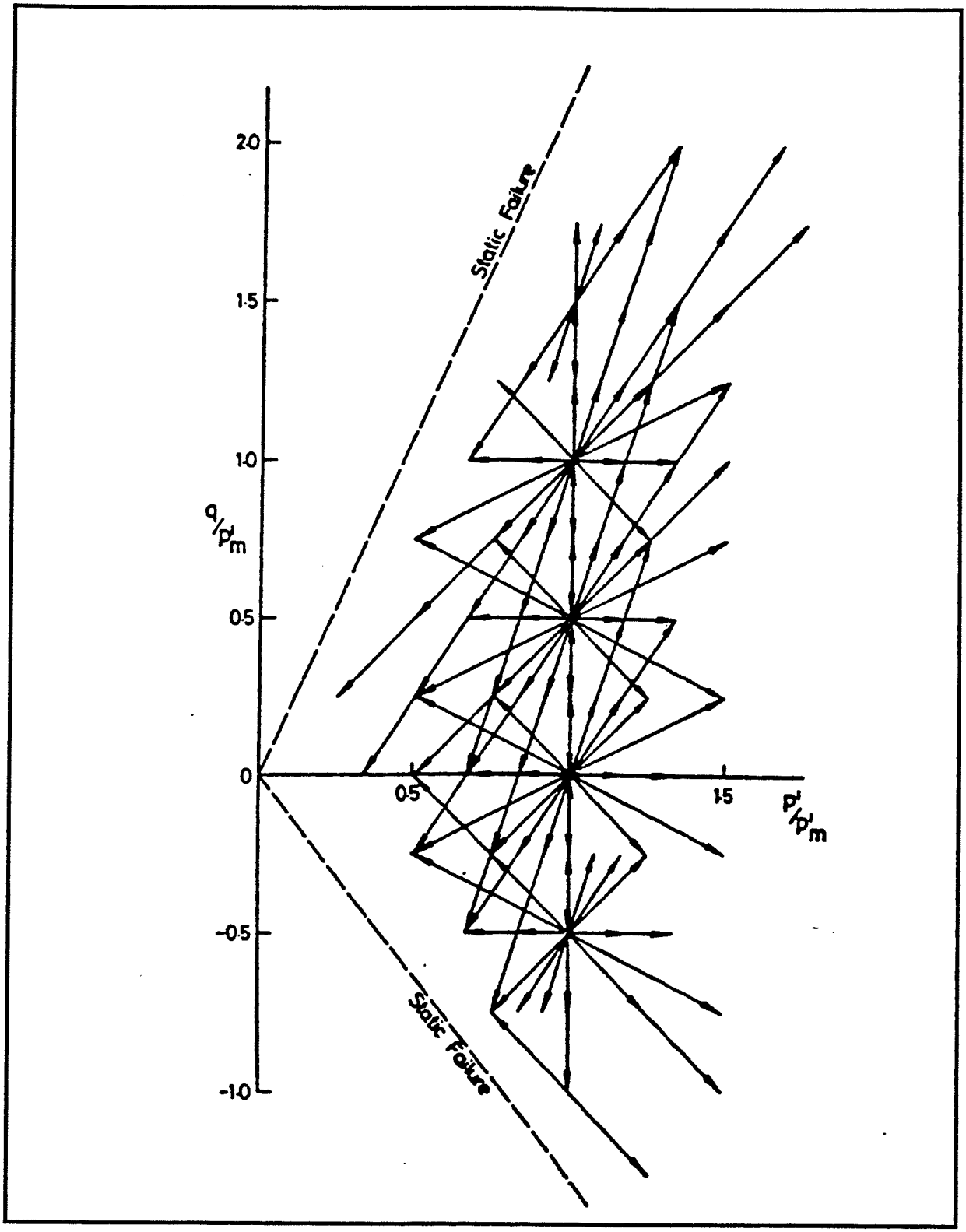

FIG. 2.15. MULTIPLE STRESS PATHS USED IN THE TESTS AT NOTTINGHAM (AFTER BROWN AND PAPAIN, 1985).

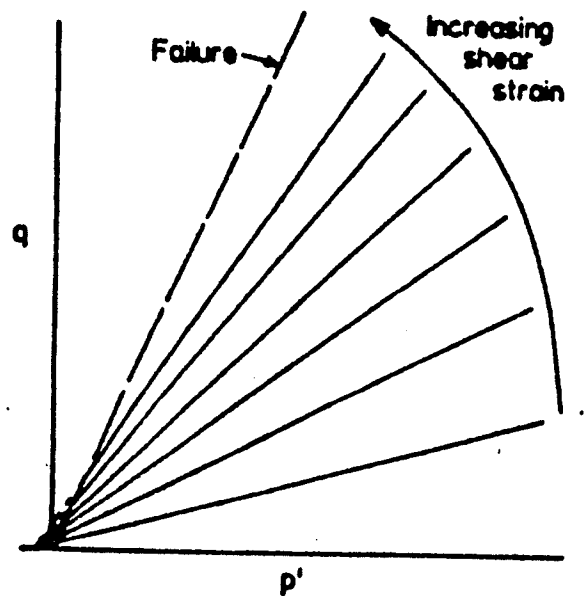

A. SHEAR STRAIN CRITERION

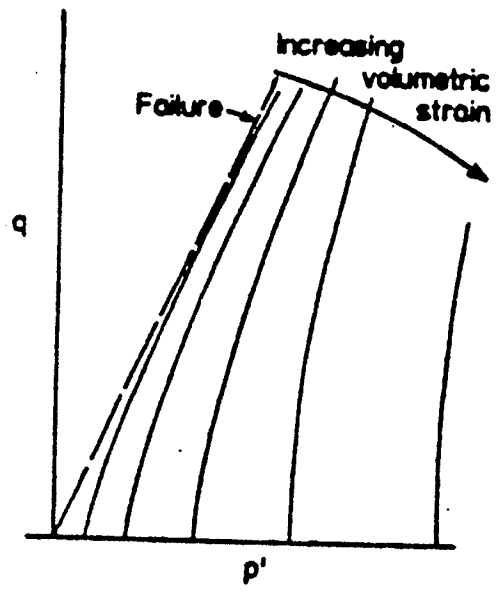

B. VOLUMETRIC STRAIN CRITERION

FIG. 2.16. STRAIN CONTOURS (AFTER BROWN, 1985).

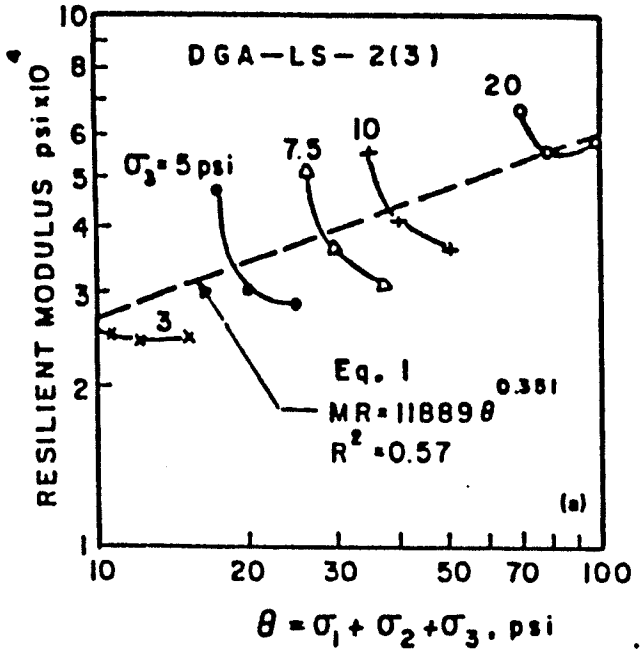

A.) MEAN NORMAL STRESS VS. RESILIENT MODULUS.

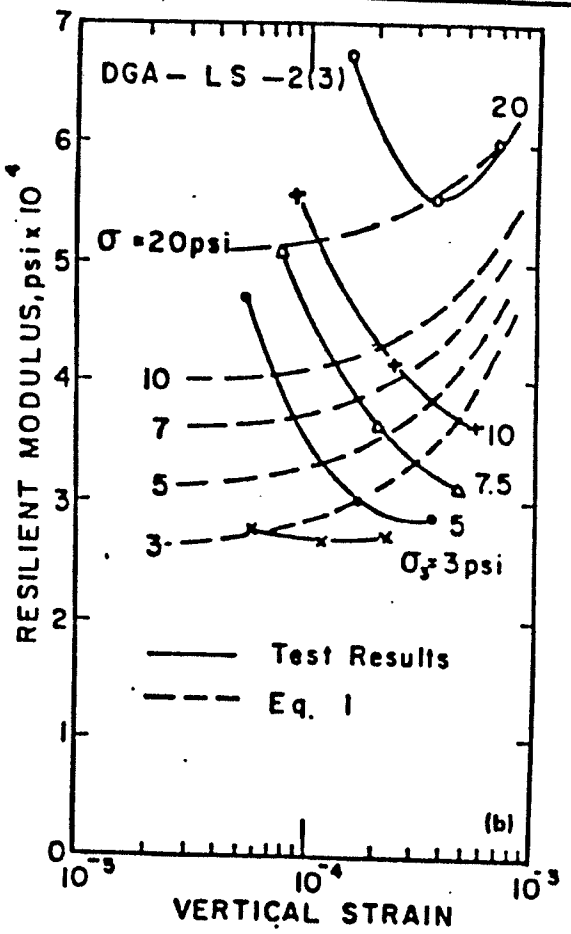

B.) VERTICAL STRAINS VS. RESILIENT MODULUS

FIG. 2.17. LABORATORY TEST RESULTS ON GRANULAR BASE MATERIALS FITTED TO K-θ MODEL. (AFTER UZAN, 1985)

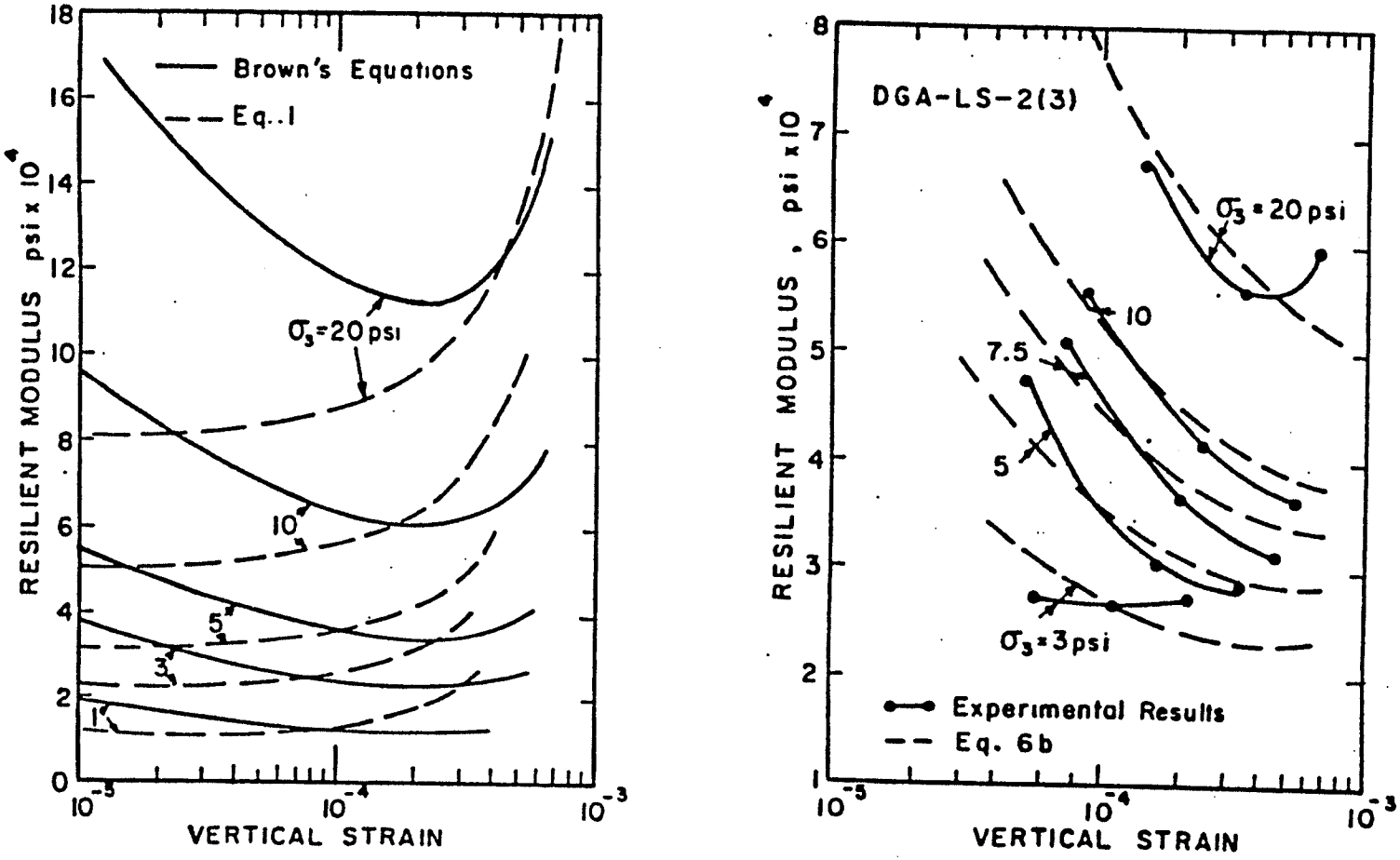

FIG. 2.18. BROWN'S MODEL FITTED TO K-θ MODEL (USING RESULTS FROM UZAN, 1985: (SEE FIG. 2.17)

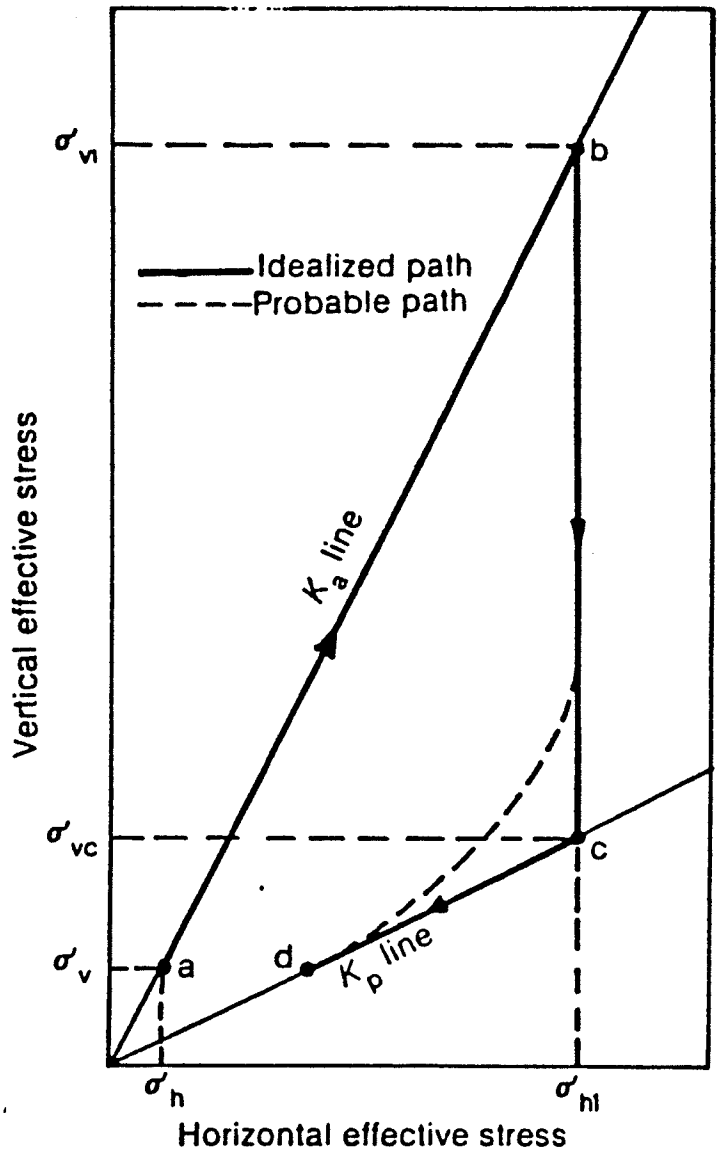

FIG. 2.19. VARIATION OF LATERAL STRESSES BEHIND A RETAINING WALL DURING COMPACTION (AFTER INGOLD, 1980)

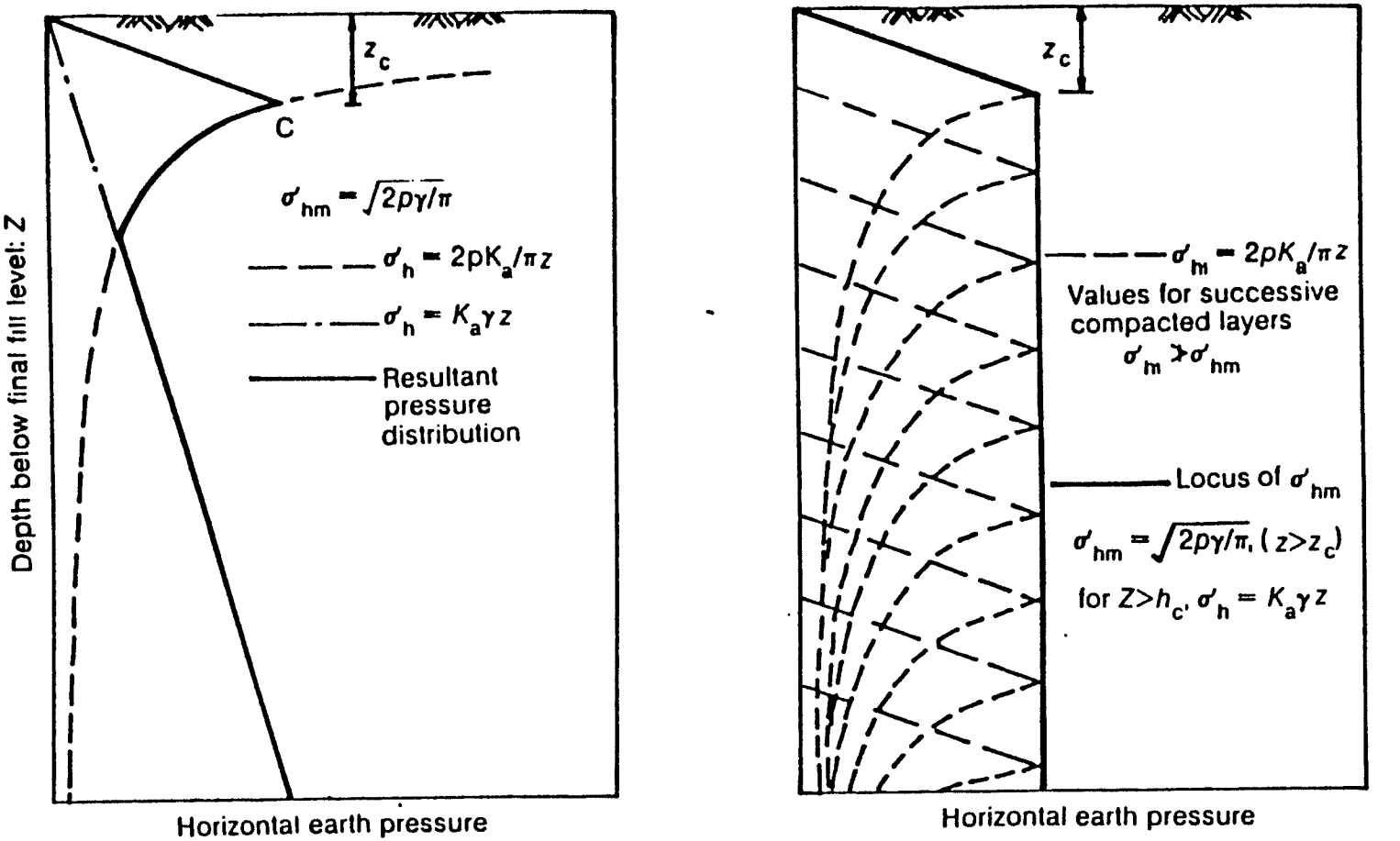

A.) FILL COMPACTED IN ONE LIFT

B.) FILL COMPACTED IN THIN LIFTS

FIG. 2.20. MAGNITUDE OF LATERAL PRESSURES BEHIND A RIGID WALL (AFTER BROMS 1971, INGOLD 1980)

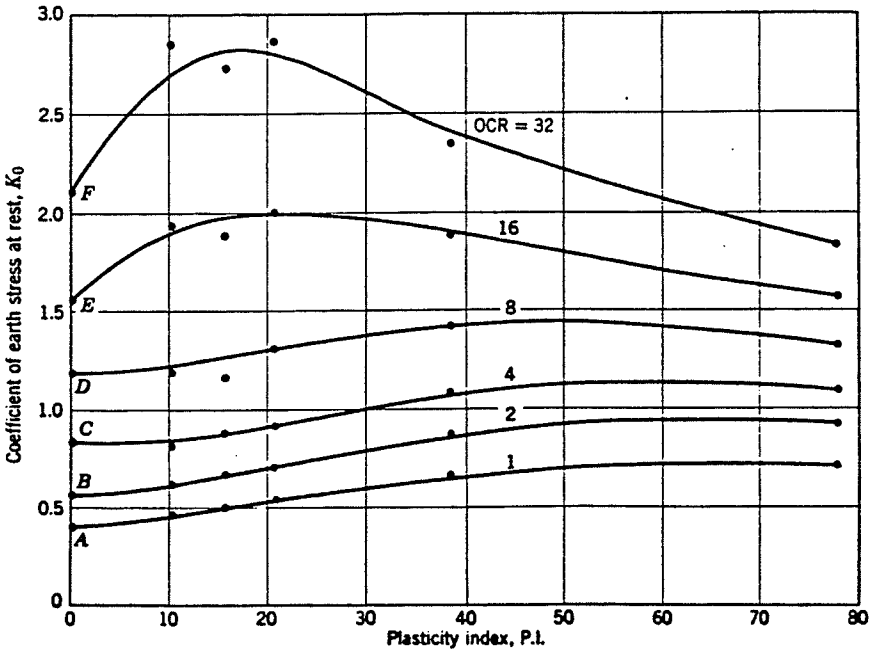

FIG. 2.21. VARIATION OF Ko WITH OVERCONSOLIDATION RATIOS (AFTER BROOKER AND IRELAND, 1965)

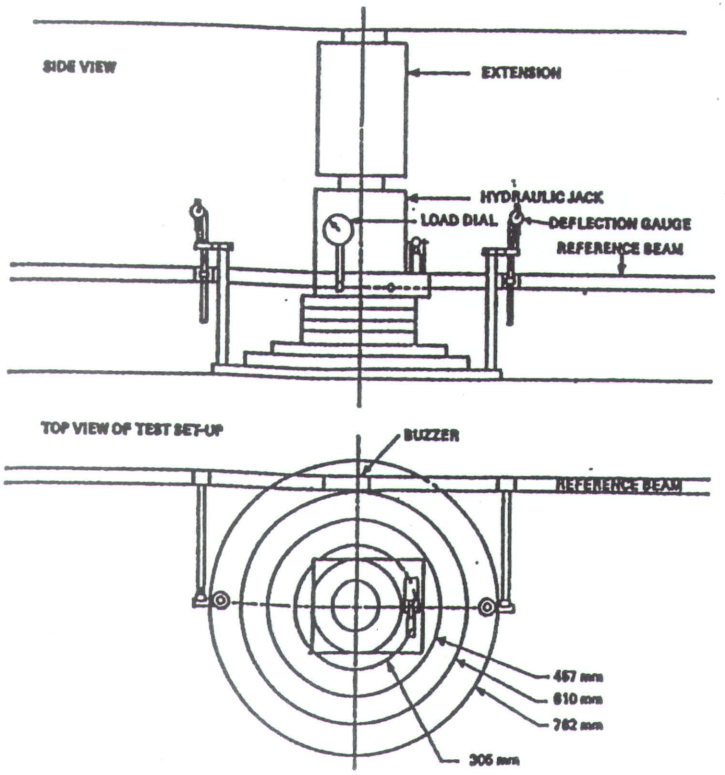

A.) SCHEMATIC.

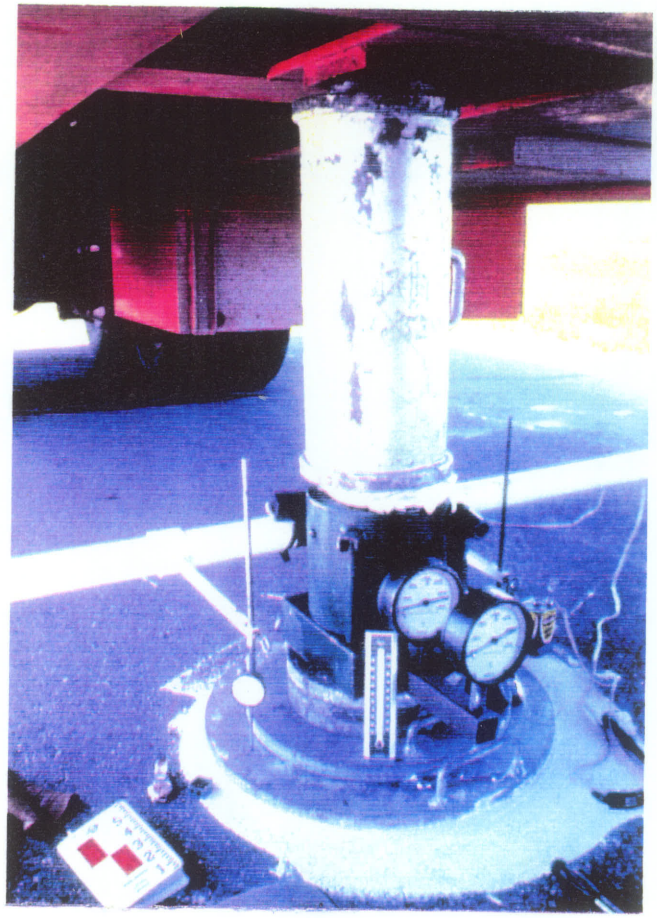

B.) PHOTOGRAPH.

FIG. 2.22. SET-UP FOR REPETITIVE AND NON-REPETITIVE PLATE LOAD TEST (TRANSPORT CANADA)

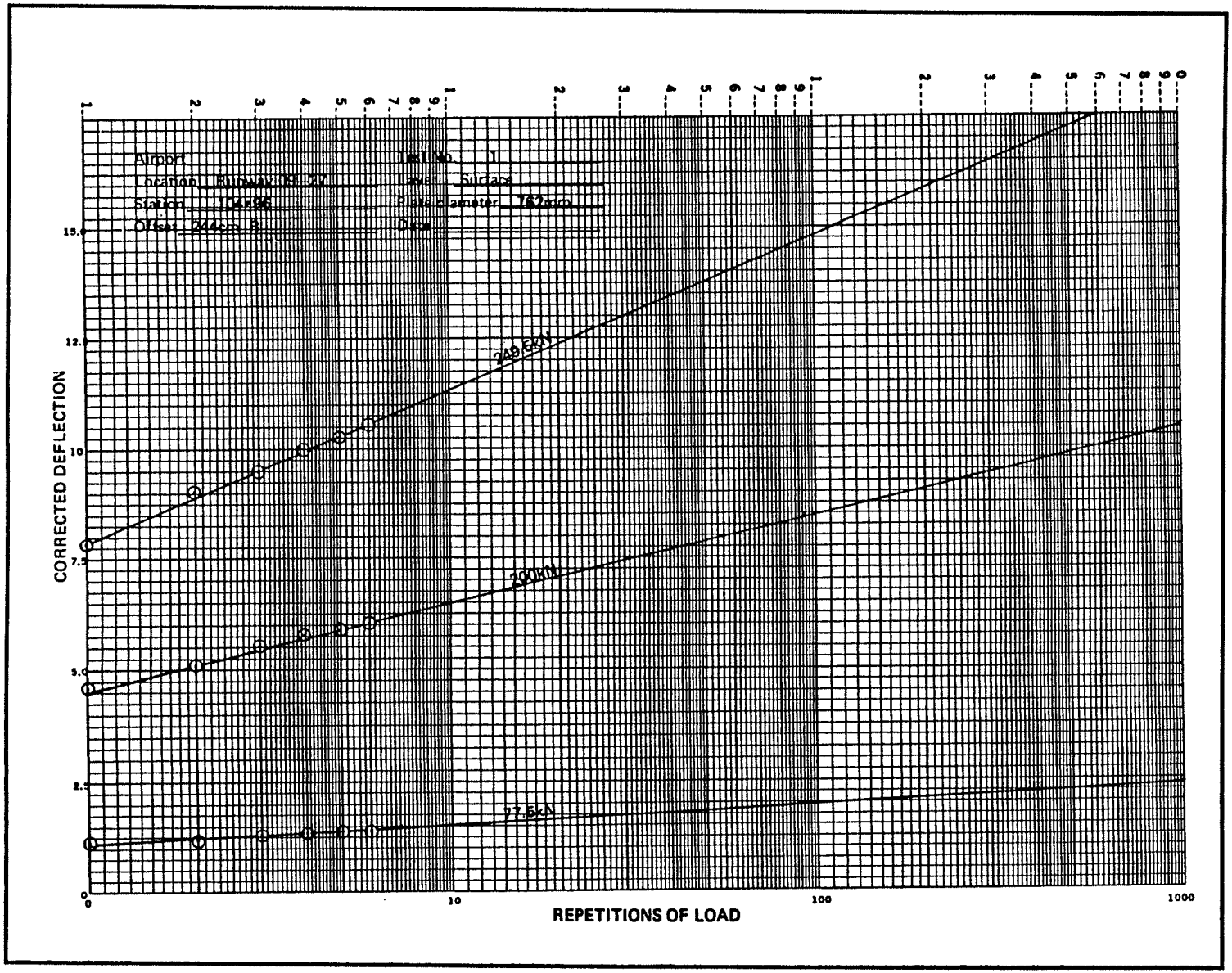

FIG. 2.23. TYPICAL RESULTS FROM A PLATE LOAD TEST.

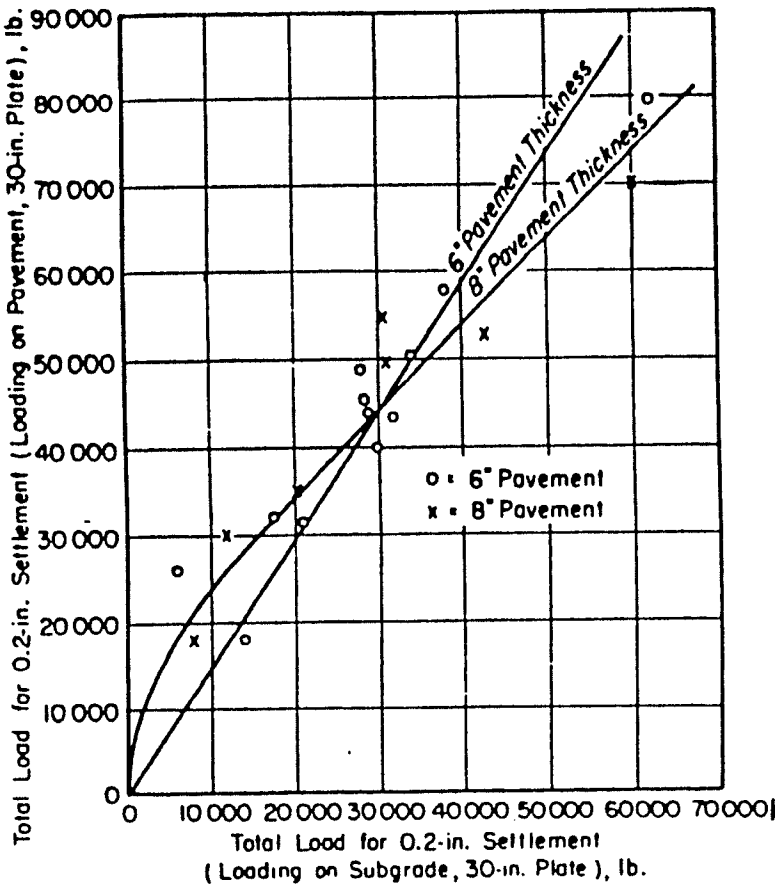

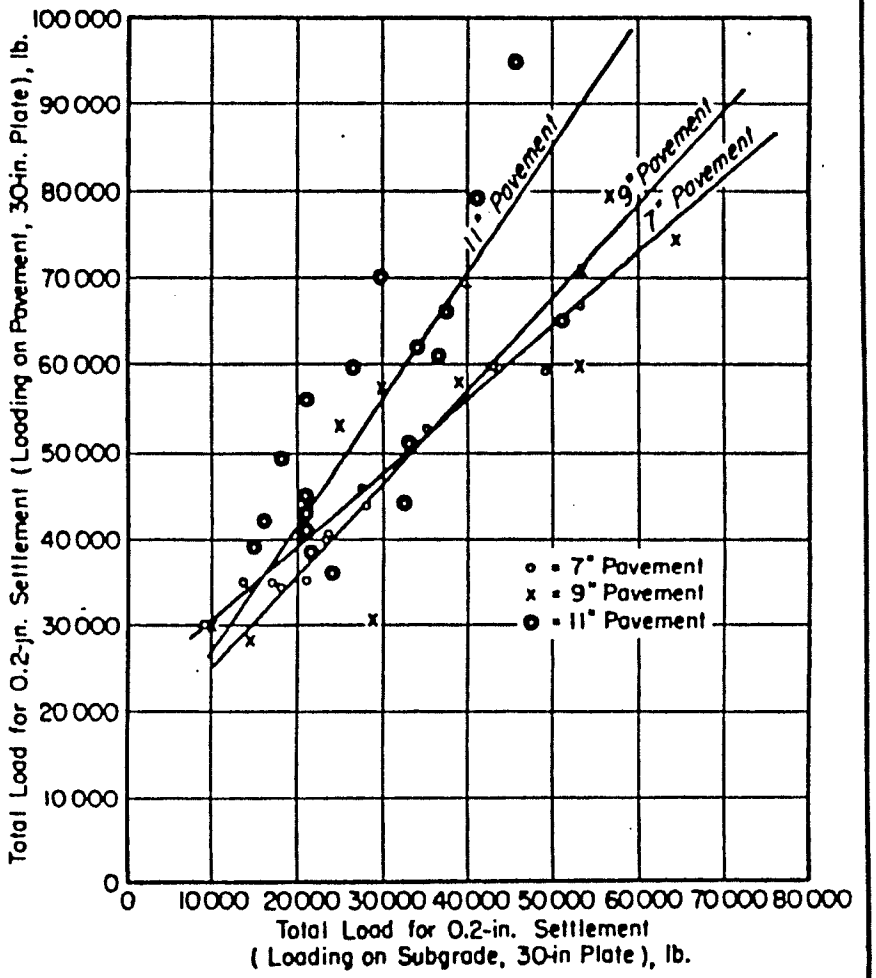

FIG. 2.24. CORRELATION BETWEEN LOAD ON SUBGRADE AND PAVEMENT (AFTER PALMER 1949).

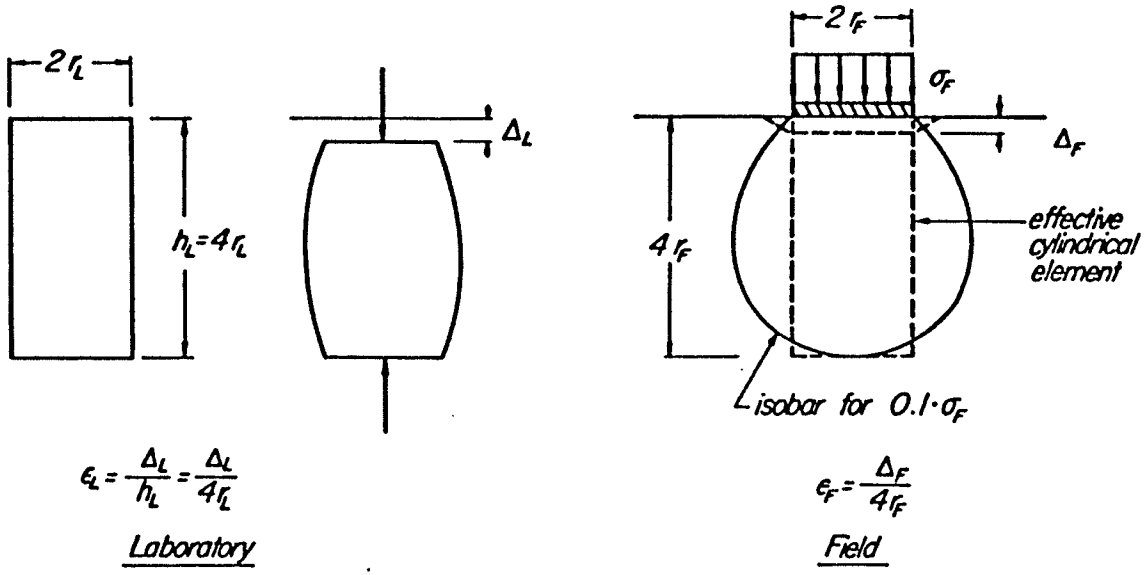

FIG. 2.25. RELATIONSHIP BETWEEN PLATE LOAD TEST AND TRIAXIAL TESTS (BURMISTER 1949, FINN AND MONISMITH 1984)

A. PHOTOGRAPH

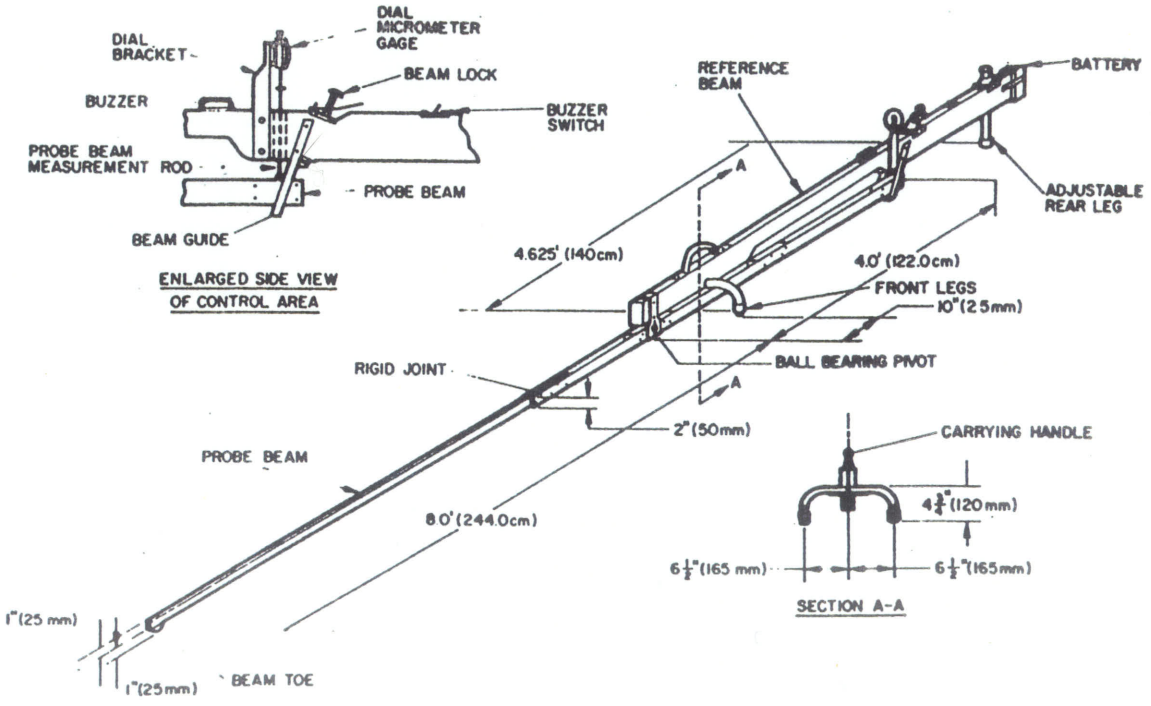

B. SCHEMATIC DETAILS

FIG. 2.26 THE BENKELMAN BEAM TEST

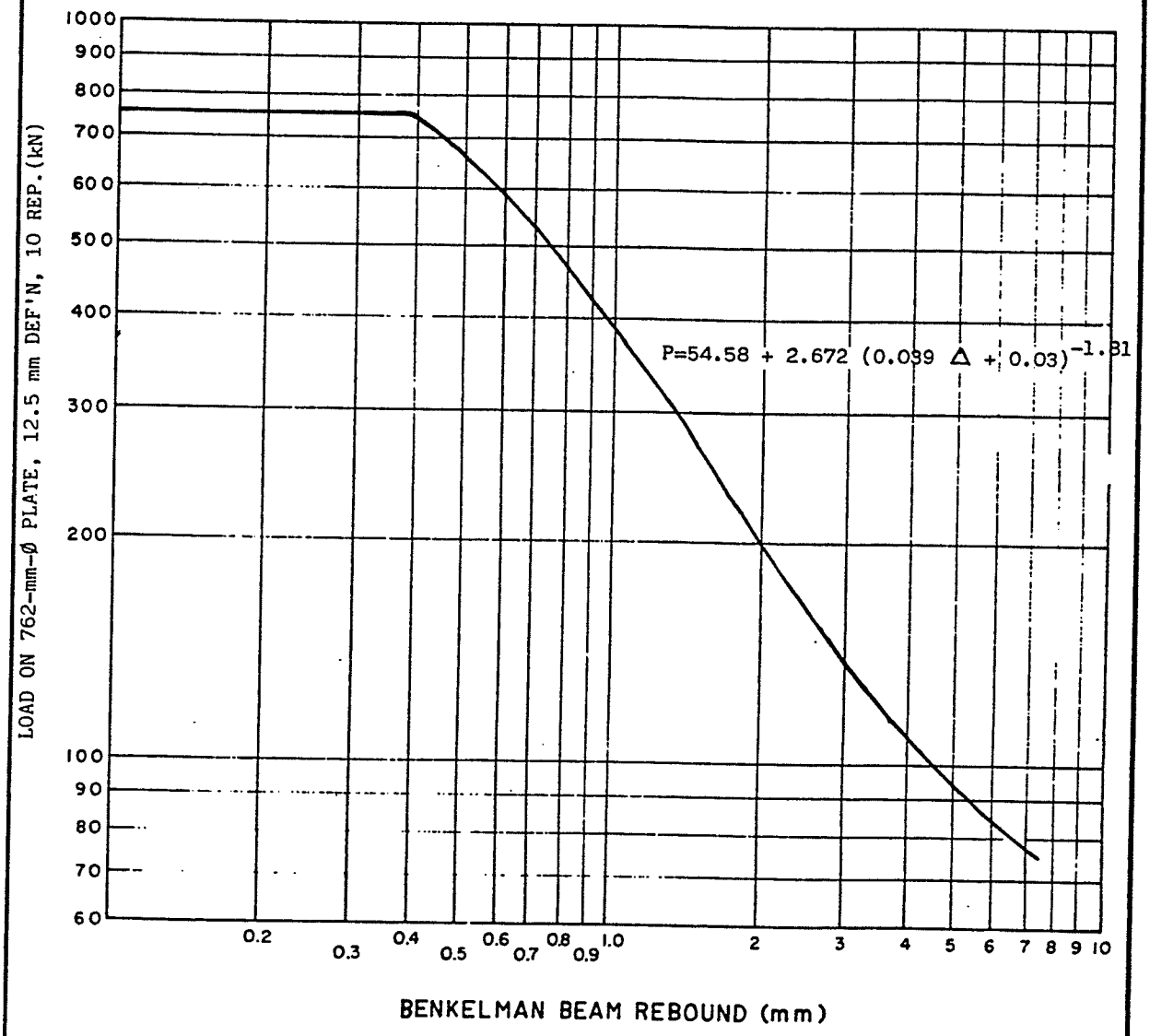

FIG. 2.27. CORRELATION BETWEEN BENKELMAN BEAM DEFLECTIONS AND SUBGRADE SUPPORT VALUE BY TRANSPORT CANADA METHOD (AFTER SEBASTYAN, 1969, TRANSPORT CANADA MANUAL SERIES AK-68-12-300).

A. THE SENSORS WITH THE STEEL WHEEL

B. THE COUNTER ROTATING MASS

FIG. 2.28. PHOTOGRAPHS OF DYNAFLECT MACHINE

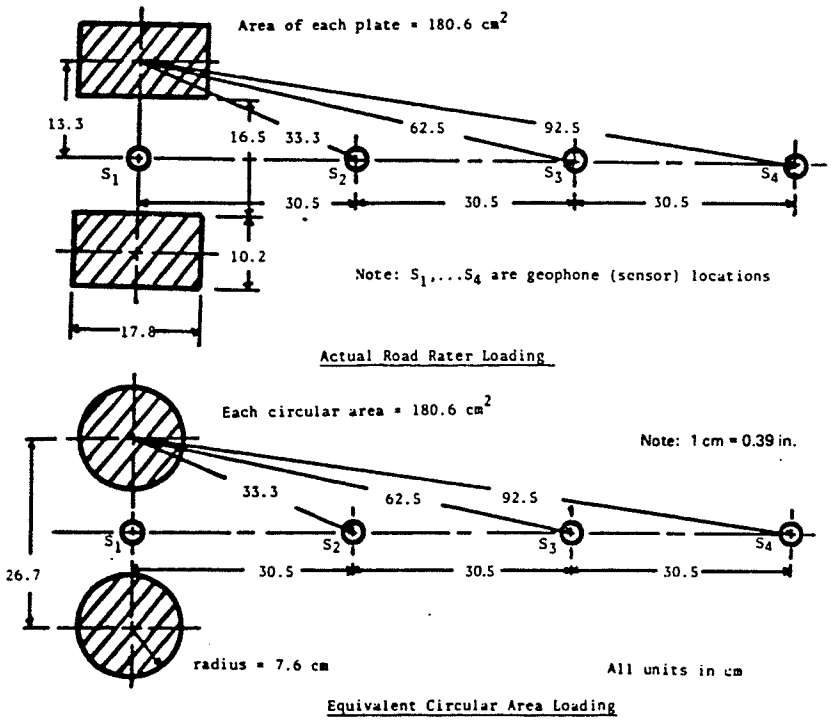

FIG. 2.29. SCHEMATIC OF A ROAD RATER MACHINE

A.) ACTUAL LOADING PADS AND DIMENSIONS

B.) EQUIVALENT CONFIGURATION FOR ANALYSIS

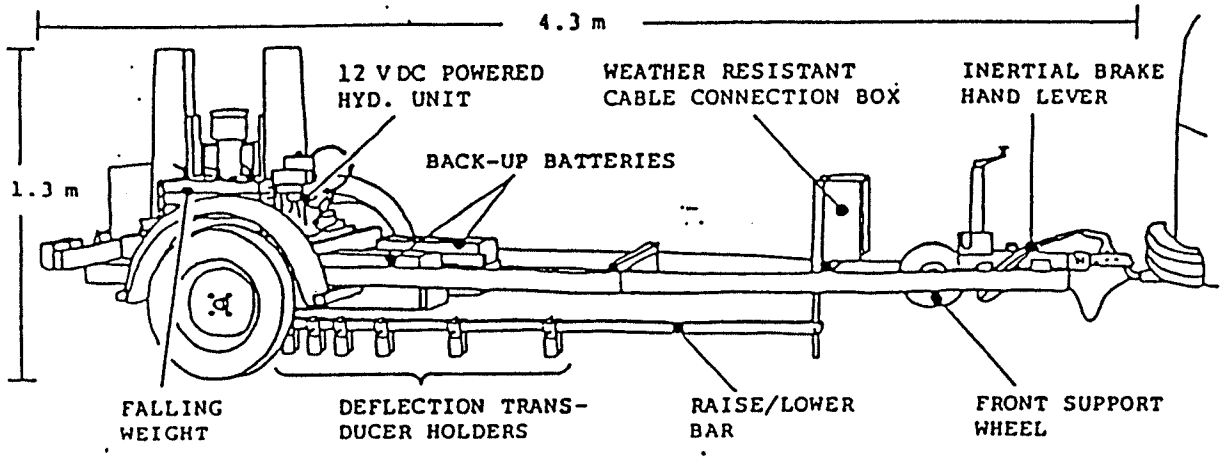

THE DYNATEST 8002 FALLING WEIGHT DEFLECTOMETER

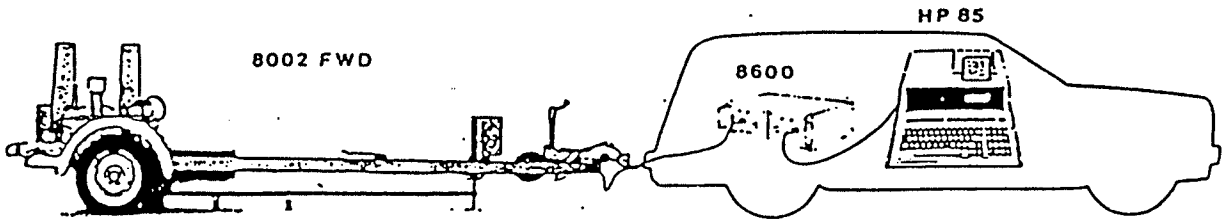

FIG. 2.30. SCHEMATIC OF THE FALLING WEIGHT DEFLECTOMETER

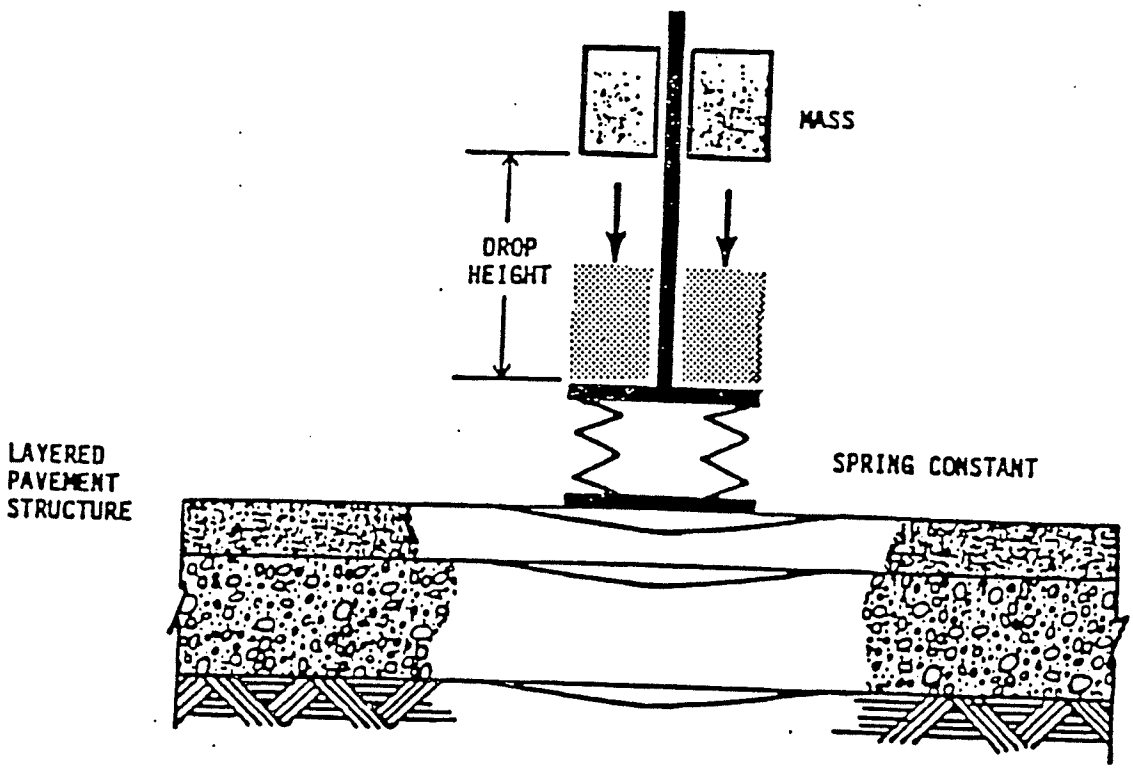

FIG. 2.31. SCHEMATIC OF THE FALLING WEIGHTS AND THE DAMPING BUFFERS ON THE FWD.

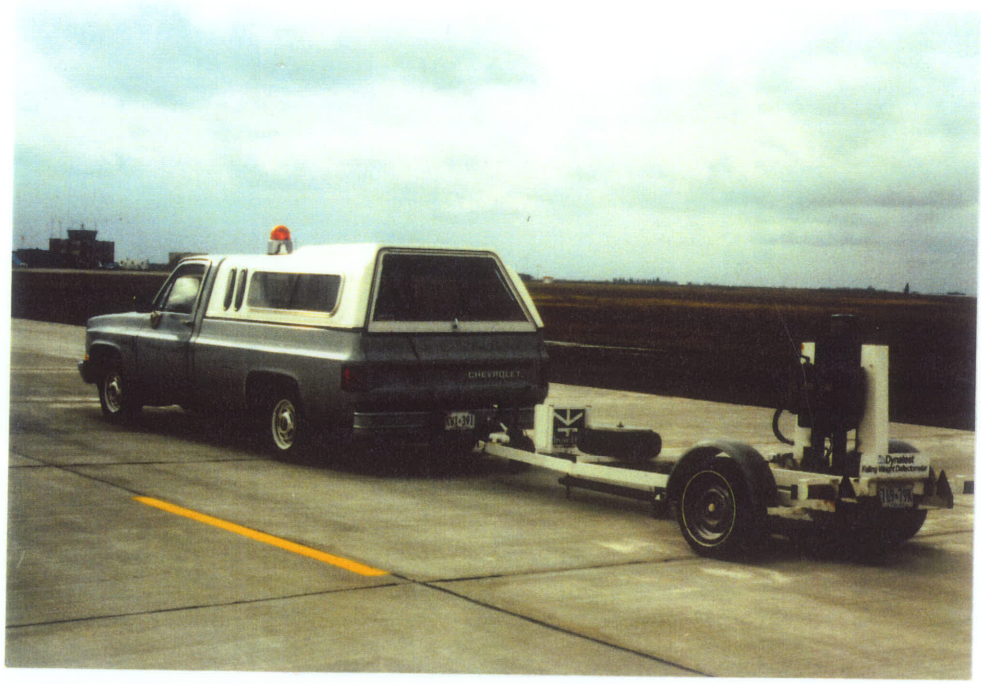

A. MODEL 8000 LIGHT WEIGHT MODEL

B. MODEL 8081, HEAVY WEIGHT MODEL

FIG. 2.32. PHOTOGRAPHS OF DYNATEST FWD (MODEL 8000) AND THE HWD (MODEL 8081)

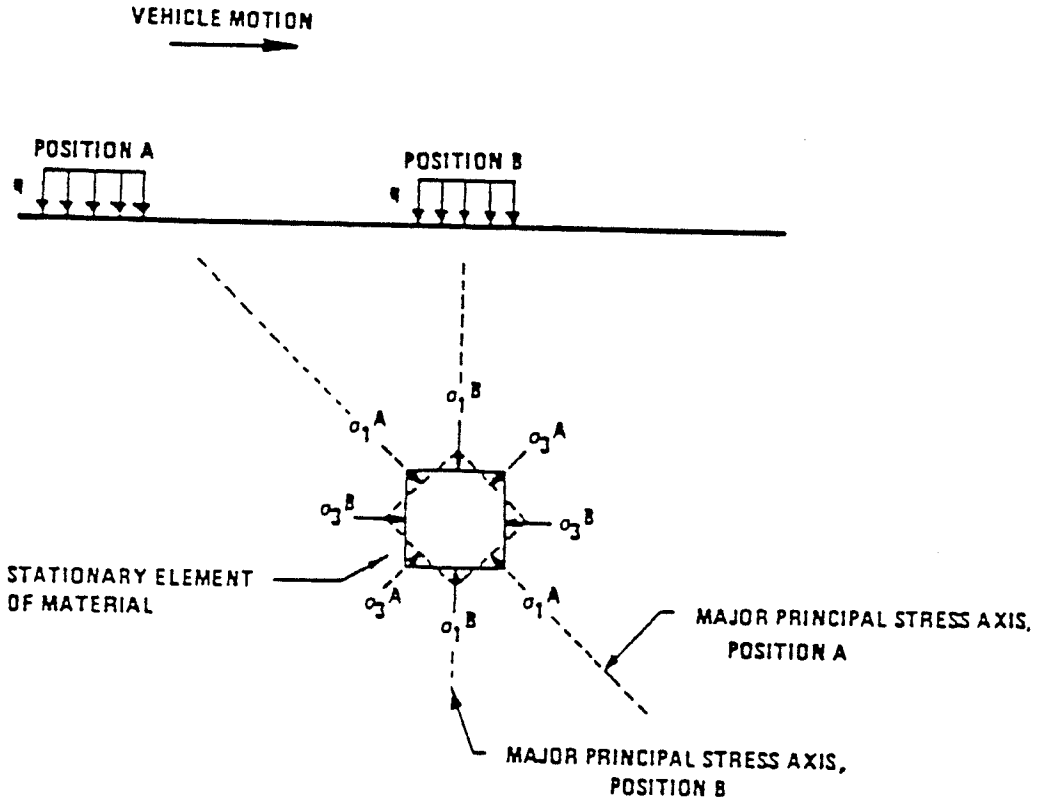

FIG. 2.33. ILLUSTAION OF THE ROTATION OF THE PRINCIPAL AXES OF A SOIL ELEMENT AS TRAFFIC PASSES BY. (AFTER HICKS AND MONISMTH, 1971)

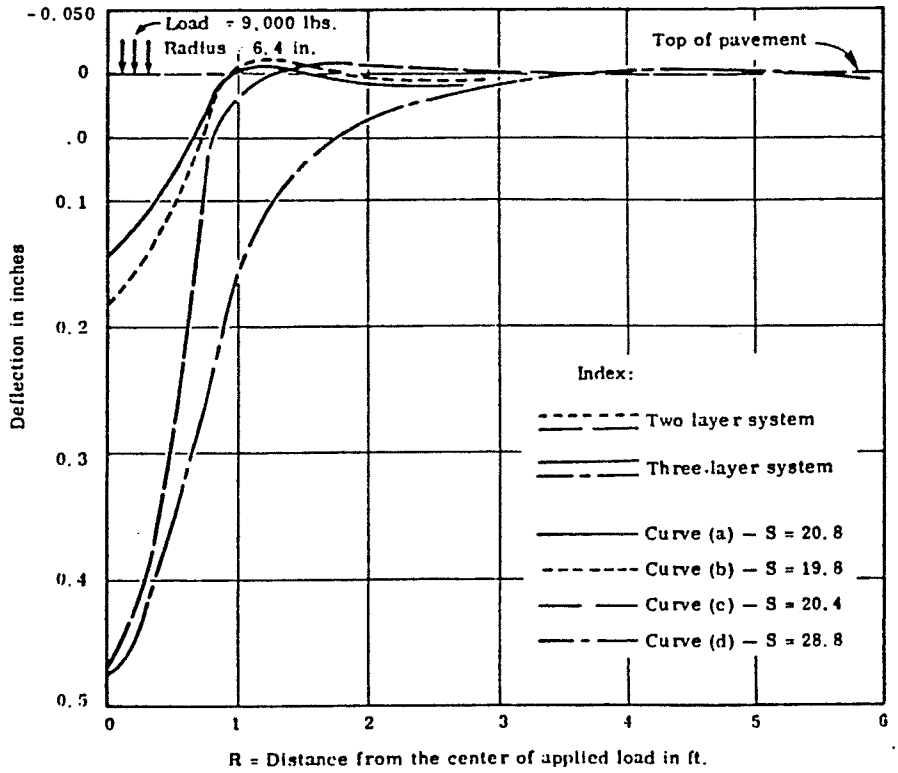

Curve Design	No. of Layers	E_s (psi)	2nd layer from top		Top layer		S	d_0
			E_2(psi)	h_2(in.)	E_1(psi)	h_1(in.)		
(a)	Three	30,000	1,000	5	30,000	2	20.8	0.147
(b)	Two	30,000	—	—	1,000	5	19.8	0.182
(c)	Two	30,000	—	—	1,000	15	20.4	0.469
(d)	Three	30,000	1,000	60	30,000	2	28.8	0.474

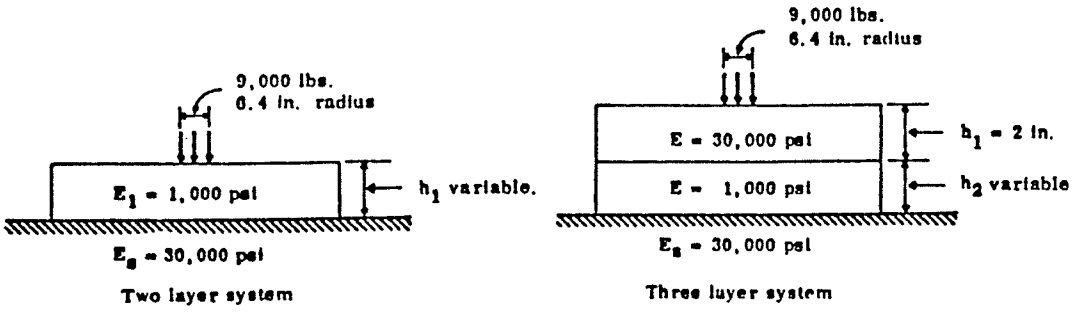

FIG. 2.34. ILLUSTRATION OF THE SPREADABILITY CONCEPT (AFTER VASWANI, 1971)

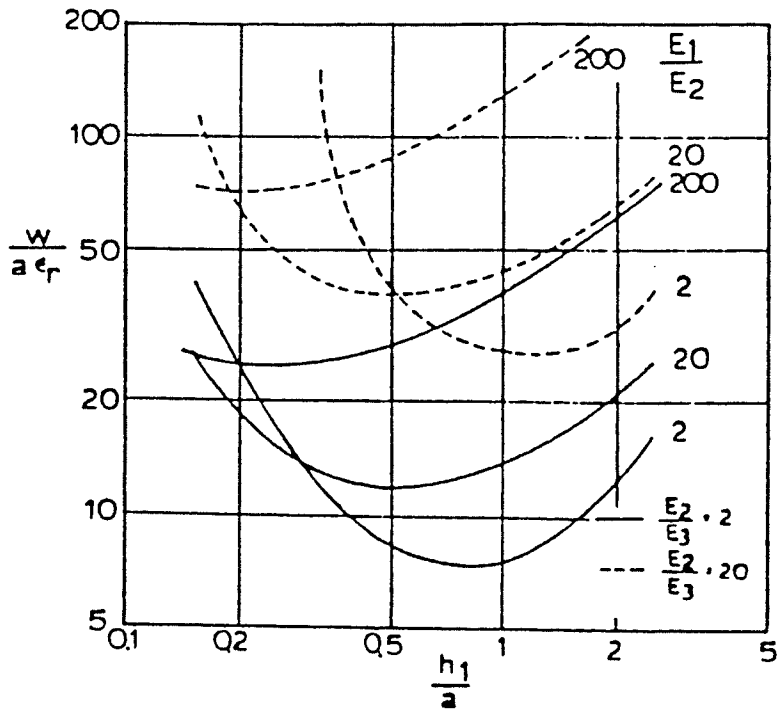

A.) DEFLECTION CRITERION

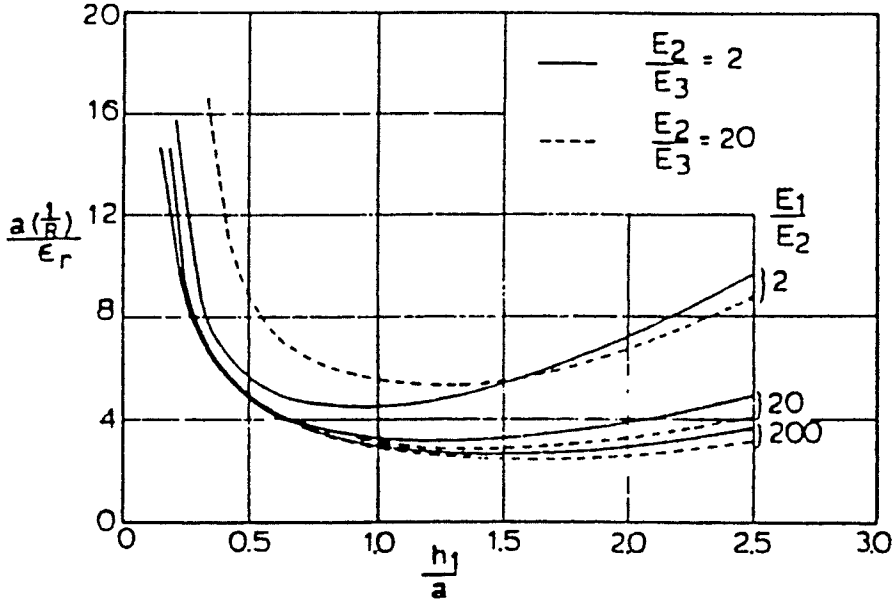

B.) CURVATURE CRITERION

FIG. 2.35. CRITERIA TO MEASURE PAVEMENT RESPONSE (AFTER HUANG, 1971)

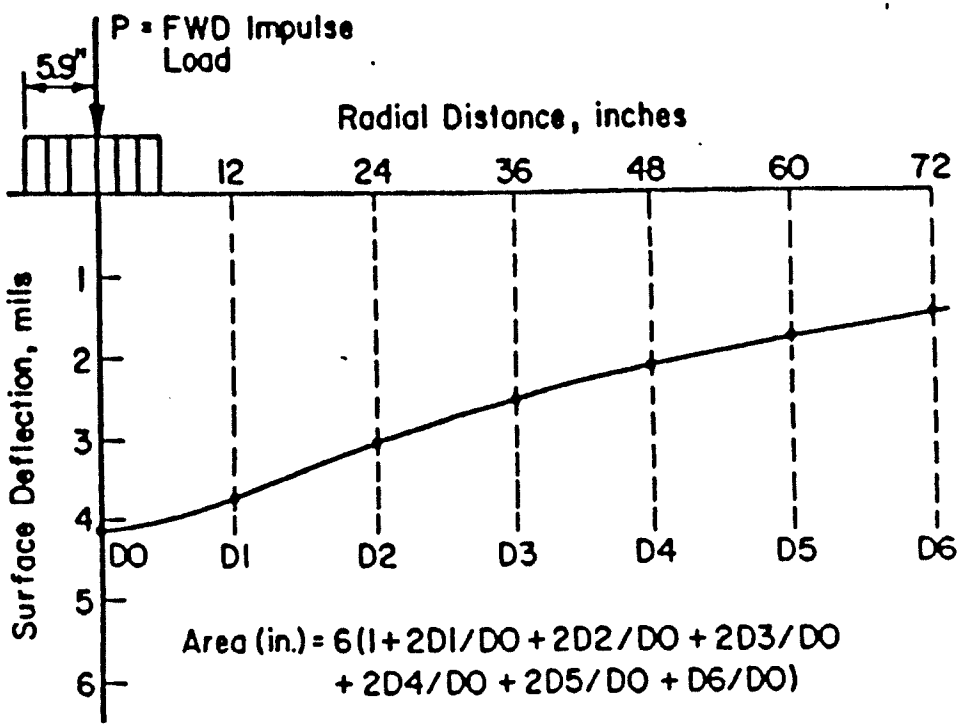

FIG. 2.36. ILLUSTRATION OF THE "AREA" CONCEPT

(AFTER HOFFMAN AND THOMPSON 1982)

	SI SYSTEM						ENGLISH SYSTEM					
R'S (MM/IN)	0	237	361	1356	1651	0	0.00	9.33	14.23	53.38	65.00	0.00
E(1) (MPA/PSI)	2760	->	->	->	->	->	401000	->	->	->	->	->
E(2) (MPA/PSI)	168	159	149	->	->	->	24400	23100	21600	->	->	->
E (3)(MPA/PSI)	74	74	75	101	115	0	10600	10700	10900	14600	16700	0
MDEF(MCR/MILS)	967.0	704.0	571.2	154.8	114.2	0.0	38.07	27.71	22.49	6.09	4.50	0.00
CDEF(MCR/MILS)	967.0	703.7	571.1	154.6	114.4	0.0	38.07	27.70	22.48	6.09	4.50	0.00

SUMMARY OF DERIVED ELASTIC MODULUS VS DYNAMIC STRESS LEVEL RELATIONSHIPS (IN SITU ONLY)

ELEMENT MODULUS(MPA/PSI): $E(2) = 575 * SIG1^{0.44}$ * $E(2) = 9510 * SIG1^{0.44}$

SURFACE MODULUS(MPA/PSI): $E(3) = 19.00 * SIG1^{-0.33}$ * $E(3) = 14400 * SIG1^{-0.33}$

ELEMENT MODULUS(MPA/PSI): (APPROXIMATE) $E(3) = 11.40 * SIG1^{-0.33}$ * $E(3) = 8670 * SIG1^{-0.33}$

NOMENCLATURE:
- R = DISTANCE FROM CENTER OF CIRCULAR LOAD
- MDEF = MEASURED DEFLECTION (FROM CURVEFIT DEFLECTION BOWL)
- CDEF = CALCULATED DEFLECTION (FROM ISSEM4 LAYERED ELASTIC SOLUTION)
- SURFACE MODULUS (SUBSCRIPT 0) = COMPOSITE MODULUS OF SEMI-INFINITE SUBGRADE

CRITICAL STRESSES AND STRAINS (LINEAR ELASTIC ASSUMPTIONS):

HORIZONTAL STRAINS, BOTTOM OF LAYERS	1 & 2:	-0.000571	-0.000094
VERTICAL STRAINS, TOP OF LAYERS	2...3:	0.002004	0.000247
VERTICAL STRESSES(MPA), TOP OF LAYERS	2...3:	0.3718	0.0172
VERTICAL STRESSES(PSI), TOP OF LAYERS	2...3:	53.92	2.50

FIG. 2.37. AN EXAMPLE OUTPUT FROM BACKCALCULATION PROCEDURE (NOTE THE STEPPED LINE SHOWING THE LATERAL INFLUENCE OF VARIOUS LAYERS)

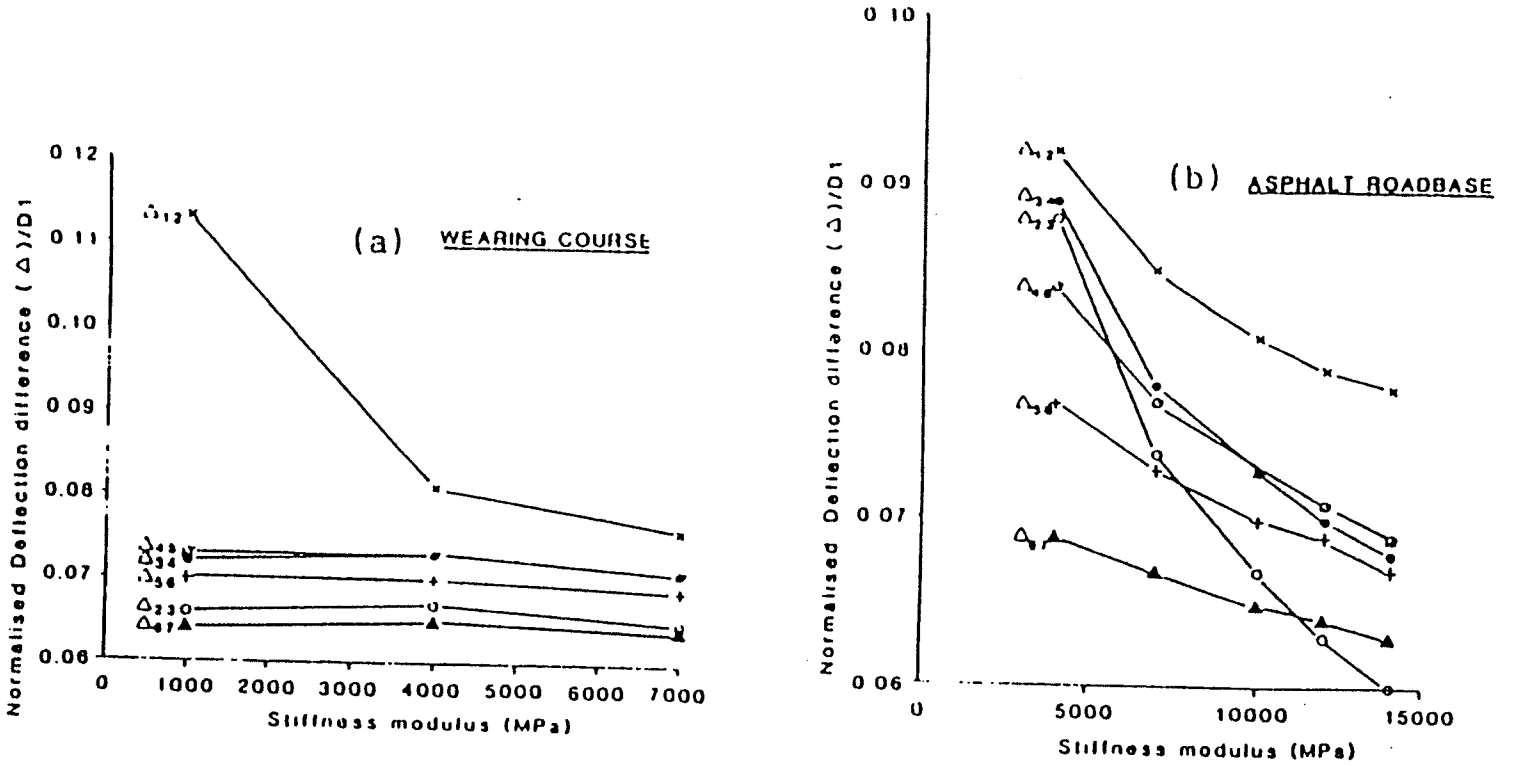

FIG. 2.38. CONTRIBUTIONS OF DIFFERENT LAYERS TO THE SHAPE OF THE DEFLECTION BASIN (AFTER BROWN ET AL 1986)

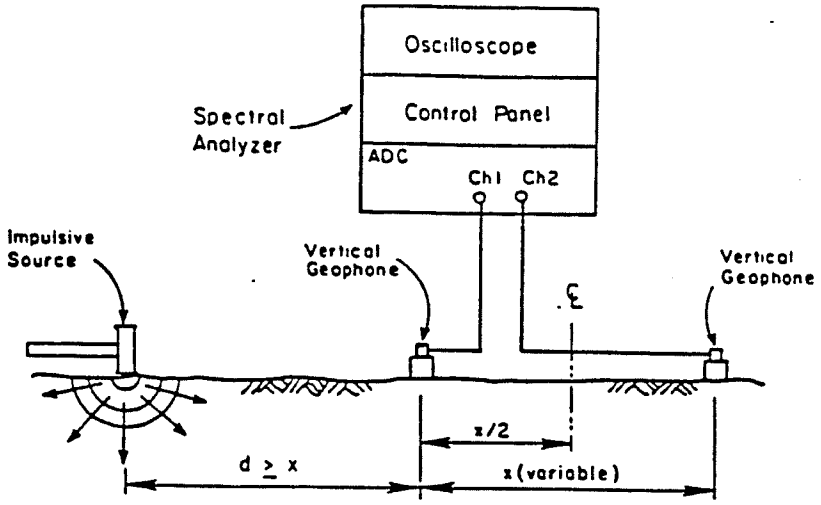

a - General Configuration

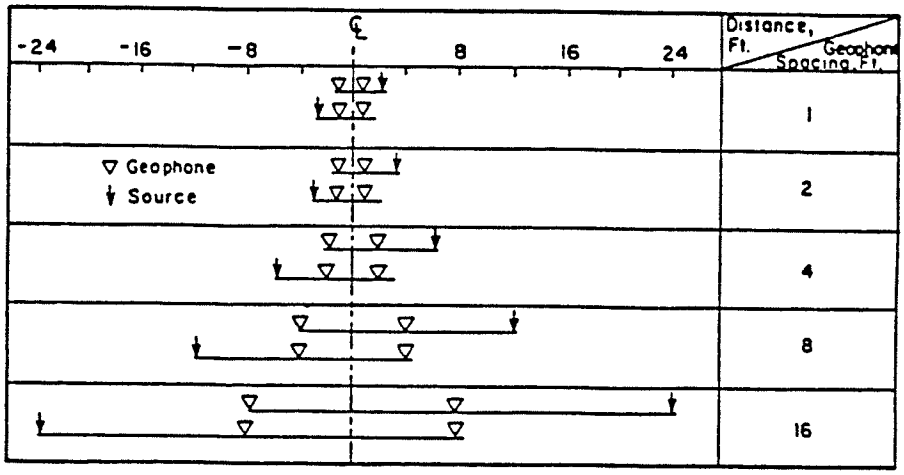

b - Schematic of Experimental Arrangement for SASW Tests

FIG. 2.39. SETUP FOR THE SURFACE WAVE SPECTRAL ANALYSIS METHOD (AFTER NAZARIAN 1989)

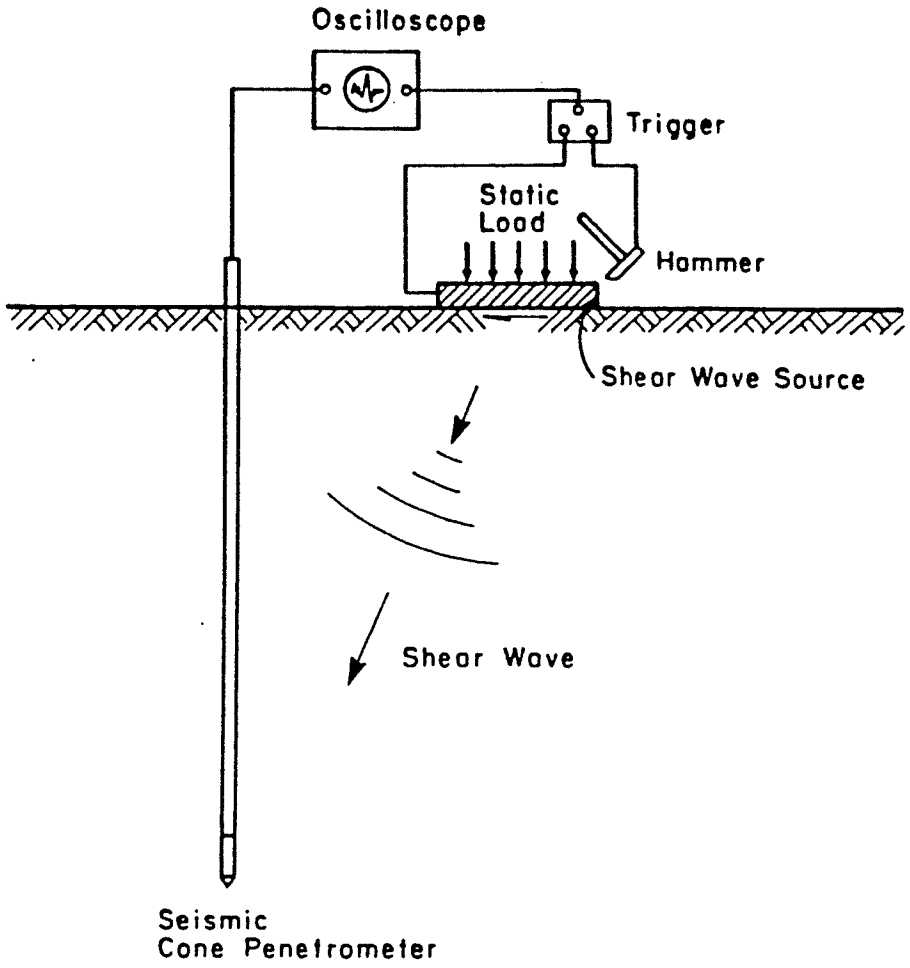

FIG. 2.40. SCHEMATIC OF A DOWNHOLE SHER WAVE TEST (AFTER CAMPANELLA ET AL 1986)

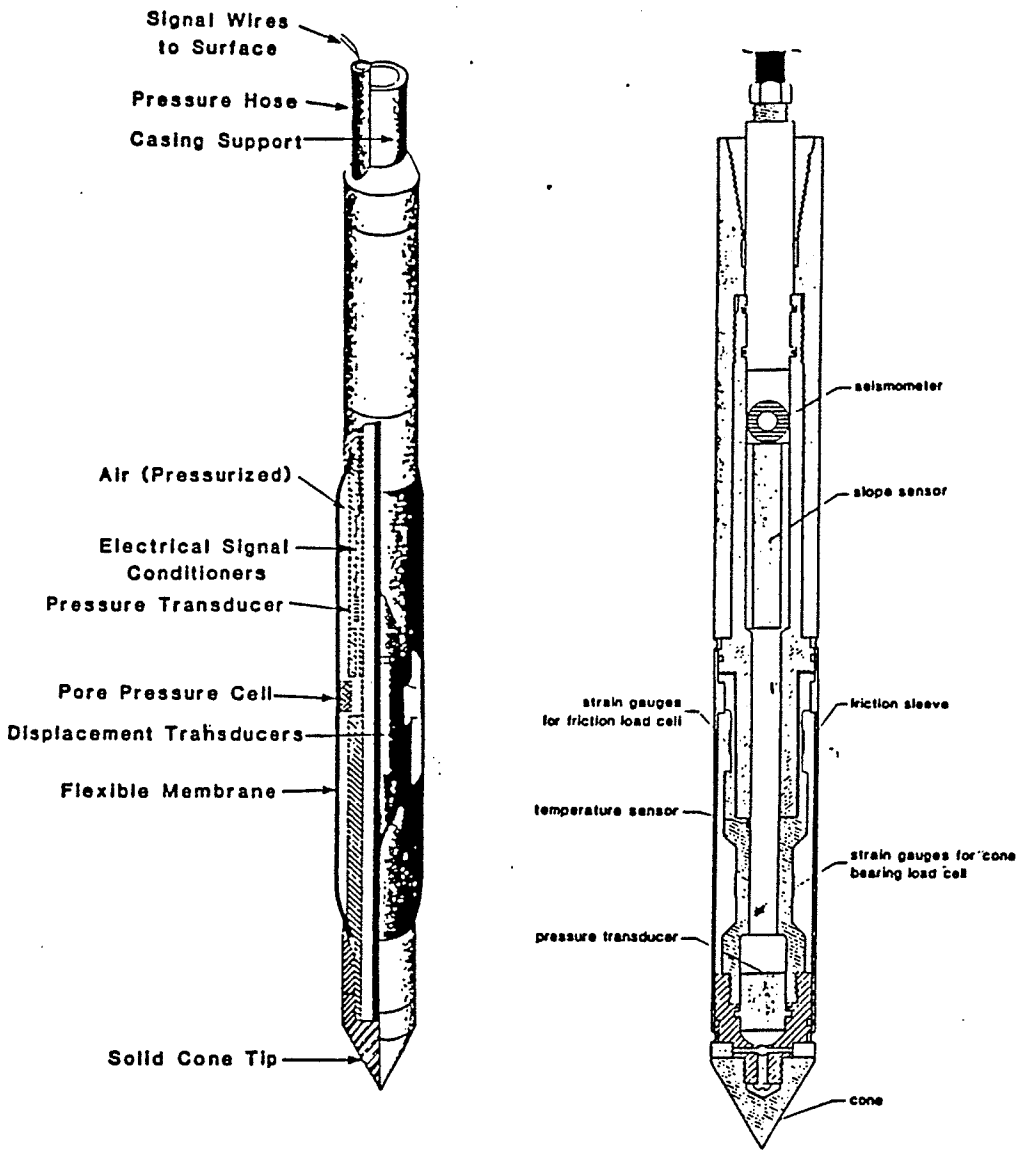

FIG. 2.41. A VIEW OF A CONE PRESSUREMETER (A) AND A SEISMIC CONE (B). (AFTER CAMPANELLA ET AL 1986, ROBERTSON ET AL 1985)

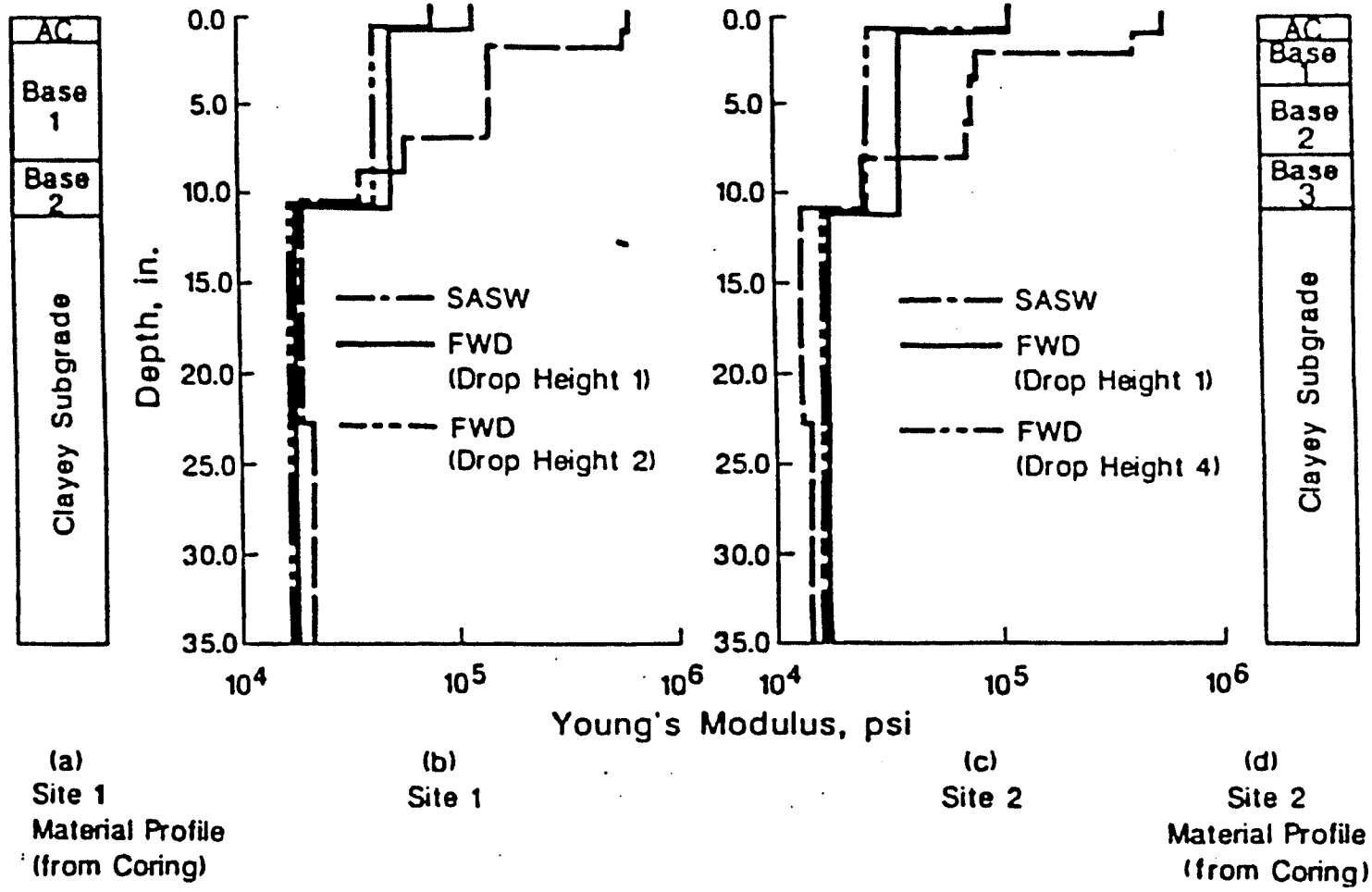

FIG. 2.42. TYPICAL RESULTS FROM THE SASW TESTS (AFTER NAZARIAN 1989)

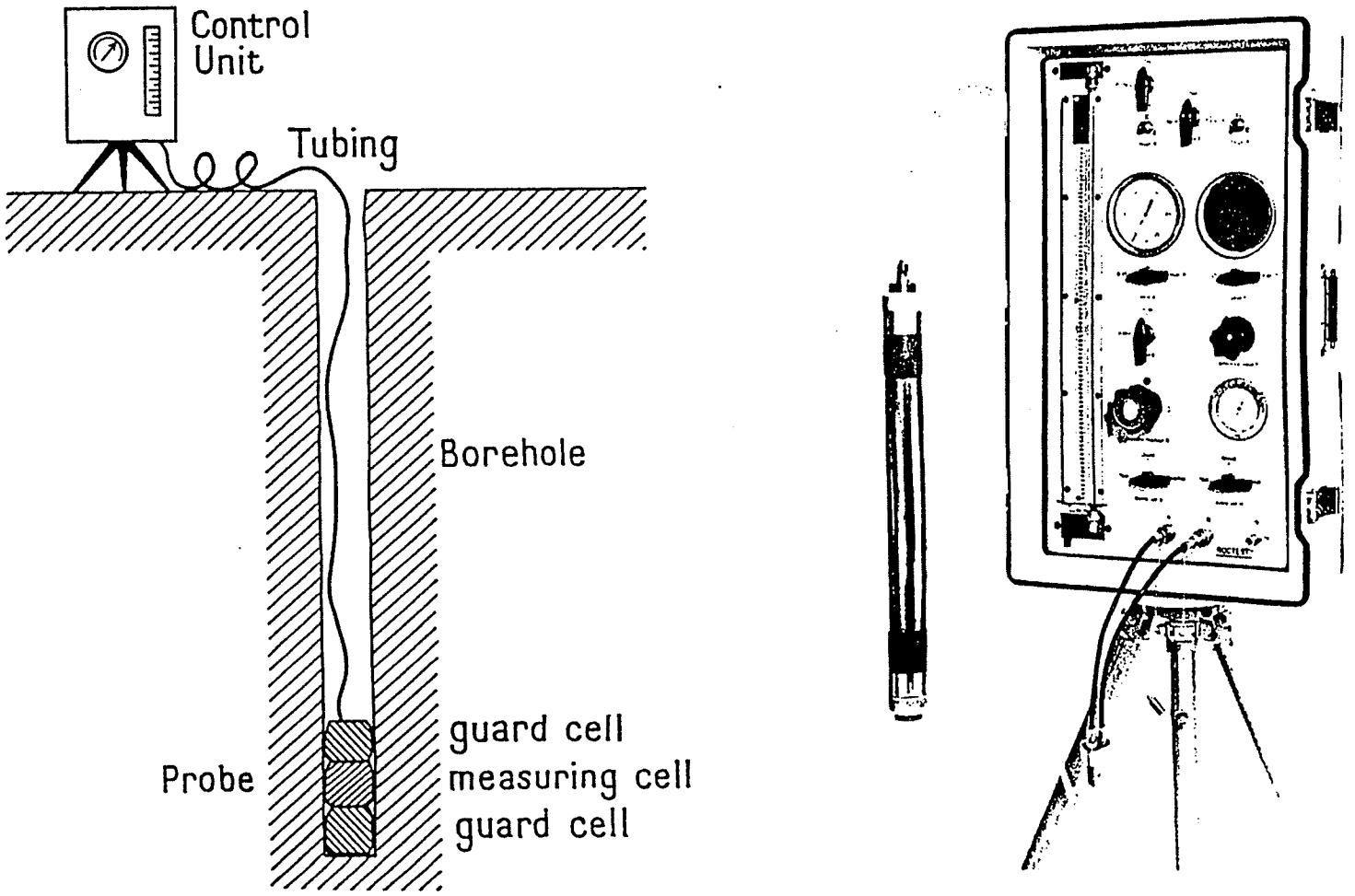

A.) SCHEMATIC VIEW.

B.) PHOTOGRAPH.

FIG. 2.43. THE MENARD PRESSURE METER (AFTER BAGUELIN ET AL, 1978).

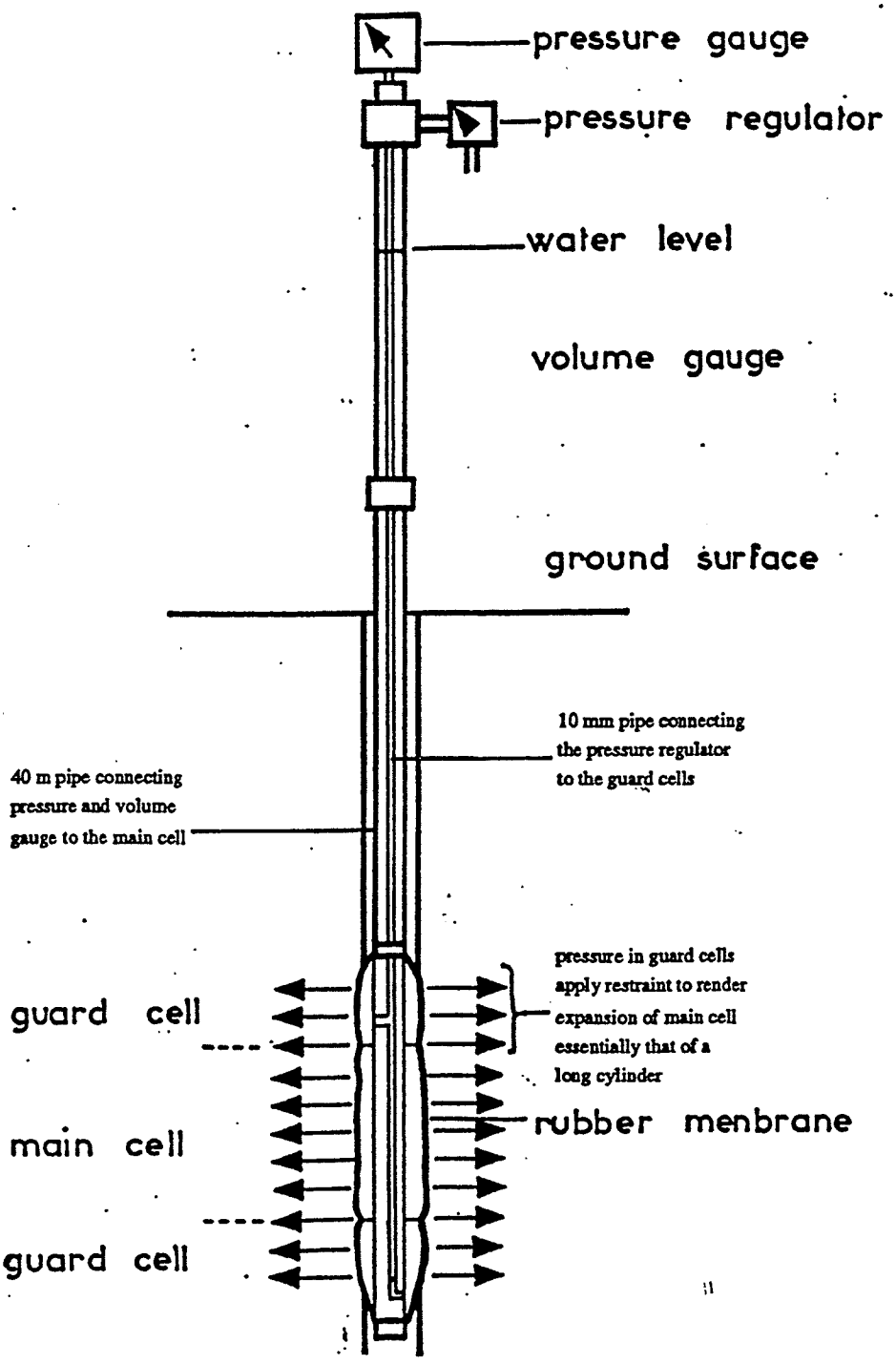

FIG. 2.44. SCHEMATIC REPRESENTATION OF THE FUNCTION OF THE GUARD CELL IN THE MENARD PRESSUREMETER

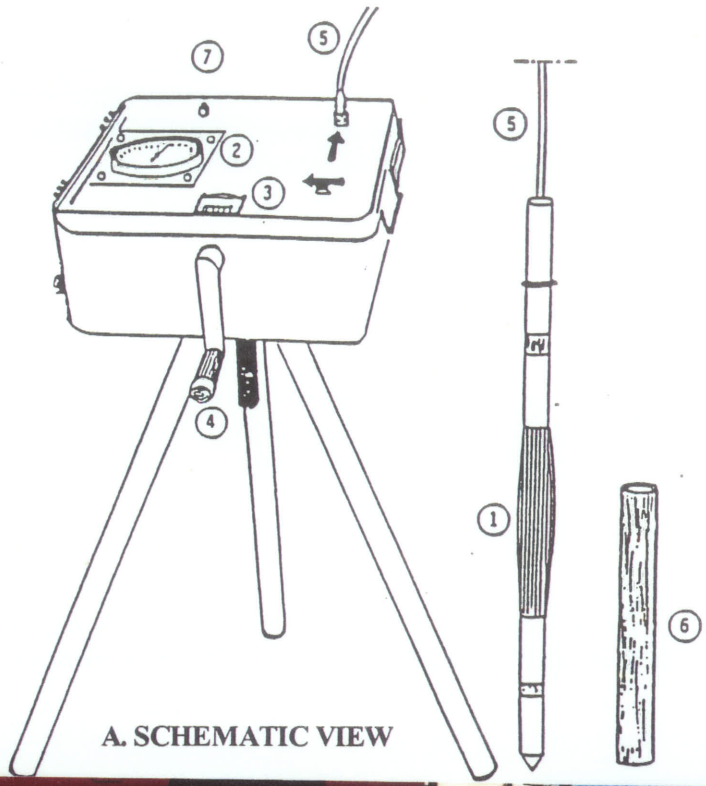

A. SCHEMATIC VIEW

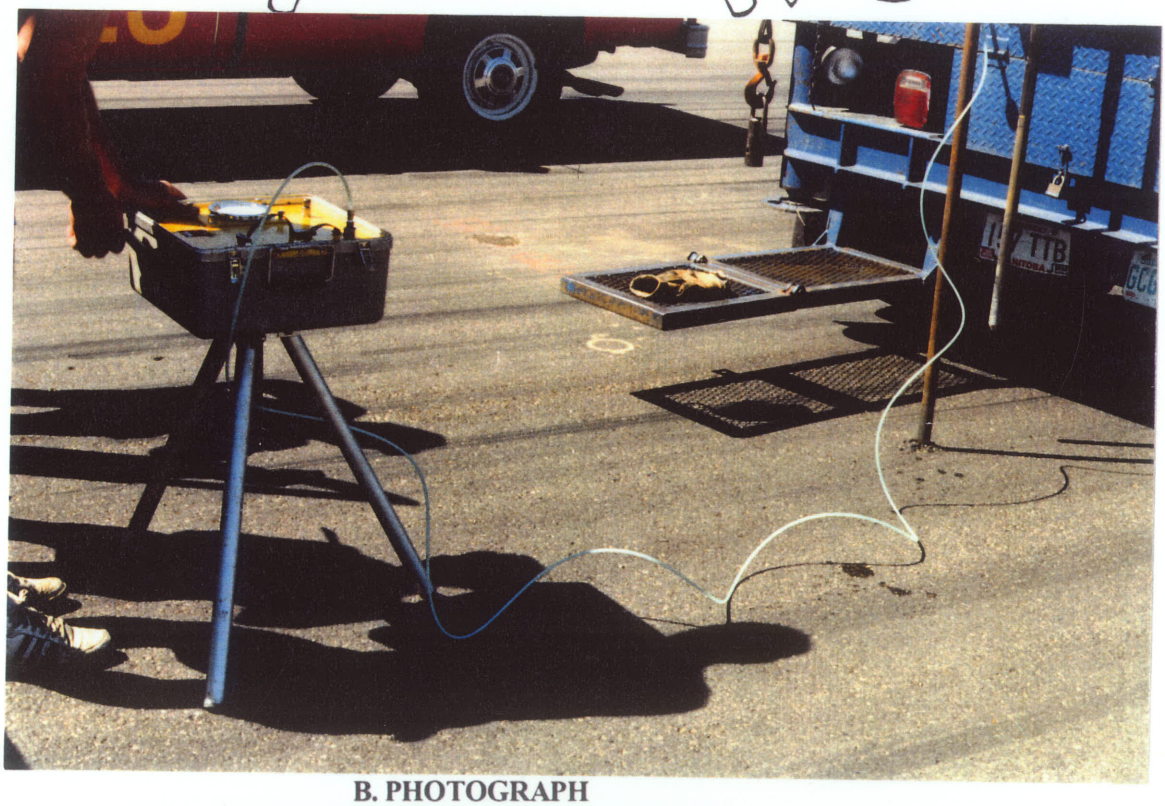

B. PHOTOGRAPH

FIG. 2.45. THE PENCEL PRESSUREMETER

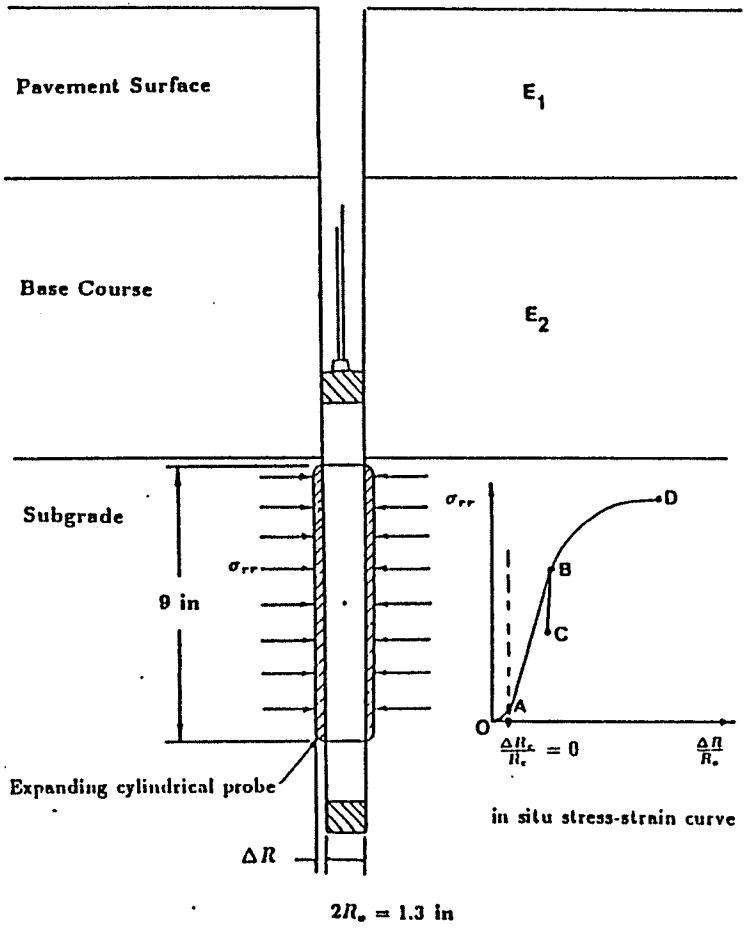

A.) SCHEMATIC OF THE TEST

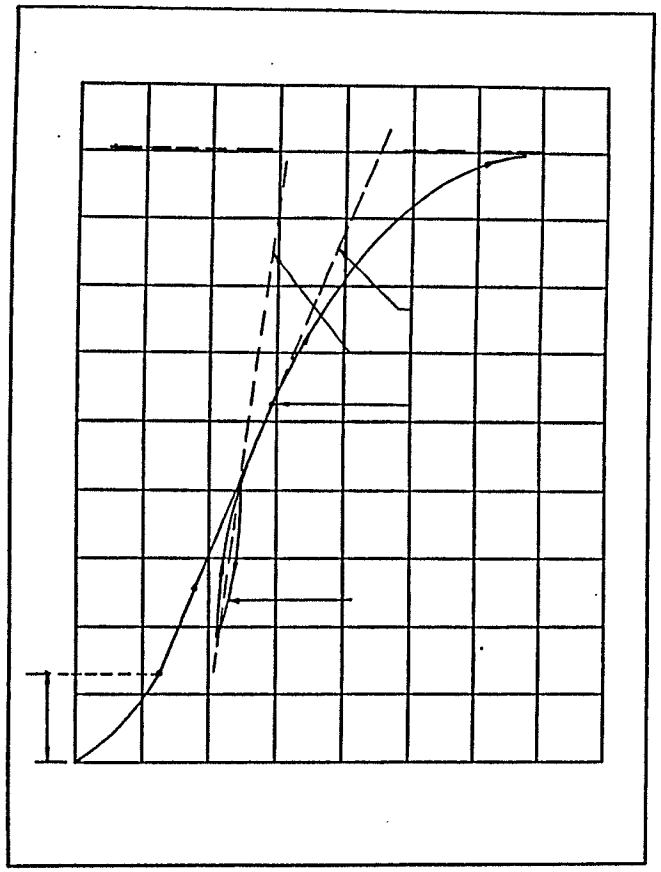

B.) TYPICAL IN-SITU RESULTS

FIG. 2.46. THE PRESSUREMETER TEST

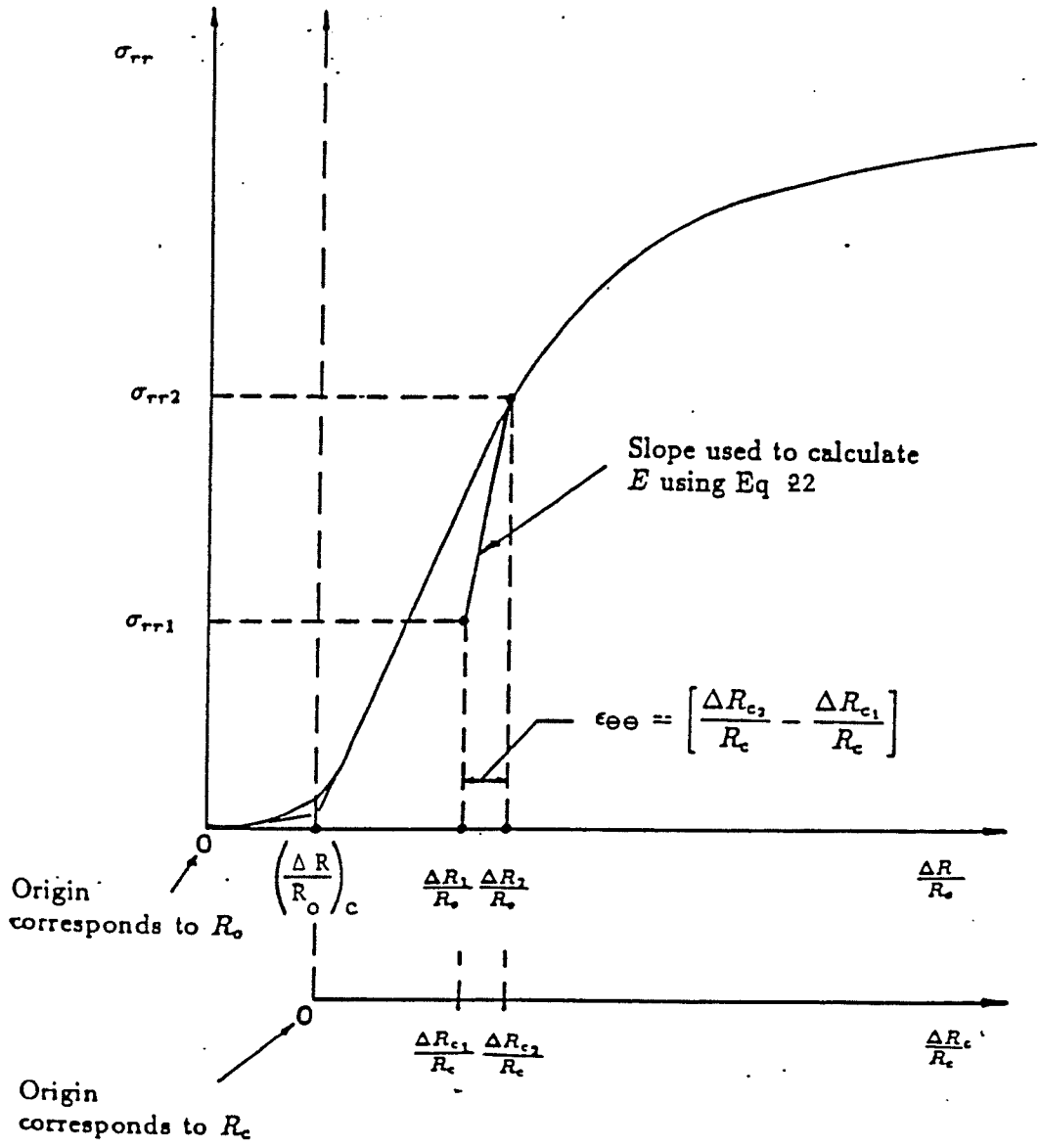

$$E = (1+\nu)\left[\left(1+\frac{\Delta R_1}{R_o}\right)^2 + \left(1+\frac{\Delta R_2}{R_o}\right)^2\right]\left[\frac{\sigma_{rr2} - \sigma_{rr1}}{\left(1+\frac{\Delta R_2}{R_o}\right)^2 - \left(1+\frac{\Delta R_1}{R_o}\right)^2}\right]$$

FIG. 2.47. CALCULATING THE MODULUS FROM A PRESSUREMETER TEST (AFTER BRIAUD ET AL 1987)

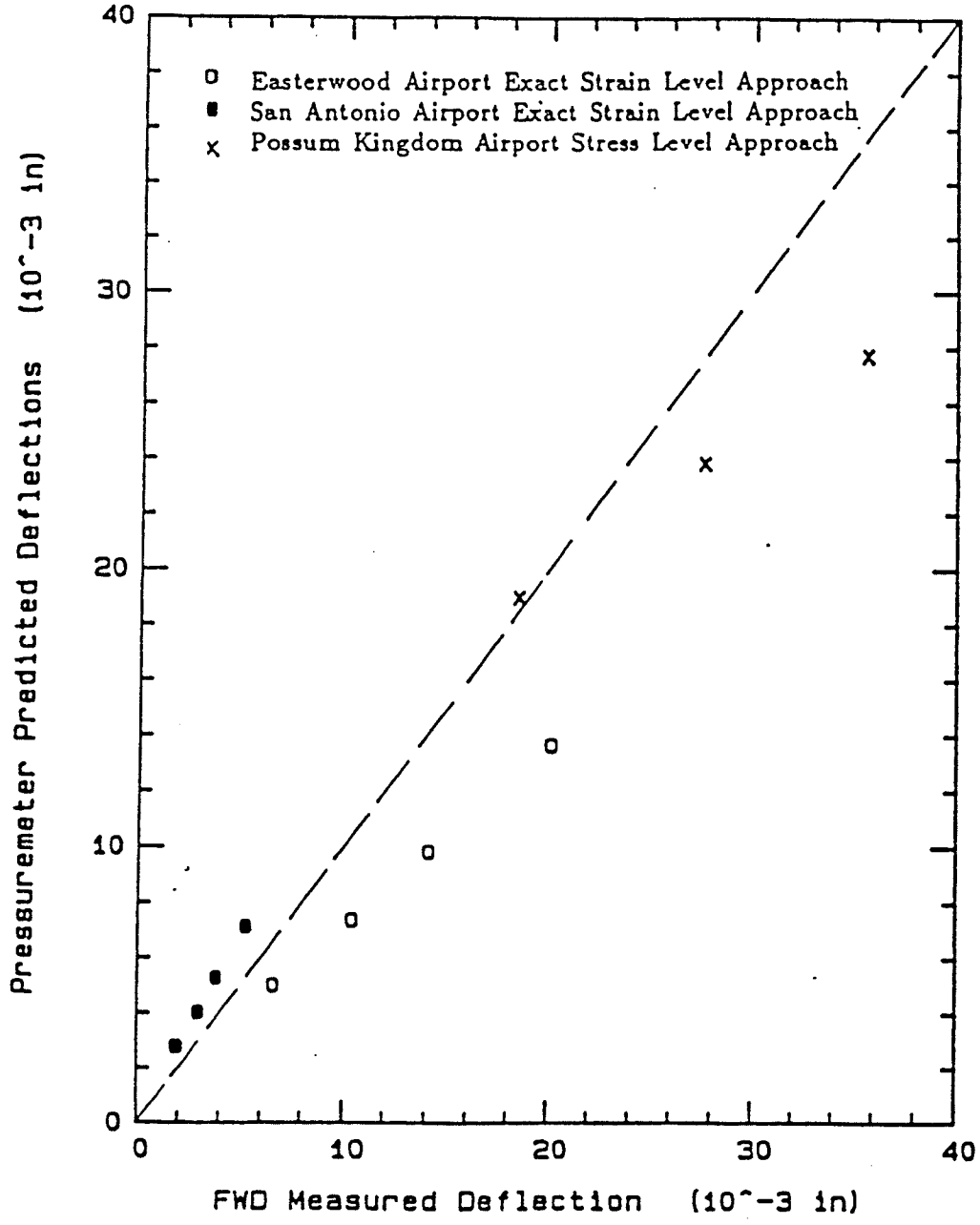

FIG. 2.48. CORRELATION BETWEEN PRESSUREMETER DEFLECTION AND MEASURED FWD DEFLECTIONS (AFTER BRIAUD ET AL 1987)

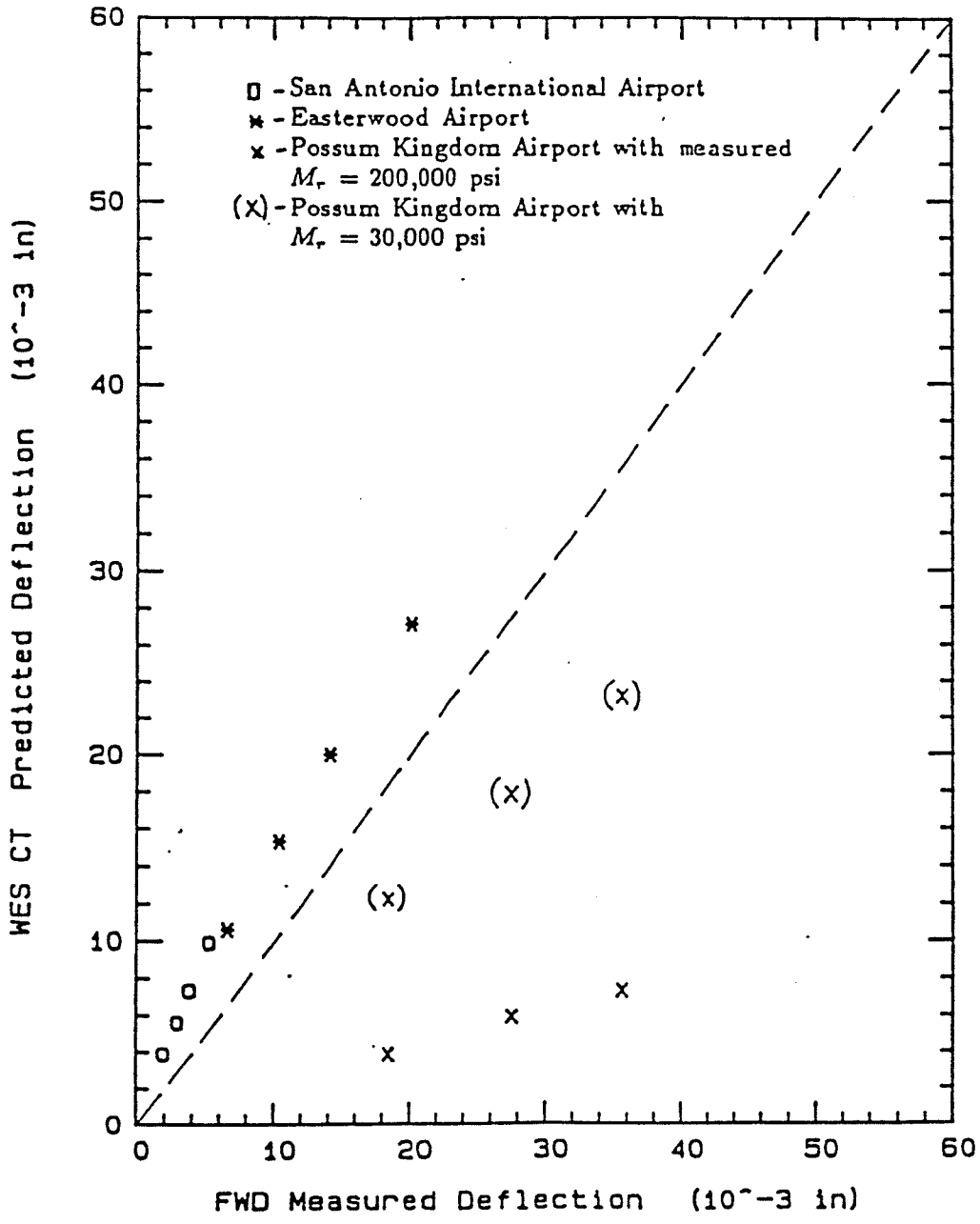

FIG. 2.49. CORRELATION BETWEEN DEFLECTION FROM CYCLIC TRIAXIAL TESTS AND MEASURED FWD DEFLECTIONS (AFTER BRIAUD ET AL 1987)

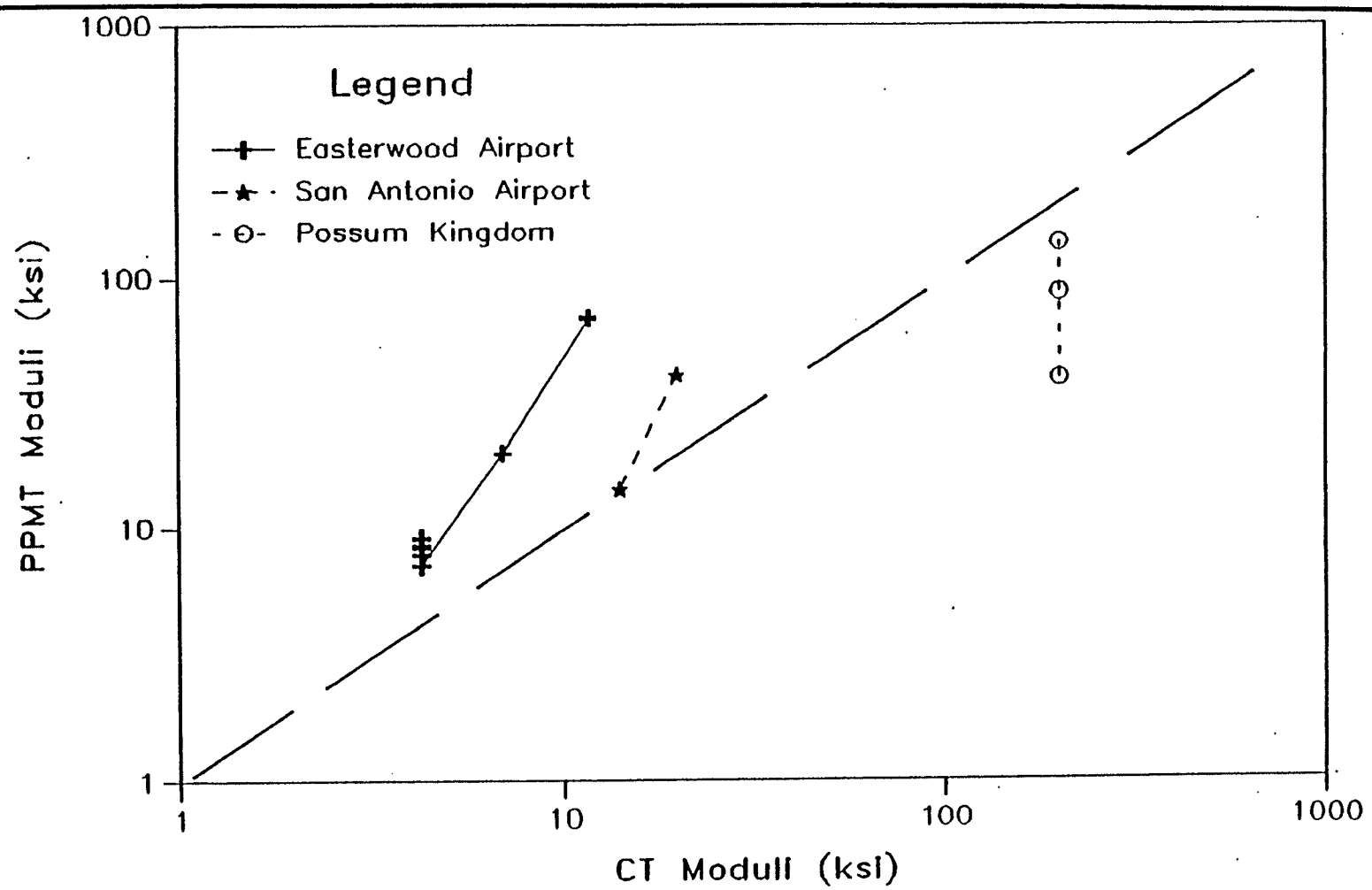

FIG. 2.50. CORRELATION BETWEEN MODULI FROM CYCLIC TRIAXIAL TESTS AND PRESSUREMETER TESTS (AFTER BRIAUD ET AL 1987)

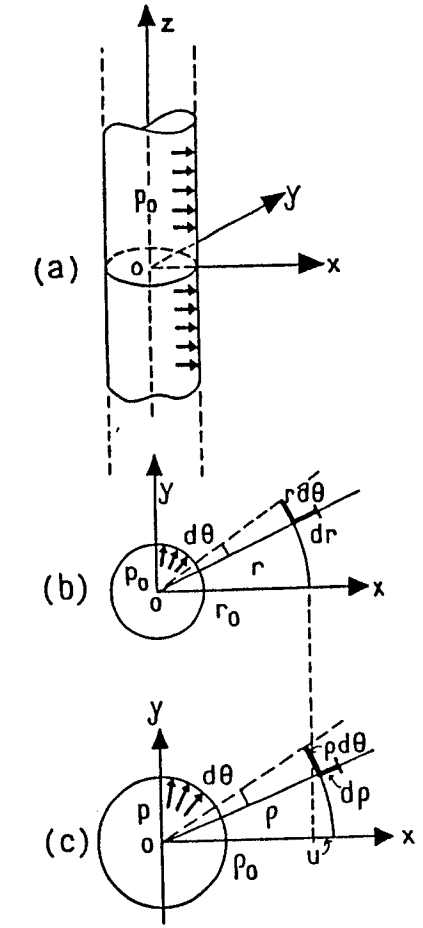

A.) THE GEOMETRY

B.) INITIAL CONDITION AT PRESSURE po

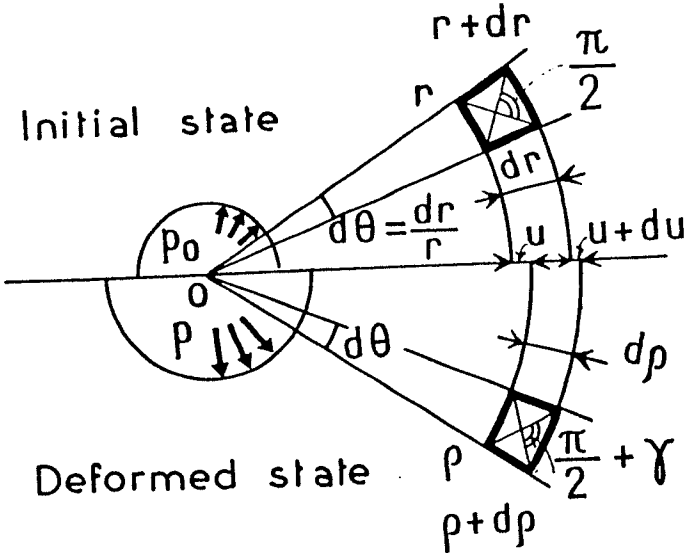

C.) AFTER INFLATING TO SOME PRESSURE p

FIG. 2.51. ILLUSTRATION OF THE EXPANSION OF A LONG CYLINDRICAL CAVITY (AFTER BAGUELIN ET AL 1978)

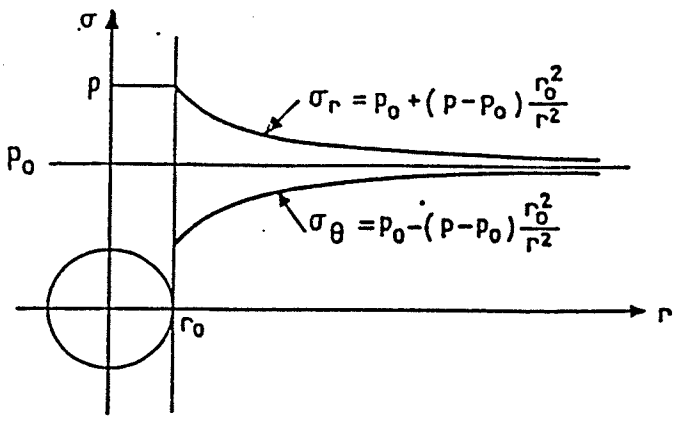

A.) STRESS DISTRIBUTION AT DIFFERENT RADIAL DISTANCES.

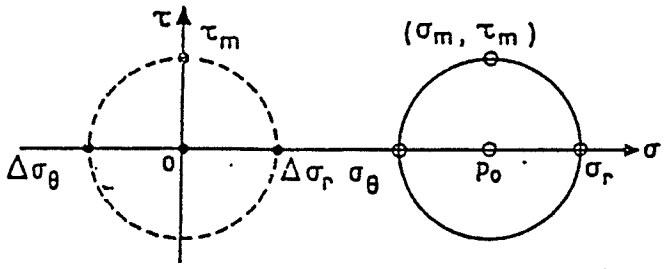

B.) MOHR CIRCLE REPRESENTATION OF STRESSES

FIG. 2.52 RADIAL AND HOOP STRESS DISTRIBUTION IN A PRESSUREMETER TEST

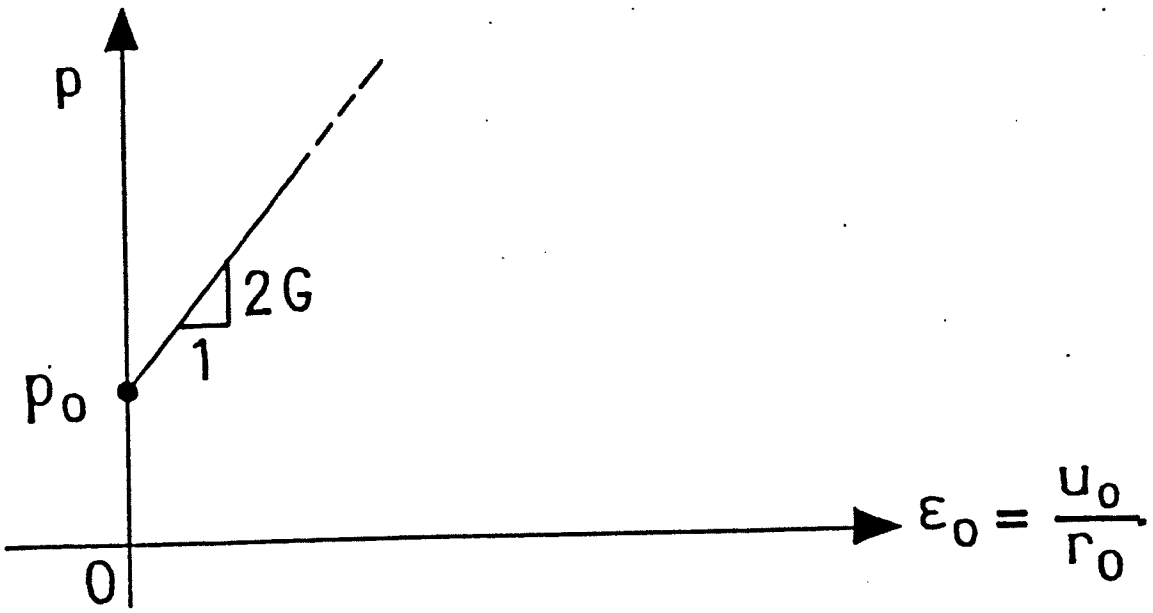

FIG. 2.53 SCHEMATIC REPRESENTATION OF THE RADIAL STRAIN VS. PRESSURE IN A PRESSUREMETER TEST (AFTER BAGUELIN ET AL, 1978)

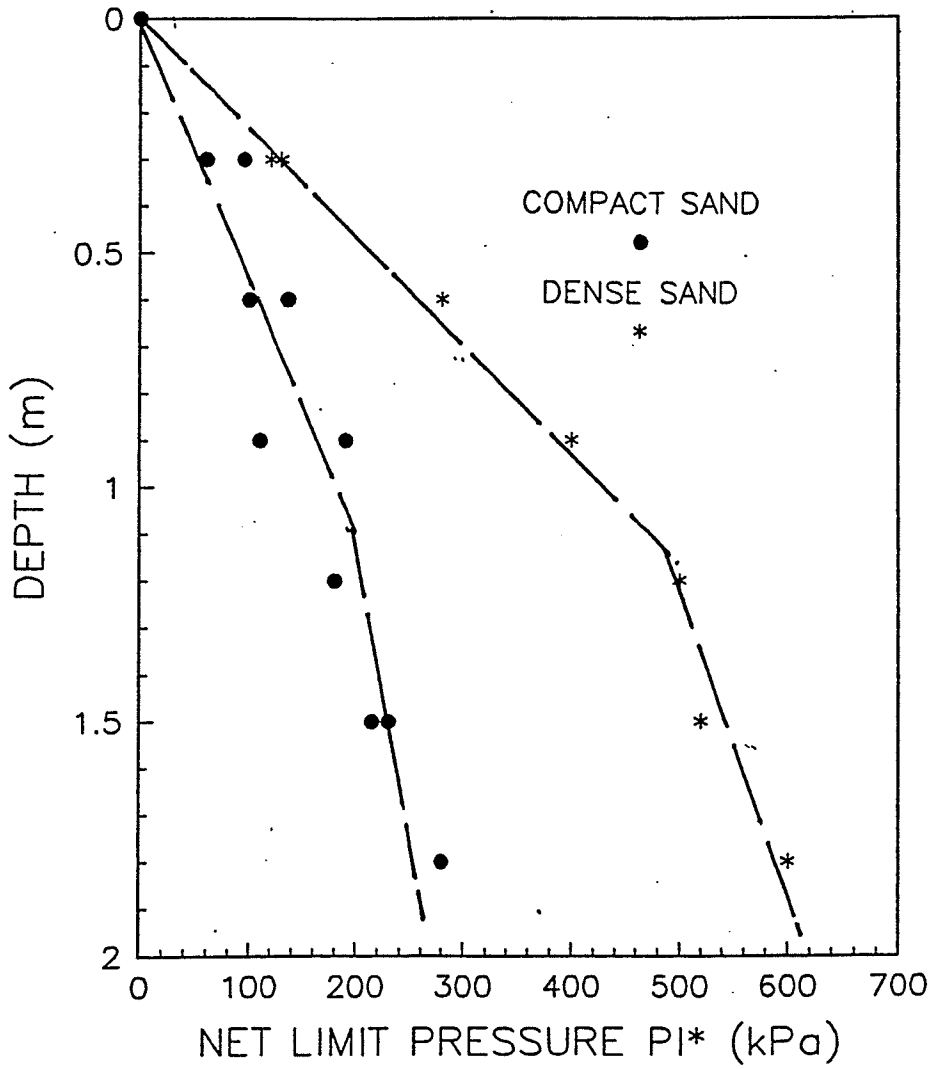

FIG. 2.54. LIMIT PRESSURE DISTRIBUTION IN SAND WITH MENARD PRESSUREMETER (AFTER BRIAUD AND SHIELDS, 1981)

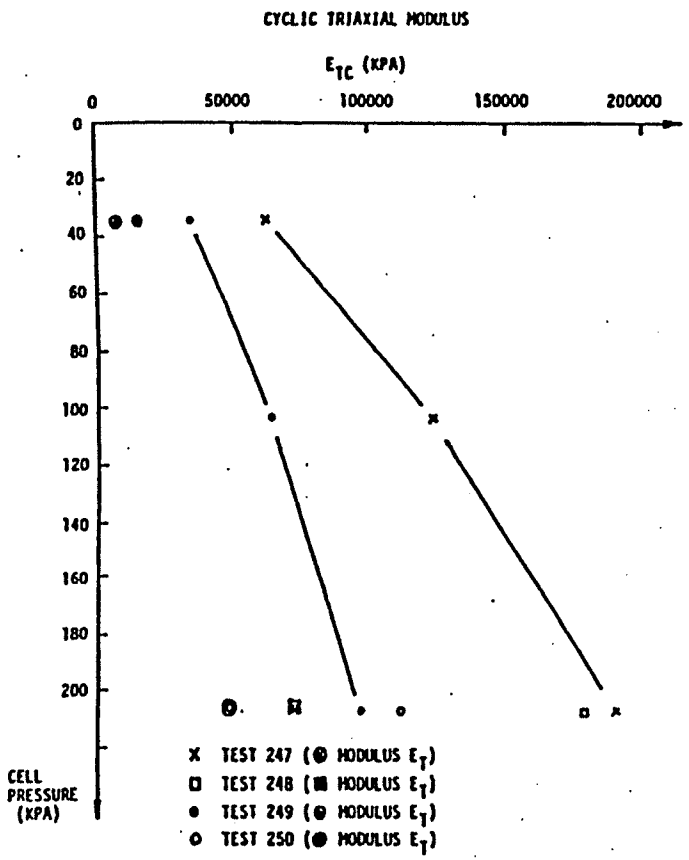

A.) SAND

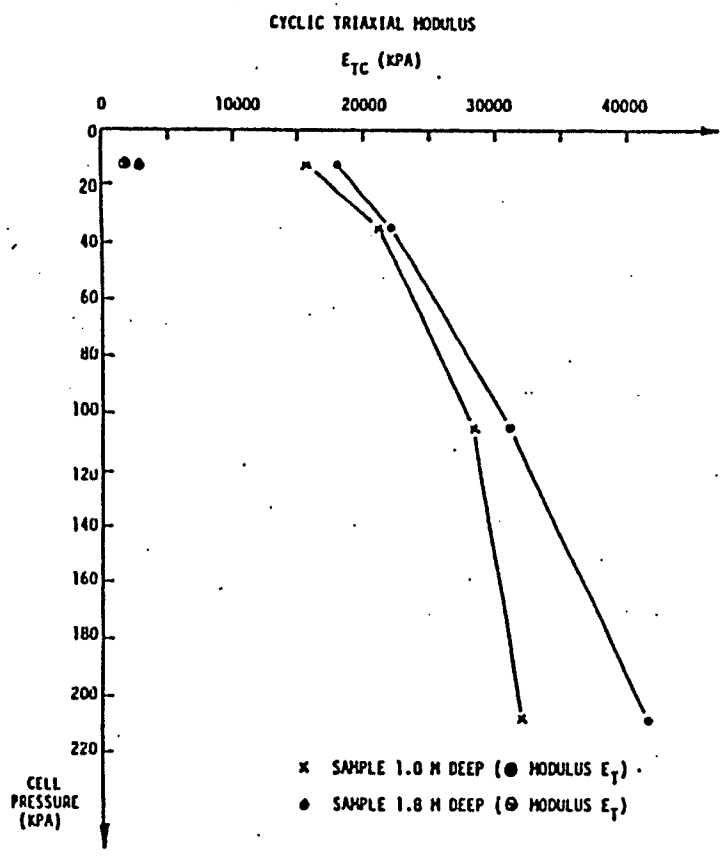

B.) CLAY

FIG. 2.55 CYCLIC TRIAXIAL TEST MODULUS VS. CELL PRESSURE IN SAND AND IN CLAY (AFTER BRIAUD AND SHIELDS, 1981)

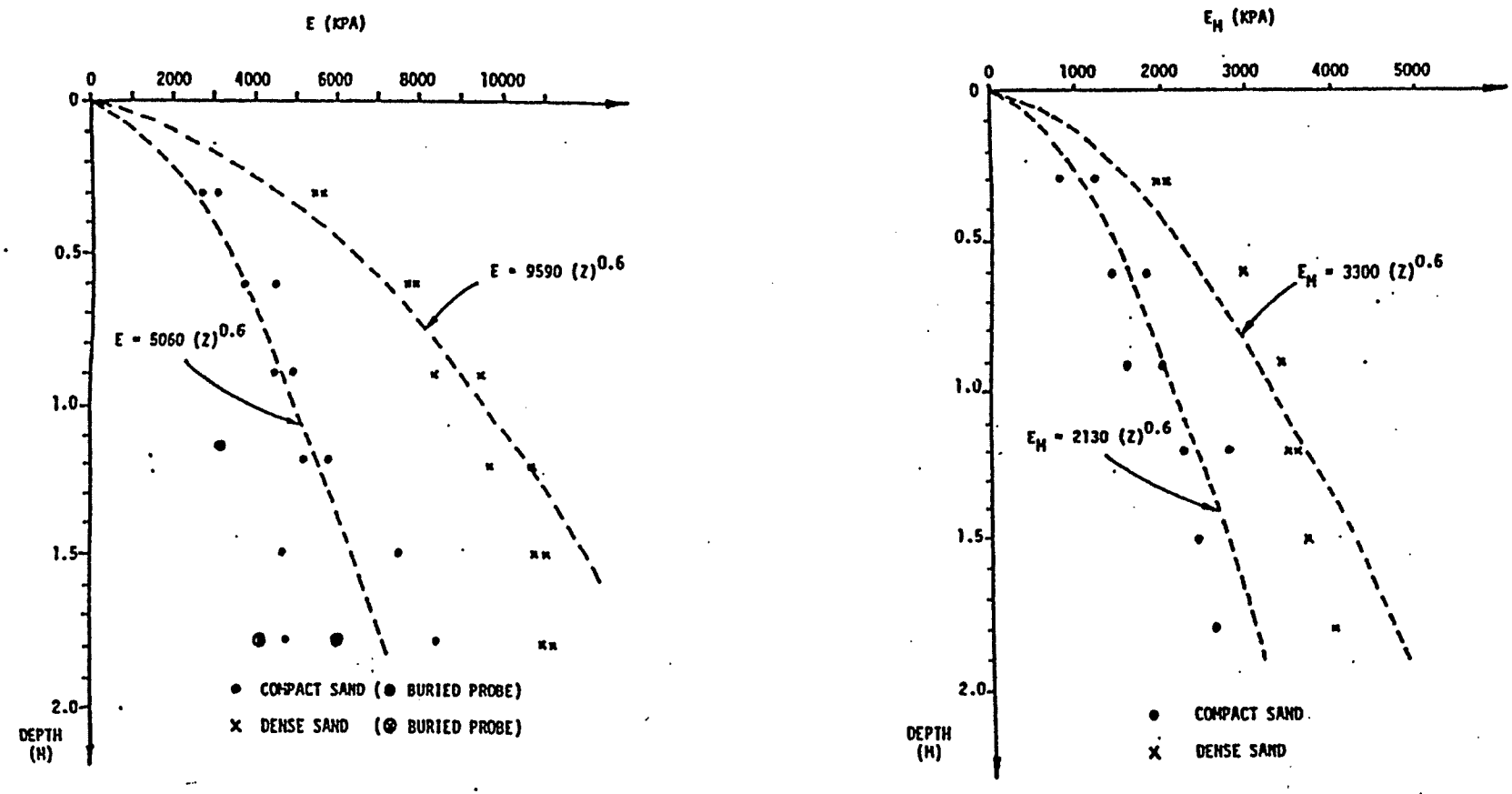

FIG. 2.56 VARIATION OF PRESSUREMETER MODULUS WITH DEPTH IN SAND BOX TESTS WITH COMPACT AND DENSE SAND (AFTER BRIAUD AND SHIELDS, 1982)

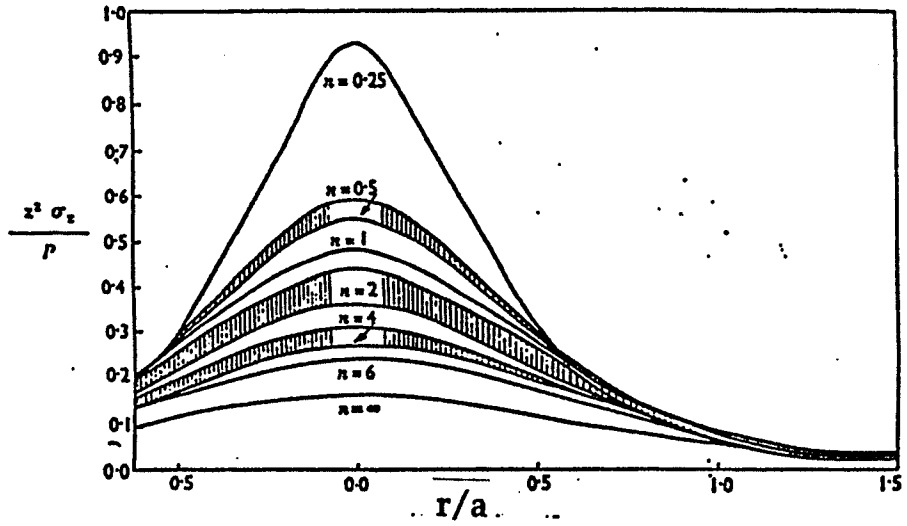

(AFTER BARDEN 1963; N= Eh/Ev = DEGREE OF ANISOTROPY)

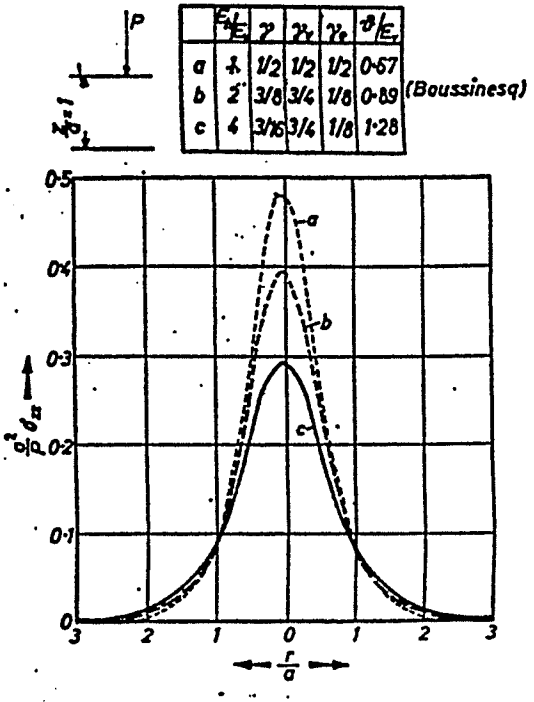

(AFTER KONING 1957)

FIG. 2.57 DISTRIBUTION OF VERTICAL STRESSES UNDER A LOADED PLATE AT DIFFERENT DISTANCES FROM THE LOAD AND FOR DIFFERENT DEGREES OF ANISOTROPY.

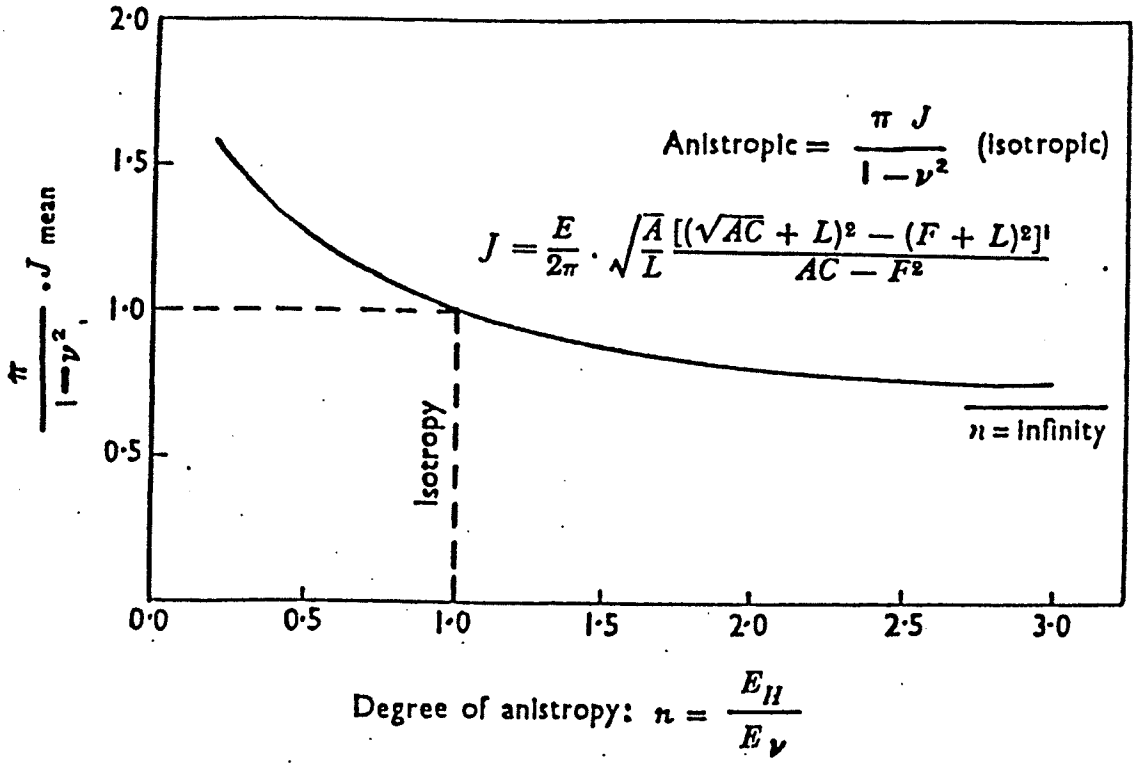

FIG. 2.58 **RELATIONSHIP BETWEEN SURFACE DEFLECTIONS FOR A LOADED ISOTROPIC AND ANISOTROPIC HALFSPACE (AFTER BARDEN, 1963)**

(A,C,F AND L ARE PARAMETERS INVOLVING ONLY THE ELASTIC CONSTANTS E AND μ)

A.) THE PARABOLOID SURFACE

B.) REPRESENTATION OF A PARTICULAR SOIL

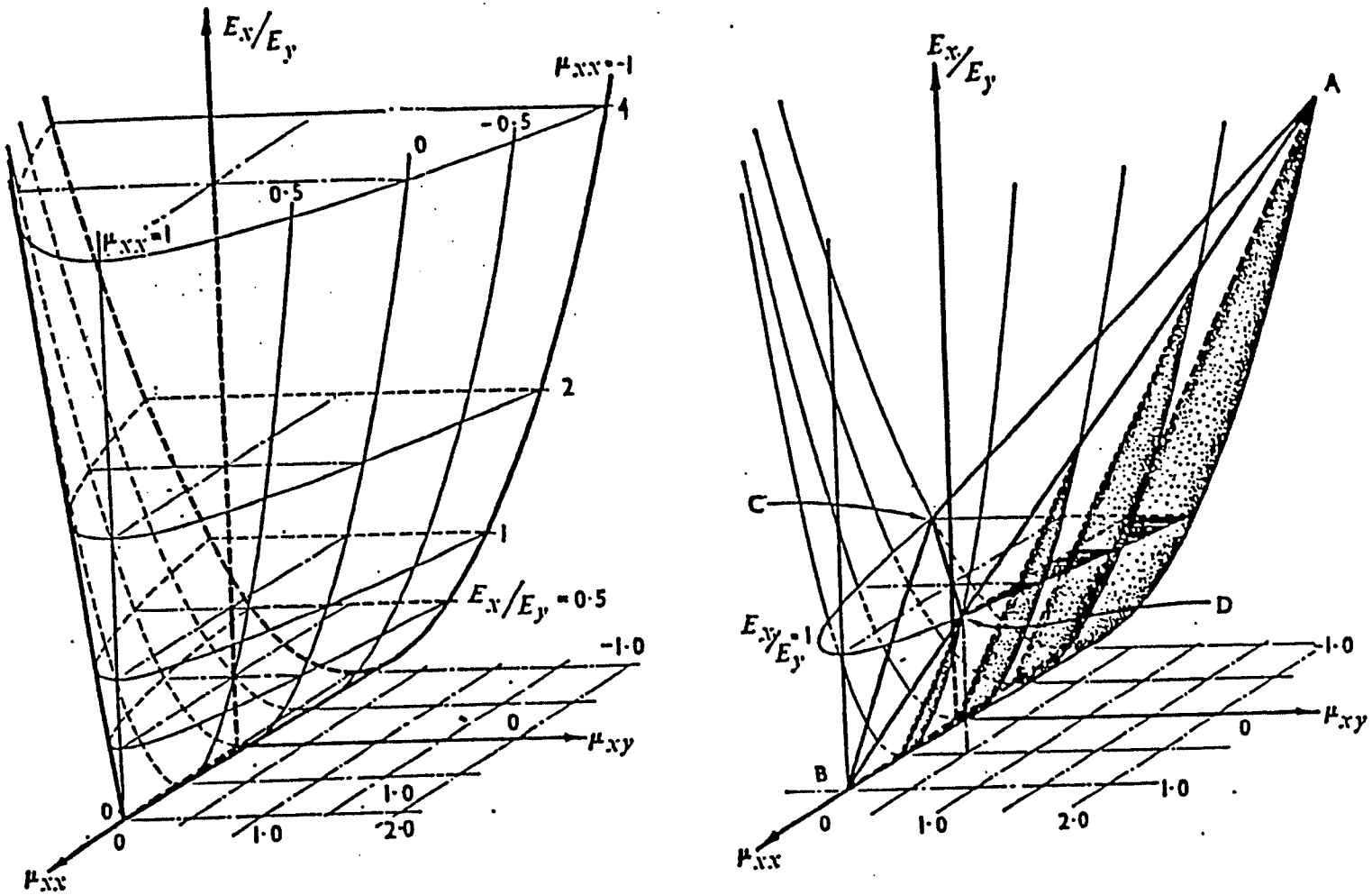

FIG. 2.59 THE BOUNDS FOR THE ANISOTROPIC PARAMETERS (AFTER PICKERING, 1970)

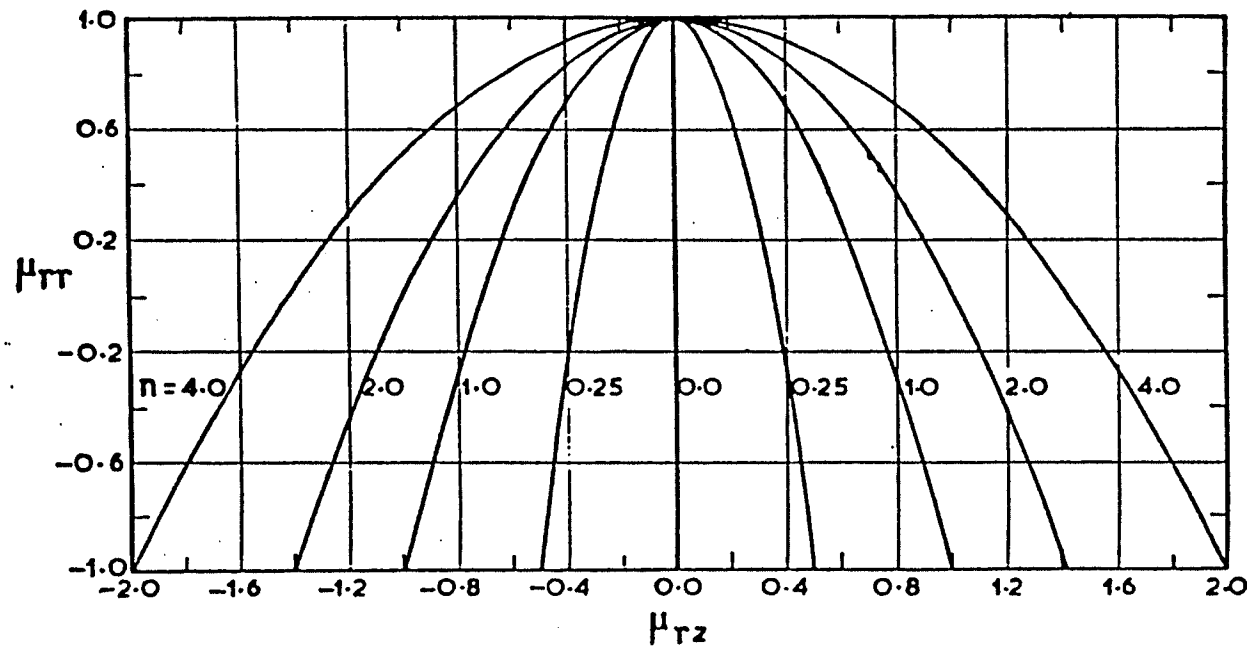

FIG. 2.60 RELATIONSHIPS BETWEEN THE DEGREE OF ANISOTROPY AND THE TWO POISSON'S RATIOS (AFTER NAYAK, 1973)

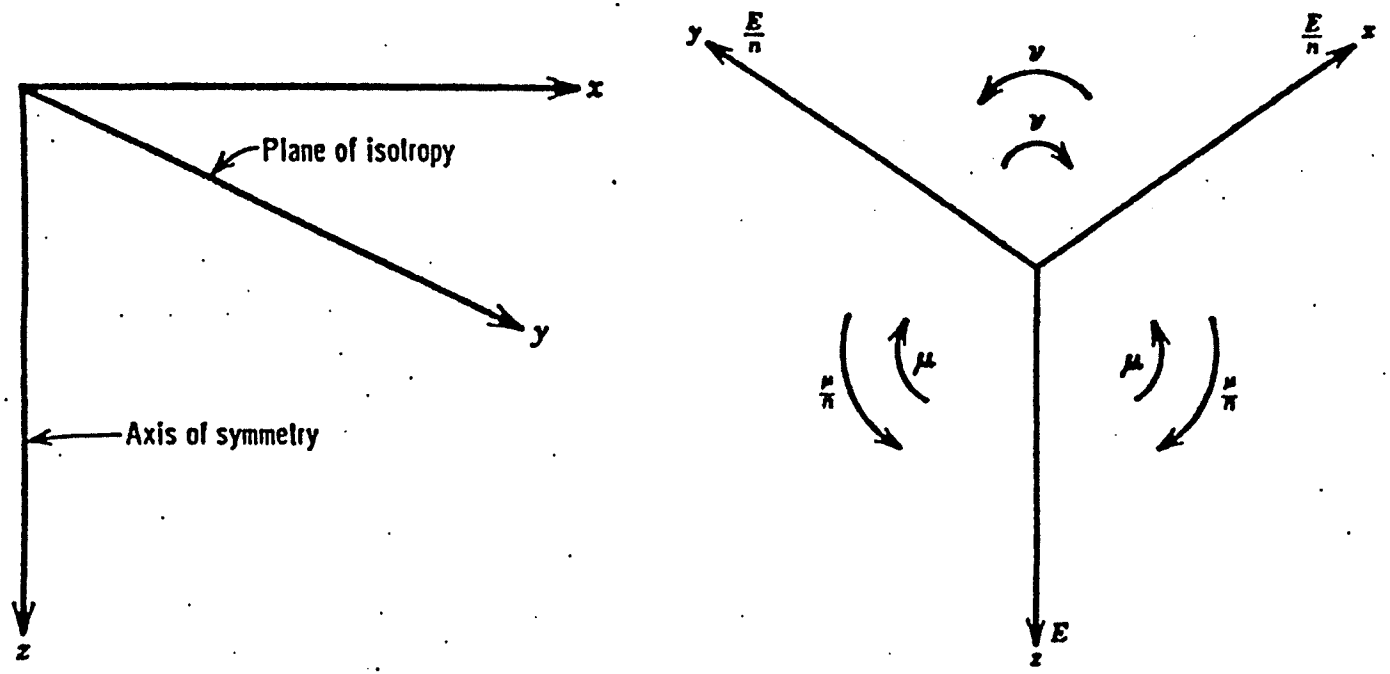

FIG. 2.61 DEFINITION OF ELASTIC PARAMETERS ACCORDING TO VAN CAULWERT (1977)

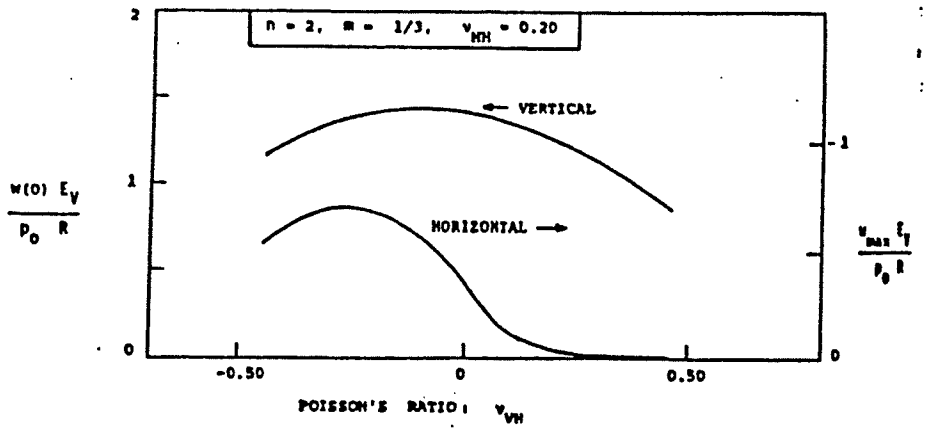

A.) POISSONS RATIO

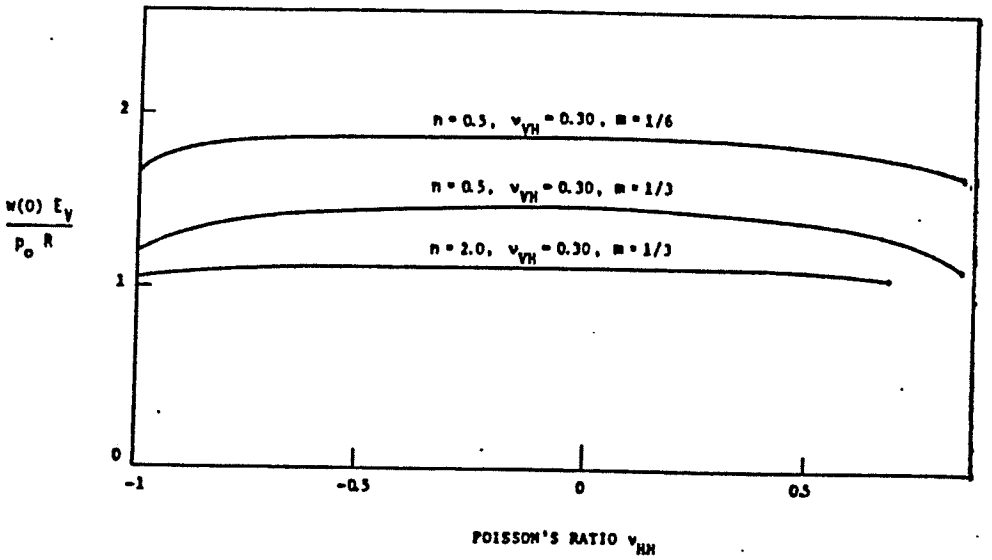

B.) POISSONS RATIO

FIG. 2.62 INFLUENCE OF THE DIFFERENT POISSON'S RATIOS ON THE SURFACE DEFLECTION OF A LOADED ANISOTROPIC HALFSPACE (AFTER GAZETAS, 1982)

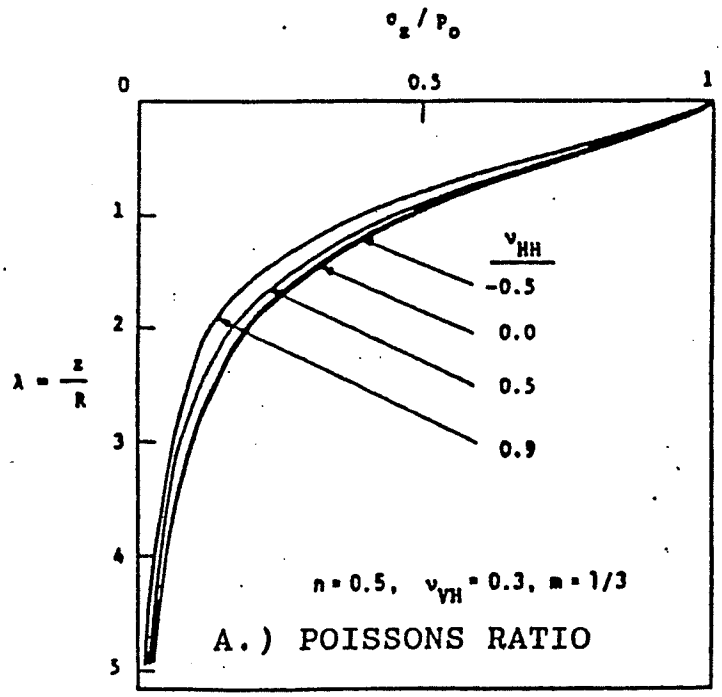

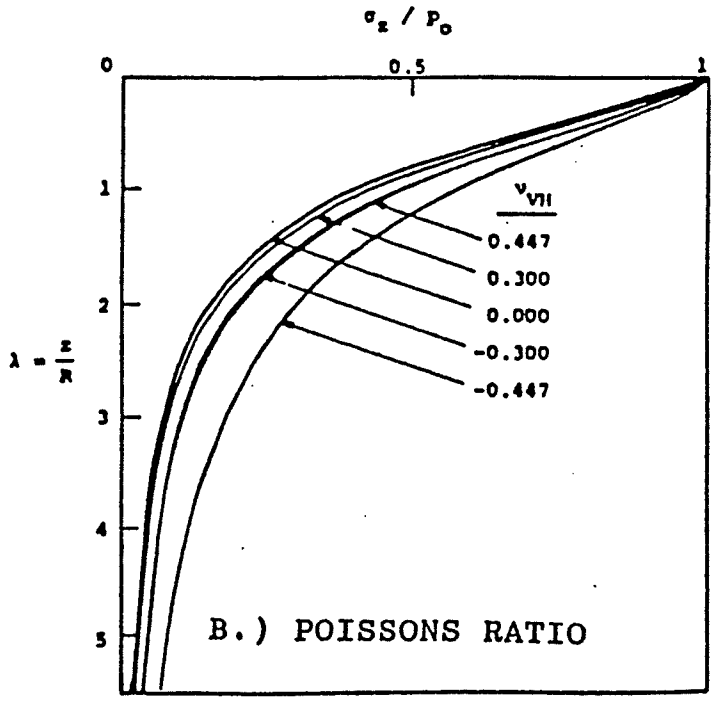

FIG. 2.63 INFLUENCE OF THE DIFFERENT POISSON'S RATIOS ON THE VERTICAL STRESSES AT DIFFERENT DEPTHS BENEATH A LOADED ANISOTROPIC HALFSPACE (AFTER GAZETAS, 1981)

TABLE 2.1: ELASTIC LAYER THEORIES FOR 2 AND 3 LAYER SYSTEMS.

AUTHOR	ASSUMPTIONS	INTERFACE	LOADING	PARAMETERS	RESULTS	COMMENTS
TWO LAYER SYSTEMS						
WESTERGAARD (1926)	Elastic plate on a subgrade. Subgrade represented by springs.	Discontinuous	Uniform circular load	Modulus of subgrade reaction	Tensile stress in the plate	Model of subgrade not realistic.
HOGG (1938)	Elastic plate on a semi infinite elastic subgrade.	Discontinuous	uniform circular load.	Young's modulus and Poisson's ratio for subgrade	Tensile stresses in the plate	Extension of Westergaard's theory
Burmister (1943)	Elastic layer on a semi infinite elastic subgrade.	a) Continuous b) Discontinuous	Besel Function.	a/h, E_1/E_2	w,zz,rr,rz in both the layers.	Theoretical work in 1943; Charts published in 1946.
Fox (1948)	Elastic layer on a semi infinite elastic subgrade.	a) Continuous b) Discontinuous	Uniform circular load.	a/h, E_1/E_2	All stresses in both layers.	Extension of Burmister's work; Tabular values.
Hank and Scrivner (1948)	Elastic layer on a semi infinite elastic subgrade	a) Continuous b) Discontinuous	Uniform circular load.	a/h, E_1/E_2	Stresses at the interface	Extension of Burmister's work; Tabular values.
Pickett and Ai (1948)	Elastic plate on a semi infinite elastic subgrade.	a) Discontinuous b) No slip at interface.	Uniform circular load.	a/h and functions of $E_1/E_2,\mu_1,\mu_2$	All stresses and deflections in both layers	Extension of Westergaard's and Burmister's theory to suit concrete pavements;
Odemark (1949)	Elastic plate on a semi infinite elastic subgrade.	Discontinuous.	Uniform circular load.	a/h and functions of $E_1/E_2,\mu_1,\mu_2$	Deflections at the surface; stresses in subgrade.	Extension of Burmister's work; Tabular and graphical results.
THREE LAYERED SYSTEMS.						
Burmister (1945)	Two elastic layers on a semi infinite elastic subgrade.	a)continuous b)discontinuous	Besel Function.	a/h, E_1/E_3, E_2/E_3	All stresses in all layers; deflections at the surface and on top of subgrade	Limited numerical evaluation.
Hank and Scrivner (1948)	Two elastic layers on a semi infinite elastic subgrade.	Continuous	Uniform circular load.	a/h, E_1/E_3, E_2/E_3	All stresses in all layers.	Extension of Burmister's work in 1945; Tabular evaluation.
Acum and Fox (1951)	Two elastic layers on a semi infinite elastic subgrade.	Continuous	Uniform circular load.	a/h, E_1/E_3, E_2/E_3	All stresses in all layers.	Further extension of Burmister's work; More extended tabular values.
Jeuffroy and Bachelez (1957)	Elastic Plate on an elastic layer on a semi infinite elastic subgrade.	Slip at first interface, no slip at second interface.	Uniform circular load.	a/h_2, functions of elasticity moduli for the layers.	w, rr, zz	Intended to model asphalt pavement on granular base/subbase.
Jones (1962)	Two elastic layers on a semi infinite elastic subgrade.	No slip.	Uniform circular load.	a/h, E_1/E_3, E_2/E_3	All stresses and deformations in all layers.	Extension of Burmister's work. Extensive tabular evaluation.
Peattie (1962)	Two elastic layers on a semi infinite elastic subgrade.	No slip.	Uniform circular load.	a/h, E_1/E_3, E_2/E_3	All stresses and deformations in all layers.	Extension of Burmister's work; Extended grphical evaluation.

Table 2.2: Some Better Known Computer Algorithms for Layered Elastic systems

Program	Source/ Author	# of Layers	# of Loads	Assumptions	Remarks
BISAR	Shell Intl. Petroleum	10	10	isotropic; linear; full continuity; temperature effects	long computer time
CHEV-5	Chevron Research	5	2	isotropic; linear; full continuity; temperature effects	
DAMA	Asphalt Institute	5	2	isotropic; nonlinear; full continuity; fatigue, temperature effects	based on CHEV-5
ELSYM-5	Univ. of California, Berkeley	5	2	isotropic; linear; full continuity	Based on CHEV-5: Recent version can handle up to 10 layers. An airport version is available.
PDMAP (PSAD)	NCHRP	5	2	Full Continuity; Linear; temperature effects; probabilistic	Long computer time
VESYS	FHWA	5	2	Full Continuity; Visco-elastic; Rutting Model; Fatigue considered	Not available to public
ILLIPAVE, ILLISLAB	Univ. Illinois, Urbana.	5	2	Full Continuity; Isotropic; Linear; temperature effects	Mainframe; PC version available Long running time
CHEVIT	U.S. Army	5	2	Full Continuity; Isotropic; Linear; Probabilistic	Based on CHEV-5
CIRCLY	Australian Road Research Board	5 +	10 +	Full Continuity; Isotropic; Linear; temperature effects	
ISSEM-4	DynaTest, California	4	4	Full Continuity; Isotropic; Linear	Specifically for FWD tests
ELMOD; ELCON	DynaTest, California	4	4	Full Continuity; Isotropic; Linear; Fatigue considered; temperature effects	Specifically for FWD tests; Remaining life calculations
SENOL-5	Univ. of Nottingham, UK	5	4	Full Continuity; Isotropic; non linear; yield criteria; temperature effects; fatigue considered	Most general yet

TABLE 2.3: McLEOD'S CONVERSION FACTORS FOR REPETITIVE PLATE LOAD TESTS.

TEST LAYER	PLATE DIAMETER ϕ (mm)	LOAD RATIOS					
		TEST DEFLECTION Δ (mm)					
		1.25	2.50	5.0	7.5	10.0	12.5
Surface	305	10.904	6.362	4.054	3.259	2.834	2.559
Subgrade	305	12.743	7.482	4.748	3.797	3.291	2.984
Surface	457	7.252	4.280	2.725	2.182	1.890	1.692
Subgrade	457	7.979	4.700	3.022	2.410	2.082	1.887
Surface	610	5.323	3.215	2.050	1.636	1.409	1.250
Subgrade	610	5.521	3.334	2.150	1.714	1.476	1.318
Surface	762	4.287	2.589	1.655	1.315	1.129	1.000
Subgrade	762	4.188	2.536	1.646	1.312	1.125	1.000
Surface	914	3.475	2.174	1.391	1.100	0.935	0.827
Subgrade	914	3.296	2.013	1.313	1.047	0.894	0.791
Surface	1067	2.940	1.871	1.199	0.945	0.799	0.703
Subgrade	1067	2.708	1.675	1.083	0.861	0.730	0.658

Note: Load ratios are average values of:

$$\frac{\text{Load (kN) on 762-mm-diameter plate, 12.5 mm deflection, 10 rep.}}{\text{Load (kN) on } \phi\text{-mm-diameter plate, } \Delta \text{ mm deflection, 10 rep.}}$$

(Source: Transport Canada: AK-Manual Series: AK-68-12-31, Table 3)

TABLE 2.4: CROSS-ANISOTROPIC MODELS FROM LITERATURE.

AUTHOR	ASSUMP-TIONS	INTERFACE	LOADING	PARA-METERS	RESULTS	COMMENTS
KONIG (1957)	Homogeneous, Cross anisotropic semi infinite elastic half space.		Uniform load. on a circular area.	E_v, E_h, ν_{hh},ν_{hv}, ν_{vh}.	all stresses and displacements. Limited numerical evaluation.	
BARDEN (1963)	Homogeneous, Cross anisotropic semi infinite elastic half space. Shear modulus invariant.		a) point load b) uniform load on a circular area.	E_v, E_h, ν_{hh},ν_{hv}, ν_{vh},	all stresses and displacements.	Assumption regarding shear modulus is not quite correct.
BHATTACHARYA (1967)	Homogeneous, Cross anisotropic semi infinite elastic half space.		point load	E_v, E_h, μ_{hh},μ_{hv}, μ_{vh}	all stresses and displacements.	singularity near the load point.
GERRARD, OR GERRARD ET AL (1967),(1969),(1970)	One, and two layer cross anisotropic elastic systems. The bottom layer is a semi infinite cross anisotropic half space.	no slip.	a) uniform strip load (plane strain) b) axisymmetric, uniform load over a circular area. c) linear shear stress. All loads applied as Besel function.	E_v, E_h, μ_{hh},μ_{hv}, μ_{vh}.	all stresses and displacements including at the interface. Complete solutions.	Theoretical work. No evaluation for specific cases. Solution based on finite differences.
Pickering (1970)	Homogeneous, Cross anisotropic semi infinite elastic half space.		No specific loading. Generalised rigorous mathematical treatment.	E_v, E_h, μ_{hh},μ_{hv}, μ_{vh}.	Bounding values for the parametrs. (see Fig. 2.61).	

TABLE 2.5: ANISOTROPIC ELASTIC CONSTANTS (AFTER GAZETAS 1981)

DESCRIPTION OF SOIL	REFERENCE	MEASURED VALUES				COMPUTED (note 1)
		n	ν_{vh}	ν_{hh}	G_{vh}/E_v	
Heavily over consolidated London clay (Ashford)	Ward (1959) Ward (1965) Gibson (1974)					
depth: 30 ft.		1.35	0.50	0.325	0.35	0.355
depth: 50 ft.		1.59	0.50	0.205	0.37	0.41
avge :		1.80	0.50	0.08	0.38	0.46
Heavily over consolidated London clay (Barbican Centre)	Atkinson (1975)	2.00	0.19	0.00	0.536	0.553
Lightly over consolidated kaolinite clay (Florida)	Saada (1978)					
$\sigma_c' = 40$ psi, $w_c = 40.7$ %		1.25	0.50	0.375	0.356	0.364
$\sigma_c' = 60$ psi, $w_c = 38.7$ %		1.36	0.50	0.322	0.362	0.378
Normally consolidated clay (Grundite)	Bianchini (1980)					
$\sigma_c' = 70$ psi, $w_c = 29.5$ %		1.17	0.50	0.415	0.355	0.353
$\sigma_c' = 60$ psi, $w_c = 38.1$ %		1.13	0.50	0.436	0.322	0.310
Colorado clay shale	Kaarsberg (1968)	1.38	0.197	0.266	0.423	0.524
Sensitive Champlian Sea clay (Canada)	Yong & Silvistry (1979)	0.62	0.35	0.20	0.205	0.187

Note: 1. Computed based on Carrier's constraining equation.
2. For further details refer to Gazetas (1981).

TABLE 2.6: ANALYSIS OF CROSS ANISOTROPIC SYSTEMS

(AFTER GERRARD (1969))

Problem Number	Geometry	Loading	No. of Layers	H_A	H_B	$\frac{(E_V)_A}{(E_V)_B}$	Layer A					Layer B				
							E_H/E_V	f/E_V	ν_H	ν_{HV}	ν_{VH}	E_H/E_V	f/E_V	ν_H	ν_{HV}	ν_{VH}
1	Plane Strain	Uniform Normal Stress(p)	1	$6x_o$	–	–	1·5	0·9	0·25	0·30	0·20	–	–	–	–	–
2	〃	〃	1	$6x_o$	–	–	3·0	1·0	0·1	0·9	0·30	–	–	–	–	–
3	〃	〃	2	$2x_o$	$4x_o$	$\frac{1}{4}$	1·5	0·9	0·25	0·30	0·20	3·0	1·0	0·1	0·9	0·3
4	〃	〃	2	$2x_o$	$4x_o$	4	3·0	1·0	0·1	0·9	0·3	1·5	0·9	0·25	0·30	0·20
5	〃	〃	1	$6x_o$	–	–	1·0	0·7 (Isotropic)	0·43	0·43	0·43	–	–	–	–	–
6	Axi-symmetric	Uniform Normal Stress (p)	2	$1·5r_o$	∞	5	1·0	0·8 (Isotropic)	0·25	0·25	0·25	2·0	0·9	0·25	0·35	0·175
7	〃	Linear Shear Stress $(s\frac{r}{r_o})$	2	$1·5r_o$	∞	5	1·0	0·8 (Isotropic)	0·25	0·25	0·25	〃	〃	〃	〃	〃
8	〃	Uniform Normal Stress (p)	2	$1·5r_o$	∞	5	3·0	1·0	0·1	0·9	0·3	〃	〃	〃	〃	〃
9	〃	Linear Shear Stress $(s\frac{r}{r_o})$	2	$1·5r_o$	∞	5	3·0	1·0	0·1	0·9	0·3	〃	〃	〃	〃	〃
10	〃	Uniform Normal Stress (p)	2	$1·5r_o$	∞	1	1·0	0·8 (Isotropic)	0·25	0·25	0·25	1·0	0·8 (Isotropic)	0·25	0·25	0·25

CHAPTER THREE

PROPOSED MODEL FOR AN ELASTIC, CROSS-ANISOTROPIC LAYERED SYSTEM

3.1 GENERAL

In the previous chapter it was shown how the generalised Hooke's law can be reduced for a cross-anisotropic medium, leaving five elastic constants to be determined (Eqns. 12 and 13). These five constants are:

In the Cartesian system: E_{xx}, E_{zz}, μ_{xx}, μ_{xz} and G_{xz}.

In Polar coordinates: E_{rr}, E_{rz}, μ_{rr}, μ_{rz} and G_{rz}.

It was also mentioned that, at present, the anisotropic parameters can be determined only in laboratory triaxial tests. *In-situ* geophysical or geotechnical tests to determine these constants have not been developed or reported. The computer algorithms, currently in use, to back-calculate the moduli from deflection basins cannot consider cross-anisotropic layers. Yet there is increasing evidence both in geotechnical engineering and in pavement engineering that anisotropy may be a significant factor in computing settlements or deflections under surface loads.

In this chapter **a layered elastic model for pavements incorporating cross anisotropy** will be suggested. A method will be proposed to derive the required five parameters for the analysis from data collected by in-situ testing. Finally, a finite-element solution will be presented for numerical evaluation of the model. In Chapter 6 the numerical solutions from the finite-element analyses will be compared to observed FWD deflections.

3.2 THE MODEL

The model proposed here is an elastic, cross-anisotropic layered system with stress-dependent layer moduli. The following assumptions are made:

1. Each layer of the pavement, except the bottom-most or the subgrade, is of finite thickness but extends laterally to infinity;
2. The subgrade extends to infinite depth or to a known depth to a rigid base;
3. Each layer except the asphaltic concrete surface layer is elastic and cross-anisotropic. The plane of isotropy is assumed to be horizontal and the axis of isotropy vertical;
4. The asphaltic surface layer is assumed to be isotropic;
5. The modulus of each layer is assumed to be stress-dependent;
6. The modulus of the asphalt surface layer is, in addition, dependent on the temperature, rate of loading and duration of loading;
7. Perfect bond is assumed to exist between the individual layers;
8. The load is applied through a circular area and is assumed to be distributed uniformly over the loaded area;
9. There are no loads outside the loaded area;
10. There are no shear forces on the loaded surface;
11. The problem can be thought of as an axisymmetrical problem.

3.2.1 Material Characterization

For the numerical evaluation, the modulus of the asphaltic concrete was determined

from the well known nomograph of van der Poel as modified by McLeod, Figs. 3.1 and 3.2[1] (see for example: Yoder and Witczak, 1974, pp. 271 and pp. 395). Brown (1982) suggests a different modification of the van der Poel nomograph based on British experience. More recently, Valkering and Stapel (1992) combined the different components of the original van der Poel's nomographs into a single nomograph and have incorporated this into the Shell design method for personal computers. However, in this study McLeod's method is used since it is felt that this will be more relevant to the Canadian conditions. The bitumen stiffness and mix characteristics were determined from cores obtained from the pavements during the field testing phase of this investigation. Further details of the evaluation of the materials will be given in Chapter 5. It is submitted that by using van der Poel's method as modified by Mcleod, the viscoelastic characteristics and the temperature dependency of asphalt modulus are accounted for (see assumption 6 above).

Anisotropy of asphaltic concrete was not considered, because there is not sufficient evidence to suggest that asphaltic concrete in a pavement structure exhibits anisotropic characteristics. The only works known to the author were due to Busching et al. (1967), (also quoted by Gerrard, 1978), Lees and Salehi (1969) and Coffman et al. (1970). Gerrard and Mulholland (1966) also quote an earlier work by Shklarsky and Livneh (1961) who presumably reported cross-anisotropic behaviour of asphaltic concrete based on laboratory tests. These latter authors reported ratios of anisotropy varying between 1.4 and 3.5. depending on the mix design.

Busching et al. start by discussing wheel-path and curb-side rutting at intersections

---

[1] Figures and Tables are included in the Appendices at the end of each chapter.

and other commonly observed distresses and hypothesize that such distresses are due to directional properties of the asphaltic concrete. Then starting with the equations of elasticity (Eqns. 5 through 13, Chapter 2) they set out to define the elastic constants to describe the behaviour of the material. They show that **six** constants, instead of five, are needed to describe the material response. This is because they recognize that the modulus of asphaltic concrete depends on other factors such as temperature, level of loading, rate of loading etc. They describe carefully conducted triaxial and diametric tests to determine these constants. They conclude that asphaltic concrete in pavements does show anisotropy and that it could be considered using the theoretical framework suggested by them. As pointed out by Finn and Nair as well as by Secor and Monismith in the discussion of this paper by Busching et al. (*loc. cit.*) there would be conceptual difficulties with their approach. If all the relevant factors were to be considered, then not the elastic theory but visco-elastic theory would be the appropriate framework to describe the response of the asphaltic concrete. Furthermore, the necessity of **six** elastic constants stemmed from not considering the strain energy requirements of an elastic continuum (the so-called Cauchy approach). Thus Busching et al. had not conclusively proven anisotropic response of asphaltic concrete. Recent studies by the Transportation Association of Canada (TAC) attribute the rutting problem to asphalt strains and mix characteristics rather than to anisotropy. In any event it is suggested that the overriding influence of temperature, loading rate and load duration would probably make anisotropy a minor consideration in characterizing the response of asphaltic concrete.

In contrast to Busching et al., Coffman et al. (1970) studied laboratory compacted specimens as well as cores and slabs taken from in-service pavements and concluded that the behaviour of asphaltic concrete can be taken to be isotropic. Lees and Salehi (1969) studied

the particle orientation of compacted asphaltic concrete both in the laboratory and from in-service pavements and showed that field compacted samples exhibit definite preferred orientation of the aggregates in the direction of rolling. However, they had not related such particle orientation to any mechanical behaviour or strength properties, anisotropic or otherwise.

Since then (i.e. late 1960's and early 1970's), considerable research has been reported on asphalt testing and layered theory. While there is a definite consensus emerging to consider anisotropy in the unbound layers no such consideration has been suggested for the asphaltic concrete. Therefore, in this study too, asphaltic concrete will be treated as an isotropic material. Rutting and cracking should be considered in a separate fatigue model and are beyond the scope of the present study. It is, therefore, submitted that, given the current state of knowledge and non availability of sophisticated testing equipment, asphalt concrete can be treated as a viscoelastic isotropic material. This can be considered in the analysis of deflection basin as suggested in this thesis.

The moduli for the unbound material (granular base, subbase and the subgrade) were obtained from *in-situ* pressuremeter tests. The measured values will be compared to the computed values. As discussed in Chapter 2, the pressuremeter test would yield only a maximum of two parameters. They are the horizontal modulus and the Poisson's ratio μ_{hh}. The other three have to be inferred. Fortunately, the anisotropy of the soils at the sites tested in this study have been investigated by others in long-term high-quality laboratory tests (Yuen, 1976; Lo et al., 1977; Graham and Houlsby, 1983; Lee and Rowe 1989). Therefore their results will be used in this study to infer the missing parameters. It is admitted that this approach is somewhat speculative. A parametric study to determine the sensitivity of the

surface deflections to errors in the inferred values of the elastic constants would have been useful. However, the optimization technique used in this thesis served the same purpose. In the following section the conceptual basis for the inferred values are presented. The numerical evaluation of the results will be shown in Chapter 5.

3.2.2 Conceptual Basis for the Inferred Anisotropic Parameters

For an anisotropic soil the five independent elastic constants cannot take any arbitrary values. They are interrelated by the following relationships (see also Chapter 2, Section 2.3):

$$E_v,\ E_h \text{ and } G_{vh} \text{ must be all positive} \tag{85a}$$

$$-1 < \mu_{hh} < 1 \tag{85b}$$

$$2\mu_{vh}^2 < n\,(1 - \mu_{hh}) \tag{85c}$$

Also Feda (1978) establishes that:

$$K_0 = (E_H / E_v) \cdot \frac{\mu_{rh}}{(1 - \mu_{hh})} = n \cdot \frac{\mu_{vh}}{(1 - \mu_{hh})} \tag{86}$$

A pressuremeter test would yield basically three values, the horizontal modulus E_{hh}, the lift-off pressure p_o and the limit pressure p_l (see Fig. 2.46b). Of these the limit pressure is of little relevance to pavement engineering. The lift-off pressure is generally taken to be approximately equal to the *in-situ* lateral stresses (e.g. Baguelin et al., 1978; Davidson, 1979; Shields et al., 1986). This is strictly true only if the probe can be placed in the hole and inflated before any stress relaxation in the ground can take place. It is generally accepted that the only equipment that comes closest to this ideal would be the self-boring pressuremeters.

However, these are very complicated and cumbersome to use. It has been, therefore, suggested that the full displacement pressuremeter would be a reasonable compromise between the self-boring pressuremeter and others (Wroth, 1984; Houlsby and Withers, 1988). In the series of tests reported here the method of insertion was not quite the same as in a full displacement test but approaches close to that. Therefore, it is suggested that the lift-off pressure may be assumed to be the *in-situ* lateral stresses. This approach will be further justified because the *in-situ* stresses are used to determine the Poisson's ratio μ_{hh} (using Eqn. (86) above), which has been shown by Gazetas (1982) as having only minor influence on surface deflections and vertical stresses. Thus it is submitted that the pressuremeter tests will yield two of the required five constants, E_{hh} and μ_{hh}. The other three constants are inferred as discussed below.

The ratio of anisotropy at these sites are taken as given by virtue of the previous laboratory investigations by others. Table 3.1,below, summarizes the results from these previous investigations.

Then using Eqns. (85), (86) and Eqn. (84) from Chapter 2 the three other parameters are inferred. Since Eqns. (85) are in fact inequalities and not equalities there would be a range of parameters possible. However, referring to Fig. 2.62 and 2.63 one can see that this range is rather narrow. Details of the test procedures, results and analyses are presented in Chapters 4 and 5.

3.2.3 Mathematical Background to the Solution

The mathematical treatment of an elastic, cross-anisotropic layered system was published by Gerrard and his associates in the late 1960's and early 1970's. This section

Table 3.1 Anisotropy Ratios for Subgrade Soils As Reported in the Literature

SITE	DEPTH (m)	PI	OCR	E_h/E_v	REF.
THUNDER BAY	10.2	45.2; soft grey silty clay	1.4	1.0	Lee and Rowe (1989)
THUNDER BAY	13.4	16.5; firm reddish brown grey varved clay	1.8 - 2.0	0.95	Lee and Rowe (1989)
WINNIPEG	4.9	77; firm brown laminated clay	1.8	1.8	Loh and Holt (1974)
WINNIPEG				1.65 - 1.8	Graham et al. (1989); Graham and Houlsby (1983)

Note: Clays from St. Andrews and Regina are very similar to Winnipeg Clay. The silty clay in Brandon is normally consolidated and is considered to be slightly anisotropic.

reproduces some of the essential steps of their formulation leading to the finite-element solution to be presented in the next section.

The starting point for the formulation of the solution is Eqn. (13) in Chapter 2 which can be written in the abbreviated form as below:

$$\{\epsilon_r,\ \epsilon_\theta,\ \epsilon_z,\ \gamma_{r\theta},\ \gamma_{\theta z},\ \gamma_{zr}\}^T = [C]\ \{\sigma_r,\ \sigma_\theta,\ \sigma_\theta,\ \tau_{r\theta},\ \tau_{\theta z},\ \tau_{zr}\}^T \qquad (87)$$

where, $\{\epsilon\}^T$ and $\{\sigma\}^T$ are the transposes of the strain and stress tensors respectively, and [C] is the coefficient matrix involving the five elastic constants. Gerrard rewrites Eqn. (87) expressing stresses in terms of strains as below:

$$\sigma_{rr} = a\,\epsilon_{rr} + b\,\epsilon_{\theta\theta} + c\,\epsilon_{zz} \qquad (88a)$$

$$\sigma_{\theta\theta} = b\,\epsilon_{rr} + a\,\epsilon_{\theta\theta} + c\,\epsilon_{zz} \tag{88b}$$

$$\sigma_{zz} = c\,\epsilon_{rr} + c\,\epsilon_{\theta\theta} + d\,\epsilon_{zz} \tag{88c}$$

$$\tau_{rz} = f \cdot \gamma_{rz} = G_{rz}\,\gamma_{rz} \tag{88d}$$

$$\tau_{r\theta} = \tau_{z\theta} = 0 \tag{88e}$$

where the constants a, b, c, d and f are the terms involving the five elastic constants and are given as below in terms of the more familiar engineering constants:

$$a = \frac{E_H\,(1 - \mu_{HV}\,\mu_{VH})}{(1 + \mu_H)\,(1 - \mu_H - 2\,\mu_{HV}\,\mu_{VH})} \tag{89a}$$

$$b = \frac{E_H\,(\mu_H + \mu_{HV}\,\mu_{VH})}{(1 + \mu_H)\,(1 - \mu_H - 2\mu_{HV}\,\mu_{VH})} \tag{89b}$$

$$c = \frac{E_H\,\mu_{VH}}{1 - \mu_H - 2\mu_{HV}\,\mu_{VH}} \tag{89c}$$

$$d = \frac{E_\mu\,(1 - \mu_H)}{1 - \mu_H - 2\mu_{HV}\,\mu_{VH}} \tag{89d}$$

The condition stipulated by Eqn. (85) should still hold. In addition Gerrard invokes a restriction imposed by Koning (1957) on the value of the shear modulus G_{vh} (or f in Gerrard's notation):

$$\frac{f}{E_H} \le \frac{-\mu_{VH}\mu_{HV} + (\mu_{VH}\mu_{HV}\,(1 - \mu_{VH}\mu_{HV})\,(1 - \mu_H)\,/\,1 + \mu_H)^{1/2}}{\mu_{HV}\,(1 - \mu_H - 2\mu_{VH}\mu_{HV})} \tag{90}$$

This is similar to the restriction imposed by Gazetas (1981). The next step is to formulate the strains in terms of displecements u, (= v for axi-symmetrical case) in the radial direction and w in the vertical direction as shown below:

$$\epsilon_{rr} = \frac{\partial u}{\partial r} \tag{91a}$$

$$\epsilon_{\theta\theta} = \frac{u}{r} \tag{91b}$$

$$\epsilon_{zz} = \frac{\partial w}{\partial z} \tag{91c}$$

$$\epsilon_{rz} = \frac{1}{2}\left(\frac{\partial u}{\partial z} + \frac{\partial w}{\partial r}\right) \tag{91d}$$

Gerrard suggests that the unknown displacements, u and w, for an axisymmetrical case are best chosen in the form of Bessel functions as shown below:

$$w = J_0(k_r) \cdot g_s(z) \tag{91a}$$

$$v = J_1(k_r) \cdot h_s(z) \tag{92b}$$

Here J_o and J_1 are Bessel functions of order 0 and 1, r is the radial distance, k is a dummy variable and g(z) and h(z) are some functions of depth. After some manipulation Gerrard arrives at the following differential equation.

$$D^4 - 2\,\frac{(ad - c^2 - cf)}{fd}\,k^2 D^2 + \frac{a}{d}\,k^4 = 0 \tag{93}$$

where D is the differential operator,

or,

$$D = \frac{\partial g}{\partial z} \tag{94}$$

$$D = \frac{\partial h}{\partial z} \tag{95}$$

depending upon whether one is solving for g(z) or h(z). This equation can again be rewritten as a quadratic in D whose roots are expressed in terms of two parameters α and β and the dummy variable k and are given by:

$$\alpha^2 = \frac{ad - c^2 - cf + f\sqrt{ad}}{2\,fd} \tag{96 a}$$

$$\beta^2 = \frac{ad - c^2 - cf - f\sqrt{ad}}{2\,fd} \tag{96 b}$$

Due to requirements that strain energy should be positive α will be always positive.

However, no such restrictions exist for β except the ones imposed by the restriction due to Koning or Gazetas on the shear modulus. Thus β can be either zero or positive. For the case β is positive, the solutions for g(z) and h(z) are:

$$g(z) = A_1 e^{(-\alpha+\beta)kz} + A_2 e^{(-\alpha-\beta)kz} + A_3 e^{(\alpha+\beta)kz} + A_4 e^{(\alpha-\beta)kz} \tag{97 a}$$

$$h(z) = q_1 A_1 e^{(-\alpha+\beta)kz} + q_2 A_2 e^{(-\alpha-\beta)kz} - q_2 A_3 e^{(\alpha+\beta)kz} - q_1 A_4 e^{(\alpha-\beta)kz} \tag{97b}$$

where q_1 and q_2 are given by:

$$q_1 = \frac{f/2 - d(-\alpha + \beta)^2}{(c + f/2)(-\alpha + \beta)} \tag{97 c}$$

$$q_2 = \frac{f/2 - d(-\alpha - \beta)^2}{(c + f/2)(-\alpha - \beta)} \qquad (97\ d)$$

For the case β is 0 (isotropy) the solutions are:

$$g(z) = C_1 e^{-\alpha kz} + C_2 Z e^{-\alpha kz} + C_3 e^{\alpha kz} + C_4 Z e^{\alpha kz} \qquad (97\ e)$$

$$h(z) = (n_1 C_1 - n_2 C_2) e^{-\alpha kz} + n_1 C_2 Z e^{-\alpha kz} + (-n_1 C_3 - n_2 C_4) e^{\alpha kz} - n_1 C_4 Z e^{\alpha kz} \qquad (97\ f)$$

where n_1 and n_2 are given by:

$$n_1 = \frac{d\alpha^2 - f/2}{(c + f/2)\alpha} \qquad (98a)$$

$$n_2 = \frac{d\alpha^2 + f/2}{(c + f/2)\alpha^2 K} \qquad (98b)$$

In either case one is left with four constants of integration for each layer. These constants are to be determined from the boundary conditions. For an N-layer system, this will be 4N constants which require 4N equations to solve. These 4N equations are obtained from the boundary conditions as follows:

1. At the surface the vertical forces and shear forces are known yielding two equations;
2. At the rigid bottom or at infinity, the vertical load is zero as is the deformation thus yielding two more equations;
3. For an N-layer system there are (N-1) interfaces. At each interface the vertical and horizontal stresses as well as the vertical and horizontal displacements for the adjoining layers must be equal. These conditions yield 4 equations at each interface (i.e 4 x (N-1) equations).

With these 4N equations the solutions for the displacements can be found. From the

displacements the strains and from the strains the stresses can be computed.

Consider two adjoining layers i and j of a multi-layer system (Fig. 3.3). The displacements and strains in layer i are given by:

$$\text{Vertical displacement } W_i = \int_0^\infty g_i(z) \cdot J_0(kr)\, dk \tag{99a}$$

$$\text{Radial displacement } U_i = \int_0^\infty h_i(z) \cdot J_1(kr)\, dk \tag{99b}$$

$$\text{Vertical strain } \epsilon_{zz} = \int_0^\infty g_i'(z) \cdot J_0(kr)\, dk \tag{99c}$$

$$\text{Radial strain } \epsilon_{rr} = \int_0^\infty k h_i'(z) \cdot J_1(kr)\, dk \tag{99d}$$

$$\text{Shear strain } \gamma_{rz} = \int_0^\infty [h_i'(z) - k g_i(z)] \cdot J_0(kr)\, dk \tag{99e}$$

Substituting for $g_i(z)$, $h_i(z)$, $g_i'(z)$, and $h_i'(z)$, from Eqns. 97 (a) and 97 (b), the displacements and strains can be computed as shown in Table 3.2. Only the results are given here. For the algebra see, for example, Spiegel (1969). Knowing the strains and using the stress-strain relationships (Eqn. (13) or Eqn. (88)), the stresses can be determined. One notices that the solutions are all in terms of known material properties only.

3.3 NUMERICAL EVALUATION OF THE RESULTS

3.3.1 General Comments

It is clear from Table 3.2 that the computation of stresses and strains is virtually impossible without computer-aided numerical techniques. Therefore, this section proposes a finite-element formulation for the evaluation of the stresses and strains at any point in the pavement as well as the surface deflections. The program presented here is an existing commercial finite-element program, **ANSYS**, marketed by Swanson Analysis Systems Inc. in Philadelphia, USA.

Before deciding upon to use this "black box" approach, many existing programs were examined. These were ISSEM 4 (Dynatest Inc.), ELSYM 5 (Berkeley), ILLIPAVE (Illinois) and two other finite element programs available with the mainframe computer at the University of Manitoba. The first three of these are extensively reported in the literature and are being used by many researchers and practising engineers all over the world. The last two were part of two graduate theses in geotechnical engineering at the University of Manitoba. ISSEM-4, ELSYM-5 and ILLIPAVE cannot consider non-homogeneity, stress dependency of materials, viscoelastic properties of asphalt, and anisotropy. They cannot consider user-imposed ***limits*** to material properties for ***each layer***. They cannot optimize the solutions to fit the measured material properties while matching the observed and computed deflection bowls. Thus many of the assumptions noted in Section 3.2. cannot be handled by these programs. Using these programs would also be a "black box" approach. Though the author could obtain the source code for ISSEM-4 and ELSYM-5, modifying these to consider a generalised pavement model proved to be a nearly impossible task. Source code for ILLIPAVE was not available.

The two programs at the University of Manitoba were written to analyze specific foundation problems. While they were smaller programs than the other three, they were also restricted in their applications. All the above objections would apply to these too. In addition, there were no algorithms to match the calculated and observed deflection basins. In other words, they were not meant to be used as a back-calculation tool.

Thus all the available programs would have involved extensive modification, debugging and testing before being used to analyze the data collected for this investigation. It is submitted that when powerful general purpose finite-element algorithms are available and which have been tried and tested on many known theoretical and practical problems, there is little additional benefit in developing a similar and new program. Therefore, all analyses reported in this thesis were done using the ANSYS finite-element program. A later section in this chapter and sections in Chapter 5 give more details and documentation of the program. In the following sections a brief overview of finite-element methods, in general, and the use of ANSYS for this study, in particular, is presented.

3.3.2 Steps in Developing a Finite-element Model (FEM).

It is not intended to go into any great details about the theory or concepts of the finite-element method (FEM). Numerous text books, journal papers, and conference proceedings have been published on this subject (see for example Mackerle, 1988). Here only the basic steps are enumerated and the implementation of these steps as relevant to the current problem on hand is discussed. The implementation of a finite-element program involves the following steps:

1. Model Definition: In this step the mesh geometry (triangular, quadrilateral, number

of nodes etc.) is defined;

2. Definition of element stiffness: This is the step where the material properties for each element in the continuum are assigned. It is in this step the various theoretical material models (such as isotropic, anisotropic, homogeneity, linearity or non linearity, etc.) are defined;

3. Definition of nodal stiffnesses: Since the elements are joined at the nodes and finally the forces and deformations are solved at these nodal points, the element stiffnesses are to be combined in some appropriate manner to define the nodal stiffness;

4. Boundary and force definition: The boundary conditions are defined here. Also the external forces acting at different points should be input;

5. Analysis: This is the step where the equations of equilibrium and compatibility are assembled and solved as a set of simultaneous equations to arrive at the dispalcements, strains and stresses;

6. Output: The results are printed out in any desired format.

Step 1. Model definition:

This step involves choosing an appropriate mesh pattern to suit the problem at hand. For analysing pavement problems, generally, a mesh as shown in Figs. 3.4 (a) and 3.4.(b) is chosen. The mesh will be of non-uniform size being finer under the load and near the surface, getting coarser as one proceeds away from the load both horizontally and vertically. In this thesis a basic pattern, as described below, is taken as the default mesh (Fig. 3.4 (a)). However, the user has the option of defining the mesh in any manner to suit the problem.

a) Horizontal Direction

It was mentioned earlier that the pavement structure could be approximated as an axi-symmetrical solid. In fixing the geometry of the model the radius of this finite cylinder should be large enough to contain the deflection bowl. Only then the back calculation process will deliver reasonable values for the resilient moduli of the layers. This is one of the drawbacks of the available programs since they cannot consider this condition. This condition implies that the vertical boundary should be a little beyond the point where the deflection bowl becomes asymptotic to the surface. In heavy pavement structures, such as airfield pavements that were tested during this study, the deflection bowls were usually large. This was confirmed by observation during the FWD testing and when some of the 1985 data was analyzed using the ISSEM-4 program. Therefore, from these initial results, it was decided to have the vertical boundary at twice the distance of the last sensor from the load point.

At this boundary, it is assumed that only vertical movements are possible, but no horizontal movements. Twenty-five node points were specified within this distance. Four of these nodes were under the loading plate, the next seventeen between the outside edge of the plate and the last sensor and the rest between the last sensor and the outer boundary as determined above. More specific details of the model and the mesh geometry are described in Chapter 5 where the theoretical basis for the analysis using ANSYS is presented.

b) Vertical Direction

The total height of the finite cylinder is taken to be approximately 15 metres from the loaded surface to the assumed depth of the rigid bottom. This depth was arrived at after some preliminary calculations using published data by Gerrard (1967) and Bhattacharya (1968).

These results are presented in Chapter 5.

The mesh distances in the vertical direction were related to the thickness of the individual layers and consider, to some extent, the usual construction practices. The asphalt surface layer is divided into two layers. This corresponds to the general practice of laying two layers of the asphaltic concrete, the lower levelling course and the upper surface course. Usually, these are two different mixes and have different mix properties. In the case of very thick asphalt layers, (such as with Full-Depth[2] Asphalt pavements) additional layers may be necessary. The granular base layer is divided into three sub-layers. With the usual pavement construction this would result in layer thickness of 200-300 mm which is generally the specified thickness of bases from the compaction point of view. Since one of the reasons for the existence of anisotropy in granular layers is compaction, it would be logical to treat each lift of compacted base as a layer and assign its appropriate material properties, if they can be measured. Using similar arguments the granular subbase, when present, is divided into four layers. Finally the subgrade is divided into layers of 1,000 mm each. Generally, this resulted in seven to ten layers of subgrade for a total height of the model approximately 15 metres. Below this depth a rigid bottom is assumed where deflections and stresses will be zero.

Step 2. Element Stiffness

The objective of this step is to formulate an expression for the stiffness of each element in the mesh so that given either the displacements or the forces, the other can be computed. The stiffness of an element is a function of its area and the properties of the

---

2 Full-Depth asphalt is the registered trade mark of Asphalt Institute, College Park, Md.

materials in that element. The area is defined by the geometry of the element described by the coordinates of the nodal points (Step 1 above). The following explanation for obtaining the element stiffness follows the presentation by Girijavallabhan and Reese (1968).

Consider a discreet element (i,j) in an axi-symmetrical medium (Fig. 3.5). The displacement within the element can be written as:

$$\{\delta\}^{ij} = \begin{Bmatrix} u^{ij} \\ w^{ij} \end{Bmatrix} = [\phi]\ \{\alpha\} \tag{100}$$

where,

$$[\phi] = \begin{bmatrix} 1 & r & z & rz & 0 & 0 & 0 & 0 \\ 0 & 0 & 0 & 0 & 1 & r & z & rz \end{bmatrix} \tag{101}$$

$$\{\alpha\}^T = \{\alpha_1\ \alpha_2\ \alpha_3\ \alpha_4\ \alpha_5\ \alpha_6\ \alpha_7\ \alpha_8\} \tag{102}$$

where, $\{\delta\}$ is the displacement vector, u and w are the displacement components in the radial and vertical directions respectively, $\{\alpha\}$ is a vector of deflection coefficients and $[\Phi]$ is a position vector. Now, strain is defined as the rate of change of deformation and hence can be written as functions of the derivatives of u and w. Since the displacements are expressed in terms of deflection coefficients $\{\alpha\}$, it is possible to write strains in terms of $\{\alpha\}$ as below:

$$\{\epsilon\} = [Q] \cdot \{\alpha\} \tag{103}$$

where $\{\epsilon\}$ represnts the strain tensor and [Q] is a vector relating strains to the displacement coefficients $\{\alpha\}$. But strains can also be related to the stresses by Eqn. (13) as below:

$$\{\epsilon\} = [C] \cdot \{\sigma\} \tag{104}$$

where [C] is the inverse of the coefficient matrix containing the elastic constants and $\{\sigma\}$ is the stress tensor. Using the strain energy principle, the work done by an external force should be equal to the energy stored by the internal strains. One can then write:

$$\text{Internal strain energy} = \frac{1}{2} \int_v \{\epsilon\}^T \{\sigma\}\, dv \tag{105}$$

$$\text{External work done} = \frac{1}{2} \cdot \{u\}^T \cdot [k] \cdot \{u\} \tag{106}$$

Equating these one obtains the expression for the element stiffness as:

$$[k] = [\phi^{-1}]^T \int_v [Q]^T [C]^{-1} [Q]\, dv \cdot [\phi]^{-1} \tag{107}$$

It will be noticed that the elements of all the matrices in Eqn. (107) are functions of the geometry and material properties only. In the finite-element algorithms these matrices are evaluated once the geometry and the material properties are given in a systematic way. The element stiffnesses are calculated with respect to the local coordinates of each element. The next step is to compute the stiffness of the assemblage, referred to the global coordinates.

Step 3. Nodal Stiffness

Once the element stiffnesses are computed it is now necessary to assemble the individual elements to the overall mesh and characterize the medium at the nodal points. The assemblage of the elements at a nodal point will give rise to a block matrix whose diagonal elements are the individual stiffnesses of the contributing elements. These matrices can then be transformed to the global axes using a transformation matrix [T] as shown below:

$$[G] = [T]^t [K] [T] \quad (108)$$

where [G] is the global stiffness matrix, [K] is the block matrix obtained at each node and [T] is the transformation matrix. It is in this step that the individual finite-element programs differ in their efficiency. Because the elements of the matrix [G] will form the coefficients of the system of equations to be solved, the computer time involved will depend on the optimization of this step and trying to keep the half band-width of the matrix to a minimum. For this reason it was decided to use existing FEM programs rather than to develop a new program.

Step 4. Boundary Conditions

The boundary conditions for an axi-symmetrical case considered here are:

1. Along the load axis there can be only vertical displacements. This is symbolized by rollers in Fig. 3.4 (a) and 3.4 (b);
2. Likewise, along the other vertical boundary only vertical displacements can take place. Therefore, this boundary is also, represented by rollers;
3. At the bottom there will be no movements, as symbolized by a rigid boundary;
4. There are only vertical loads acting on a small area at the centreline. There are no other loads anywhere. The vertical loads are lumped as point loads at each of the nodes covered by the radius of the loading plate;
5. At the loaded surface, the deflections are given by the FWD tests. Therefore, the deformation of the surface is known. The surface deformation can be specified more tightly if a curve-fitting routine such as the one that the ISSEM 4 program uses, is employed. This curve-fitting routine fits the curve at every 30 mm and is constrained

to accept the deflections at the sensor points as measured in the field (see the input data at the top part of Fig. 4.8 (a) and (b)). The fitted curve forms the constant conditions at the free surface;

6. Because of the axi-symmetrical nature, only one half of the cross section needs to be considered.

Step 5. Analysis

Finite elment algorithms are generally classified into two categories: (1) the incremental method and (2) the iterative method.

The incremental method is shown schematically in Fig. 3.6. In this method the load is applied in small increments. Since the increments will be chosen to be small, the modulus for the analysis will be the tangent modulus. In Fig. 3.6 the tangent modulus at O for the first load increment OA is estimated and the computation carried out. If the same modulus were used for the next increment then the strains would be as at point B_0 instead of B. Hence the modulus is estimated again and the computations carried out. This procedure is repeated till the full load is applied. The advantages of this method are:

1. Non-linear problems can be treated as series of linear problems. If the increments are chosen small enough, the error in the estimated tangent modulus is likely to be small;
2. Because the loads are in increments, the computations are in a way like a triaxial test. Thus one can trace the stress path to the full load. If one sets a yield criterion then one will also know whether at any stage of loading failure is imminent, or in the case of pavements, whether tensile stresses in unbound materials are developing.

The disadvantage of the method is the amount of computer time required. Refinement to the

incremental method would be to choose smaller increments and doing an iterative routine within each increment so that the modulus need not be estimated at the end of load increment but can be obtained from computations (see for example Valliappan, 1974; Naylor, 1978).

The iterative method is shown schematically in Fig. 3.7. In this technique the full load is applied at once with an estimated initial or seed modulus. This might, for example, yield a strain at point 1 which is far removed from the actual stress-strain path. Then a correction is made which might result in the conditions as shown by point 2. This process is repeated until the calculated strains or stresses are within an acceptable tolerance of the true stress-strain curve. The advantage of this method is essentially the speed of computations. For an unambigous and fairly well understood stress-strain path this method would result in acceptable results. The disadvantage is that the stress path cannot be traced nor can a failure criterion be specified by this method. However, since the FWD can apply up to eight steps of load one can circumvent this difficulty by applying different loads below the design load and carry out an iterative analysis. This way the stress path can be traced.

As far as this writer is aware, except for the SENOL program from the University of Nottingham, all the programs used for the backcalculation of moduli of pavement layers use the iterative method.

Whether one uses the iterative or the incremental method, one has to have a material-response model so that the program can make the corrections at every step to arrive at the proper modulus value for the next step. In this thesis the material models were taken as outlined under Section 3.2.1 and are repeated below:

1. The asphalt modulus was determined from properties of the mix obtained from cores taken from the pavements, and using the van der Poel nomograph;

2. The moduli of the unbound layers were estimated from the results of the pressuremeter tests and are assumed to vary within the limits suggested by Lam (1982) and Emery (1983);

3. Anisotropy was considered by specifying a probable range of anisotropic ratios (E_v/E_h) for the materials actually found in the pavement structure. These ratios were obtained from published research results as mentioned in Section 3.2.1.

Existing back-calculation procedures are not capable of considering restricting bounds for the material properties of the different layers. Thus, they usually arrive at modulus values which are artificially high or low that do not necessarily correspond to the actual materials in the pavement structure (D'Amoto and Witczack, 1980). Therefore, it is submitted that while they deliver ***a mathematical solution*** to the problem, that solution does not necessarily reflect the actual material properties or the true system stiffness of the pavement structure.

In order to achieve this objective of finding a possible mathematical solution as well as to satisfy the bounds imposed for the probable material properties, the finite-element program must be able to perform iterative calculations to match the observed and computed deflection basins by choosing a combination of material properties ***within the range specified by the user.*** This process is not unlike linear programming or optimization procedures common in the operations research field. None of the existing programs can achieve this objective. Since ANSYS has this capability, it was proposed to use this program as a backcalculation tool in this study. Chapter 5 presents the ANSYS algorithm and a discussion of this optimization procedure.

Step 6. Output

The format of the output is more a preference of the programmer or the user, rather than a feature of the FEM. Generally, these outputs have to be redsigned and re-processed with other spreadsheet, database, or graphics programs to make them easily readable and understandable. Parts of the output from the FEM program used in this thesis is included as Appendices to Chapter 6.

3.4 ANALYSIS USING ANSYS

3.4.1 General

In the previous sections it was argued that in order to solve for the stresses and strains within a pavement structure, numerical techniques are to be resorted to. It was suggested that the most powerful numerical technique available today is the finite-element model. The assumptions involved in building such a model were listed. A conceptual model of a layered elastic system to represent a pavement structure was presented. The actual physical model used in this study was also presented (Fig. 3.4a). The mathematical basis for the finite-element techniques for pavement problems according to Girijavallabhan and Reese (1968) and the mathematical basis for the layered elastic solution according to Gerrard (1968) were discussed. It was noted that many of the existing commercial programs for back-calculating FWD data were inadequate in that they arrived at ***a mathematical solution*** which does not necessarily represent the physical pavement structure or the material making up that structure. Therefore, it was argued that pavement problems are best solved by developing a general-purpose finite-element program which permits the treatment of the layered elastic system in the most general way capable of considering non-homogeneity, non-linearity, stress and

temperature dependency of the moduli, etc.. In addition the program should be able to perform some form of iterative calculations so that it can arrive at the **most probable combination of material properties** that are **consistent with the actual physical structure** being analyzed. It was suggested that the ANSYS finite-element algorithm satisfies these criteria and hence was used in the analysis phase of this study.

3.4.2 A Short Overview of the ANSYS Model

Chapter 5 discusses the ANSYS algorithm in more detail. That chapter also presents the mathematical theory of ANSYS, as well as the user-defined codes used in building the pavement model at the different test sites. The basic building block of the model presented in Fig. 3.4 (and in Chapter 5) is the four noded isoparametric plane elastic solid. The theory of this element type is discussed in Chapter 5. Finally, in the later chapter a discussion of the optimization module as employed by the ANSYS program is presented.

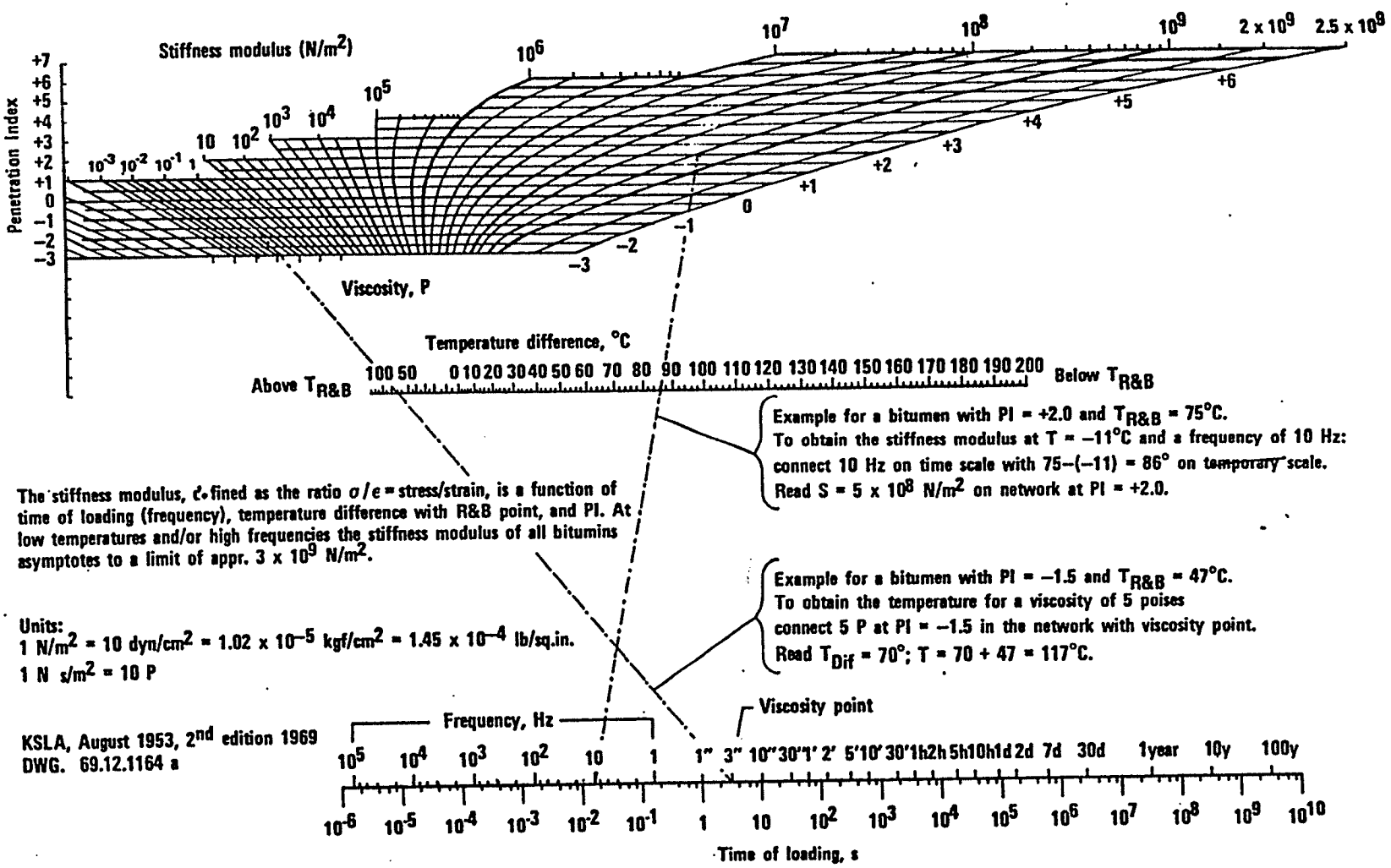

Fig. 3.1. Determination of asphalt cement and mix stiffness

(After van der Poel)

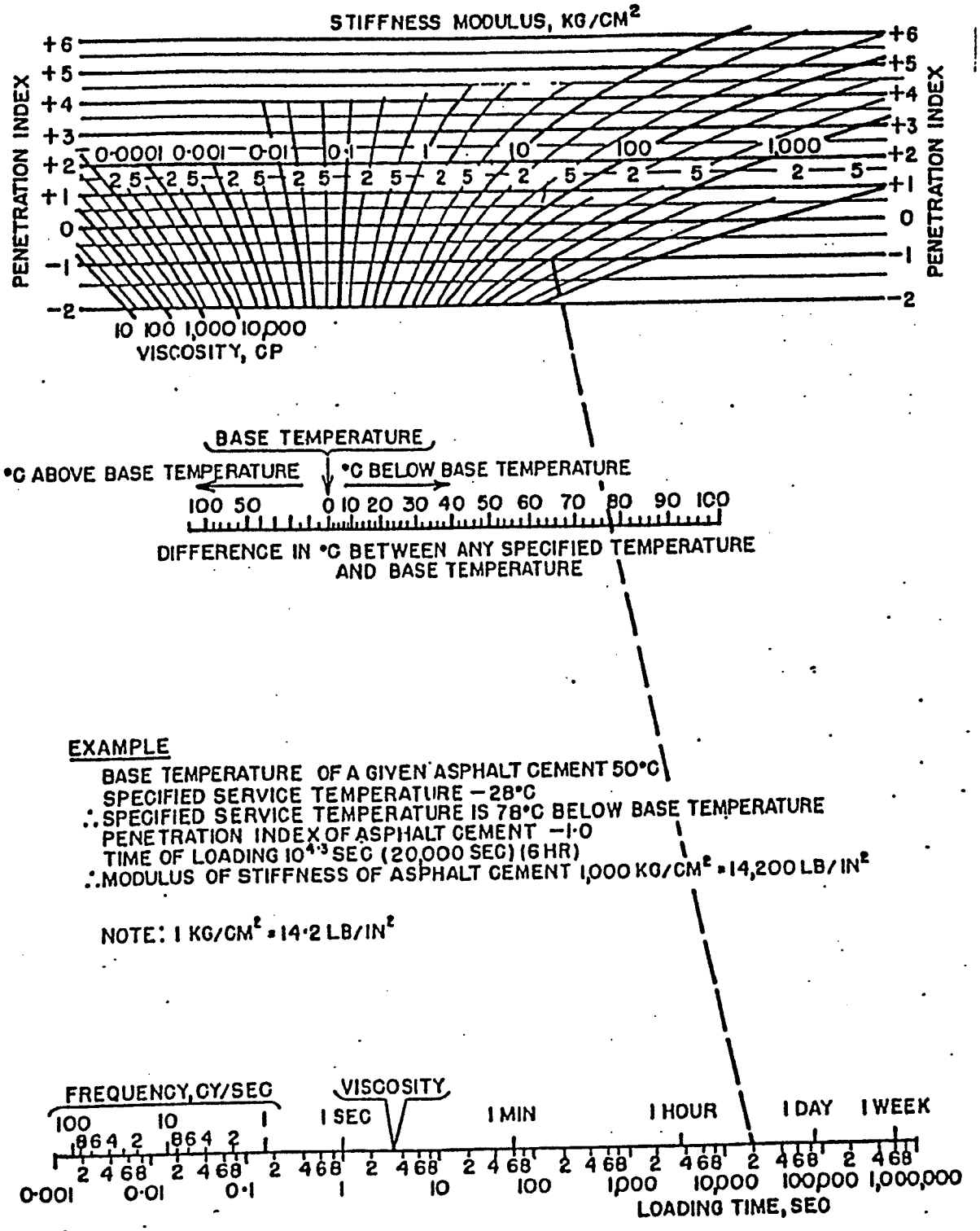

Fig. 3.2. Modification of van der Poel's nomograph by McLeod

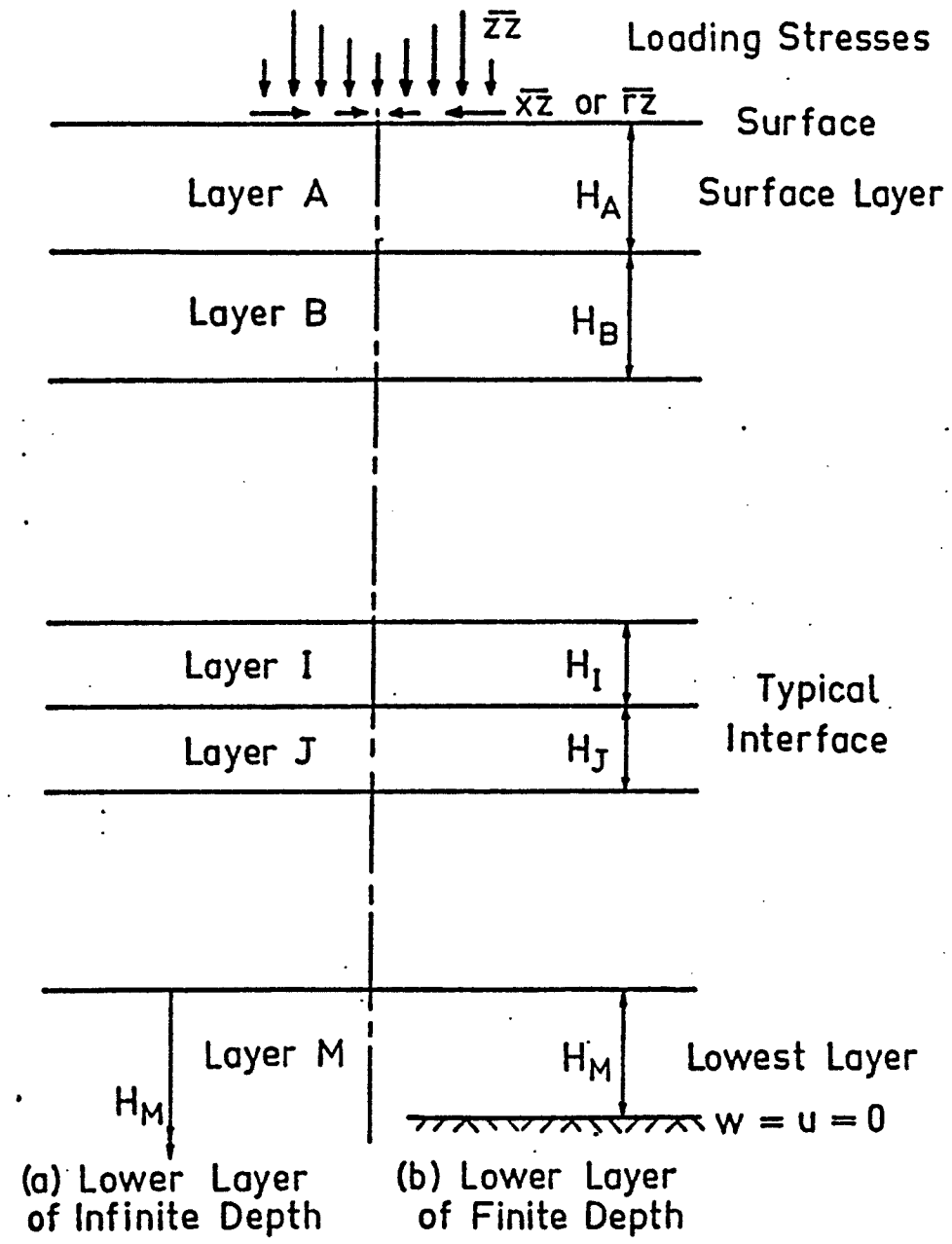

FIG. 3.3. TYPICAL LAYERED SYSTEM (AFTER GERRARD, 1967)

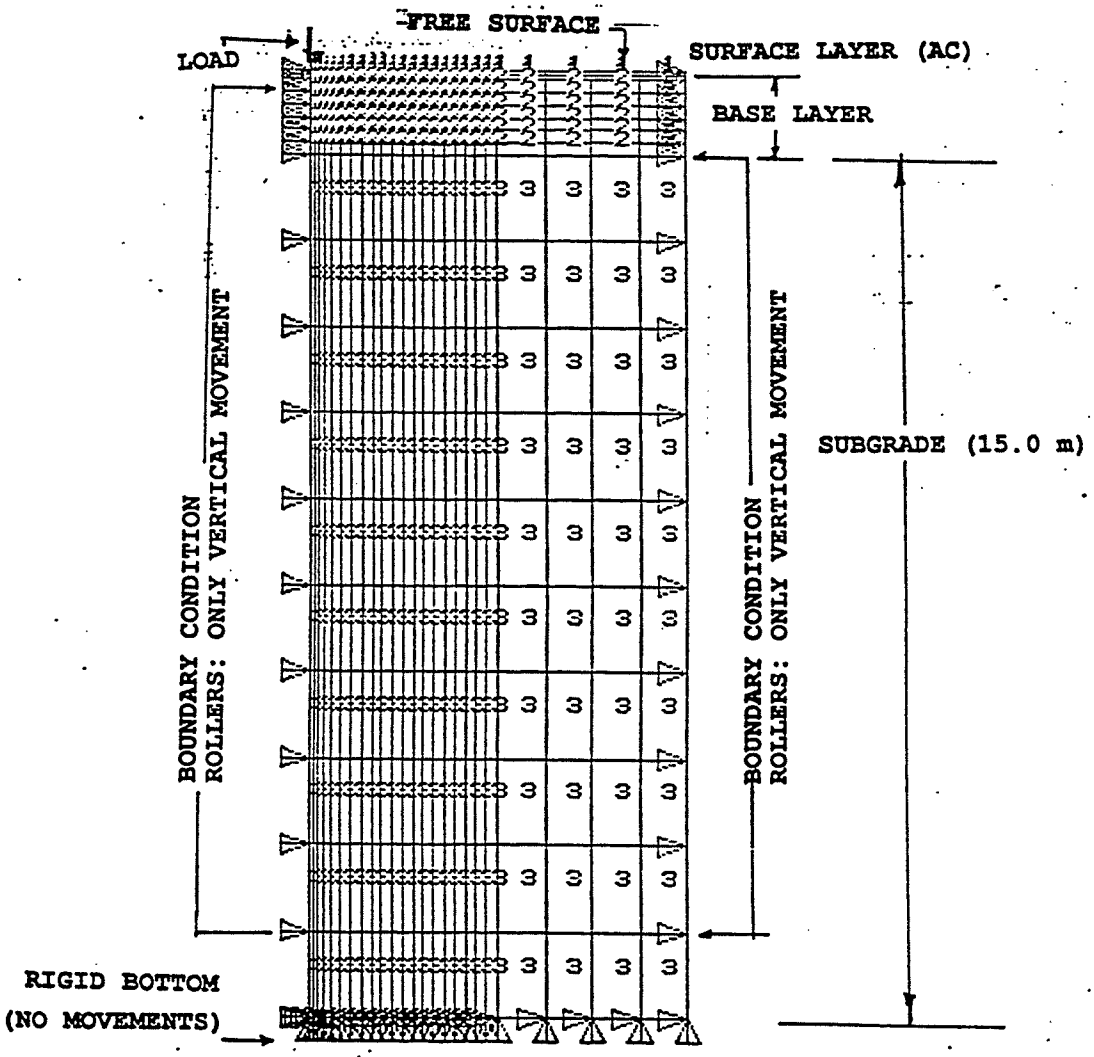

FIG. 3.4.(A): TYPICAL FINITE ELEMENT MODEL TO APPROXIMATE THE LAYERED ELASTIC SYSTEM

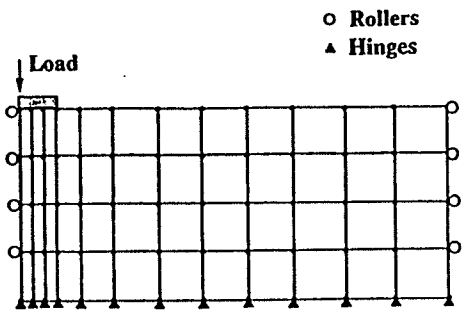

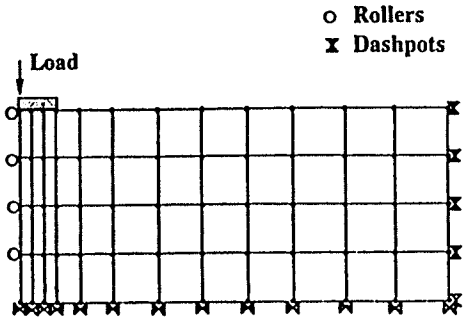

(a) FOR STATIC AND DYNAMIC ANSLYSIS
DASH POTS FOR DYNAMIC EFFECTS (ONG ET AL, 1992)

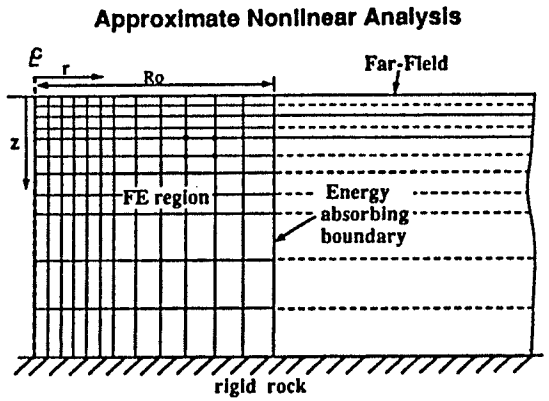

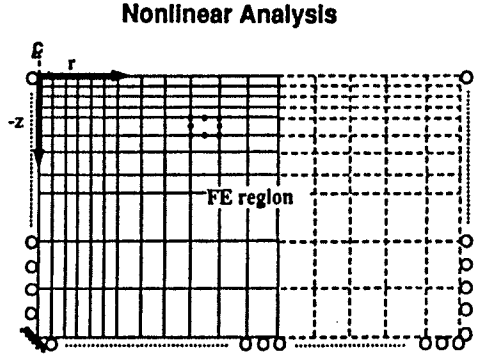

(b) NON LINEAR MODELS (Chang ET AL, 1991)

FIG. 3.4 (B): OTHER FINITE ELEMENT MODELS THAT MAY BE USED TO APPROXIMATE LAYERED ELASTIC SYSTEMS

b = height of the element

r,z,θ = local cylindricsl coordinates

u_{ij} = nodal dispalcement in r direction at nodal point (i,j)

w_{ij} = nodal dispalcement in z direction at nodal point (i,j)

a_j, a_{j+1} = coordinates of nodal points in r direction

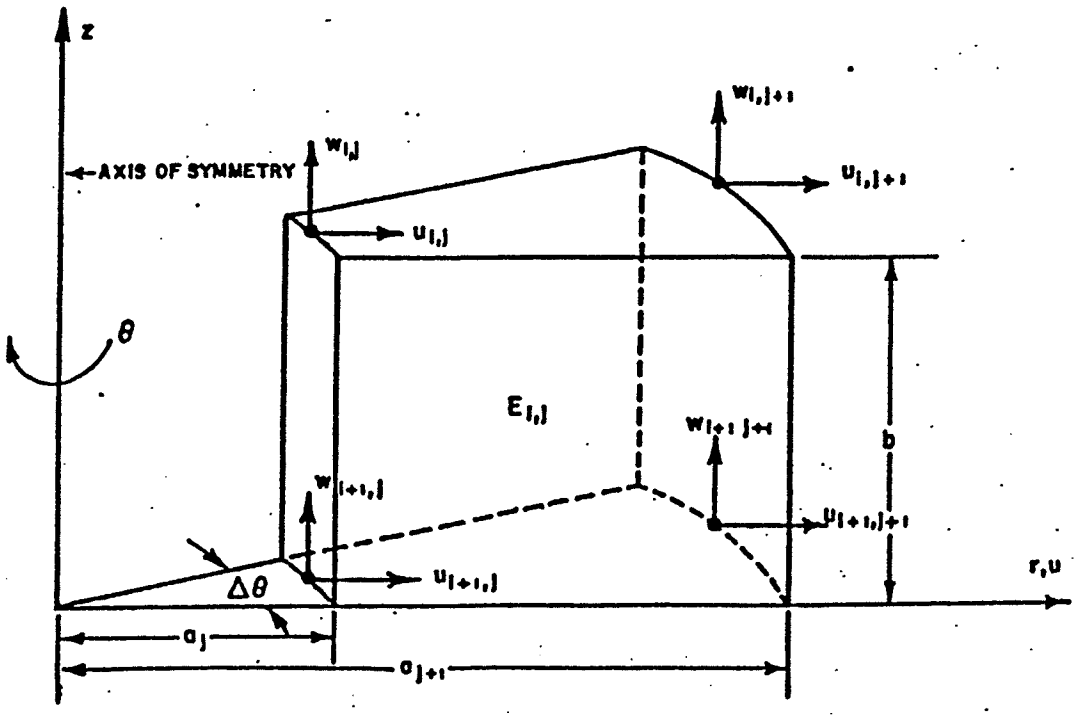

FIG. 3.5 NODAL AND ELEMENT STIFFNESS IN AN AXI-SYMMETRICAL FINITE ELEMENT MODEL

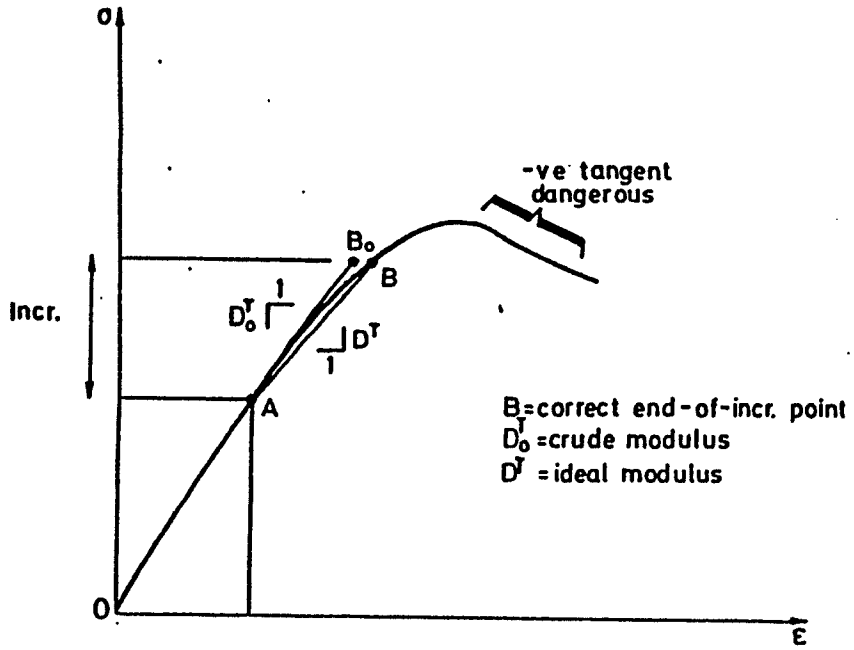

FIG. 3.6: CONCEPT OF INCREMENTAL METHOD

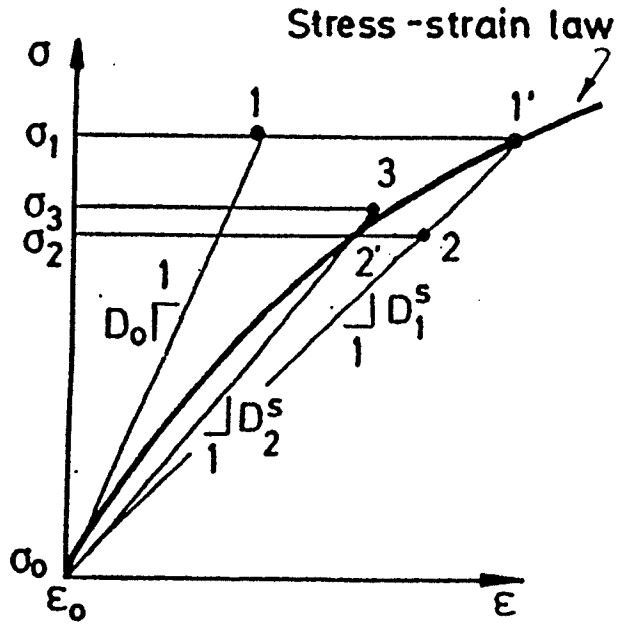

FIG. 3.7 CONCEPT OF ITERATIVE METHOD

AFTER NAYLOR, 1978)

Table 3.2. Summary of Displacements and Strains in layer i.

Function	$\beta^2 > 0$	$\beta^2 = 0$
Vertical Deflection W_i	$\frac{(A_2+A_3)}{\sqrt{l^2z^2+r^2}} + \frac{(A_1+A_4)}{\sqrt{m^2z^2+r^2}}$ where, $l^2=(\alpha+\beta)^2;\ m^2=(\alpha-\beta)^2$	$\frac{1}{\sqrt{(\alpha^2z^2)+r^2}}\ [c_1+c_3+z(c_2+c_4)]$ where, $\alpha z = p$
Radial Deflection U_i	$\left[\begin{array}{l} \frac{q_1}{r}\ [(A_1-A_4) - \frac{mz}{\sqrt{m^2+r^2}}] \\ + \frac{q_2}{r}\ [(A_2-A_3) - \frac{lz}{\sqrt{l^2+r^2}}] \end{array}\right]$	$\left[\begin{array}{l} \frac{1}{r}(1 - \frac{p}{\sqrt{p^2+r^2}})\ (n_1c_1 - n_2c_2 + n_1c_2) \\ - \frac{1}{r}(1 + \frac{p}{\sqrt{p^2+r^2}})\ (n_1c_3 + n_2c_4 + n_1c_4) \end{array}\right]$ where, $p = \alpha z$
Vertical Strain ε_{zz}	$\left[\begin{array}{l} -(A_2+A_3)\ (l^2z)\ (l^2z^2+r^2)^{(-\frac{3}{2})} \\ -(A_1+A_4)\ (m^2z)\ (m^2z^2+r^2)^{(-\frac{3}{2})} \end{array}\right]$	$\left[\begin{array}{c} (C_2+C_4)\ (p^2+r^2)^{(-\frac{3}{2})} \\ -[C_1+C_3+z(C_2+C_4)]\ 2\alpha^2z\ (p^2+r^2)^{(-\frac{3}{2})} \end{array}\right]$ where $p = \alpha z$
Radial Strain ε_{rr}	$\left[\begin{array}{c} -\frac{q_1}{r^2}\ (A_1 - A_4) - \frac{q_2}{r^2}\ (A_2 - A_3) \\ -q_1.m.z\ [2(m^2z^2+r^2)^{(-\frac{3}{2})} + \frac{1}{r^2}(m^2z^2+r^2)^{(-\frac{1}{2})}] \\ -q_2.l.z\ [2(l^2z^2+r^2)^{(-\frac{3}{2})} + \frac{1}{r^2}(l^2z^2+r^2)^{(-\frac{1}{2})}] \end{array}\right]$	$\frac{1}{r^2}\ (Y-X) + 2p\ (p^2+r^2)^{-\frac{3}{2}}\ (X+Y)$ $-\frac{1}{r^2}\ p\ (p^2+r^2)^{-\frac{1}{2}}\ (X+Y)$ where, $X = n_1C_1 - n_2C_2 + n_1C_2$ $Y = n_1C_3 + n_2C_4 + n_1C_4$ $p = \alpha z$

CHAPTER FOUR

FIELD TESTING PROGRAM

4.1 GENERAL

The field testing reported, herein, formed part of a larger study undertaken by Transport Canada[1], to establish a correlation between plate load test results and the results from non-destructive testing such as the Falling Weight Deflectometer (FWD). The objective of Transport Canada was to determine whether the time-consuming, expensive and operationally very disruptive plate load tests could be replaced with a much faster, lighter, and less disruptive testing technique without compromising their design standards or creating any abrupt discontinuity in their design procedures. These procedures were developed by Transport Canada in the early 1940's and had served them well for over 50 years and through a period of rapid growth and advancement in the aviation industry.

Transport Canada was kind enough to permit the author to participate in their test program at their expense and collect the data he needed for this study. Because of administrative and budgetary constraints, all the tests were not done in a few months nor even in one year, but spanned a period of three years between 1985 and 1988. The test data from their study was evaluated by Trow Ltd., of Toronto, Canada in 1985. Excepting some passing comments in a later section, this firm's report is considered beyond the scope of this thesis. Furthermore, Transport Canada had extended these tests to many airports across the country

---

1 Transport Canada is a Department in the Ministry of Transport of the Government of Canada. This Department regulates and sets standards for the construction and maintenance of civil aviation airports in Canada.

in later years. By the end of 1993, this series of tests will have been completed. Another thesis was completed in 1991 at the Royal Military College in Kingston, Ontario, Canada (Fenton, 1991), using the data up to that year. This latter thesis addresses specifically the question of correlation between the Plate Load tests and FWD tests.

The objective of the present study is the ***in-situ*** characterization of material properties in the pavement structure. In the literature one finds that FWD testing and the back-calculation procedures themselves are often referred to as in-situ testing. However, the aim of this thesis is:

1. To demonstrate an independent and direct means of *measuring* these material properties (primarily the layer moduli); and
2. To determine whether any correlations could be established between the measured and back-calculated moduli.

Also, the study started with a focus on the unbound layers only. As explained in a previous chapter, the modulus of asphaltic surface material was to be established using the nomographs developed by Van der Poel and later modified by McLeod.

4.2 ADDITIONAL FIELD TESTS FOR THIS STUDY

With the above objectives in mind, the additional tests that were performed were:

1. Pressuremeter tests at selected stations using the PENCEL pressuremeter;
2. Tests on asphaltic concrete cores recovered from the same stations;
3. Simple geotechnical tests such as classification tests on the unbound materials recovered from the same stations.

Details of these tests are given in later sections in this chapter.

4.3 SITES TESTED

From the first series of tests in 1985, four airports representing different traffic, environmental, and geotechnical conditions were chosen. They also represented a broad spectrum of pavement structures. These sites were Thunder Bay in Ontario, St.Andrews and Brandon in Manitoba and Regina in Saskatchewan. In the second series in 1988, the tests included again St. Andrews and Regina but extended also to Saskatoon in Saskatchewan. Fig. 4.1[2] shows the geographical location of these sites. Table 4.1 gives some pertinent statistics regarding their climatological and overall geotechnical conditions. The reason for repeating the tests at St.Andrews and Regina was that there were too few data collected at these sites in 1985. There were also other differences in the testing procedures between the series in 1985 and in 1988. For instance, the 1985 series used the lighter Dynatest 8,000 FWD with a 300 mm diameter loading plate while the latter series used the heavier Heavy Weight Deflectometer (HWD) with a 450 mm diameter plate.

Fig. 4.2 to 4.6 show the plan layout of the airside facilities at these airports and the locations of the field tests. At Regina, Saskatoon and St.Andrews (the 1988 series) the FWD tests were done, by Transport Canada, for the purpose of arriving at rehabilitation strategies for these facilities. Hence the tests were done on hundreds of points on each runway. However not all were used for this study. Only a few randomly selected points along the wheel paths of the aircraft (i.e. 3 m left and 3 m right of the centreline and on-centreline) were chosen and analyzed. Care was taken to ensure that the entire runway was covered by the points chosen. Of these again, only five points were chosen for comparing anisotropic and

---

[2] All figures and tables (with the exception of Table 4.1) are included in the Appendices at the end of the chapters.

TABLE 4.1 Environmental and Geotechnical Conditions at the Test Sites (30 year records)

SITE	THUNDER BAY	BRANDON	ST.ANDREWS	REGINA	SASKATOON
LATITUDE	N 48° 22'	N 49°55'	N 50° 03'	N 50° 26'	N 52° 10'
LONGITUDE	W 89° 19'	W 99°57'	W 97° 02'	W 104° 40'	W 106° 42'
TEMP.° C MAX. AVG. MIN.	 32.9 2.3 -35.7	 35 1.5 - 38.1	 35.7 1.2 -39.6	 35.9 2.2 -38.6	 34.9 1.6 -39.1
PRECIP. RAIN(cm) SNOW(cm)	 52.7 213.0	 33.9 116.9	 38.3 85.6	 28.7 115.7	 24.5 113.1
SUBGRADE TYPE	SP/SM ML/CL	CL/ML	CH	CH	ML/CL
BUILT TESTED AGE AT TEST	1984 1985 1 YR	1983 1985 2 YRS	1968, 1970 1988 20,18 YRS	1979 1988 9 YRS	1976 1988 12 YRS
DESIGN AIRCRAFT	B-727	B-737	DC-3	B-727	B-727

isotropic models. Tables 4.2 to 4.6 show the stations and the pavement structures at these locations. The pavement structures were determined from actual coring. These were the depths or layer thicknesses used for the finite-element analyses later.

4.4 TEST LAYOUT

4.4.1 1985 Test Series

The 1985 test series reported herein pertains to two sites, Thunder Bay, Ontario and Brandon, Manitoba. As mentioned earlier, these were part of an investigation by Transport Canada. The test layout was accordingly decided by their engineers. In this series they

followed the standard test layout that had been adopted for their Benkelman Beam tests. By this procedure, the deflection test at any station is not a single test precisely at the specified station but the mean of six tests done on five points along the circumference of a circle 1.5 m and at the centre which is the exact location of the chosen station on the runway. Fig. 4.7 shows this set-up schematically. Thus the deflection reported for any station will be the mean of all the six stations. For the Benkelman Beam tests, Transport Canada would report the standard deviation from the mean so that some idea of a measure of variability around any particular location on the runway could be gained. It should be mentioned that the sensors of the FWD were always placed parallel to the direction of traffic and not in the radial directions from the centre. This was somewhat unfortunate because by placing the sensor beam radially, not only the non-homogeneity in the pavement construction could have been determined but also the anisotropic behaviour of the pavement structure could have been studied.

In this study, the loads and deflections at each of the seven FWD sensor locations was averaged and reported as the deflection at the particular station. Tables 4.7 and 4.8 show the variations in the applied loads and the deflection responses of the pavements. The coefficient of variation is generally low particularly for the loads and for deflections at the sensors farther from the load. The variations are somewhat larger at the nearer sensors, particularly below the load. The nearer sensors are influenced by all the layers but predominantly by the asphaltic layer. Thus the higher variation could indicate the variability in the top layers of the pavement. The 1985 test series was also conducted with the lighter Dynatest 8000 FWD. It was felt that the maximum loads and the small- diameter loading plate would generate smaller pressure bulbs. Thus the deeper layers were not even "feeling" the impact of the load.

The effect of plate size on the pavement response, layer moduli and stress distribution requires further study.

4.4.2 1988 Test Series

The 1988 series of tests in this study and a subsequent study by Transport Canada used the heavier Dynatest 8001 Heavy Weight Deflectometer (HWD). The two studies were not conducted at the same sites. For this study the testing was done at St.Andrews, Saskatoon and Regina. The loading pattern was not as in the 1985 tests. The auxiliary test points on a circle around the station were dispensed with. Instead a high density testing program on several longitudinal profile lines on the runway and at closer spacing, which was more appropriate in a routine design situation, was carried out. Thus, for this series, the deflections reported herein are not the average deflections but the only deflections that were measured.

4.4.3 Loads

In all cases it was attempted to simulate the traffic at that particular airport. As shown in Table 4.1 the design aircraft ranged from Boeing B-737 to B-727. However, many other types of aircraft with different weight and tire pressure combinations were using these facilities. Therefore, the loading represented a spectrum of tire pressures ranging from 500 kPa to 1,500 kPa. In Brandon and in Thunder Bay (1985 series) four load steps were applied: 500 kPa, 800 kPa, 1,200 kPa and 1,500 kPa. The loads were applied through a 300 mm diameter plate. In the 1988 series four loads were applied, but the highest load (the 1,500 kPa load) was applied twice. Thus the load steps were 700 kPa, 1,200 kPa and 1,500 kPa for Regina and Saskatoon while they were 500 kPa, 750 kPa and 900 kPa for St.

Andrews. The loads were applied through a 450 mm diameter plate at Regina and at Saskatoon whereas a 300 mm plate was used at St. Andrews. The last mentioned airport is a trainer airport with a high volume of predominantly light aircraft and consequently had a light pavement structure. As it turned out, even the 900 kPa load indicated that the pavement had probably failed. These results will be presented in a later chapter and discussed. Again the detailed printout of the large number of tests showed that the FWD or HWD could apply loads with high precision and reproducibility.

4.4.4 Deflection Measurement

The FWD and the HWD used in the two series measured the pavement response with seven accelerometers. The location of these sensors could be varied within certain limits. For the 1985 series the sensors were at 0, 300, 610, 915, 1,219, 1,524 and 1,829 millimetres[3] from the load point. During the subsequent analysis by the ISSEM-4 program, many sections could not be analyzed because the program was not able to define the deflection basin with sufficient accuracy. A typical example of such an ISSEM-4 run is shown in Fig. 4.8 (b). Thus, in the 1988 series the sensors were placed farther away from the load in order to be able to better define the tapering end of the deflection basin. The sensor distances in the 1988 series were 0, 300, 450, 1,000, 1,400, 1,800 and 2,250 millimetres.

---

[3] These measurements are converted units from the imperial units of 0, 1, 2, 3, 4, 5 and 6 feet.

4.4.5 Temperature Measurements

Temperature measurements were recorded by the machine with a built-in sensor and also manually by a surface thermometer. In addition, a thermometer was stuck in a small hole in the pavement so that temperatures could be measured between 50 and 75 mm below the surface. Air temperatures were obtained each hour from the meteorological stations at each airport.

4.5 IN-SITU MATERIAL TESTS

Immediately after the completion of the deflection tests, the pavements were cored at these locations. This coring program helped to determine the pavement structure, to recover samples of asphalt and unbound materials for further laboratory tests and to perform the pressuremeter tests.

Pressuremeter tests were done in the granular materials and in the subgrade. Generally, the pressuremeter test could be done only at one depth in the granular material because this layer was not usually thick enough to permit more test locations. Often, due to the age of the pavements and probably due to the quality of materials placed during the original construction, a clear distinction between the high-quality crushed granular base and pit-run granular subbase material was difficult to ascertain. In the subgrade material, generally, two pressuremeter tests were done; the first one immediately below the interface of the subgrade and the granular construction and the next one metre below the first one. Tables 4.2 through 4.6 show the location of pressuremeter tests at the different sites.

4.5.1 Procedure for Pressuremeter Tests

The pressuremeter was inserted in the ground with the help of a drill rig. It is believed that the procedure would be closest to what Houlsby and Withers (1988) called the full-displacement pressuremeter tests. A solid rod with a conical point which is almost identical to the point at the end of the pressuremeter was pushed into the ground with the hydraulics of the drill rig. The rod and the cone were approximately 3 mm larger in diameter than the pressuremeter itself. Once the hole has been made to the required depth, the rod was withdrawn and the pressuremeter lowered into the hole without any delay. This usually resulted in a good fit of the instrument in the hole without allowing the soil to relax too much.

All pressuremeter tests were cyclic tests. In order to determine the point at which the unload-reload cycles should begin, a pilot hole would be first made. The pressuremeter test was carried out to define the complete pressuremeter curve. From this curve, the pseudo-elastic range was visually estimated using a "zoom-mode" on the computer screen. The unload point was, generally, about 80% of the point where the linear segment started deviating toward plastic behaviour (Fig. 4.9). In the case of granular base layers, the initial part was very steep and often showed no transition to a plastic range (see for example Fig. 4.10). In these cases the unload point was arbitrarily chosen between 300 kPa and 500 kPa loading. The unloading would be generally carried out over three to five steps, i.e. 15 to 25 cc of water pumped out. The soil was not completely unloaded. Complete unloading would have taken the soil very quickly over the plastic range in the unloading stage. Once in the plastic range it is difficult to estimate the rebound secant modulus.

Cyclic tests consisted of three unload-reload cycles. The author is aware that Briaud et al (1986) recommended 10 unload-reload cycles to clearly define the modulus, E_r.

However, in this series it was found that the modulus E_r remained fairly steady over three cycles. Therefore, it was decided that three cycles were as good as ten. It may be worthwhile to investigate the influence of number of cycles to the variation in the modulus values and its relevance in the pavement analysis and design.

Calibration of the pressuremeter was carried out at the beginning of each day or whenever the sheath was changed. It was found that the calibration did not change significantly for extended period of times.

Evaluation of pressuremeter tests were done using a computer algorithm, called PRESSRED, developed by Briaud and his colleagues in Texas A & M University. Examples of output from this program are shown in Fig. 4.11 and Fig. 4.12. A complete set of pressuremeter results are shown in Appendix 4-I.

4.5.2 Testing of Asphalt Cores

Asphalt cores were usually obtained in duplicate at each test location. The cores were visually inspected and notes made of their condition. Then they were used for extraction, aggregate gradation, penetration and viscosity tests. All tests were done in accordance with relevant ASTM standards. Asphalt penetrations were determined at 4°C, 25°C and 40°C, while viscosities were determined at 60°C 100°C and at 135°C. The results are plotted on the Shell bitumen chart as suggested by van der Poel and by Bell (1983).

Results of asphalt testing are presented in Figs. 4.13 to 4.17. and in Table 4.9.

4.5.3 Geotechnical Tests

Bulk samples of base and subgrade materials were recovered at each test location. These were tested for grain size distribution, plasticity and moisture content. The results are presented in Figs. 4.18 to 4.22 as well as in Table 4.10.

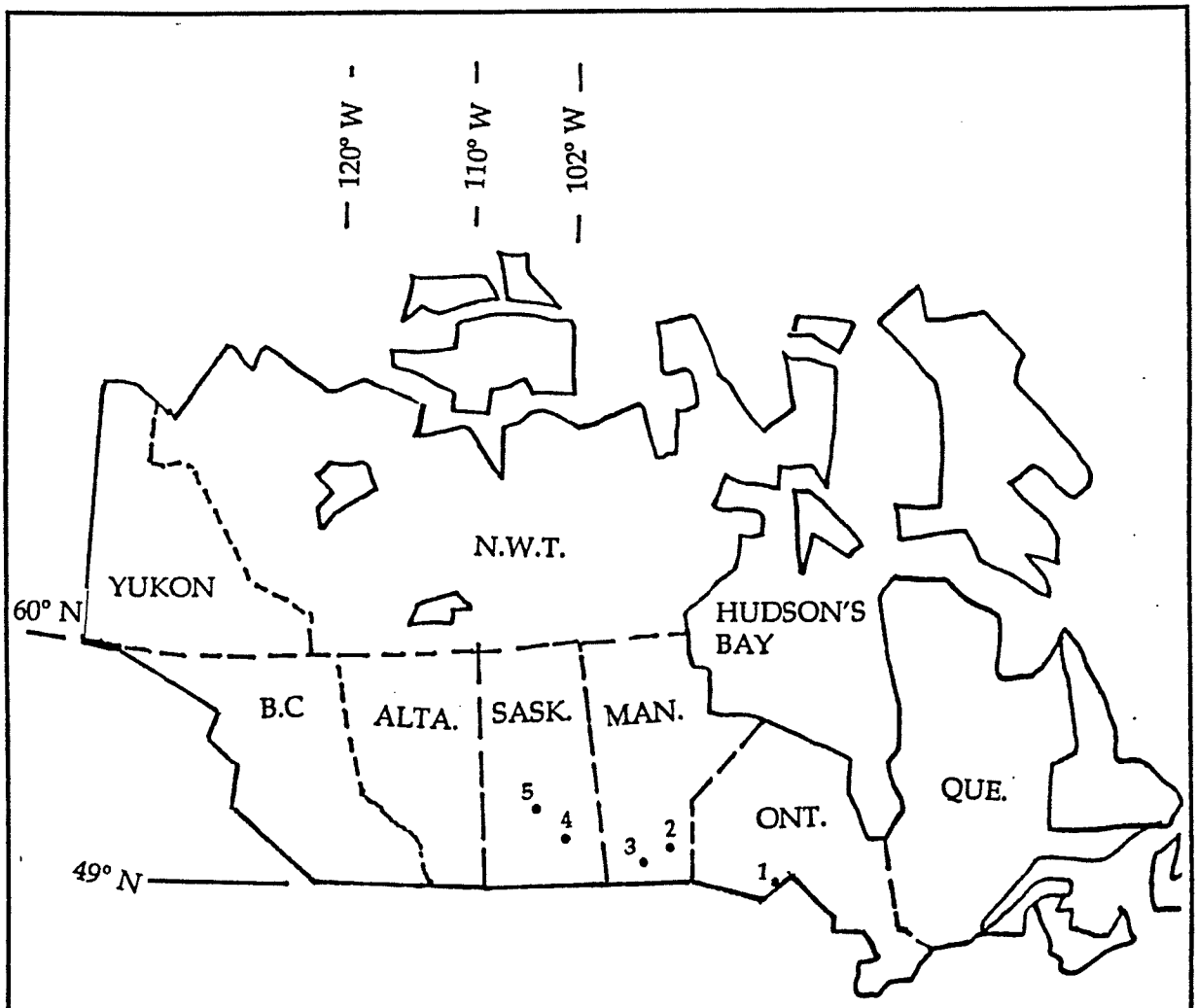

1. THUNDER BAY

2. ST. ANDREWS

3. BRANDON

4. REGINA

5. SASKATOON

FIG. 4.1. GEOGRAPHIC LOCATIONS OF THE SITES

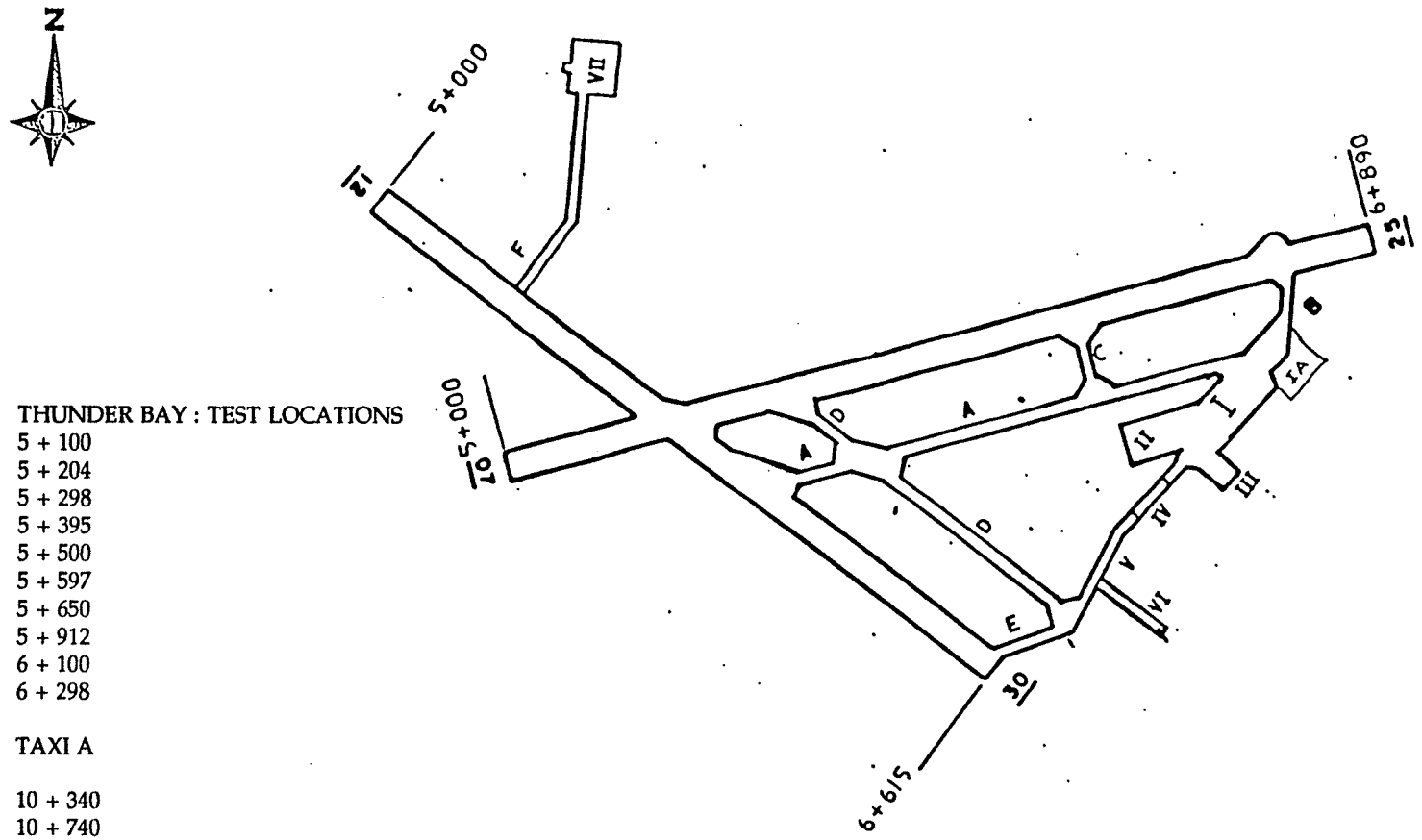

FIG. 4.2. TEST LOCATIONS IN THUNDER BAY AIRPORT

BRANDON: TEST LOCATIONS

RUNWAY 08-26

STA. 4 + 950
STA. 5 + 090
STA. 5 + 183
STA. 5 + 278
STA. 5 + 384
STA. 5 + 488
STA. 5 + 588
STA. 5 + 691
STA. 5 + 787
STA. 5 + 895 *
STA. 5 + 978 *
STA. 6 + 108
STA. 6 + 206 *
STA. 6 + 303
STA. 6 + 435
STA. 6 + 500
STA. 6 + 539 *
STA. 6 + 613

* NOT ANALYZED

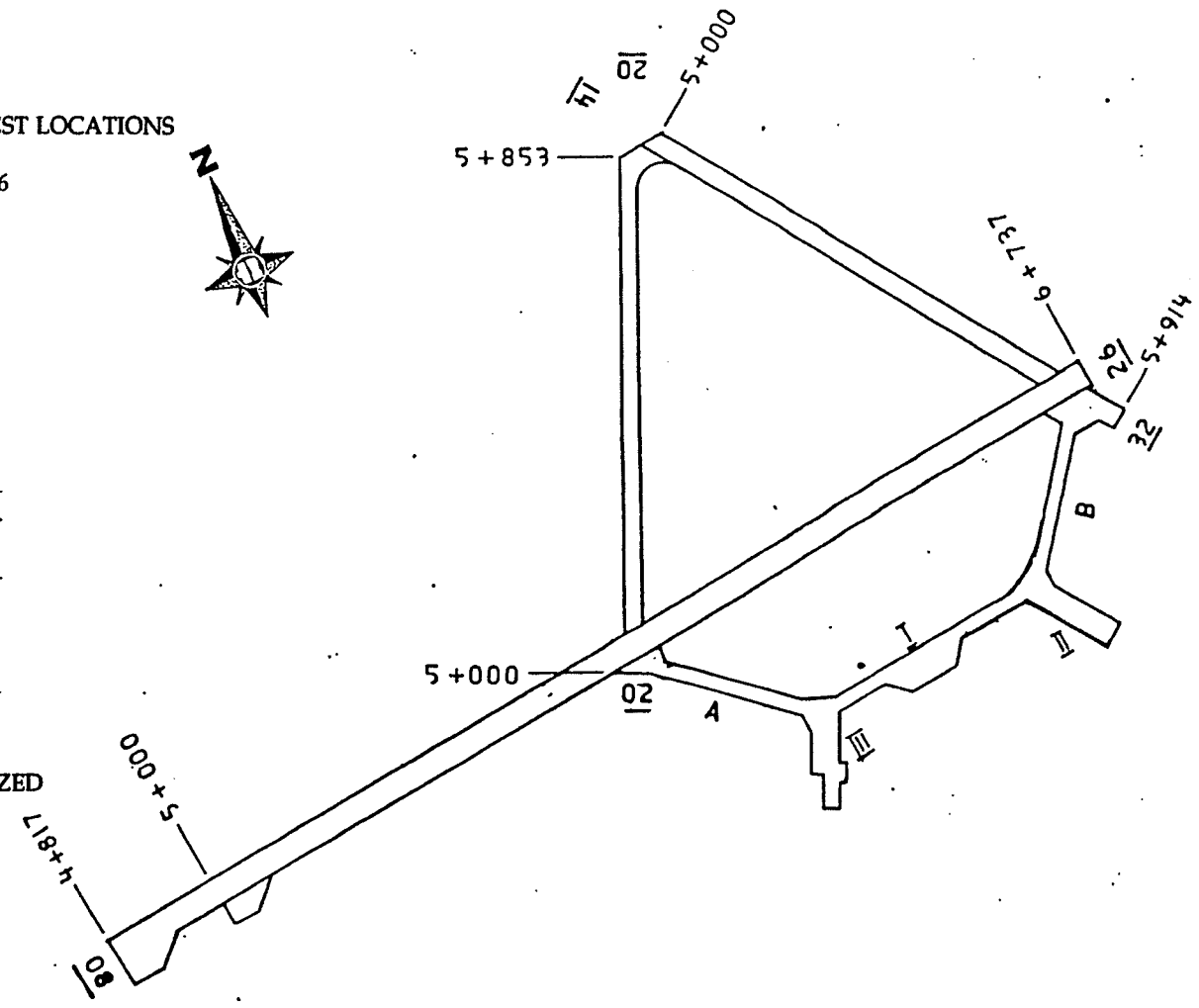

FIG. 4.3. TEST LOCATIONS IN BRANDON AIRPORT

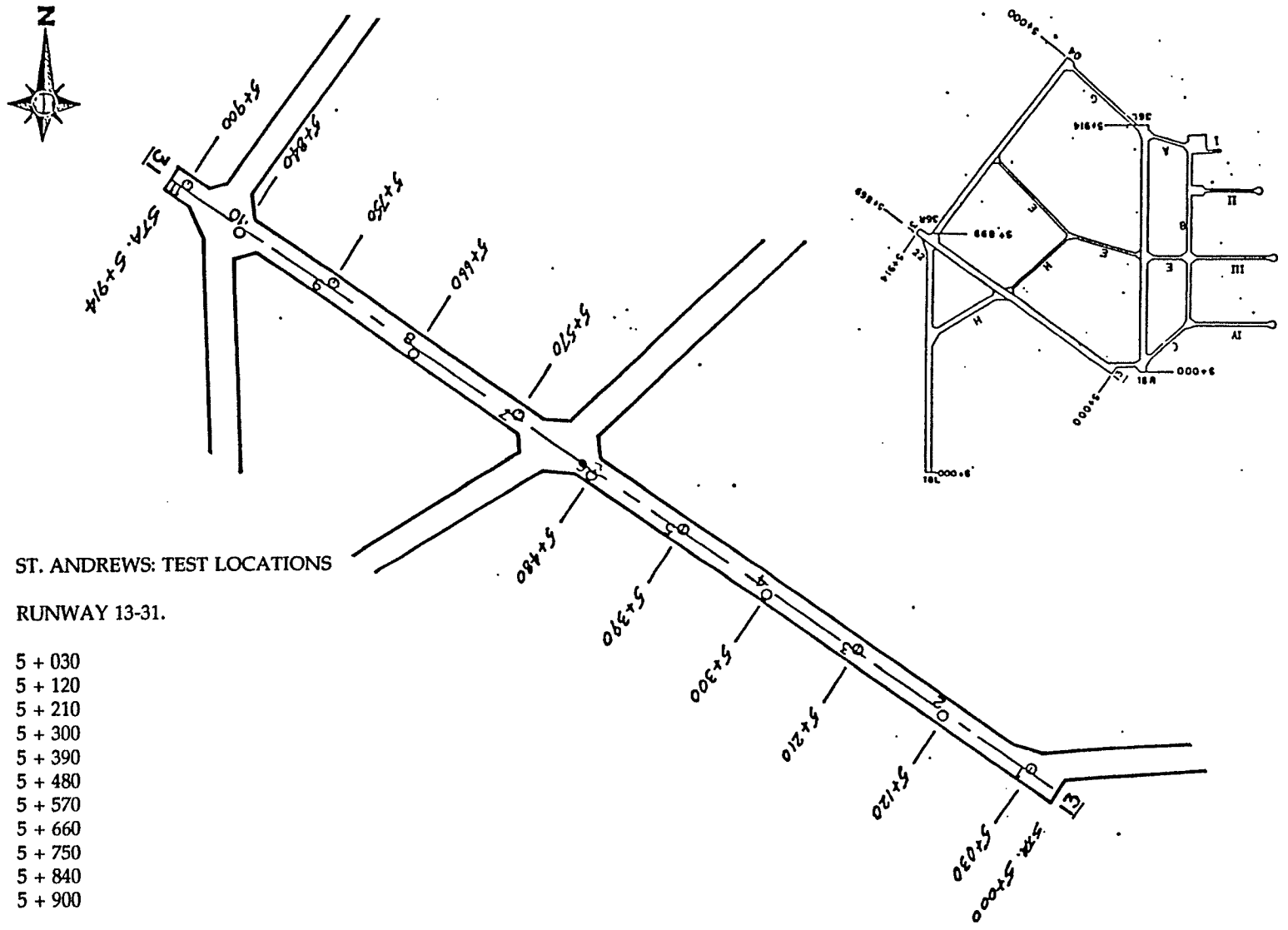

FIG. 4.4. TEST LOCATIONS IN ST. ANDREWS AIRPORT

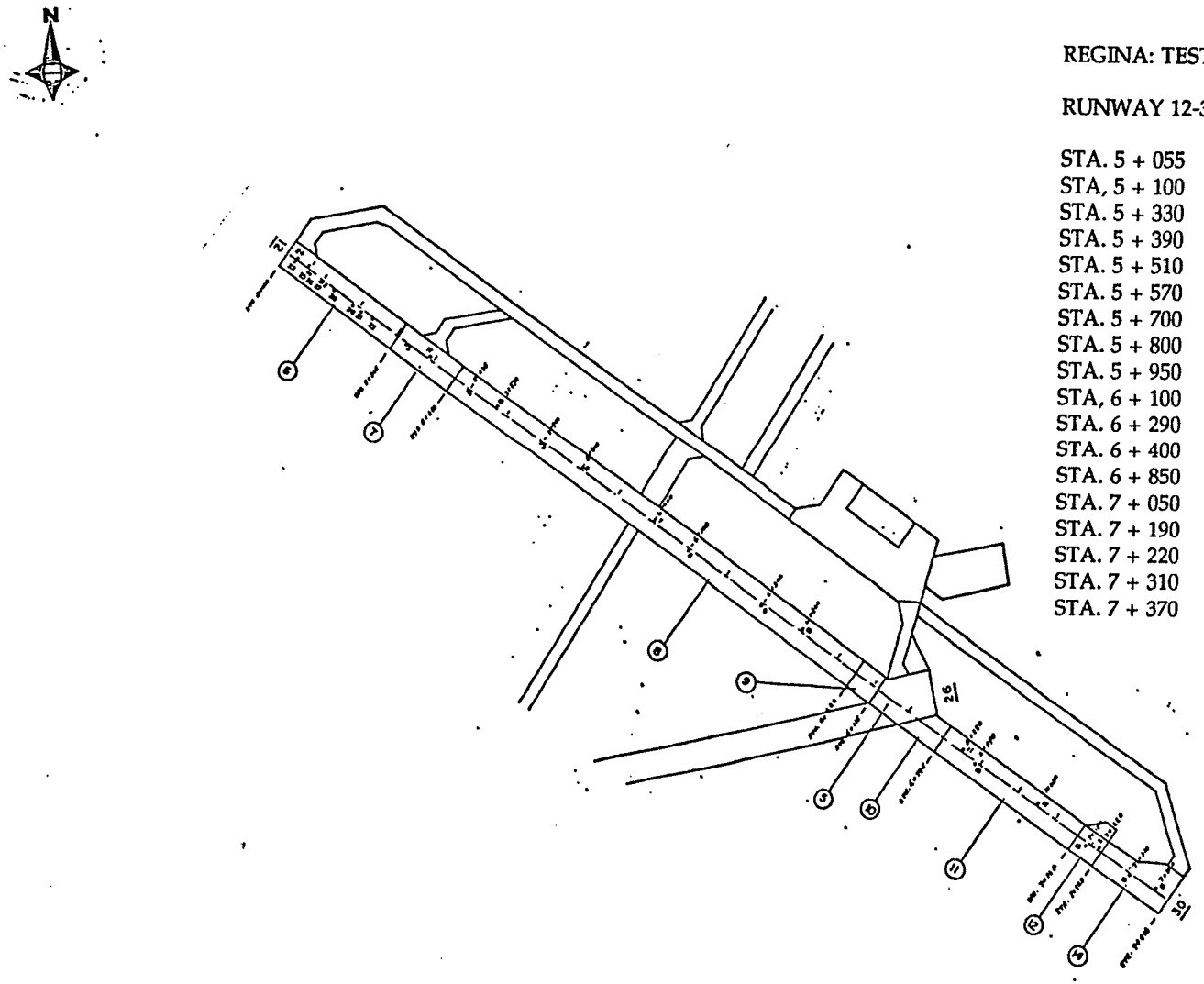

FIG. 4.5. TEST LOCATIONS IN REGINA AIRPORT

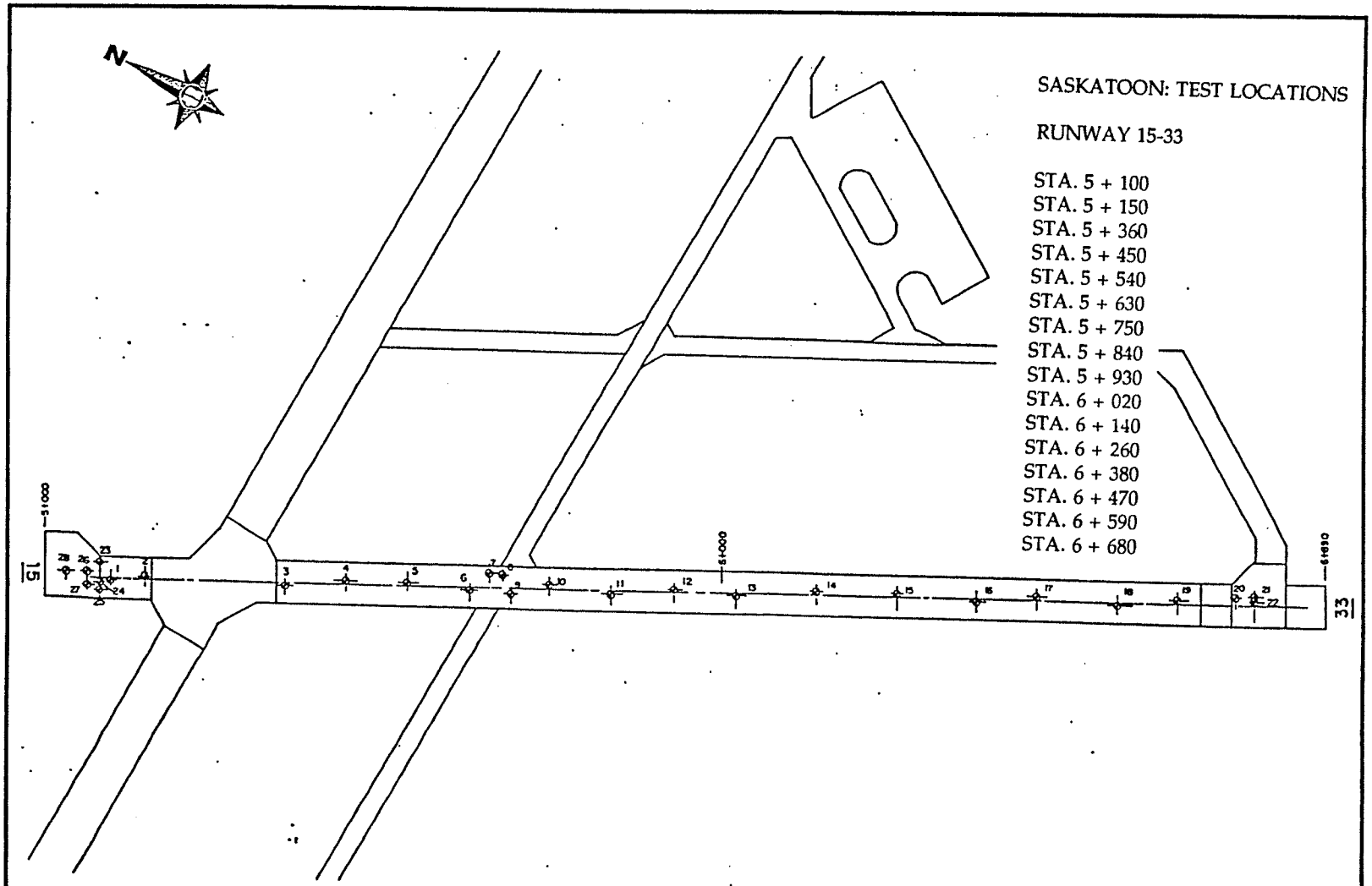

FIG. 4.6. TEST LOCATIONS IN SASKATOON AIRPORT

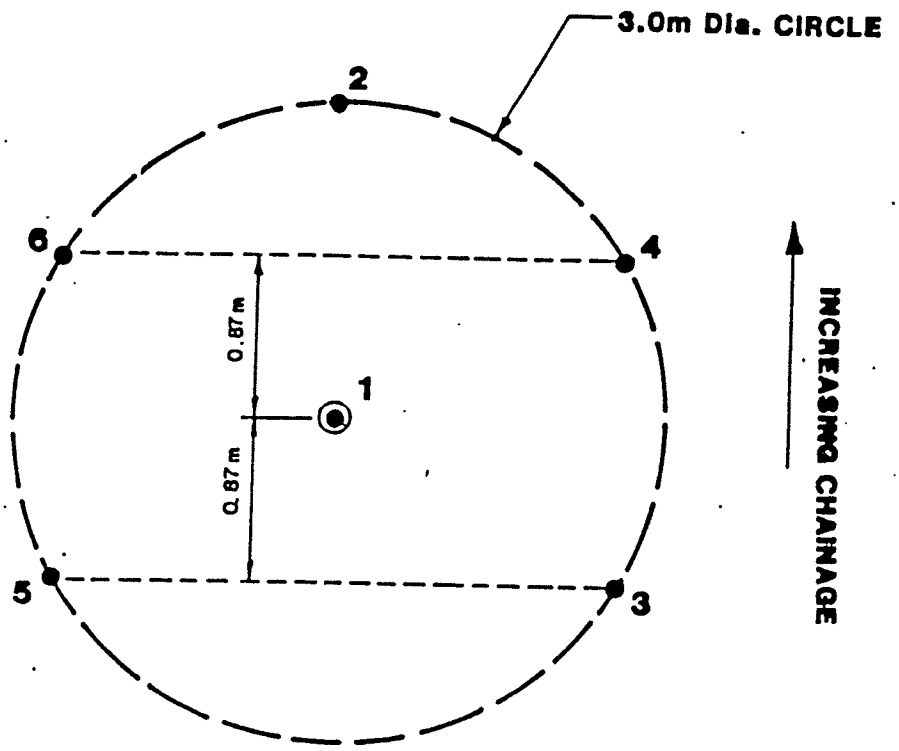

DENOTES THE TEST STATION

DENOTES ADDITIONAL TEST LOCATIONS

FIG. 4.7. SCHEMATIC FOR FWD TESTS IN THE 1985 SERIES

```
 ******   ****    ****   ******  **    **    ***
  **    *  *  *  *    *  *    *  * *  * *   * **
  **    *     *  *       *       *  * * *  *  * **
  **     ****    ****    ****    *  *  *  * ******
  **         *       *  *       *     *     **
  **    *  *  *  *    *  *    *  *     *     **
 ******   ****    ****   ******  ***    ***   ***

PROPRIETARY PROGRAM BY:
   DYNATEST CONSULTING, INC
   P.O. BOX 71 / 209 BALD STREET
   OJAI, CALIFORNIA  93023
   TELEPHONE:  (805) 646-2230
                     646-5531

         INPUT DATA (UNDER COLUMN NUMBER):
<-------------------------------------------------------------------->
              1      2      3      4      4      5      6      7
 2  5  8      8      4      2      0      8      6      4      2
<-------------------------------------------------------------------->
E2 1 THUNDER BAY: RWY 07-25: STA. 5+600: 3 m R: LOC. MEAN-3
     0.    300.    610.    915.   1219.   1524.   1829.
   146.    109.     99.     89.     77.     74.     62.
          1148.    150.
    6
    4      100.    200.
    1      240.    .30    7500.
    2      170.    .35   20000.
    3      110.    .35     130.
    4              .35     120.
<-------------------------------------------------------------------->


DEFLECTION BASIN VALUES FROM CURVE FITTING ROUTINE:    (NOTE - POSITION = DISTANCE FROM CENTER OF LOAD IN MM; DEFLECTION IN MM)

*(INCLUDES MEASURED PTS.)* <---------------------------- (EXTRAPOLATED OR INTERPOLATED) ----------------------------> *
*    POSITION DEFLECTION *   POSITION DEFLECTION *   POSITION DEFLECTION *   POSITION DEFLECTION *   POSITION DEFLECTION *
*       0.0    0.1460  *     30.0    0.1451  *     60.0    0.1425  *     90.0    0.1387  *    120.0    0.1341  *
*     150.0    0.1289  *    180.0    0.1236  *    210.0    0.1186  *    240.0    0.1143  *    270.0    0.1109  *
*     300.0    0.1090  *    331.0    0.1079  *    362.0    0.1068  *    393.0    0.1058  *    424.0    0.1048  *
*     455.0    0.1038  *    486.0    0.1029  *    517.0    0.1019  *    548.0    0.1010  *    579.0    0.1000  *
*     610.0    0.0990  *    640.5    0.0980  *    671.0    0.0970  *    701.5    0.0960  *    732.0    0.0950  *
*     762.5    0.0941  *    793.0    0.0931  *    823.5    0.0921  *    854.0    0.0911  *    884.5    0.0900  *
*     915.0    0.0890  *    945.4    0.0879  *    975.8    0.0868  *   1006.2    0.0856  *   1036.6    0.0844  *
*    1067.0    0.0832  *   1097.4    0.0819  *   1127.8    0.0807  *   1158.2    0.0794  *   1188.6    0.0782  *
*    1219.0    0.0770  *   1249.5    0.0761  *   1280.0    0.0756  *   1310.5    0.0754  *   1341.0    0.0754  *
*    1371.5    0.0755  *   1402.0    0.0756  *   1432.5    0.0756  *   1463.0    0.0754  *   1493.5    0.0749  *
*    1524.0    0.0740  *   1554.5    0.0728  *   1585.0    0.0716  *   1615.5    0.0703  *   1646.0    0.0690  *
*    1676.5    0.0678  *   1707.0    0.0665  *   1737.5    0.0653  *   1768.0    0.0641  *   1798.5    0.0630  *
*    1829.0    0.0620  *   1865.6    0.0608  *   1902.2    0.0597  *   1938.8    0.0586  *   1975.4    0.0575  *
*    2012.0    0.0565  *   2048.6    0.0555  *   2085.2    0.0545  *   2121.8    0.0536  *   2158.4    0.0527  *
*    2195.0    0.0519  *


ITERATION SUMMARY:

FINAL CENTERLINE E-VALUES FOR LOOP 1 = 7500.0013919.50  365.47  295.40
1.1 * ET(5) IS GE ET(6), ET(5)=1319.4  ET(6)=1383.3  ;TRY LARGER TH(3) FOR RERUN
```

HERE THE RUN WAS ABORTED BECAUSE THE SEED MODULI AND THICKNESS COMBINATION COULD NOT LEAD TO A MATCH BETWEEN OBSERVED AND COMPUTED DEFLECTION BASINS. THE SYSTEM SUGGESTS TO FICTITIOUSLY ALTER THE LAYER THICKNESS TO SUIT THE COMPUTATION!

FIG. 4.8-A. EXAMPLE OF AN ABORTED ISSEM-4 RUN

```
 ******   ****    ****   ******  **    **     ***
  **    *   *  *   *  *  *    *  * *  * *   * **
  **    *      *      *  *       *  * ** *   * **
  **     ****    ****    ****    *  *  * *   ******
  **         *       *  *       *      *     **
  **    *    *  *    *  *    *  *      *     **
 ******   ****    ****   ******  ***    ***    ***

PROPRIETARY PROGRAM BY:
   DYNATEST CONSULTING, INC
   P.O. BOX 71 / 209 BALD STREET
   OJAI, CALIFORNIA  93023
   TELEPHONE:  (805) 646-2230
               646-5531

         INPUT DATA (UNDER COLUMN NUMBER):
<-------------------------------------------------------------------->
             1      2      3      4      4      5      6      7
 2  5  8     6      4      2      0      8      6      4      2
<-------------------------------------------------------------------->
E1 1 REGINA FWD TESTS 1985: RUNWAY 12-30: STA.5+498: 3 m R: LOC. MEAN-1
     0.    300.    610.    914.   1219.   1524.   1829.
   123.    104.     89.     72.     59.     51.     42.
           618.    150.
    6
    3
    1     330.    .30   10000.
    2    1070.    .35     200.
    3             .35     100.
<-------------------------------------------------------------------->
```

DEFLECTION BASIN VALUES FROM CURVE FITTING ROUTINE: (NOTE - POSITION = DISTANCE FROM CENTER OF LOAD IN MM; DEFLECTION IN MM)

(INCLUDES MEASURED PTS.)		(EXTRAPOLATED OR INTERPOLATED)							
POSITION	DEFLECTION	POSITION	DEFLECTION	POSITION	DEFLECTION	POSITION	DEFLECTION	POSITION	DEFLECTION
0.0	0.1230	30.0	0.1226	60.0	0.1216	90.0	0.1199	120.0	0.1179
150.0	0.1156	180.0	0.1131	210.0	0.1106	240.0	0.1081	270.0	0.1059
300.0	0.1040	331.0	0.1023	362.0	0.1007	393.0	0.0992	424.0	0.0978
455.0	0.0964	486.0	0.0949	517.0	0.0935	548.0	0.0921	579.0	0.0906
610.0	0.0890	640.4	0.0874	670.8	0.0857	701.2	0.0839	731.6	0.0821
762.0	0.0803	792.4	0.0786	822.8	0.0768	853.2	0.0751	883.6	0.0735
914.0	0.0720	944.5	0.0705	975.0	0.0691	1005.5	0.0677	1036.0	0.0663
1066.5	0.0649	1097.0	0.0636	1127.5	0.0624	1158.0	0.0612	1188.5	0.0601
1219.0	0.0590	1249.5	0.0580	1280.0	0.0571	1310.5	0.0563	1341.0	0.0555
1371.5	0.0548	1402.0	0.0541	1432.5	0.0533	1463.0	0.0526	1493.5	0.0518
1524.0	0.0510	1554.5	0.0501	1585.0	0.0492	1615.5	0.0483	1646.0	0.0473
1676.5	0.0464	1707.0	0.0454	1737.5	0.0445	1768.0	0.0436	1798.5	0.0428
1829.0	0.0420	1865.6	0.0411	1902.2	0.0402	1938.8	0.0394	1975.4	0.0386
2012.0	0.0379	2048.6	0.0371	2085.2	0.0364	2121.8	0.0358	2158.4	0.0352
2195.0	0.0346								

ITERATION SUMMARY:

```
CURVE FITTING RANGE EXCEEDED, NLP = 1 IERR = 2, ET(J) = 2065.3, GMXXP =1829.0, J = 5
FINAL CENTERLINE E-VALUES FOR LOOP 1 =12981.70  239.56  125.59
CURVE FITTING RANGE EXCEEDED, NLP = 2 IERR = 2, ET(J) = 2254.0, GMXXP =1829.0, J = 4
```

HERE THE RUN WAS ABORTED BECAUSE THE DEFLECTION SENSORS DID NOT REACH FAR ENOUGH OUT FROM THE LOAD TO RESONABLY WELL DEFINE THE DEFLECTION BASIN.

FIG. 4.8-B. EXAMPLE OF AN ABORTED ISSEM-4 RUN

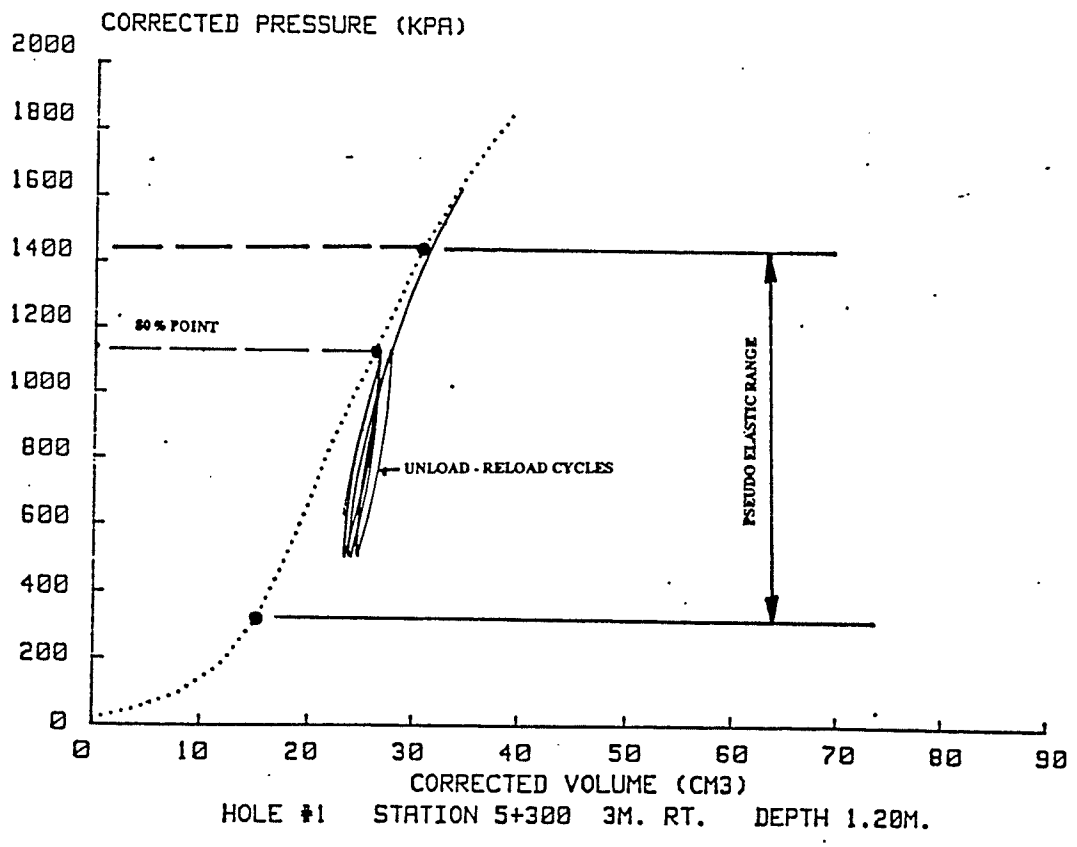

NOTE:

1. DETERMINE THE PSEUDO ELASTIC RANGE
2. MARK 80 % POINT OF THE UPPER LIMIT OF THIS RANGE
3. START UNLOAD - RELOAD CYCLES OVER 3 TO 4 VOLUME STEPS
4. MINIMUM NUMBER OF CYCLES THREE

FIG. 4.9. DETERMINING THE UNLOAD-RELOAD POINTS FROM A PILOT HOLE

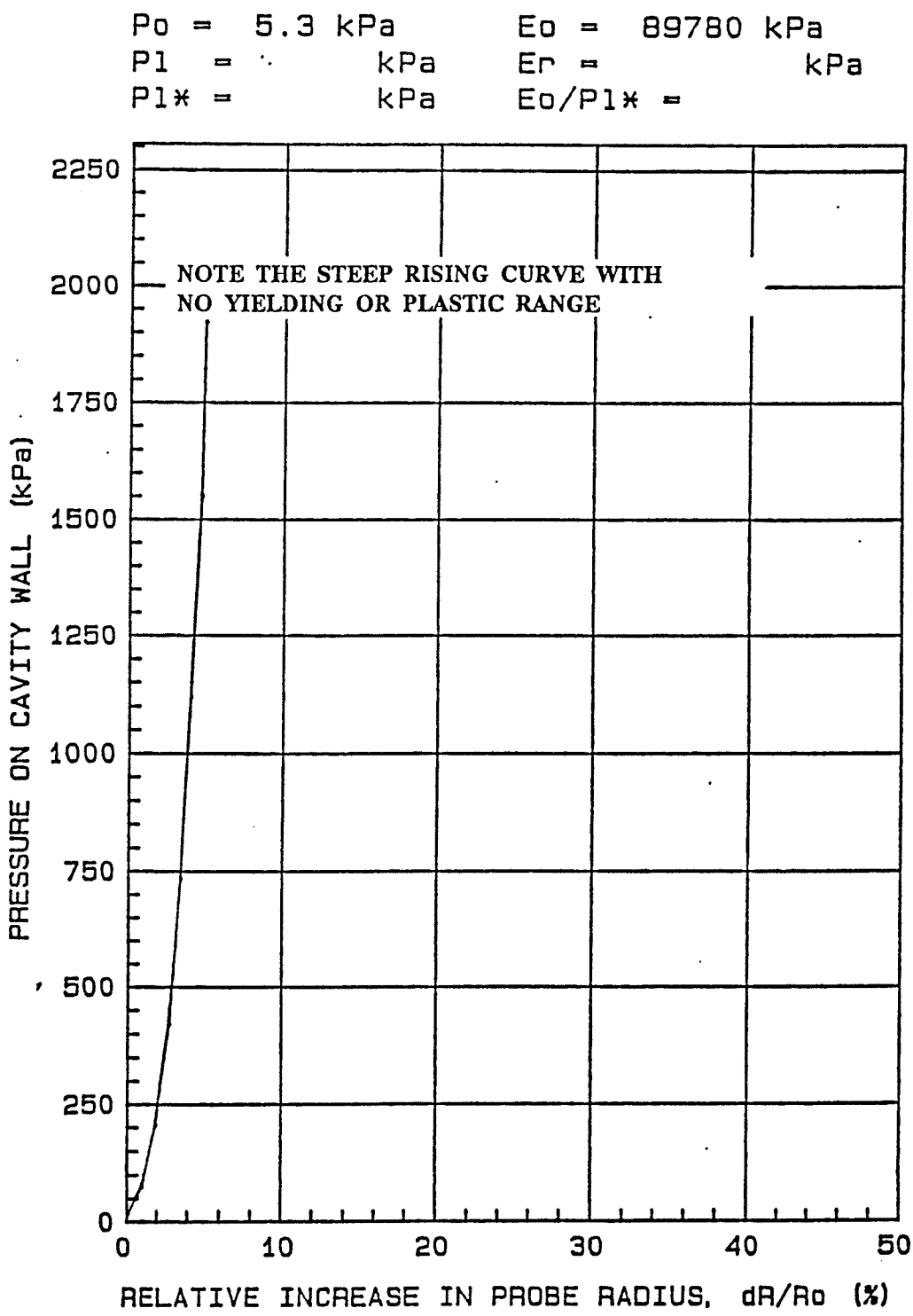

FIG. 4.10. TYPICAL PRESSURE METER CURVE FOR GRANULAR BASE

Regina R/W12-30:October/88:6+300:3mRt:Hole#9:2.25m.

POINT NUMBER	VOLUME MEASUREMENT	PRESSURE MEASUREMENT	CORR. VOL. INCREASE (cm^3)	dR/Ro (%)	CORRECTED PRESSURE (kPa)
1	0.000	300.0	0.00	0.00	27.00
2	5.000	370.0	4.76	1.01	82.00
3	10.000	405.0	9.64	2.04	102.00
4	15.000	435.0	14.54	3.07	122.00
5	20.000	465.0	19.44	4.08	147.00
6	25.000	480.0	24.39	5.09	157.00
7	20.000	345.0	19.39	4.07	27.00
8	15.000	265.0	14.39	3.03	-48.00
9	10.000	200.0	9.39	1.99	-103.00
10	5.000	175.0	4.39	0.93	-113.00
11	0.000	130.0	-0.61	-0.13	-143.00
12	5.000	220.0	5.00	1.06	-68.00
13	10.000	300.0	10.00	2.12	-3.00
14	15.000	360.0	14.80	3.12	47.00
15	20.000	425.0	19.57	4.11	107.00
16	25.000	465.0	24.44	5.10	142.00
17	20.000	330.0	19.44	4.08	12.00
18	15.000	250.0	14.44	3.04	-63.00
19	10.000	200.0	9.44	2.00	-103.00
20	5.000	155.0	4.44	0.95	-133.00
21	0.000	120.0	-0.56	-0.12	-153.00
22	5.000	185.0	5.00	1.06	-103.00
23	10.000	255.0	10.00	2.12	-48.00
24	15.000	330.0	14.90	3.14	17.00
25	20.000	395.0	19.68	4.13	77.00
26	25.000	450.0	24.49	5.11	127.00
27	20.000	325.0	19.49	4.09	7.00
28	15.000	235.0	14.49	3.06	-78.00
29	10.000	195.0	9.49	2.01	-108.00
30	5.000	150.0	4.49	0.96	-138.00
31	0.000	110.0	-0.51	-0.11	-163.00
32	5.000	170.0	5.00	1.06	-118.00
33	10.000	250.0	10.00	2.12	-53.00
34	15.000	320.0	14.93	3.15	7.00
35	20.000	385.0	19.71	4.13	67.00
36	25.000	450.0	24.49	5.11	127.00
37	30.000	475.0	29.40	6.11	147.00
38	35.000	495.0	34.34	7.10	162.00
39	40.000	510.0	39.29	8.08	172.00
40	45.000	520.0	44.25	9.06	177.00
41	50.000	530.0	49.22	10.03	182.00
42	55.000	540.0	54.18	11.00	187.00
43	60.000	550.0	59.15	11.95	192.00
44	65.000	555.0	64.13	12.90	192.00
45	70.000	560.0	69.11	13.84	192.00
46	75.000	570.0	74.08	14.77	197.00
47	80.000	575.0	79.06	15.69	197.00
48	85.000	575.0	84.06	16.62	192.00
49	90.000	580.0	89.05	17.53	192.00

Po = 24.3 kPa Pl = 190.0 kPa Pl* = 165.7 kPa
Eo = 7248 kPa Er = 8458 kPa Eo/Pl* = 43.7

FIG. 4.11. EXAMPLE OF PRINTOUT OF CALCULATION FROM PRESSRED PROGRAM (TEXAS A & M UNIVERSITY)

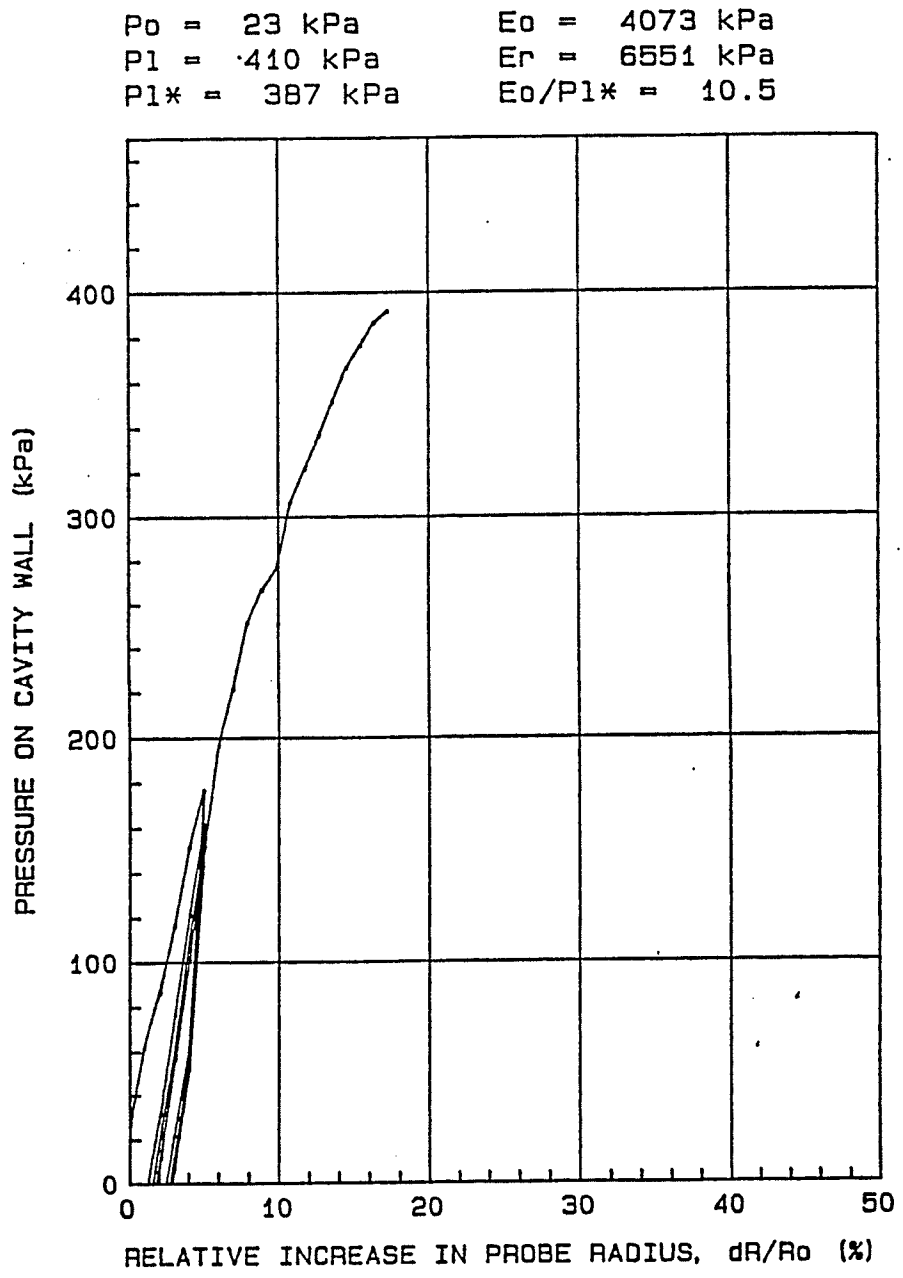

FIG. 4.12. EXAMPLE OF A PRESSUREMETER CURVE OBTAINED USING THE PRESSRED PROGRAM FROM TEXAS A & M UNIVERSITY

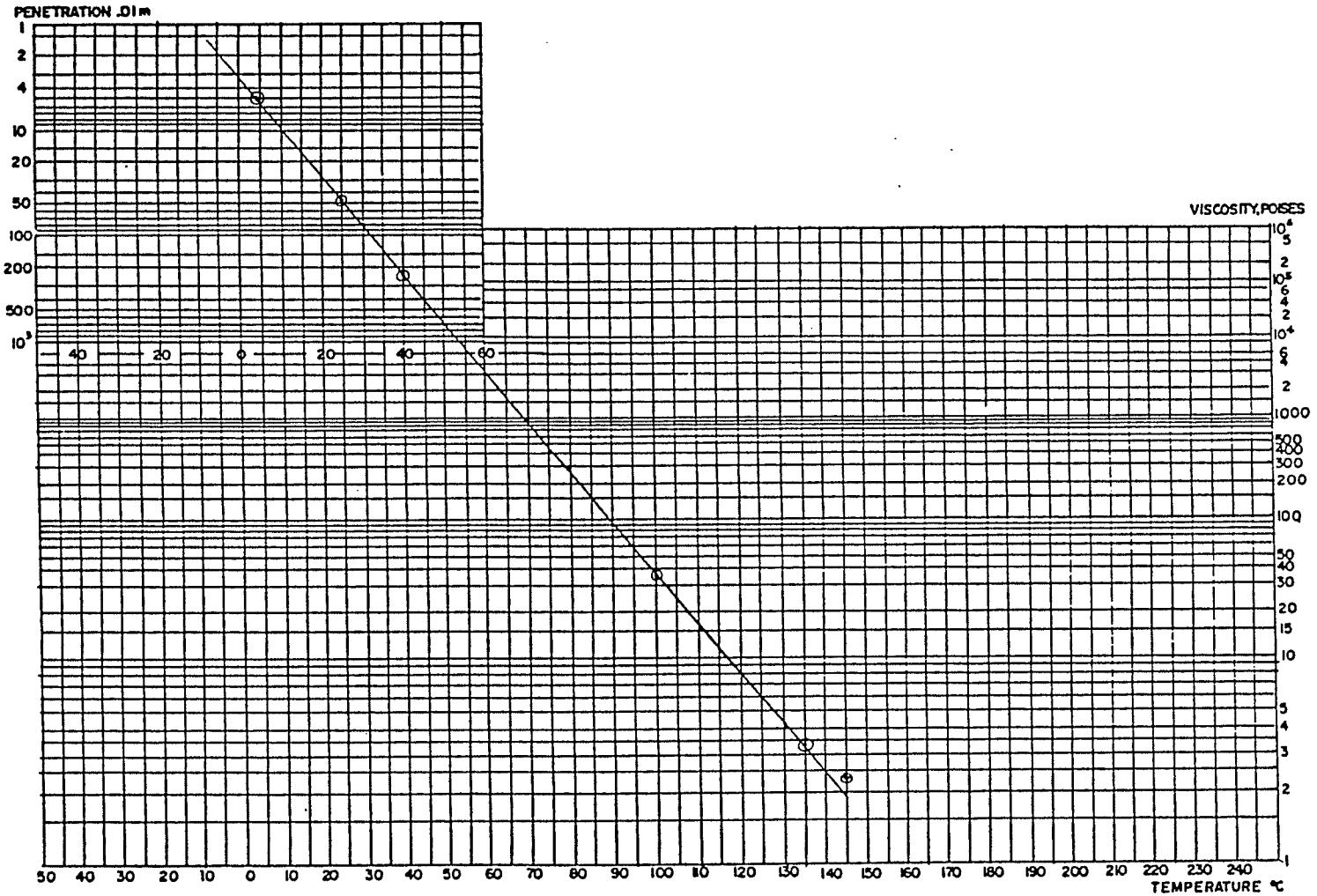

FIG. 4.13. SHELL BITUMEN CHART FOR ASPHALT CEMENT RECOVERED FROM CORES IN THUNDER BAY

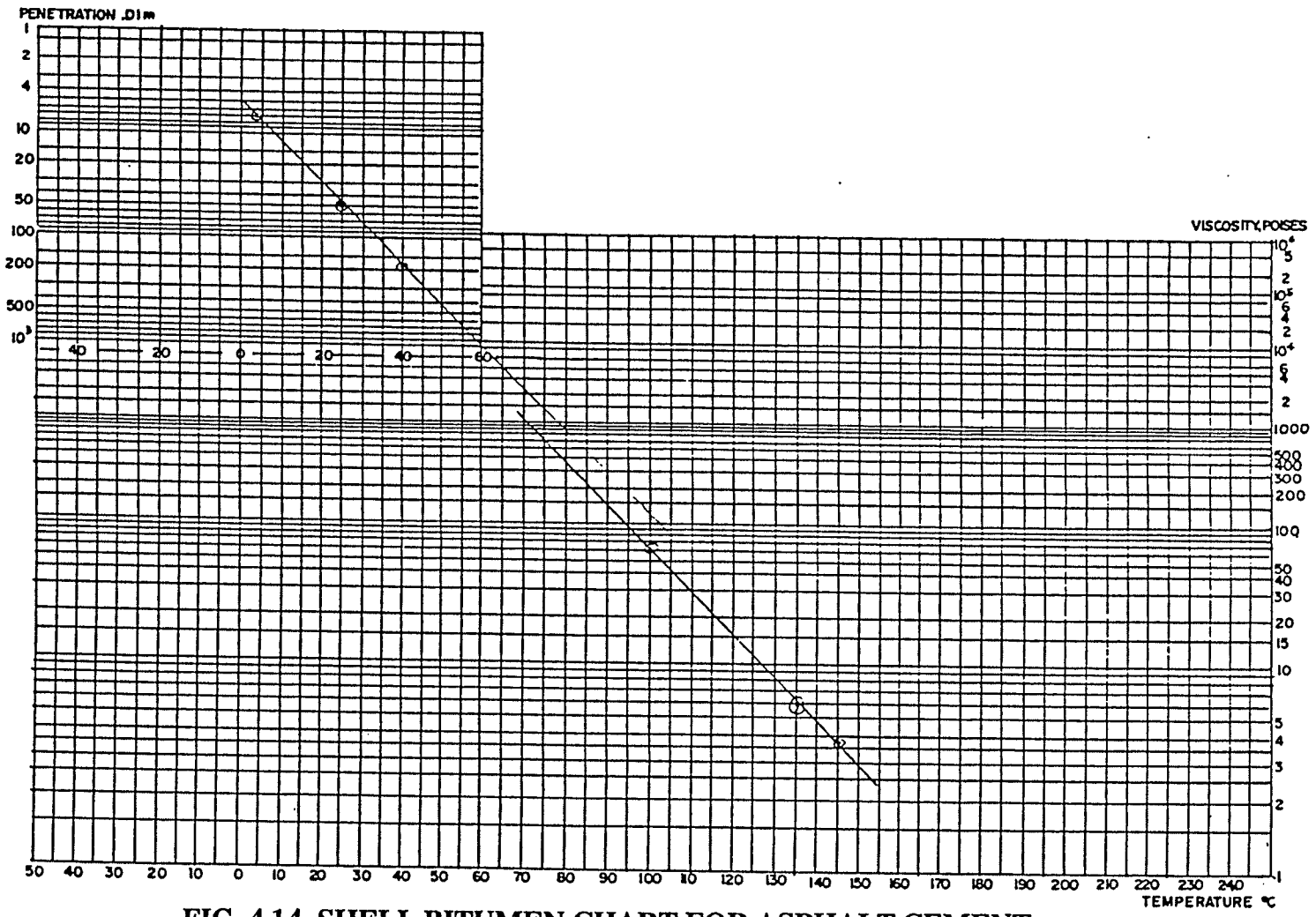

FIG. 4.14. SHELL BITUMEN CHART FOR ASPHALT CEMENT RECOVERED FROM CORES IN BRANDON

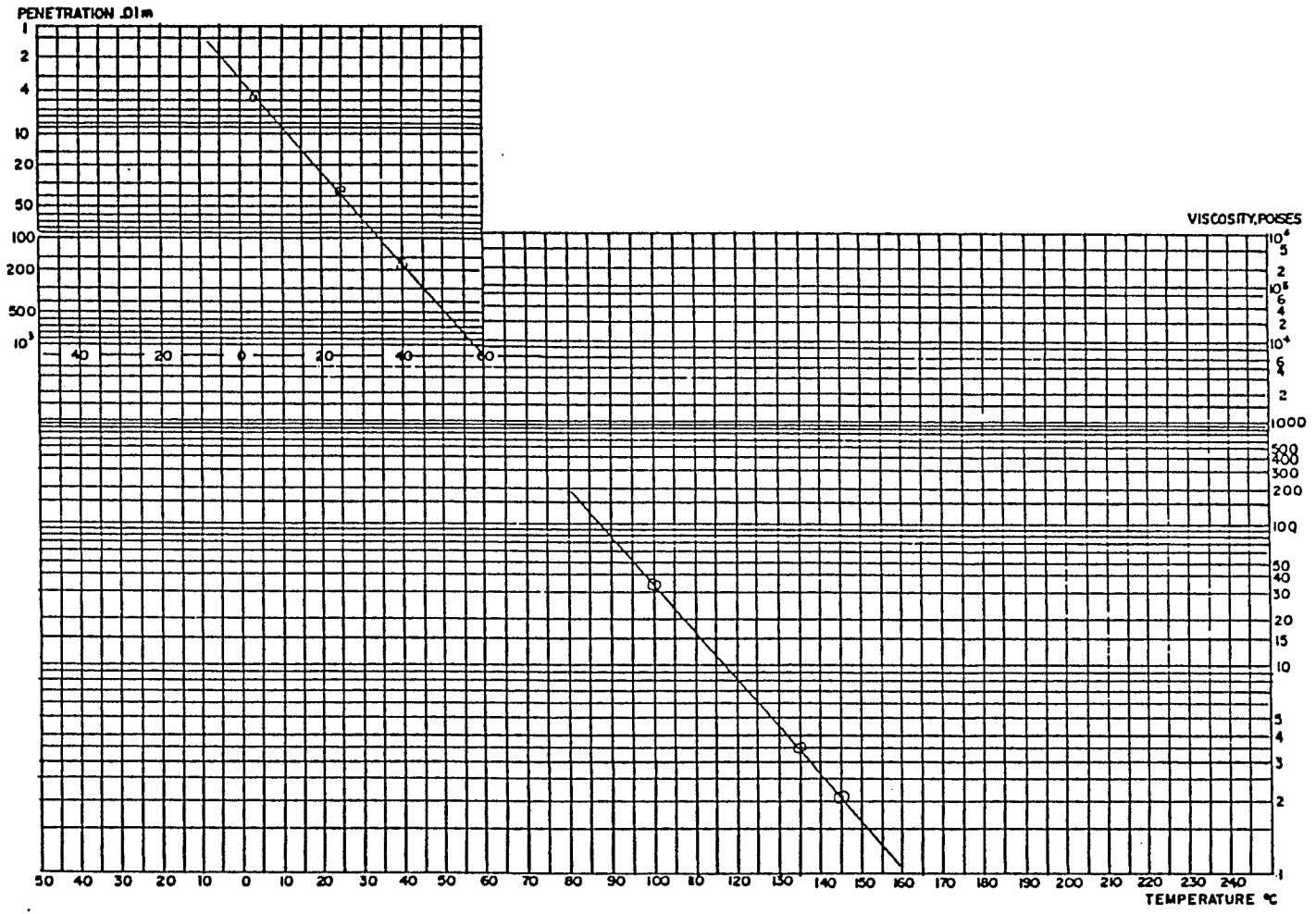

FIG. 4.15. SHELL BITUMEN CHART FOR ASPHALT CEMENT RECOVERED FROM CORES IN St. ANDREWS

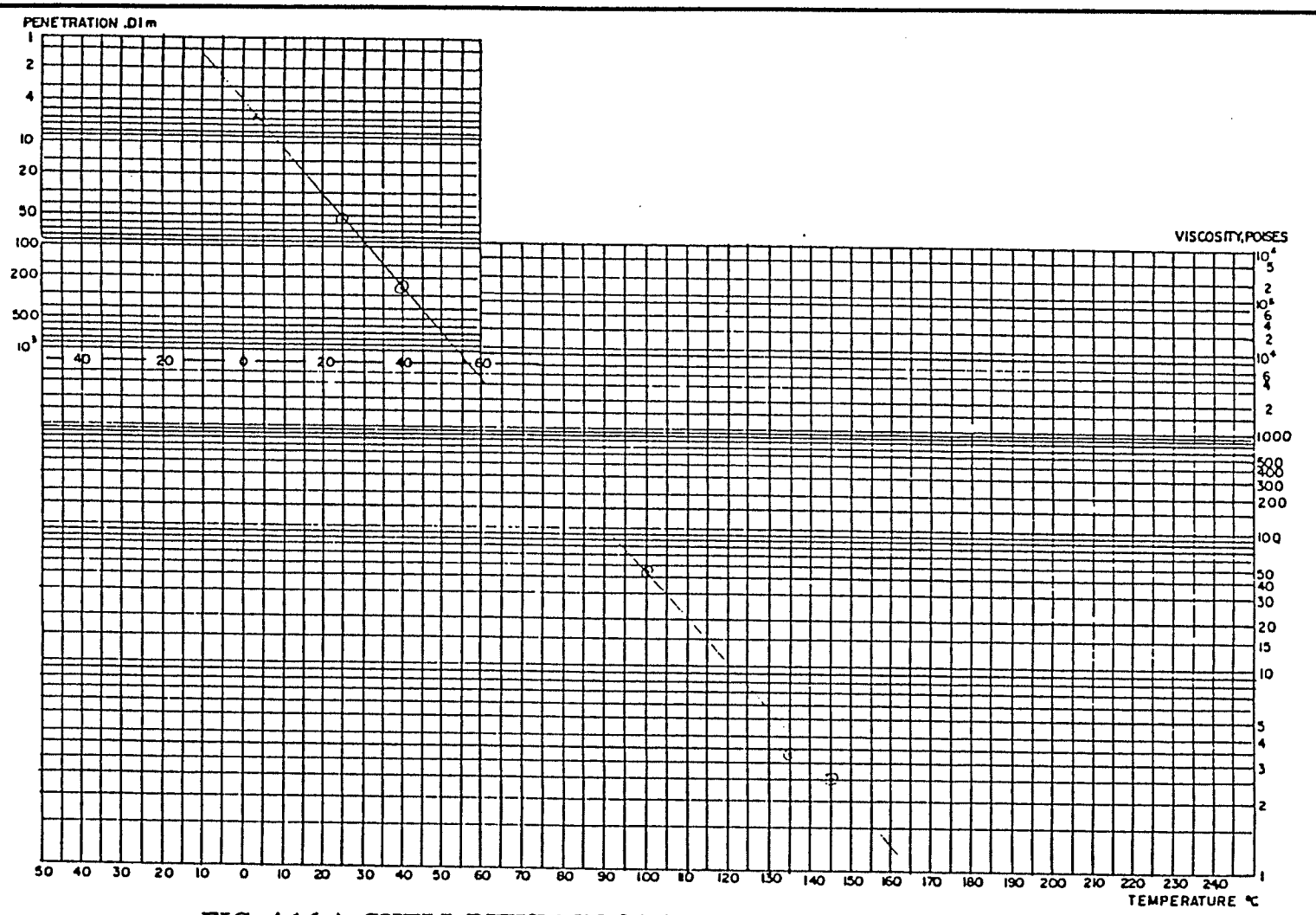

FIG. 4.16-A. SHELL BITUMEN CHART FOR ASPHALT CEMENT RECOVERED FROM CORES IN REGINA (1966 LOWER COURSE)

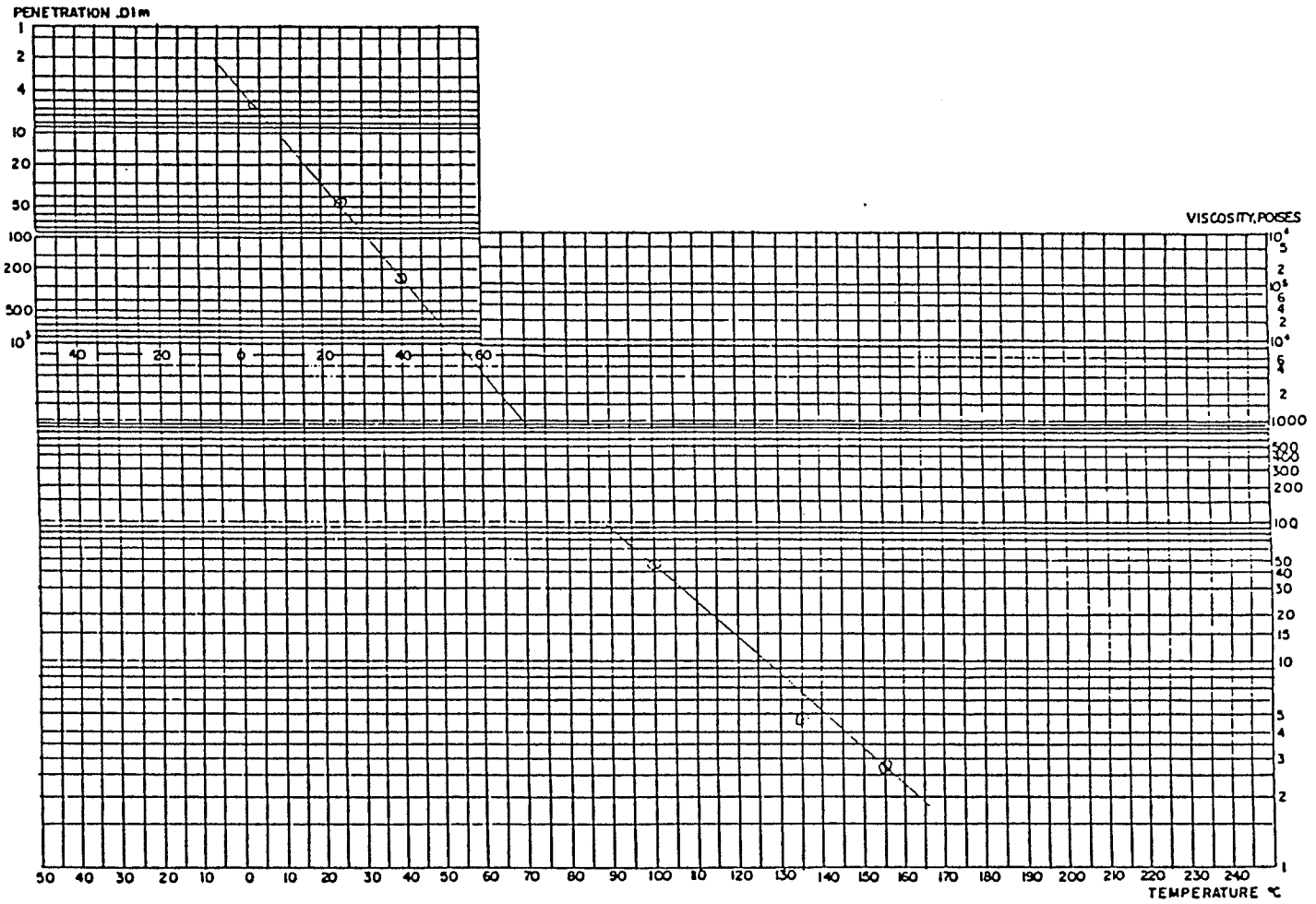

FIG. 4.16-B. SHELL BITUMEN CHART FOR ASPHALT CEMENT RECOVERED FROM CORES IN REGINA (1966 UPPER COURSE)

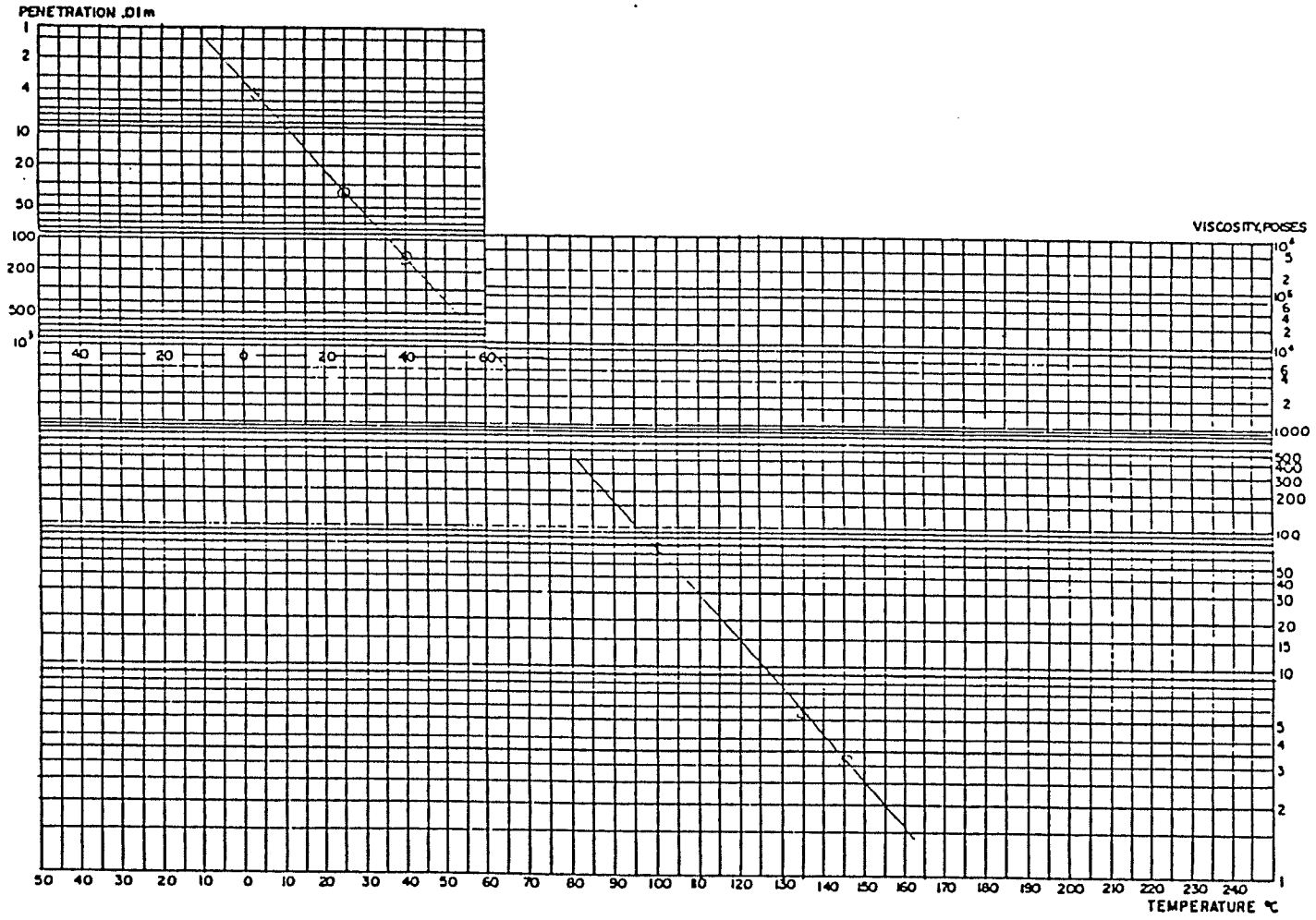

FIG. 4.16-C. SHELL BITUMEN CHART FOR ASPHALT CEMENT RECOVERED FROM CORES IN REGINA (1967 UPPER COURSE)

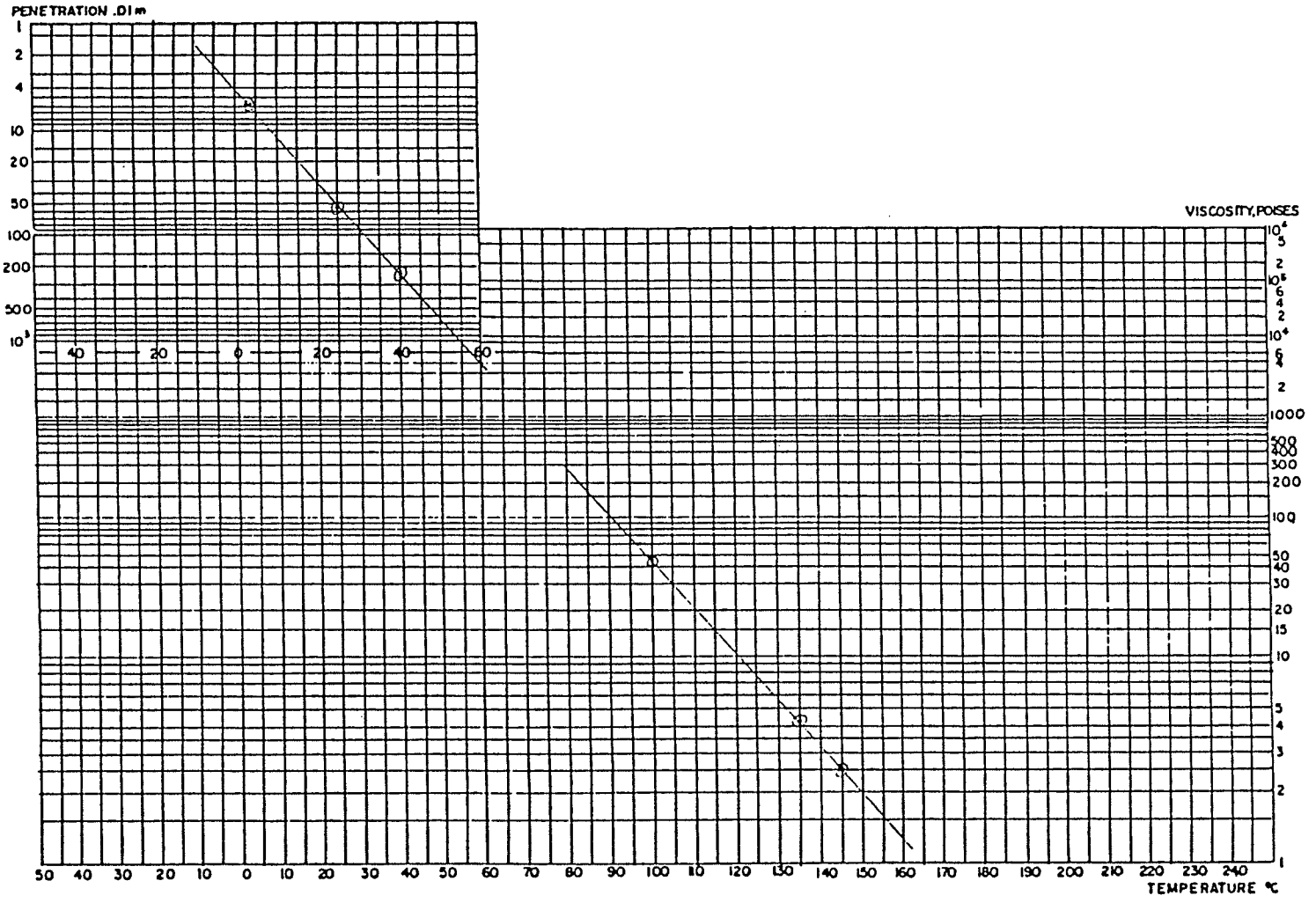

FIG. 4.16-D. SHELL BITUMEN CHART FOR ASPHALT CEMENT RECOVERED FROM CORES IN REGINA (1967 LOWER COURSE)

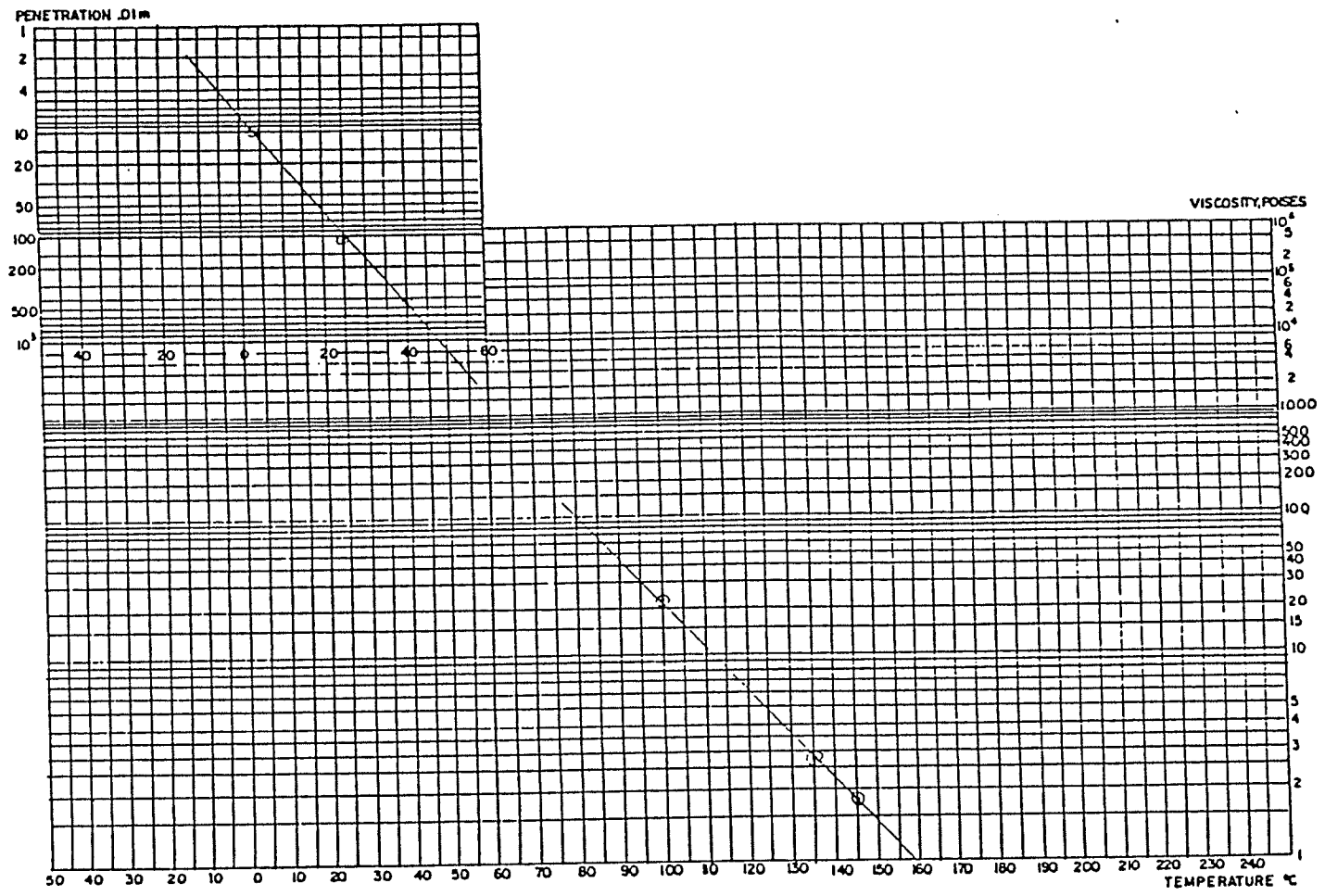

FIG. 4.16-E. SHELL BITUMEN CHART FOR ASPHALT CEMENT RECOVERED FROM CORES IN REGINA (1979 LOWER COURSE)

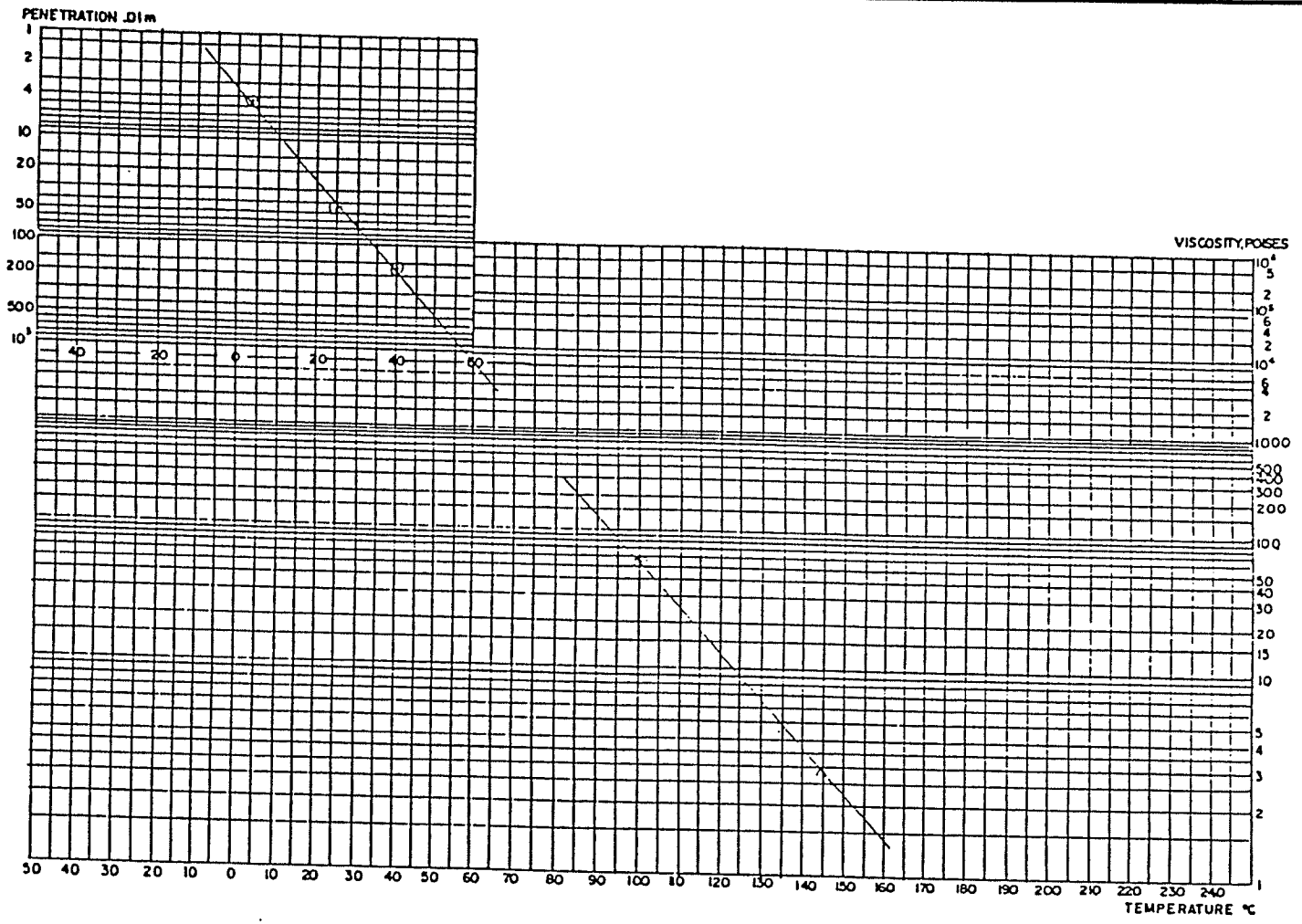

FIG. 4.16-F. SHELL BITUMEN CHART FOR ASPHALT CEMENT RECOVERED FROM CORES IN REGINA (1979 UPPER COURSE)

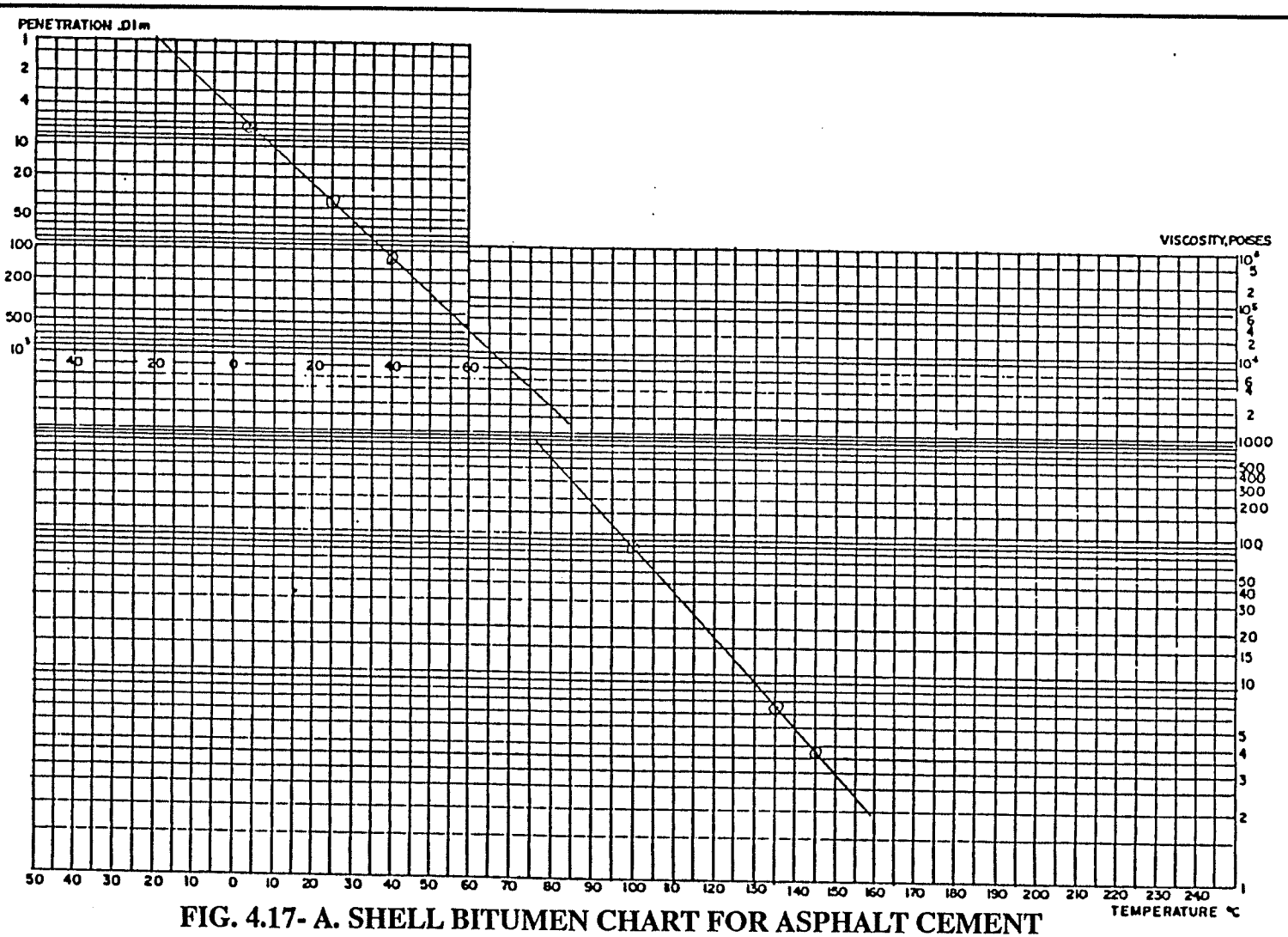

FIG. 4.17- A. SHELL BITUMEN CHART FOR ASPHALT CEMENT RECOVERED FROM CORES IN SASKATOON (1976 UPPER COURSE)

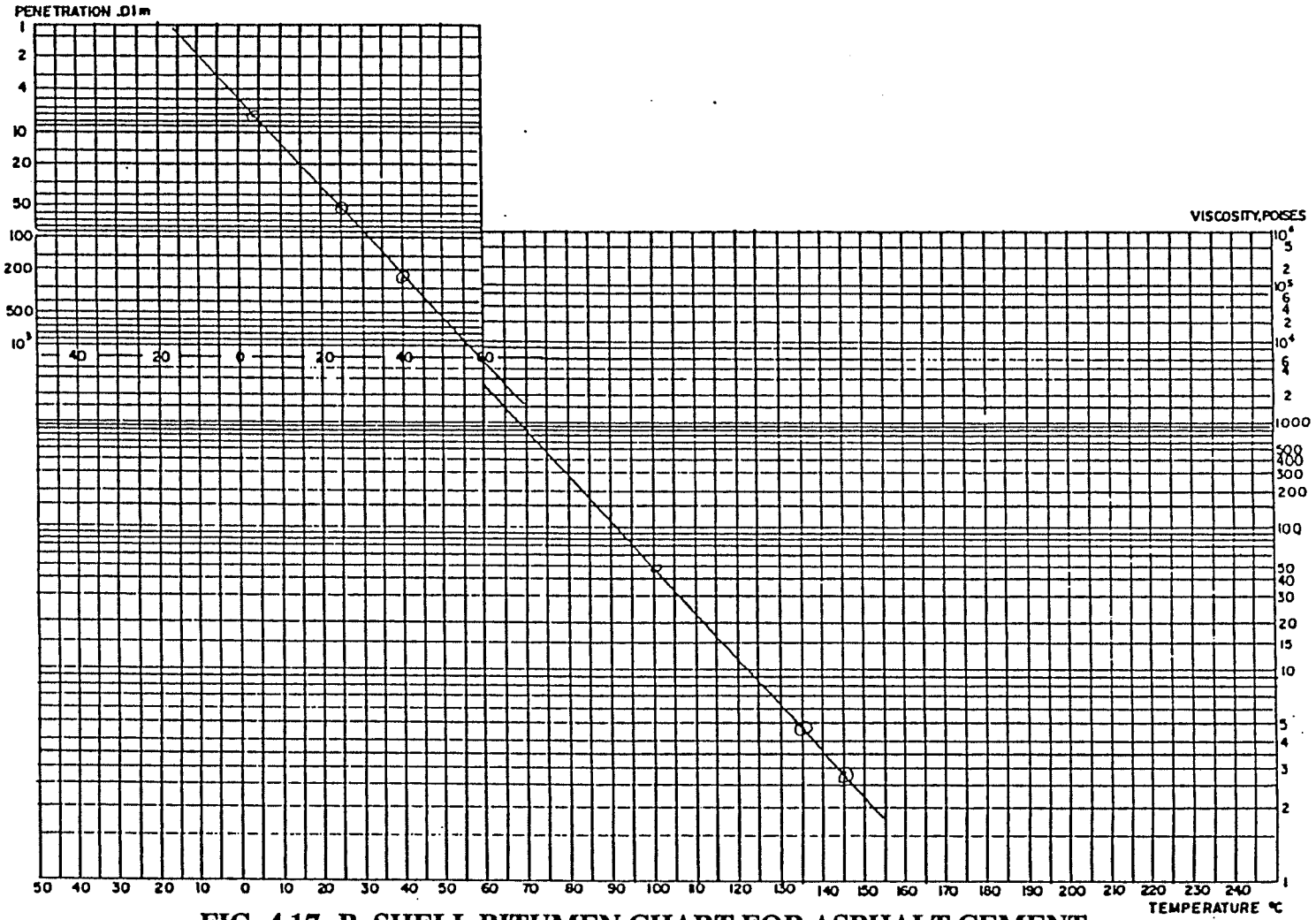

FIG. 4.17- B. SHELL BITUMEN CHART FOR ASPHALT CEMENT RECOVERED FROM CORES IN SASKATOON (1961 LOWER COURSE)

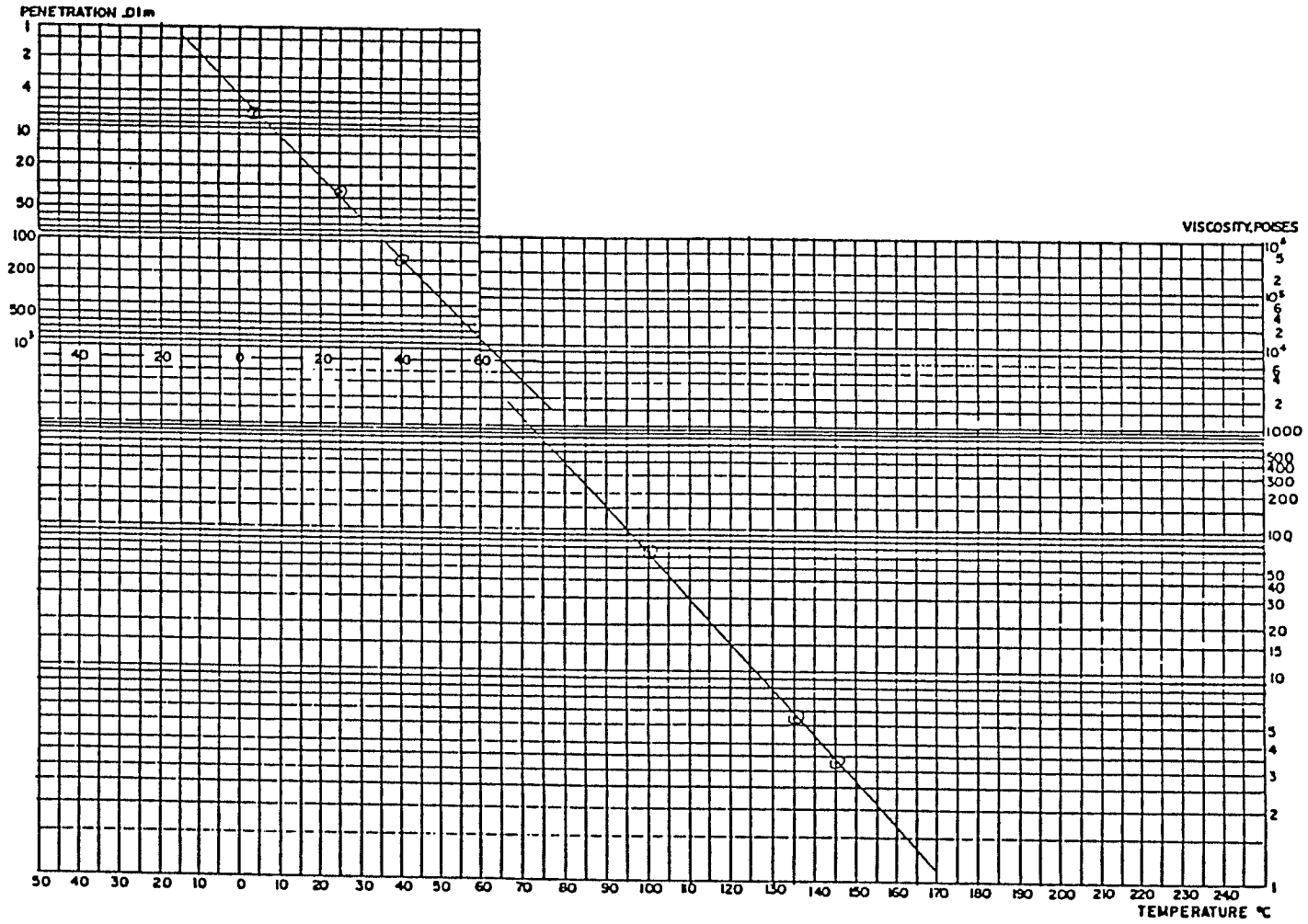

FIG. 4.17- C. SHELL BITUMEN CHART FOR ASPHALT CEMENT RECOVERED FROM CORES IN SASKATOON (1961 UPPER COURSE)

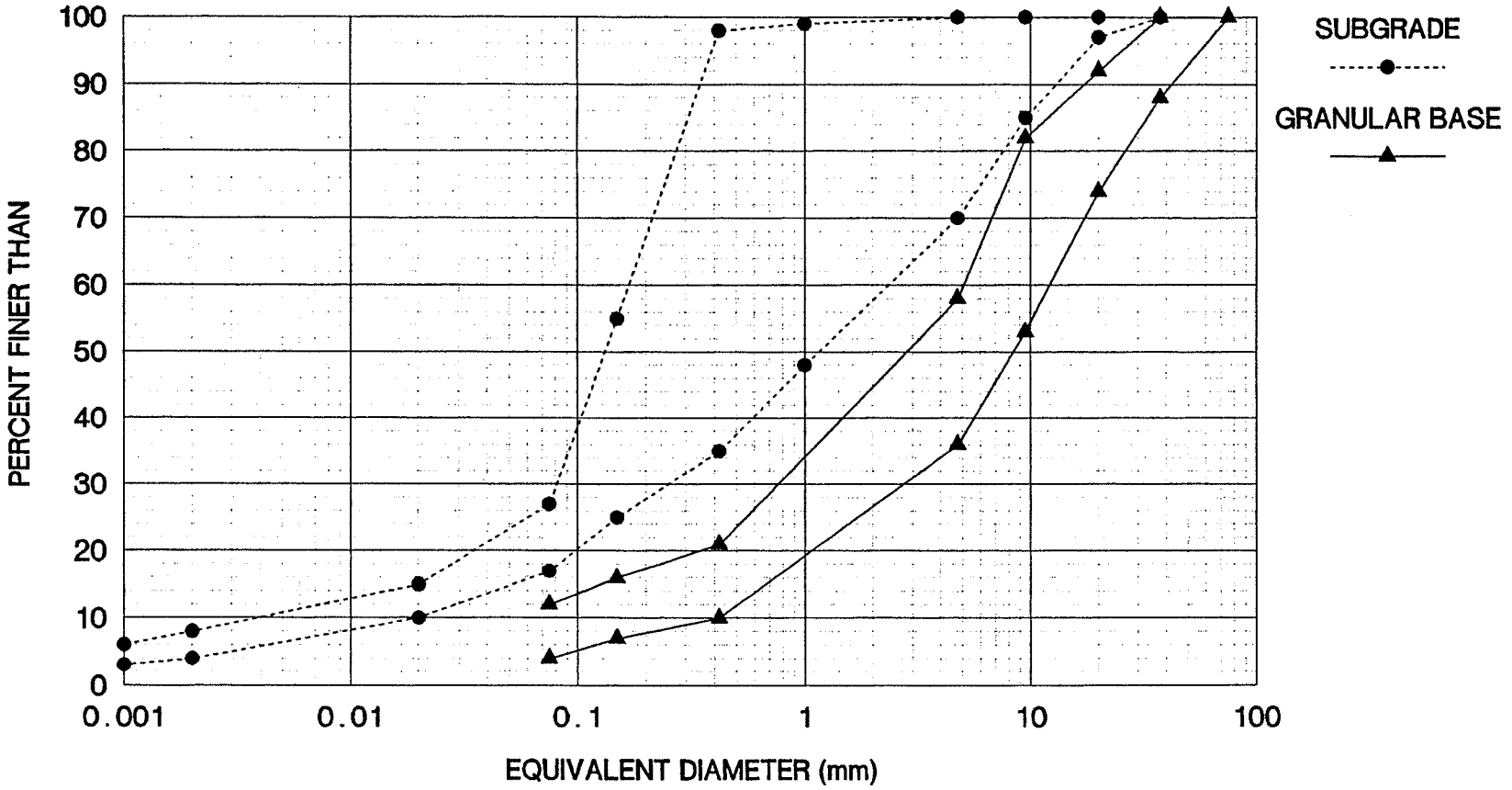

FIG. 4.18. GRAIN SIZE DISTRIBUTION OF UNBOUND MATERIALS IN THUNDER BAY

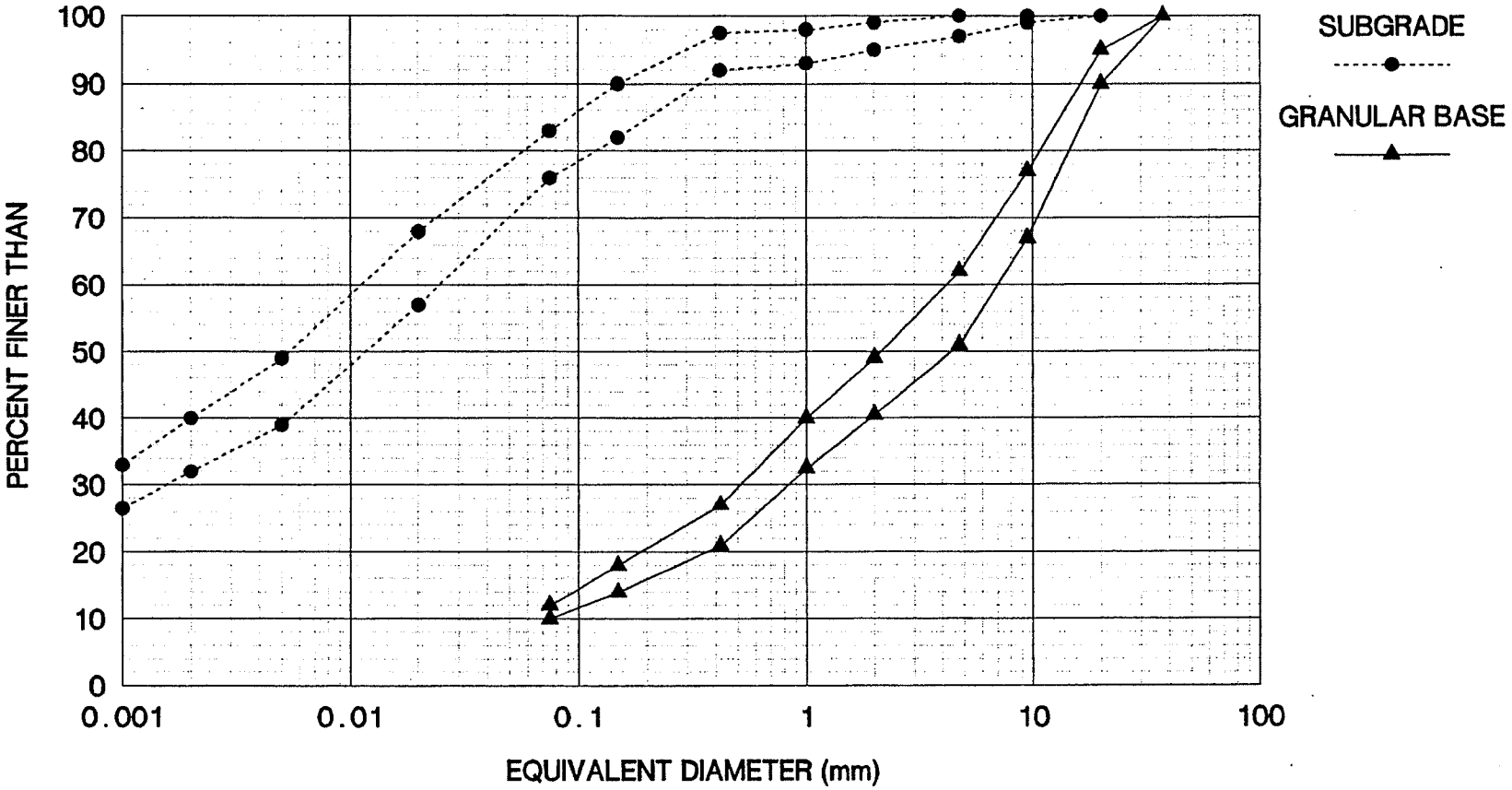

FIG. 4.19. GRAIN SIZE DISTRIBUTION OF UNBOUND MATERIALS IN BRANDON

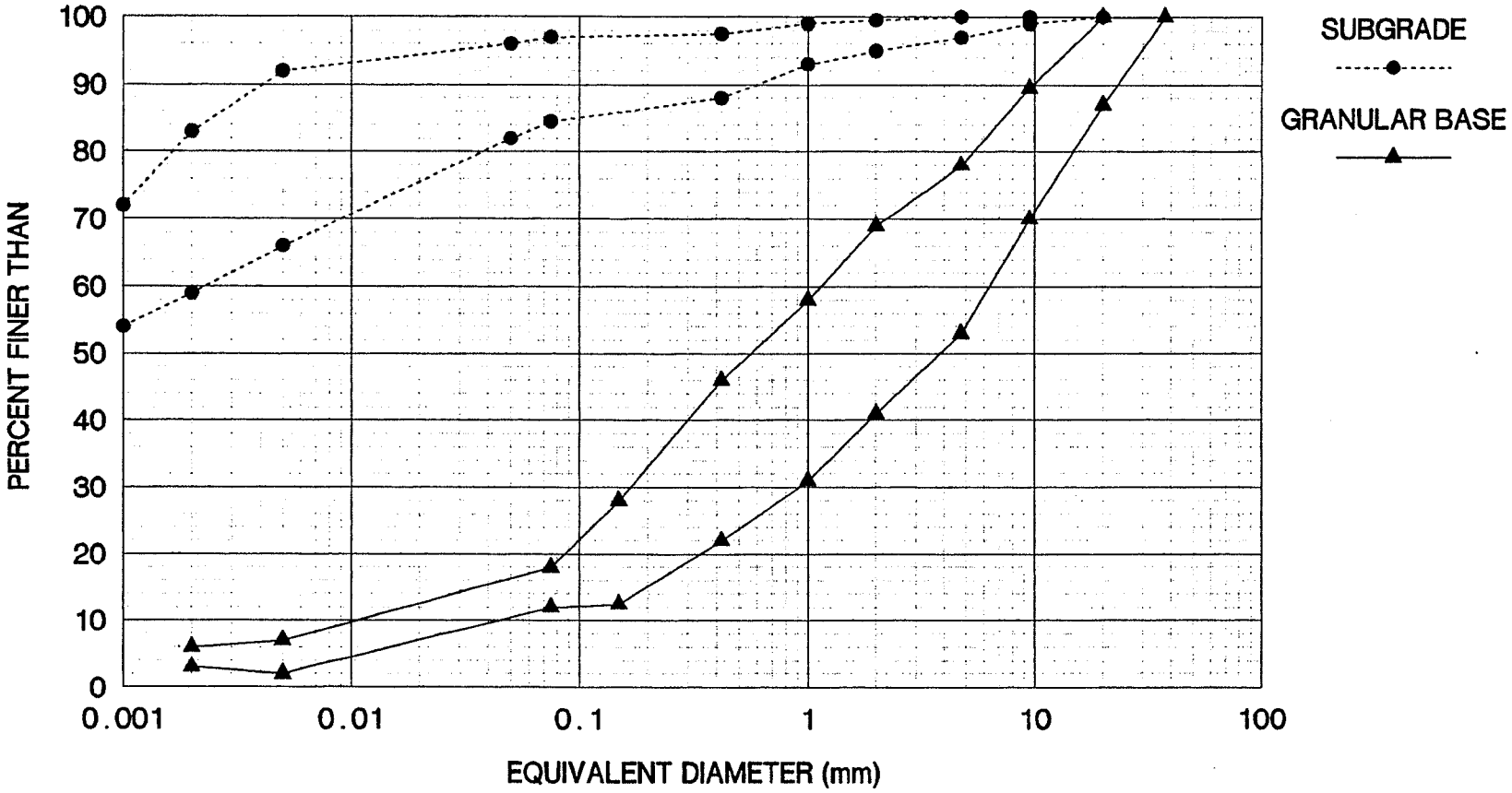

FIG. 4.20. GRAIN SIZE DISTRIBUTION OF UNBOUND MATERIALS IN ST. ANDREWS

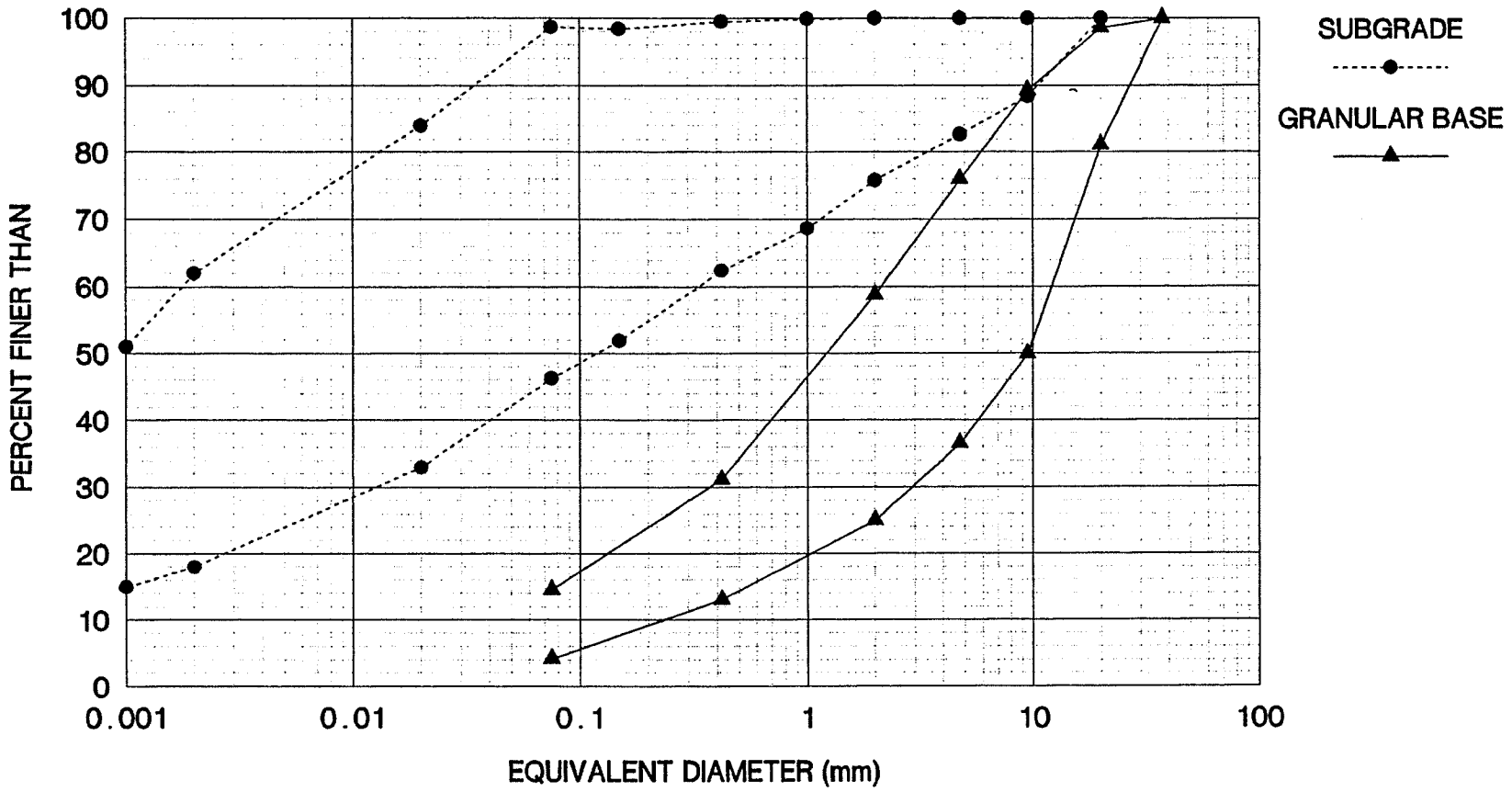

FIG. 4.21. GRAIN SIZE DISTRIBUTION OF UNBOUND MATERIALS IN SASKATOON

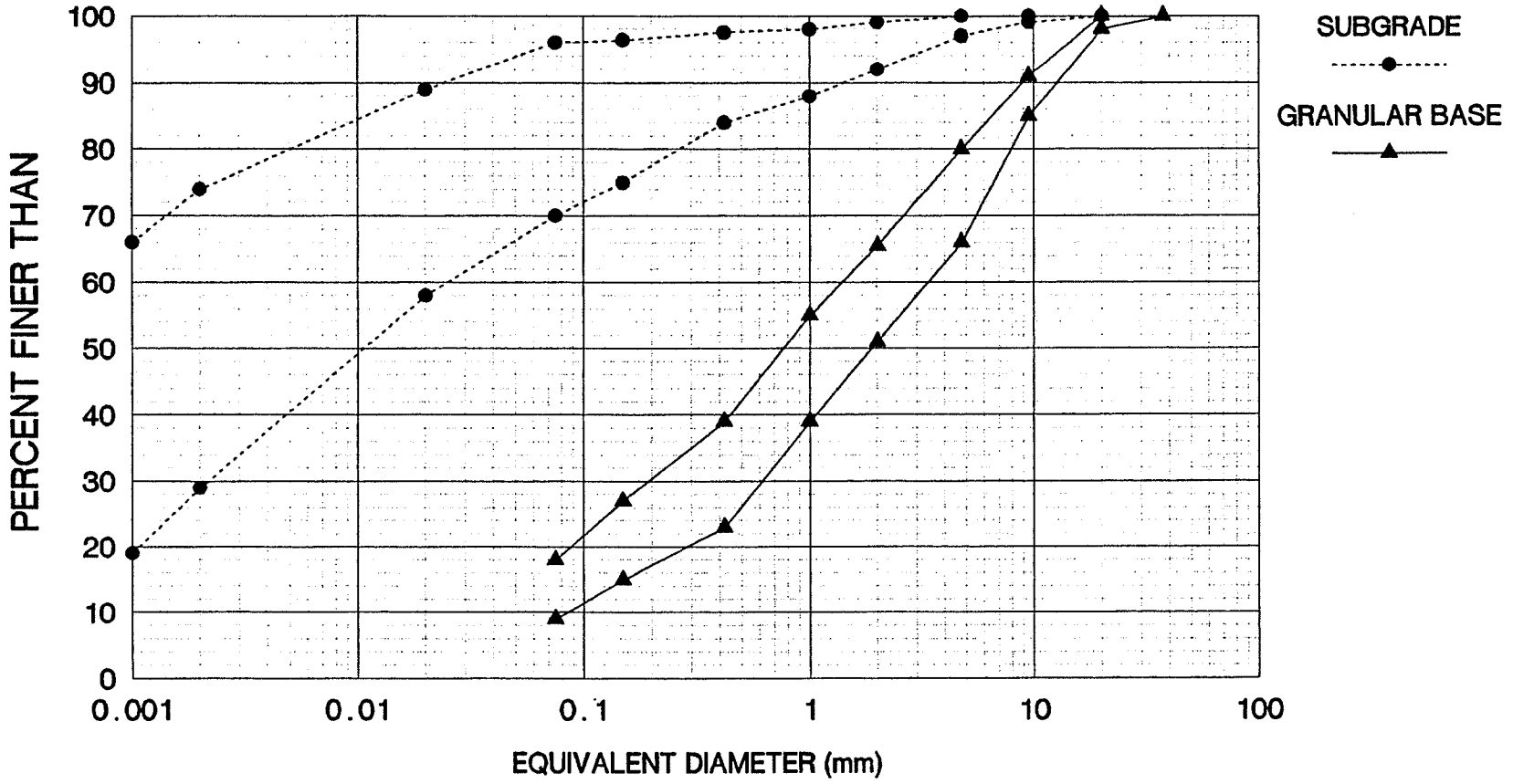

FIG. 4.22. GRAIN SIZE DISTRIBUTION OF UNBOUND MATERIALS IN REGINA

TABLE 4.2. TEST LOCATIONS AND PAVEMENT STRUCTURE IN THUNDER BAY AIRPORT.

STATION	PAVEMENT STRUCTURE (mm)	YEAR OF CONST.	USC	ANALYSIS SYST.	DEPTH TO PMT (m)
5 + 100	AC 70 AC 100 AC 100 BASE 280 SB 600 SG	1984 1965 1954 1954 1954	 GP,GW SW,SM SP,SM	5L 4P	 0.6 1.5 2.5
5 + 300	AC 70 AC 100 AC 70 BASE 230 SB 680 SG	1984 1965 1954 1954 1954	 GP,GW SM	5L 4P	 0.6 1.5 2.5
5 + 500	AC 70 AC 100 AC 70 PCC 170 SB 110 SG	1984 1965 1954 1942 1942	 SW,SM SP,SM	5L 4P	 1.5 2.5
5 + 650	AC 80 AC 100 AC 70 PCC 190 SB 100 SG	1984 1965 1954 1942 1942	 SM SP,ML	5L 4P	 1.5 2.5
6 + 100	AC 100 AC 100 AC 70 PCC 180 SB 100 SG	1984 1965 1954 1942 1942	 SW SM	5L 4P	 1.5 2.5
TAXI A 10 + 740	AC 135 BASE 300 SB 905 SG	1983 1983 1983	 SW SM ML	3L 4P	 0.75 2.00

TABLE 4.3. TEST LOCATIONS AND PAVEMENT STRUCTURE IN BRANDON AIRPORT.

STATION	PAVEMENT STRUCTURE (mm)	YEAR OF CONSTR.	USC	ANALYSIS SYSTEM	DEPTH TO PMT (m)
5 + 400	AC 110 BASE 990 SG	1983 1957/83	SW-SM CL	3L 4P	0.6 1.5
5 + 600	AC 120 BASE 1100 SG	1983 1957/83	SW-SM CL	3L 4P	0.6 1.5
5 + 900	AC 120 BASE 1040 SG	1983 1957/83	SW-SM CL	3L 4P	0.6 1.5
6 + 300	AC 120 BASE 980 SG	1983 1957/83	SW-SM CL	3L 4P	0.6 1.5
6 + 500	AC 110 BASE 990 SG	1983 1957/83	SW-SM CL	3L 4P	0.6 1.5
4 + 950	AC 100 EC 300 SB 350 SG	1983 1983 1983	SP-SM CL-ML	4L 4P	NO TEST

NOTE: EC IS ECONOCRETE: A LEAN CONCRETE BASE.

TABLE 4.4. TEST LOCATIONS AND PAVEMENT STRUCTURE IN ST. ANDREWS AIRPORT.

STATION	PAVEMENT STRUCTURE (mm)	YEAR OF CONSTR.	USC	ANALYSIS SYSTEM	DEPTH TO PMT (m)
5 + 030	AC 45 BASE 150 [1] SB 300 [1] SG	1968 1968 1968	 SW-SM SW-SM CH	3L 3P	 0.25 0.70 1.70
5 + 120	AC 40 BASE/ SB 470[1] SG	1968 1968	 SW-SM CH	3L 3P	 0.26 0.75 1.75
5 + 480	AC 50 BASE/ SB 470 SG	1968 1968	 GP-SW SM CH	3L 3P	 0.25 0.75 1.75
5 + 660	AC 50 BASE/ SB 550 SG	1968 1968	 SW-SM CH	3L 3P	 0.28 0.80 1.80
5 + 840	AC 50 BASE/ SB 460 SG	1968 1968	 SW-SM CH	3L 3P	 0.23 0.70 1.70

NOTE 1.: IT WAS DIFFICULT TO DISTINGUISH BETWEEN BASE AND SUB BASE MATERIAL UNDER THIS PAVEMENT, THOUGH CONSTRUCTION RECORDS SHOWED THAT 150 mm OF GRANULAR BASE (GW-GP) WAS PLACED IN 1968.

TABLE 4.5. TEST LOCATIONS AND PAVEMENT STRUCTURE IN REGINA AIRPORT.

STATION	PAVEMENT STRUCTURE (mm)	YEAR OF CONSTR.	USC	ANALYSIS SYSTEM	DEPTH TO PMT (m)
5 + 510	AC 40 AC 120 AC 90 AC 80 BASE[1] SB 1070 SG	1979 U[2] 1979 L[2] 1967 1953 1953	 SM CH	6L 3P	 0.68 1.20 2.20
5 + 990	AC 45 AC 110 AC 115 AC 60 BASE/ SB 710 SG	1979 U 1979 L 1967 1953 1953	 SW-SM CH	6L 3P	 0.67 1.20 2.20
6 + 290	AC 55 AC 110 AC 115 AC 95 BASE/ SB 740 SG	1979 U 1979 L 1967 1953 1953	 SW-SM CH	6L 3P	 0.71 1.25 2.25
6 + 890	AC 40 AC 70 AC 115 AC 120 BASE/ SB 780 SG	1979 U 1979 L 1962 1953 1953	 SW-SM CH	6L 3P	 0.72 1.30 2.30
7 + 310	AC 35 AC 70 AC 95 PCC 265 BASE/ SB 355 SG	1979 U 1979 L 1966 1960 1960	 SP	5L 3P	 0.65 1.05 2.05

NOTE 1: BASE AND SUB BASE ARE NOT EASILY DISTINGUISHABLE
NOTE 2: U = UPPER COURSE; L = LOWER COURSE.

TABLE 4.6. TEST LOCATIONS AND PAVEMENT STRUCTURE IN SASKATOON AIRPORT.

STATION	PAVEMENT STRUCTURE (mm)	YEAR OF CONSTR.	USC	ANALYSIS SYSTEM	DEPTH TO PMT (m)
5 + 360	AC[1] 30 AC 95 BASE 655 AC[1] 55 BASE/SB 175 SG	1976 1961 1961 1947 1947	 GP-SP SP-SM CLAY TILL	5L 3P	 0.50 1.30 2.30
5 + 630	AC 35 AC 115 BASE 550 AC 150 BASE/SB 350 SG	1976 1961 1961 1947 1947	 GP-SP GP-PLASTIC CLAY TILL	5L 3P	 0.50 1.00 1.50 2.10
5 + 840	AC 40 AC 110 BASE 600 AC 125 BASE/SB 425 SG	1976 1961 1961 1947 1947	 GP-SP SP-PLASTIC CLAY TILL	5L 3P	 0.50 1.10 1.50 2.10
6 + 140	AC 35 AC 105 BASE 590 AC 70 BASE/SB 600 SG	1976 1961 1961 1947 1947	 GP GP-SP (PL) CH	5L 3P	 0.50 1.20 1.80 2.80
6 + 470	AC 35 AC 90 BASE 615 AC 95 BASE/SB 465 SG	1976 1961 1961 1947 1947	 GW GP-SP (PL) CH	5L 3P	 0.50 1.00 1.60 2.50

NOTE: 1) THE 1961 SURFACE WAS BADLY CRACKED. THE THIN OVERLAY IN 1976 REFLECTED ALL THE 1961 CRACKS.

2) THE 1947 AC WAS TOTALLY STRIPPED AND WAS NO MORE THAN GRAVEL

TABLE 4.7. TYPICAL FWD RESULTS AND VARIABILITIES FROM TESTS IN THUNDER BAY (1985 SERIES)

SITE: THUNDER BAY DATE: 8 OCT.,85

FACILIT RWY 12-30

STATION 5+300 OFFSET: 3 m R LOCATION: 1 to 6

FWD DEFLECTION DATA

	LOAD LEVEL 1	2	3	4	
kPa	730	1001	1305	1479	MEAN
	33	19	20	13	STD. DEV.
	4.5%	1.9%	1.5%	0.8%	CV %
SENSOR	DEFLECTIONS IN MICRONS				
1	135	209	280	317	
	11	16	25	34	
	8.1%	7.8%	9.0%	10.7%	
2	109	168	225	253	
	5	7	9	10	
	4.9%	4.1%	4.1%	4.1%	
3	80	124	165	186	
	2	2	3	2	
	2.7%	1.4%	1.6%	1.3%	
4	57	89	119	133	
	1	1	2	2	
	2.0%	1.6%	1.7%	1.7%	
5	40	64	85	97	
	1	1	2	2	
	2.5%	2.1%	1.9%	1.6%	
6	31	49	67	75	
	1	2	2	2	
	4.1%	4.1%	3.4%	3.0%	
7	24	38	52	60	
	1	1	1	1	
	3.9%	2.8%	2.0%	2.5%	
	0.49	0.49	0.49	0.49	RIGIDITY FACTOR (Vaswani)

NOTE: THE FIRST ROW IS THE AVERAGE FOR THE SIX LOCATIONS
THE SECOND ROW IS THE STANDARD DEVIATION FROM THE MEAN
THE THIRD ROW IS THE COEFFICIENT OF VARIATION.

TABLE 4.8: TYPICAL FWD TESTS AND VARIABILITIES FROM TESTS IN BRANDON (1985 SERIES)

SITE: BRANDON DATE: 22 OCT.,85

FACILITY RWY 08-26

STATION: 5+900 OFFSET: 3 m R LOCATION: 1 to 6

FWD DEFLECTIO N DATA

	LOAD LEVEL 1	2	3	4	
kPa	588	844	1192	1360	MEAN
	5	5	5	5	STD. DEV.
	0.9%	0.5%	0.4%	0.4%	CV%
SENSOR #	DEFLECTIONS IN MICRONS				
1	405	574	826	947	
	8	27	230	173	
	2.1%	4.7%	27.9%	18.2%	
2	271	389	539	605	
	4	6	10	16	
	1.6%	1.4%	1.8%	2.7%	
3	147	216	305	344	
	4	6	8	8	
	3.0%	2.8%	2.7%	2.4%	
4	83	125	181	206	
	3	5	6	7	
	3.9%	3.9%	3.4%	3.4%	
5	57	85	121	138	
	2	3	4	3	
	3.1%	3.5%	3.6%	2.0%	
6	45	68	97	112	
	2	2	4	2	
	3.5%	3.3%	4.3%	1.9%	
7	37	55	79	92	
	1	2	2	2	
	2.6%	4.0%	2.7%	2.0%	
	0.34	0.35	0.34	0.34	RIGIDITY FACTOR (Vaswani)

NOTE:
THE FIRST ROW IS THE AVERAGE PRESSURE OR DEFLECTIONS.
THE SECOND ROW IS THE STANDARD DEVIATION OF THE MEAN.
THE THIRD ROW IS THE COEFFICIENT OF VARIATION.

TABLE 4.9.A: TEST RESULTS ON ASPHALTIC CONCRETE CORES

SITE: BRANDON **FACILITY: RUNWAY 08-26**

	<—— AGGREGATE GRADATION ——> (% PASSING mm)							BITUMEN %	<—— BITUMEN VISCOSITY / PENETRATION ——>					
									<——PEN dmm——>		<--VISCOSITY (Poises)-->			
STATION	25	12.5	4.75	2.00	0.425	0.180	0.075		4 C	25 C	40 C	100 C	135 C	145 C
	100	93.2	60.9	43.5	19.3	9.7	6.4	5.92	7.0	50.0	188.0	57.8	5.5	3.5
	100	96.6	61.8	44.7	18.9	9.4	6.5	5.57	7.0	50.3	188.0	58.9	5.7	3.6
	100	96.6	67.2	48.9	20.5	10.5	7.3	5.46	7.0	48.8	188.0	64.5	6.0	3.8
MEAN	**100**	**95.5**	**63.3**	**45.7**	**19.6**	**9.9**	**6.7**	**5.65**	**7.0**	**49.7**	**188.0**	**60.4**	**5.7**	**3.6**

TABLE 4.9.B: TEST RESULTS ON ASPHALTIC CONCRETE CORES

SITE: ST. ANDREWS **FACILITY: RUNWAY 13-31**

	<—— AGGREGATE GRADATION (% PASSING mm) ——>							BITUMEN %	<—— BITUMEN VISCOSITY / PENETRATION ——>					
									<——PEN dmm——>			<–VISCOSITY (Poises)–>		
STATION	25	12.5	4.75	2.00	0.425	0.180	0.075		4 C	25 C	40 C	100 C	135 C	145 C
5 + 030	100	100	62.2	46.7	18.2	12.5	6.7	5.39	5.0	45.0	253.0	17.5	2.1	1.35
5 + 120	100	98.4	64.7	48.7	21.5	14.8	8.5	5.47	4.3	37.0	202.0	22.9	2.5	1.59
5 + 300	100	100	59.7	45.8	20.6	13.6	7.2	4.92	4.8	44.0	201.0	20.3	2.5	1.60
5 + 480	100	98.9	60.2	45.7	20.0	13.1	7.2	5.17	5.5	43.0	199.0	21.7	2.5	1.57
5 + 660	100	98.0	60.1	46.1	22.4	10.1	5.2	6.13	5.8	36.0	156.0	55.8	5.0	3.02
5 + 840	100	98.6	61.3	46.1	24.2	10.6	5.2	6.24	5.5	43.0	195.0	45.7	4.5	2.73
MEAN	**100**	**99.0**	**61.4**	**46.5**	**21.2**	**12.5**	**6.7**	**5.55**	**5.2**	**41.3**	**201.0**	**30.7**	**3.2**	**1.98**

TABLE 4.9.C: TEST RESULTS ON ASPHALTIC CONCRETE CORES

SITE: REGINA **FACILITY: RUNWAY 12-30**

	<—— AGGREGATE GRADATION ——> (% PASSING mm)							BITUMEN %	<—— BITUMEN VISCOSITY / PENETRATION ——>					
									<——PEN dmm——>			<–VISCOSITY (Poises)–>		
STATION	25	12.5	4.75	2.00	0.425	0.180	0.075		4 C	25 C	40 C	100 C	135 C	145 C
5 + 510	100	99.5	71.0	55.5	21.3	10.8	7.2	5.9	3.0	38.5	120.0	55.0	5.7	3.10
5 + 950	100	99.2	71.5	52.4	19.1	10.1	7.0	5.9	5.0	51.0	198.0	42.0	4.4	3.00
6 + 290	100	99.4	72.4	54.1	21.4	11.7	7.5	5.96	4.5	45.0	172.0	53.1	4.9	2.86
6 + 890	100	99.6	71.6	53.8	21.5	11.5	7.2	5.9	4.5	42.0	177.0	52.6	8.0	2.82
7 + 310	100	99.8	72.4	54.0	26.0	14.4	8	6.1	5.0	43.0	188.0	48.2	4.6	2.71
MEAN	**100**	**99.5**	**71.8**	**54.0**	**21.9**	**11.7**	**7.4**	**5.95**	**4.4**	**43.9**	**171.0**	**50.2**	**5.5**	**2.90**

TABLE 4.9.D: TEST RESULTS ON ASPHALTIC CONCRETE CORES

SITE: SASKATOON **FACILITY: RUNWAY 15-33**

	<—— AGGREGATE GRADATION ——> (% PASSING mm)							BITUMEN %	<—— BITUMEN VISCOSITY / PENETRATION ——>					
									<——PEN dmm——>			<--VISCOSITY (Poises)-->		
STATION	25	12.5	4.75	2.00	0.425	0.180	0.075		4 C	25 C	40 C	100 C	135 C	145 C
5 + 360	100	100	68.1	49.2	19.5	8.5	5.1	5.5	5.8	31.2	110.0	90.0	6.9	4.10
5 + 630	100	100	69.7	50.8	19.8	9.0	5.0	5.69	4.8	31.5	130.0	70.0	6.3	4.10
5 + 840	100	100	71.0	51.1	19.8	9.0	5.3	5.37	6.2	31.8	150.0	63.0	5.5	4.10
6 + 140	100	100	68.5	48.2	18.5	7.8	3.8	4.97	6.5	38.0	140.0	55.0	5.3	3.30
6 + 470	100	100	65.3	46.8	17.6	7.5	3.5	5.65	5.5	37.3	162.0	55.0	4.9	3.80
MEAN	**100**	**100**	**68.5**	**49.2**	**19.0**	**8.4**	**4.5**	**5.44**	**5.8**	**34.0**	**138.4**	**66.6**	**5.8**	**3.88**

TABLE 4.9.E: TEST RESULTS ON ASPHALTIC CONCRETE CORES

SITE: THUNDER BAY **FACILITY: RUNWAY 12-30**

	<—— AGGREGATE GRADATION ——> (% PASSING mm)							BITUMEN %	<—— BITUMEN VISCOSITY / PENETRATION ——>					
									<——PEN dmm——>			<–VISCOSITY (Poises)–>		
STATION	25	12.5	4.75	2.00	0.425	0.180	0.075		4 C	25 C	40 C	100 C	135 C	145 C
5 + 100	100	95.9	57.1	40.9	27.6	19.9	7.1	5.92	5	43.3	185	61.00	5.79	3.54
5 + 300	100	93.9	70.3	53.6	30.3	12.4	7.0	5.88	5	46.8	185	54.73	5.20	3.28
5 + 500	100	92.7	65.9	45.3	21.6	13.7	7.6	5.19	6	42.3	256	20.87	2.45	1.62
5 + 650	100	96.0	71.7	49.4	22.5	14.7	9.1	5.38	6	34.0	252	32.55	3.41	2.19
6 + 100	100	93.6	67.4	46.4	22.9	14.6	8.1	5.77	6	45.8	256	21.72	2.83	1.68
TXTB10+740	100	97.0	69.8	46.7	23.2	14.7	7.9	5.71	6	52.8	256	18.77	4.98	1.56
MEAN	**100**	**94.9**	**67**	**47.1**	**24.7**	**15**	**7.8**	**5.64**	**5**	**44.2**	**228**	**34.94**	**3.66**	**2.31**

TABLE 4.10.A. RESULTS OF LABORATORY TESTS ON GRANULAR AND SUBGRADE MATERIALS AT BRANDON

STATION	DEPTH (m)	LAYER	MOIST. CONT. (%)	LL (%)	PL (%)	PI (%)	qu (kPa)
5 + 400	0.60	B	5.3				
	1.20	SG	26.3	41.8	15.8	26	
5 + 600	0.60	B	5.4				
	1.30	SG	19.9				
5 + 900	0.60	B	6.3				
	1.30	SG	18.4	35.7	14.5	21.2	
6 + 300	0.60	B	4.5				
	1.20	SG	15.8				
6 + 500	0.60	B	6.0				
	1.30	SG	19.9	35.2	15.2	20	

TABLE 4.10.B. RESULTS OF LABORATORY TESTS ON GRANULAR AND SUBGRADE MATERIALS AT ST. ANDREWS.

STATION	DEPTH (m)	LAYER	MOIST. CONT. (%)	LL (%)	PL (%)	PI (%)	qu (kPa)
5 + 030	0.25	B	7.6			NP	
	0.70	SG	16.1	38.5	15.4	23.1	
	1.70	SG	34.8	88.7	29.9	58.8	180
5 + 120	0.30	B	7.3			NP	
	0.75	SG	32.5	84.5	31.1	53.4	250
	1.75	SG	42.3	96.0	30.3	65.7	170
5 + 480	0.25	B	6.4			NP	
	0.75	SG	33.1	73.7	30.9	42.8	270
	1.75	SG	43.2	101.1	29.6	71.5	150
5 + 660	0.28	B	4.3			NP	
	0.80	SG	36.0	76.4	30.9	45.5	275
	1.80	SG	38.1	94.8	30.3	64.5	180
5 + 840	0.20	B	5.3			NP	
	0.70	SG	38.9	83.0	31.1	51.9	280
	1.70	SG	39.7	97.3	30.3	67.0	260

TABLE 4.10.C. RESULTS OF LABORATORY TESTS ON GRANULAR AND SUBGRADE MATERIALS AT REGINA

STATION	DEPTH (m)	LAYER	CONT. (%)	LL (%)	PL (%)	PI (%)	qu (kPa)
5 + 510	0.65	B	5.7				
	1.20	SG	27.7	77.2	26.3	50.9	400
	2.20	SG	31.7				300
5 + 990	0.70	B	5.6				
	1.20	SG	33.9	77.6	26.3	51.3	375
	2.20	SG	32.3	81.4	25.3	56.1	290
6 + 290	0.70	B	5.7				
	1.25	SG	31.8				350
	2.25	SG	33.6	81.4	25.3	56.1	275
6 + 890	0.72	B	6.8				300
	1.30	SG	30.8				250
	2.30	SG	31.5				
7 + 310	0.65	B	6.6				
	1.15	SG	29.8	81.7	26.3	55.4	350
	2.15	SG	32.3				325

TABLE 4.10.D. RESULTS OF LABORATORY TESTS ON GRANULAR AND SUBGRADE MATERIALS AT SASKATOON.

STATION	DEPTH (m)	LAYER	MOIST. CONT. (%)	LL (%)	PL (%)	PI (%)	qu (kPa)
5 + 360	0.40	B	3.2				
	0.90	B	8.1				
	1.30	SG	9.9	35.2	23.8	11.4	400
5 + 630	0.69	B	5.2				
	1.10	B	5.2				
	2.10	SG	10.8	24.6	18.4	6.2	100
5 + 840	0.50	B	3.3				
	1.10	B	8.4				
	1.50	SG	23.3	60.9	24.9	36.0	250
6 + 140	0.40	B	2.4				
	0.60	B	3.7				
	2.80	SG	10.9	28.7	18.4	10.3	300
6 + 470	0.50	B	2.3				
	1.00	B	4.8				
	1.60	SG	25.4	79.0	26.8	52.2	375

TABLE 4.10.E. RESULTS OF LABORATORY TESTS ON GRANULAR AND SUBGRADE MATERIALS AT THUNDER BAY

STATION	DEPTH (m)	LAYER	MOIST. CONT. (%)	LL (%)	PL (%)	PI (%)	qu (kPa)
5 + 100	0.24	B	7.6				
	0.42	B	6.8				
	1.20	SG	19.2			NP (SM)	
5 + 300	0.3	B	6.9				
	0.6	SB	6.5				
	1.2	SG	18.7			NP (SM)	
5 + 500	0.50	SB	6.6				
	0.65	SG	22.5			NP (SP-SM)	
5 + 650	0.47	SB	10.3				
	0.57	SG	9.1			NP (SP-SM)	
6 + 100	0.44	SB	6.2				
	0.54	SG	18.1			NP (SM)	
TAXI A	0.13	B	3.7				
10 + 740	0.43	SB	4.5				
	1.48	SG	23.2			NP (SM)	